

# ABSTRACT OF THESIS

Name of Candidate SHEILA WILSON  
Address [REDACTED]  
Degree Ph.D. Date November 1972  
Title of Thesis STUDIES IN NUCLEAR MAGNETIC RESONANCE WITH SPECIAL  
REFERENCE TO PARAMAGNETIC EFFECTS.

The effects of the presence of paramagnetic species on Nuclear Magnetic Resonance (N.M.R.) spectra and applications of these effects are reviewed, with special reference to systems in which structural analysis of organic compounds is facilitated.

The paramagnetic shifts in the signals of slightly oxidised ferrocene derivatives have been found to be relatively small while considerable line-broadening occurs. Selective changes in the relaxation times for the protons have been observed.

The intermolecular contribution to the linewidth of the signals of a nitroxide free radical has been effectively eliminated by using very dilute solutions of the free radicals, thus allowing observation of the intramolecular contribution for use in structure determination. The dependence of the intermolecular contribution on the solvent viscosity has been demonstrated and evidence has been found for selective broadening arising from intermolecular association, probably hydrogen bonding.

Complex formation between cobalt(II) perchlorate and ligands such as cyanides, alcohols and amides in deuteroacetone solution has been shown to give rise to substantial paramagnetic shifts with relatively little line-broadening, the reagent being superior to cobaltous acetylacetonate in structure determination of organic compounds.

The lanthanide complexes, trisdipivalomethanato europium(III) and praseodymium(III),  $\text{Eu}(\text{DPM})_3$  and  $\text{Pr}(\text{DPM})_3$ , were also examined as shift reagents, for comparison with the cobalt perchlorate system. Europium nitrate and praseodymium nitrate were found to be useful shift reagents for a diol, all the other reagents studied being of doubtful value.

The method of progressive saturation has been developed on both the R10 (60 MHz) and HA 100 (100 MHz) N.M.R. spectrometers. Relative values for relaxation times have been obtained and used in connection with the ferrocene derivatives and the cobalt complexes of amides.



STUDIES IN NUCLEAR MAGNETIC RESONANCE  
WITH SPECIAL REFERENCE TO  
PARAMAGNETIC EFFECTS

by

SHEILA WILSON, B.Sc.



Thesis presented for the degree of Doctor of  
Philosophy of the University of Edinburgh in  
the Faculty of Science.

November, 1972.



This thesis describes the results of research carried out in the University of Edinburgh during the period 1968-1971, under the supervision of Dr. J.C.P. Schwarz, to whom I wish to express my most sincere thanks for the constant help and encouragement during that period.

Grateful acknowledgment is also made to Professor J.I.G. Cadogan, for the provision of laboratory facilities, and to the Science Research Council for financial support.

I also wish to thank Mr. J. Allan and Miss F.A.K. Maclean for help with some of the preparative aspects of this work, and Mrs. E.P. Groves and Mr. A. King for instrumental advice and help with modifications to the spectrometers.



## CONTENTS

		<u>Page</u>
	SUMMARY	
PART I	INTRODUCTION	1
PART II	A REVIEW OF THE N.M.R. OF PARAMAGNETIC SPECIES	4
	(A) Introduction	4
	(B) Contact Shifts	4
	(C) Pseudocontact Shifts	7
	(D) Relaxation Times	9
	(E) Chemical Exchange	11
	(F) Chemical Spin-Decoupling	12
	(G) Applications	12
	(a) Stable compounds - metallocenes	15
	(b) Configurational equilibrium complexes	15
	(c) Complexes with ligand exchange	17
	(d) Lanthanide "shift reagents"	20
	(e) Free radicals	24
	(f) Relaxation studies	27
PART III	FERROCENES	29
	(A) Experimental	30
	(a) General	30
	(b) Preparation of compounds	32
	(c) Preparation of solutions	44
	(B) Shift Studies	47
	(C) Linewidth Studies	56
	(D) Stability of Ferricenium Cations	60
	(E) Conclusion	61
PART IV	FREE RADICALS	62
	(A) Experimental	63
	(a) Preparation of compounds	63
	(b) Preparation of solutions for N.M.R. measurements	64



	<u>Page</u>
(B) Preliminary Investigations	66
(a) Alcohol nitroxide	66
(b) Tosylate nitroxide	67
(C) More Detailed Study of the Concentration Effect for the Tosylate Nitroxide	69
(D) Viscosity Effect with Tosylate Nitroxide	72
(E) Selective Broadening Arising from Intermolecular Association	73
(F) Conclusion	76
 PART V	
COBALT COMPLEXES	77
(A) Experimental	79
(a) Preparation of compounds	79
(b) Preparation of solutions for N.M.R.	84
(c) Instrumental conditions	86
(B) Detailed Investigation of Simple Model Compounds: Ethyl Cyano- acetate and Propionitrile	86
(a) Ethyl cyanoacetate	86
(b) Nature of the complex and solution	93
(c) Propionitrile	98
(d) Shifts in the absence of com- plex formation	101
(C) Investigation of More Complex Molecules	103
(a) Cyanide ligands	104
(b) Alcohol ligands	119
(c) Amide ligands	146
(d) Ketone ligands	174
(e) Ester ligands	177
(f) Conclusion	179
(D) Cobaltous Acetylacetonate Complexes	181



	<u>Page</u>
PART VI	LANTHANIDE COMPLEXES 189
(A)	Experimental 190
(a)	Preparation of shift reagents 190
(b)	Preparation of solutions for N.M.R. 191
(B)	Trisdipivalomethanato-Lanthanide (III) Shift Studies 192
(a)	Trisdipivalomethanato-europium(III) 192
(b)	Trisdipivalomethanato-praseodymium(III) 199
(C)	Lanthanide Nitrate Shift Studies 203
(a)	Europium nitrate dihydrate 203
(b)	Praseodymium nitrate monohydrate 208
(D)	Conclusion 219
PART VII	COMPARISON OF SHIFT REAGENTS 220
(A)	Cyanide Ligands 220
(B)	Alcohol Ligands 222
(a)	Simple alcohols 222
(b)	Diols 223
(C)	Amide Ligands 224
(D)	Summary 226
(E)	Experimental Comparison 226
(a)	Ease of preparation of solutions 226
(b)	Cost of solutions 228
(F)	Conclusion 229
PART VIII	PROGRESSIVE SATURATION STUDIES 230
(A)	Introduction 230
(B)	Experimental 236
(C)	Progressive Saturation Using the R10 Instrument 236
(a)	Instrumental conditions and accuracy checks 236
(b)	Instrumental calibration to evaluate absolute values of $T_1 T_2$ 240
(c)	Conclusion 249



	<u>Page</u>
(D) Progressive Saturation Using the HA 100 Instrument	249
(a) Instrumental conditions and accuracy checks	249
(b) Instrumental calibration to evaluate absolute values of $T_1 T_2$	255
(c) Measurement of the radio- frequency field by Torrey oscillations	261
(d) Progressive saturation of the integral	263
(e) Conclusion	265
(E) Applications of Progressive Saturation	266
(a) Ferrocene derivatives	266
(b) Amide studies	267
BIBLIOGRAPHY	268



## SUMMARY

The effects of the presence of paramagnetic species on Nuclear Magnetic Resonance (N.M.R.) spectra and applications of these effects are reviewed, with special reference to systems in which structural analysis of organic compounds is facilitated.

The paramagnetic shifts in the signals of slightly oxidised ferrocene derivatives have been found to be relatively small while considerable line-broadening occurs. Selective changes in the relaxation times for the protons have been observed.

The intermolecular contribution to the linewidth of the signals of a nitroxide free radical has been effectively eliminated by using very dilute solutions of the free radicals, thus allowing observation of the intramolecular contribution for use in structure determination. The dependence of the intermolecular contribution on the solvent viscosity has been demonstrated and evidence has been found for selective broadening arising from intermolecular association, probably hydrogen bonding.

Complex formation between cobalt(II) perchlorate and ligands such as cyanides, alcohols and amides in deuterio-acetone solution has been shown to give rise to substantial paramagnetic shifts with relatively little line-broadening, the reagent being superior to cobaltous acetylacetonate in structure determination of organic compounds.

The lanthanide complexes, trisdipivalomethanato europium(III) and praseodymium(III),  $\text{Eu}(\text{DPM})_3$  and  $\text{Pr}(\text{DPM})_3$ ,



were also examined as shift reagents, for comparison with the cobalt perchlorate system. Europium nitrate and praseodymium nitrate were found to be useful shift reagents for a diol, all the other reagents studied being of doubtful value.

The method of progressive saturation has been developed on both the R10 (60 MHz) and HA 100 (100 MHz) N.M.R. spectrometers. Relative values for relaxation times have been obtained and used in connection with the ferrocene derivatives and the cobalt complexes of amides.



PART IINTRODUCTION

Nuclear Magnetic Resonance (N.M.R.) spectroscopy has been extensively used in most branches of chemistry, but only in more recent times has it been found to have widespread application in paramagnetic systems. Paramagnetic species have a strong influence on N.M.R. spectra, causing changes in the resonance positions and broadening of the signals, often rendering the spectra unobservable. Because of the latter effect paramagnetic systems were initially little studied. However, situations were discovered in which relatively narrow signals were observed and physical and inorganic chemists were soon utilising the shift changes and the broadening to obtain information about physical processes, types of bonding, electron distributions, stereochemistry and exchange rates.

Recently it has become apparent that the selective shifts and line-broadening produced by paramagnetic species can be valuable to the organic chemist in structure determination in molecules whose N.M.R. spectrum is complex. A number of studies including some in this laboratory<sup>1,2</sup> indicated that selective broadening can reveal which protons lie closest to the paramagnetic centre. Also, selective shifts of the resonance positions can separate overlapping signals (often rendering second-order spectra first-order) and at the same time indicate the proximity of the protons to the paramagnetic centre and their relative positions



within the molecule. The method of selective broadening requires signals that are sufficiently separated for their linewidths to be measurable which, consequently, limits the scope of the technique; the use of selective shifts requires that the paramagnetic probe produces substantial changes in the resonance positions, while broadening is minimal, so that peaks become distinct and fine structure is still observable.

It was the aim of this work to investigate a variety of paramagnetic probes, both in stable entities and in ligand exchange situations, with a view to exploring their utility for either selective broadening or selective shifts. The ease of sample preparation, the value of the information obtained and the scope of application were factors that were also considered in the assessment of the various systems.

In the first such system examined, the ferrocene nucleus was used as a probe; this can conveniently be oxidised to the paramagnetic ferricenium cation. The ferrocene-ferricenium system is discussed in Part III. It proved unsatisfactory for a number of reasons but led on to an investigation of the potentialities of selective saturation of paramagnetic-broadened resonances, described in Part VIII.

Attention then focussed on the possibilities of complex formation with cobalt(II) ion, provided by cobalt perchlorate in deuteroacetone solution. The partial success of this system using some cyanide molecules as ligands prompted a further study of a wider variety of ligands. This work is detailed in Part V.



The appearance in the literature of rare-earth paramagnetic shift reagents induced a brief investigation of these systems, for comparison with the cobalt perchlorate system and the previously used cobaltous acetylacetonate system, as presented in Parts VI and VII.

Part IV describes some preliminary work carried out with a rather different probe involving free radical nitroxides.

There follows first a review of the effects of paramagnetic species on N.M.R. spectra and of some of the applications of these effects, a knowledge of which is helpful in the interpretation of the results of these studies.



## PART II

### A REVIEW OF THE N.M.R. OF PARAMAGNETIC SYSTEMS

#### (A) INTRODUCTION

The introduction of paramagnetic species into a solution can affect the N.M.R. spectra of that solution considerably. This is the result of the unpaired electron(s), whose large magnetic moment,  $10^3$  times that of a nucleus, causes strong local magnetic fields at the nuclei.

Three of the effects which may be observed are:

- 1) a change in the resonance position of the N.M.R. signals;
- 2) a broadening of the signals due to more rapid relaxation;  
and
- 3) a change in the multiplicity of the signals from coupled nuclei.

We shall consider briefly the mechanisms responsible for the shift and relaxation effects and some of their applications to problems in physical, inorganic and organic chemistry.

#### (B) CONTACT SHIFTS

The presence of unpaired electron spin at the resonating nucleus gives rise to an interaction between the two spins, named the Fermi contact interaction. The electronic spin can be aligned with or against the applied magnetic field thus increasing or decreasing the field which the nucleus experiences. This might be expected to result in a doublet of coupling constant,  $A$ , the Electron Spin Resonance (E.S.R.) hyperfine coupling constant, but in fact



this is not observed as the signals would be too broad. If, however,  $1/\tau_s \gg A$  and/or  $1/T_e \gg A^3$ , where  $\tau_s$  is the electronic relaxation time and  $T_e$  is the electronic exchange time, then the nucleus will see one time-averaged magnetic field and a single resonance is observed. This is shifted from its diamagnetic position due to the unequal Boltzmann distribution of populations between the two electronic spin states. Under these conditions, E.S.R. resonances are too broad for resolution and so E.S.R. and N.M.R. techniques are thus complementary to each other.

The contact shift expression has been derived from the effective Hamiltonian given by McConnell and Chestnut<sup>3</sup> from Fermi's<sup>4</sup> expression, to be

$$\frac{\Delta H}{H} = \frac{\Delta \nu}{\nu} = -\frac{4}{9} A \frac{\gamma_e}{\gamma_I} \frac{g\beta S(S+1)I(I+1)}{kT}$$

which, for the proton with  $I = \frac{1}{2}$ , reduces to

$$\frac{\Delta H}{H} = -A \frac{\gamma_e}{\gamma_I} \frac{g\beta S(S+1)}{3kT}.$$

$H$  and  $\nu$  define the resonance field and frequency,  $\gamma_e$  and  $\gamma_I$  are the electronic and nuclear magnetogyric ratios,  $g$  is the electronic  $g$  factor,  $\beta$  is the Bohr magneton and  $I$  the nuclear spin quantum number, the remaining symbols having their previously defined or usual meaning.

The equation has been modified several times<sup>5-10</sup>, the most general form, where not all the unpaired electron spin is delocalised, being<sup>9</sup>

$$\frac{\Delta H}{H} = -A \frac{\gamma_e}{\gamma_I} \frac{g\beta S(S+1)}{6S'kT}$$



where  $S'$  is the total spin of unpaired electrons involved in the delocalisation, and  $S$  is the total unpaired electron spin.

Recently, the assumptions underlying these equations have been discussed and cases in which they are not fulfilled have been considered<sup>11</sup>.

In some systems there is an equilibrium between diamagnetic and paramagnetic forms of a chelate in solution. For such systems, Eaton<sup>12</sup> proposed the equation

$$\frac{\Delta H}{H} = -A \frac{\gamma_e}{\gamma_H} \frac{g\beta S(S+1)}{2SkT [\exp(\Delta G/RT)+3]}$$

where  $\Delta G$  is the free energy difference between the two forms. The free energy term was later corrected by Horrocks<sup>13</sup> to  $[\exp(\Delta G/RT)+1]$ .

Spin density can be transferred from a metal nucleus to ligand nuclei by two main mechanisms. If unpaired spin density resides in metal orbitals of  $\sigma$ -symmetry and is transferred to the  $\sigma$ -orbitals of the ligands, the magnetic field at the protons is reinforced by the electron spin magnetic field, and the proton resonances are all shifted to lower applied fields. If the metal atom has orbitals of  $\pi$ -symmetry containing unpaired electrons, their spin density may be transferred into the ligand  $\pi$ -systems by  $d\pi-d\pi$  or  $d\pi-p\pi$  bonding. This latter results in the proton resonances being shifted alternately to higher and lower applied fields.

Analysis of the signs and relative magnitudes of the contact shifts has been widely used to investigate the type of metal-ligand bonding present. Fitzgerald and Drago<sup>14</sup>



have given evidence that  $\pi$ -delocalisation is possible although the bonding is  $\sigma$ -type, and Eaton, Josey and Benson<sup>15</sup> have shown that spin density can be distributed from a  $\pi$ -system into orbitals of  $\sigma$ -symmetry. Doubt has also been thrown on the conclusions of some of the work by Horrocks and Johnston<sup>16</sup> who have shown that delocalisation of spin density in  $\sigma$ -systems can give rise to shifts similar to those arising from  $\pi$ -delocalisation.

### (C) PSEUDOCONTACT SHIFTS

Pseudocontact interaction results from the dipolar interaction between the nuclear moment and the electron spin magnetisation. If the metal ion possesses an anisotropic  $g$  tensor, the interaction is not averaged by tumbling, and shifts are observed.

Subsequent to the work of Bloembergen and Dickinson<sup>17,18</sup>, McConnell and Robertson<sup>19</sup> deduced two equations for pseudocontact shifts for complexes of axial symmetry in solution

$$\frac{\Delta H}{H} = \frac{-g^2 S(S+1)}{27kT} (g_{\parallel} + 2g_{\perp})(g_{\parallel} - g_{\perp}) \frac{(3\cos^2\chi - 1)}{r^3} \text{ for } \tau_s \gg \tau_c$$

and, with the signs corrected<sup>20</sup>,

$$\frac{\Delta H}{H} = \frac{-g^2 S(S+1)}{45kT} (3g_{\parallel}^2 + g_{\parallel}g_{\perp} - 4g_{\perp}^2) \frac{(3\cos^2\chi - 1)}{r^3} \text{ for } \tau_c > \tau_s$$

where  $\tau_c$  is the dipolar correlation time, and  $g_{\parallel}$  and  $g_{\perp}$  the electronic  $g$  tensors parallel and perpendicular to the principal symmetry axis,  $r$  is the distance between the paramagnetic centre and the magnetic nucleus, and  $\chi$  is the angle between the distance vector and the principal symmetry axis.



The initial assumption that the former was the more usual case was disputed by LaMar<sup>20</sup> who stated that  $\tau_c > \tau_s$  is more generally true and the latter equation should therefore be used.

LaMar, Horrocks and Allen<sup>21</sup> have extended the equations to complexes which are not axially symmetric, where the three principal  $g$  values,  $g_1$ ,  $g_2$  and  $g_3$ , are different.

As with the contact shifts, the pseudocontact expressions may have alternative forms depending on the nature of the basic assumptions<sup>11</sup>.

The fact that most Ni(II) complexes have an isotropic  $g$  factor, and so no pseudocontact interactions, while Co(II) complexes show  $g$  factor anisotropy has been used<sup>22</sup> in comparative studies of complexes of the two ions, to derive information about pseudocontact interactions. Assuming that the ratios of the contact shifts of the various protons in the complexes are the same for the two ions, the pseudocontact shifts in the cobalt complexes can be calculated. Wicholas and Drago<sup>23</sup> have criticised the assumption that the contact shift ratios will remain constant for different metal ions, but Horrocks<sup>24</sup> defends the procedure as being valid provided certain basic assumptions hold. Drago<sup>25</sup> claims that it is extremely difficult to predict when the delocalisation mechanism will be the same and so estimation of the pseudocontact shifts by this method will be unreliable.



## (D) RELAXATION TIMES

Two characteristic times were introduced by Bloch<sup>26</sup> to describe relaxation processes. The first, the thermal, spin-lattice or longitudinal relaxation time,  $T_1$ , characterises the time required for the spin system to come to equilibrium with the other degrees of freedom, the lattice, that is for the Boltzmann distribution of populations in the spin states to be re-established. This process involves a change in energy of the total spin system.  $T_1$  characterises the rate of decay of magnetisation in the direction of the applied field.

The second, the spin-spin or transverse relaxation time,  $T_2$ , describes processes in which the energy of the total spin system is unchanged.

Irradiation constrains the spins to precess in phase thus generating a component of the magnetisation perpendicular to the applied magnetic field; on removal of the irradiation the spins gradually lose phase at a rate characterised by  $T_2$ , which thus describes the rate of decay of the transverse magnetisation. Bloembergen, Purcell and Pound<sup>27</sup> have given the relationship between the normalised Lorentzian line-shape function,  $g(\nu)$ , and  $T_2$  as

$$g(\nu) = \frac{2T_2}{1 + 4\pi^2(\nu - \nu_0)^2 T_2^2}$$

where  $\nu$  is absorption frequency and  $\nu_0$  the frequency of maximum absorption. From this, the relationship between  $T_2$  and linewidth at half peak-height,  $\Delta\nu_{\frac{1}{2}}$ , is

$$\Delta\nu_{\frac{1}{2}} = 1/\pi T_2$$



Since the magnetic moment of an electron is of the order of  $10^3$  times that of a nucleus, the addition of paramagnetic ions to a diamagnetic solution can have a strong influence on the relaxation times. Bloembergen, Purcell and Pound<sup>27</sup> derived an expression for  $T_1$  in the presence of paramagnetic ions. This was developed more fully by Solomon<sup>28</sup> who gave expressions for the effect of dipole-dipole interactions on  $T_1$  and  $T_2$ , which was later modified by Bloembergen<sup>29</sup> to include scalar interactions. The resulting Solomon-Bloembergen equations<sup>30</sup> are

$$\frac{1}{T_{1M}} = \frac{2}{15} \frac{S(S+1)g^2\beta^2\gamma_I^2}{r^6} [3\tau_c + \frac{7\tau_c}{1+\omega_s^2\tau_c^2}] + \frac{2}{3} \frac{S(S+1)A^2}{\hbar^2} \frac{\tau_e}{(1+\omega_s^2\tau_e^2)}$$

$$\frac{1}{T_{2M}} = \frac{1}{15} \frac{S(S+1)g^2\beta^2\gamma_I^2}{r^6} [7\tau_c + \frac{13\tau_c}{1+\omega_s^2\tau_c^2}] + \frac{1}{3} \frac{S(S+1)A^2}{\hbar^2} [\tau_e + \frac{\tau_e}{1+\omega_s^2\tau_e^2}]$$

The symbols have the same definitions as before,  $\omega_s$  being the electronic Larmor precession frequency and  $\tau_c$  and  $\tau_e$  being the correlation times characterising the dipolar and the hyperfine interactions respectively.

$\tau_c$  and  $\tau_e$  are given by<sup>31</sup>

$$\frac{1}{\tau_c} = \frac{1}{\tau_e} + \frac{1}{\tau_r}$$

$$\text{and } \frac{1}{\tau_e} = \frac{1}{\tau_s} + \frac{1}{\tau_h}, \text{ where}$$

$\tau_s$  is the electronic relaxation time of the paramagnetic species,  $\tau_r$  is the characteristic time for tumbling of the paramagnetic ion or complex and  $\tau_h$  is the chemical exchange time for nuclei between the co-ordination sphere and bulk medium.

For very short electronic relaxation times for which



$\omega_s^2 \tau_e^2 \ll 1$ , the Solomon-Bloembergen equations simplify to

$$\frac{1}{T_{1M}} = \frac{1}{T_{2M}} = \frac{4}{3} \frac{S(S+1)g^2 \beta^2 \nu_I^2 \tau_s}{r^6} + \frac{2}{3} \frac{S(S+1)A^2 \tau_s}{\hbar^2}$$

In this case resonances are not greatly broadened. When  $\omega_s^2 \tau_e^2 \gg 1$ , resonances may be broadened so much they cannot be detected.

Sternlicht<sup>32</sup> has derived expressions for  $T_1$  and  $T_2$  in the case of paramagnetic ions with anisotropic  $g$  factors.

An expression for the relaxation times of nuclei outside the co-ordination sphere has been given by Luz and Meiboom<sup>33</sup> by averaging the dipole-dipole interaction over the volume between the sphere of closest approach and infinity.

The Bloembergen-Solomon formulation has been extended to include the temperature dependences of the correlation times governing the various contributions to  $T_1$  and  $T_2$ <sup>34</sup>, and has also been used to interpret the frequency dependence of the relaxation times<sup>35</sup>.

#### (E) CHEMICAL EXCHANGE

The expressions which have been given above refer to situations where the paramagnetic species and the resonating nuclei are components of a stable entity. If a ligand bound to a metal ion is exchanging with ligand in the bulk diamagnetic solution, changes in both shift and linewidth may be observed. If the exchange is very slow two peaks will be observed, one for the diamagnetic state and one for the paramagnetic. If the exchange is very fast an average resonance is found. At intermediate rates, the situation



is more complex. These various cases have been considered in detail by Swift and Connick<sup>36</sup> in their investigation of the temperature and frequency dependence of the transverse relaxation time.

#### (F) CHEMICAL SPIN-DECOUPLING

Decoupling of spin-spin N.M.R. splittings is normally brought about by irradiation with a strong RF field at the frequency of absorption of one nuclei, but it can also be achieved chemically by the rapid relaxation produced by a paramagnetic species<sup>37-42</sup>. If the local fluctuating fields due to the paramagnetic ion are sufficiently strongly felt at a magnetic nucleus, they may cause that nucleus to exchange so rapidly between its spin states that a neighbouring nucleus observes only one averaged state and so becomes decoupled from that nucleus. The nucleus being so relaxed must therefore lie fairly close to the paramagnetic centre to experience a strong enough field<sup>43,44</sup>, and the effectiveness of the relaxation will vary according to the transition metal employed<sup>45</sup>.

#### (G) APPLICATIONS

The effects of unpaired electron spins on N.M.R. spectra have been applied to the elucidation of a great variety of problems. Initially most of the interest was focussed on the investigation of the nature of metal complexes, particularly with regard to the metal-ligand bonding and the mechanisms for the delocalisation of the electron spin. Another early type of application which continues to be



fruitful is the use of paramagnetic effects in studying the rates of ligand exchange and of other exchange processes. More recently, as in the present thesis, attention has been turned towards employing these effects in the determination of the structure and stereochemistry of organic molecules. These applications are now reviewed briefly according to the class of compound involved.

Other applications which are not reviewed in detail here include the use of paramagnetic probes in the study of micellisation and micelle structure<sup>2</sup> and in investigations involving molecular motion<sup>46,47</sup>, particularly with regard to macromolecules.

For most purposes it is essential that the effect of the paramagnetic species should not be such as to make the N.M.R. signals unobservable on normal high resolution spectrometers. In particular, in practical applications of contact and pseudocontact shifts it is usually desirable that the ratio of the shift change to the broadening of the signals should be large. Examination of the Solomon-Bloembergen equations given earlier (Section D) shows that metal atoms with short electronic relaxation times will tend to give narrow lines.

Two other mechanisms can contribute to line-narrowing, these being rapid exchange of ligand between complexed and uncomplexed sites, and rapid interconversion between two magnetically distinct configurations of a stable chelate.

The magnitude of the shift change depends on the magnitude of its two components. Large contact shifts arise



from a large coupling constant,  $A$ , which is dependent on the spin density at the resonating nucleus. The contact shift depends on  $A$  while the line-broadening depends on  $A^2$ , so that, although the greater is the value of  $A$  the greater is the shift observed, small values of  $A$  will give rise to better shift to linewidth ratios. The size of the pseudo-contact contribution to the shift for axial symmetry depends on the geometric factor  $(3\cos^2\chi-1)r^{-3}$  and on the anisotropy of the  $g$ -factor. The dipolar contribution to the linewidth depends on  $r^{-6}$  and the square of the average  $g$ -factor,  $g^2$ . It is thus apparent that the two factors which are most effective in generating a large shift to linewidth ratio are as follows. Firstly, the closer the protons are to the main symmetry axis, where  $\chi = 0$  or  $180^\circ$ , the larger will be the shifts without affecting the linewidths; and, secondly, the greater the anisotropy of the  $g$ -factor, that is the greater the absolute magnitude of  $(g_{||}-g_{\perp})g^{-2}$ , the larger again will be the shifts. The second of these factors applies equally to all protons in the paramagnetic species and so is more important than the first. The short electronic relaxation times of Co(II), Ni(II), V(III) and Cr(II) make them the most favourable ions of the first row transition metals, while the even greater potential of the lanthanides, Eu(III) and Pr(III) and to a lesser extent Yb(III), which has recently been shown, arises from short electronic relaxation times combined with highly anisotropic  $g$ -factors.

Although free radicals have relatively long electron relaxation times, giving rise to extensive line-broadening,



and have almost isotropic g-factors, N.M.R. spectra of these species can be observed under certain circumstances and have interesting applications which are considered separately below.

(a) Stable compounds - metallocenes

The first compound examined was nickelocene<sup>5</sup> which was found to give upfield shifts relative to diamagnetic metallocenes. Later<sup>48</sup>, manganocene and cobaltocene were found also to give upfield shifts while downfield shifts were observed for vanadocene and chromocene. Attention has focussed mainly on the nature of bonding and mode of spin delocalisation in these systems<sup>49-51</sup>.

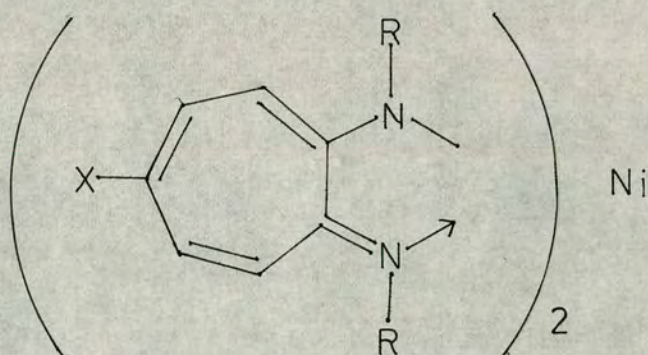
Ferrocene, though diamagnetic itself, is fairly readily oxidised to the paramagnetic ferricenium cation. In solutions containing both species, rapid electron transfer<sup>52</sup> between the species occurs with subsequent line-narrowing of the paramagnetic resonance signals, rendering them observable. The N.M.R. spectra of a number of ferrocene/ferricenium systems have been investigated<sup>53</sup>, not only because ferrocene has many stable derivatives, but also because the E.S.R. of the cation<sup>54</sup> is observable, yielding further information, notably the anisotropic g values.

(b) Configurational equilibrium complexes

With these chelates there is rapid intramolecular interconversion between diamagnetic square-planar and paramagnetic tetrahedral configurations.

The most investigated complexes of this type have been the nickel(II) aminotroponeimineates.





Eaton, Phillips and co-workers, studying a variety of derivatives substituted at the nitrogen atom or at the  $\gamma$  position of the ring, deduced the metal-ligand bonding to be  $\pi\pi$ - $d\pi$  with spin density distributed through the  $\pi$ -system of the ligand<sup>55-57,12</sup>. They also studied the thermodynamics of the equilibrium<sup>58</sup>, and the effect of having two different ligands chelated to the Ni<sup>59</sup>. Complexes of V, Cr, Mn, Fe and Co have also been investigated<sup>60</sup>. In their  $^{13}\text{C}$  studies of the Ni complexes, Doddrell and Roberts<sup>61</sup> have found predominant  $\sigma$  delocalisation of spin density.

The nickel bis-salicylaldimines form a similar group of complexes<sup>62</sup> with comparably sharp lines but shifts which are five times smaller. The position of the equilibrium is strongly dependent on the nature of the substituent at the nitrogen atom. The paramagnetic tetrahedral form has been found to predominate increasingly in the order closed chain alkyl < open chain alkyl < aryl<sup>63,64</sup>, and *n*-propyl < sec. alkyl < tert. butyl<sup>65</sup>. Eaton and co-workers<sup>66</sup> have proposed that the unpaired spin is delocalised through the  $\pi$  system, and have also observed the shifts on addition of pyridine. The closely related bis(*o*-hydroxy-naphthalaldimine)-nickel(II)



complexes<sup>67</sup> and the bis( $\beta$ -ketoamino)-nickel(II) complexes<sup>68</sup> also show the planar-tetrahedral equilibrium. In the cobalt(II) complex<sup>69</sup> of the latter, the equilibrium position is moved markedly towards the tetrahedral configuration.

A third group of this type is the bis-tertiary phosphine nickel dihalides<sup>70,71</sup>. N.M.R. studies of these have yielded information about the rates of interconversion of the two forms.

### (c) Complexes with ligand exchange

A number of systems have been examined in which paramagnetic ions have been added to a solution containing a potential ligand, or in which a paramagnetic complex is added to a solution containing excess of the same ligand or a different ligand. As the ratio of metal ion to ligand concentration increases, so does the fraction of ligand complexed; this increases the shifts from the diamagnetic line positions and the linewidths. Metal ion concentrations can thus be chosen, for a given substrate concentration, so as to give the most favourable shifts and linewidths.

Nickel(II) and cobalt(II) have been studied with ligands such as pyridines<sup>72-74</sup>, bipyridines<sup>75,76</sup> and their N-oxides<sup>77,78</sup>, amines<sup>14,79</sup> and phosphines<sup>80,81</sup>. The shifts have been employed to examine mechanisms of metal-ligand spin transfer and delocalisation of spin in saturated and conjugated ligand systems. Evidence for both  $\sigma$  and  $\pi$  delocalisation of spin in pyridine-type ligands of tetrahedral and octahedral complexes has been found<sup>73-76</sup>, while the N-oxides



appear to have predominantly  $\pi$  delocalisation<sup>78</sup>. However, the metal-ligand bonding in the case of amines is necessarily  $\sigma$ , yet  $\pi$  delocalisation is observed in benzylamine<sup>14</sup>. In alkylamines delocalisation is  $\sigma$ -type<sup>79</sup>, as expected. The kinetics of the phosphine ligand exchange have been investigated<sup>80,81</sup>. Structural information has been derived from the pseudocontact shifts in the cobalt complexes by comparison with the analogous nickel complexes to eliminate the contact contribution<sup>76,78</sup>. Solvation studies have included other transition metals, Cr(III), Fe(III), Mn(II), Cu(II), Fe(II)<sup>82,83</sup>.

The acetylacetonates of nickel(II) and cobalt(II), [bis(2,4-pentanedionato)nickel(II) and cobalt(II)], exist as octahedrally co-ordinated polymeric species in non-co-ordinating solvents<sup>84</sup>, but, when basic ligands are introduced, an equilibrium mixture is formed in which the added ligand co-ordinates to the metal, reducing the degree of polymerisation<sup>85,86</sup>. In the presence of excess ligand, usually two ligand molecules are accepted by each metal atom in a trans configuration, the two acetylacetonate groups forming an equatorial plane. The exchange rate of the ligands is found to be rapid.

The shifts of ligands such as pyridines<sup>87,89</sup>, bipyridines<sup>90,91</sup>, amines<sup>92-98,88</sup>, pyridine-N-oxides<sup>99-102</sup>, phosphines<sup>103,88,89</sup>, isonitriles<sup>103</sup> and cyanides<sup>101</sup> have been used to determine electron spin densities, and configuration and geometry. Electron spin densities in the pyridines, amines and pyridine-N-oxides indicate the same



pattern type of delocalisation as found above, while  $^{13}\text{C}$  studies<sup>88,89</sup> have confirmed the presence of  $\sigma$  delocalisation in pyridine, aniline and triphenylphosphine ligands. The last named also have  $\pi$  delocalisation.  $\pi$  delocalisation was also found in isonitriles. Again the pseudocontact shifts in the cobalt complexes have been utilised for structure determination<sup>95,99,100,102</sup>.

Complexes of this type have been used as "shift reagents" to simplify the spectra of the ligands by selective shift changes which result in an expanded range of resonance positions. Compounds which have been examined in this way include amines<sup>92,97,98</sup>, alcohols<sup>97,98,104</sup> and furans<sup>105</sup>.

The acetylacetonate proton resonance shifts have been found to be independent of the nature of the ligand with the nickel complexes, but sensitive to the ligand in the cobalt complexes<sup>106</sup>. The acetylacetonate proton shifts in tris-acetylacetonato-vanadium(III) have suggested  $\pi$  delocalisation of spin density in the chelate<sup>107</sup>; in unsymmetrical tris- $\beta$ -diketonates of the same metal, assignments of cis and trans configurations were possible<sup>108</sup>.

A type of system which strictly does not involve ligand exchange but which is sufficiently related to be included here is that involving ion-pairs where either the cation or the anion is paramagnetic. If it is accepted that unpaired spin density cannot be transferred from one ion to the other in an ion-pair, the shifts observed in the diamagnetic component of the ion-pair can only be due to pseudocontact effects arising from magnetic anisotropy in the paramagnetic



ion. Examples of ion pair systems which have been studied are  $[(\text{CH}_3)_4\text{N}]_3[\text{Fe}(\text{CN})_6]^{109}$ ,  $[\text{Bu}_4\text{N}][(\text{C}_6\text{H}_5)_3\text{PMI}_3]^{110}$ ,  $[\text{Bu}_4\text{N}][\text{M}(\text{AA})_3]^{111}$  and  $[(\text{C}_6\text{H}_5)_4\text{As}][(\text{C}_6\text{H}_5)_3\text{PMI}_3]^{112}$ , where M is Co(II) or Ni(II).

(d) Lanthanide "shift reagents".

In the last section, mention was made of the use of acetylacetonates, particularly the cobalt complex, in signal assignment and structure determination by selective shifting of the resonance lines from their diamagnetic positions.

Milner and Pratt<sup>113</sup> noted some time ago that the large shifts observed on complexing amines and amino acids with Co(II) and Ni(II) ions could sometimes yield structural information. Progress in this field was impeded however by poor shift to linewidth ratios. When sufficient paramagnetic reagent had been introduced to give the required separation of resonance signals, the lines proved too broad to be useful. Certain rare-earth ions were known to cause very little line-broadening while giving large paramagnetic shifts but the problem remained of finding a suitable system for organic chemists.

In 1969, Hinckley<sup>114</sup> found that the dipyrindine adduct of trisdipivalomethanato-europium(III), [europium(III) 2,2,6,6-tetramethylheptane-3,5-dione], gave sizeable shifts and very little broadening when added to cholesterol monohydrate. He found that the methyl signals of (+)-camphor were also assignable<sup>115</sup> using this shift reagent. By analysing graphically the shifts produced in two bifunctional steroids<sup>116</sup>,



he separated the small contact shifts from the pseudo-contact shifts and found the relative proportion of complexing at the two functional groups in each molecule. However, Sanders and Williams<sup>117</sup> showed that trisdipivalomethanatoeuropium(III),  $\text{Eu}(\text{DPM})_3$ , itself, is more efficient in effecting large shifts. Shifts were observed with alcohols, ketones, ethers, esters and amines. He found that the proton resonances of alcohols and amines were strongly shifted, ketones rather less so, and ethers and esters less strongly still.

Since its discovery, the complex has been widely used with many ligands, including alcohols<sup>118-126</sup>, amines<sup>121,126-133</sup>, ketones<sup>120,121,133-135</sup>, aldehydes<sup>121</sup>, esters<sup>121,136-138</sup>, ethers<sup>121</sup>, epoxides<sup>139,140</sup>, oximes<sup>141,142</sup>, amides<sup>143-146</sup>, sulphoxides<sup>147,148</sup>, carbohydrates<sup>146,149-151</sup>, steroids<sup>118,152-154</sup>, terpenes<sup>118,155,156</sup>, polymers<sup>157,158</sup> and organo-metallic compounds<sup>159,160</sup>.

Hart and coworkers<sup>161</sup> discovered that the praseodymium complex,  $\text{Pr}(\text{DPM})_3$ , gave upfield shifts whereas the europium complex gave downfield shifts, and the former shifts were considerably greater in magnitude, thus greatly increasing the utility of the method. The praseodymium reagent has been utilised<sup>151,158,162-169</sup> less extensively than its europium analogue.

The complexes of Sm, Tb, Ho and Yb have been evaluated by Crump, Sanders and Williams<sup>170</sup> who found none of them as good as the Eu or Pr complexes. A greater number of the lanthanide complexes has been investigated by Bhacca and



coworkers<sup>171</sup>, and Horrocks and Sipe<sup>172</sup>. Upfield resonance shifts for the substrate ligand are obtained with the complexes of Pr, Nd, Sm, Tb, Dy and Ho, while downfield shifts are observed for Eu, Er, Tm and Yb. Gd produces negligible shifts and considerable broadening. The Yb complex has been utilised as a shift reagent<sup>173</sup>. Bhacca<sup>171</sup> proposed that the temperature dependence observed with the Eu-shifted spectrum of 2-heptanone could be used as a technique for increasing the utility of these shift reagents.

Complete assignments of the  $^1\text{H}$ <sup>161</sup> and  $^{13}\text{C}$ <sup>174</sup> spectra of borneol have been made using the praseodymium reagent. It is noteworthy that the proportionality constant  $K_{\text{C}}$  for the best fit of the carbon-13 data is  $1.16K_{\text{H}}$  where  $K_{\text{H}}$  is the corresponding constant for the proton data. This is fairly close to the equality of the proportionality constants expected if the shifts were purely pseudocontact in nature.

Three optically active shift reagents of europium have been used to determine enantiomeric purity, a particularly interesting application. Whitesides and Lewis<sup>175</sup> have used tris[3-(tert-butylhydroxymethylene)-(+)-camphorato]Eu(III), while others have used tris[3-(trifluoromethylhydroxymethylene)-(+)-camphorato]Eu(III)<sup>176</sup> and the Eu complex of 3-heptafluorobutanoyl-(+)-camphor<sup>177</sup>.

The partially fluorinated complex, tris(1,1,1,2,2,3,3-heptafluoro-7,7-dimethyl-4,6-octanedionato)Eu(III), Eu(fod)<sub>3</sub>, has proved<sup>178</sup> a superior shift reagent to Eu(DPM)<sub>3</sub>. The fluorocarbon moieties increase the solubility of the complex, and the electron withdrawing influence of the fluorines



increases the ability of the metal to co-ordinate with weak donor ligands.  $\text{Eu}(\text{fod})_3$  has been used with amides<sup>179</sup> and dioxans<sup>180</sup> and both  $\text{Eu}(\text{fod})_3$  and  $\text{Pr}(\text{fod})_3$  have been used with poly(methylmethacrylate) polymer<sup>181</sup>.

The shifts generated by these lanthanide complexes have been generally taken to be dipolar in origin, although small contact contributions may be present<sup>125,182</sup>. Pseudo-contact shifts in axially symmetric complexes depend on the geometric factor  $(3\cos^2\chi-1)r^{-3}$  [see Section C]. The principal axis is not readily defined in these complexes<sup>183</sup> but is usually taken to be that involving the metal-ligand bond. Many authors have neglected the angle dependence<sup>114, 115, 118, 121, 127, 137, 147, 167</sup> and have found good correlation of shifts with  $r^{-3}$ . Where there is little variation in the angle for the different protons in the ligand, this approximation can be justified, but examples have been found where the angular dependence is not only significant but can change the direction of the shifts<sup>122, 168</sup>. Some authors have found better correlation using  $r^{-2}$  dependence<sup>118, 141, 184</sup>, but their measurement of  $r$  as proton-oxygen rather than proton-metal distance seems to have little justification. The distance dependence has been discussed by Goodisman and Matthews<sup>185</sup>. Much of the work on lanthanide shift reagents can be criticised for other reasons. The hygroscopic nature of the reagents causes experimental difficulties which are not always appreciated and the usual assumption that a single axially symmetric 1:1 complex is formed has been insufficiently examined<sup>186</sup>. Fortunately, however,



the utility of these reagents as a practical tool in organic chemistry usually does not depend on a rigorous understanding of the physical chemistry and theory of the systems.

Recently, studies of the stoichiometry have been carried out in some of the systems and equilibrium constants have been derived for a number of shift reagents and ligands<sup>187-191</sup>. It has also been pointed out that constancy of the relative shifts of various nuclei in the ligand as the nature of the lanthanide metal atom is varied can be used as a test as to whether the shifts are entirely due to pseudocontact terms arising in an axially symmetric situation<sup>192</sup>. This depends on the fact that contact terms, axial pseudocontact terms and the two contributions to the non-axial pseudocontact terms all change by different factors when the metal atom is varied.

#### (e) Free radicals

Although free radicals in the solid state had been studied by N.M.R. since 1958, it was not until 1966 that solution studies proved possible. The conditions for narrow lines,  $1/\tau_s \gg A$  and/or  $1/T_e \gg A$ , [see Section B] are not generally true for free radicals in solution and the mechanisms for line narrowing found with metal complexes are not applicable, with the result that spectra usually are very broad. However, if the radicals are in high concentration, spin exchange causes a decrease in  $T_e$  rendering the condition  $1/T_e \gg A$  true. Low viscosities and high temperatures also favour this situation, and, naturally, the condition is more readily attained for low values of the



the electron-nuclear coupling constant,  $A$ <sup>193</sup>.

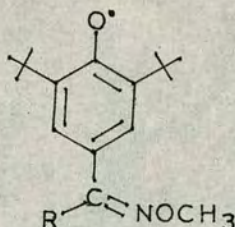
The E.S.R. spectra of free radicals have been observed and interpreted for a long time, but the N.M.R. spectra have several advantages. E.S.R. can give the magnitude of  $A$ , but the contact shifts observed in N.M.R. spectra can give not only the magnitude but also the sign of  $A$ , a great advantage when studying electron spin delocalisation. Coupling constants are evaluated directly from the paramagnetic shifts which are almost entirely Fermi contact in origin, free radicals having very nearly isotropic  $g$  factors. This means that the N.M.R. spectra are more readily interpreted than are the E.S.R. spectra. N.M.R. can also be used for much smaller coupling constants.

As mentioned above, in concentrated solutions of free radicals, the condition  $1/T_e \gg A$  is realised and lines are relatively narrow. Kreilick<sup>194,195</sup> has studied various nitroxide radicals in concentrated solutions and found their coupling constants in good agreement with their E.S.R. spectra. He found that the coupling constants depended on geometry and the substituents present, but were independent of solvent<sup>195</sup>.

A concentrated solution of free radicals is also achieved by using a dilute solution of the radical in a solvent which is also a free radical. Spin exchange between the solvent and solute molecules rapidly averages the electron spin levels of the solute molecules, and the N.M.R. spectrum of the solute can be observed. Thus Kreilick<sup>196-199</sup> has examined various phenoxy radicals in di-*t*-butylnitroxide



solvent. With the phenoxy radicals



where R is a cyclic<sup>196,197</sup> or straight chain<sup>198</sup> aliphatic group, he observed spectra from two different geometric isomers in most cases. The coupling constants for the various groups of protons in the radicals were found to depend on the relative geometries of the molecules. Long range couplings through the aliphatic rings or chains were observed in most cases of the former and in each case of the latter.

Kreilick also investigated the linewidths of a further series of phenoxy radicals<sup>199</sup>. Since the Fermi contact contribution to the linewidth is proportional to  $A^2$  and it becomes dominant at larger A values, the measured linewidth should be proportional to  $A^2$ , which he found to be true at larger A values. Again he found the A values in good agreement with the E.S.R. values.

A very recent discovery in the N.M.R. of free radicals arises from the ability of the radicals to hydrogen bond with protic substances<sup>200,201</sup>. The contact shifts induced serve as a sensitive probe for elucidation of the character of the hydrogen bond and the mode of electron spin distribution on the proton donor molecule. Dimethyl and di-*t*-butyl nitroxides have been hydrogen bonded, for example,



with methanol, acetylene, chloroform and phenol. Shifts and broadening of signals as a result of hydrogen bonding was observed independently in our own work.

#### (f) Relaxation studies

Relaxation studies in paramagnetic systems have not been so numerous as isotropic shift studies, but linewidths and relaxation times have provided useful information in certain situations.

Linewidths can be used to elucidate the kinetics of chemical exchange processes. Using the Swift and Connick expressions<sup>36</sup> it is possible to evaluate the lifetime of a ligand molecule in the coordination sphere of a paramagnetic ion<sup>81</sup>. Solvation studies have yielded rates of exchange of solvent molecules between the first coordination sphere and the bulk solvent<sup>202-204,33</sup>, coordination numbers<sup>204-207</sup>, and preferential solvation in binary solvent mixtures<sup>208</sup>. Paramagnetic ions involved in these studies have included Mn(II)<sup>202</sup>, Cu(II)<sup>202,205</sup>, Co(II)<sup>202,205-208</sup>, Ni(II)<sup>202,208</sup>, Fe(III)<sup>202</sup> and Np(V)<sup>203</sup>. The relative effectiveness of various paramagnetic ions in broadening the <sup>17</sup>O N.M.R. of water has been investigated<sup>209</sup>. Various ions have also been used in a study of the relationship between proton relaxation times produced by the ions and the magnetic moment of the ion<sup>210</sup>.

Similarly electron and hydrogen transfer studies have been accomplished. For example, Dietrich and Wahl<sup>52</sup> have investigated the rates of electron transfer between osmium(II) and osmium(III) dipyridines, between ferrocene and the ferricenium cation and between the iron(II) and iron(III)



complexes of 1,10-phenanthroline. Hydrogen atom transfer has been studied, for example, by Kreilick and Weissman<sup>211</sup>, between a series of hydroxylic compounds and their corresponding oxy free radicals.

The kinetics of the planar-tetrahedral interconversion in four-coordinated complexes [see Section b] has also been examined.

It is also possible to obtain structural information from linewidth studies. Binding sites of paramagnetic ions in molecules of biological interest have been investigated. Shulman and coworkers<sup>31,212</sup> have used Mn(II), Co(II), Ni(II) and Cu(II) in their<sup>31</sup>P study of metal-ion binding to nucleic acids. They have also studied<sup>46,47</sup> the change in the spin-lattice relaxation time,  $T_1$ , of the water protons in aqueous solutions of nucleic acids and metal ions. When the metal ion is bound to a large molecule such as DNA the rotation of its hydration sphere becomes slower, so that its effectiveness in reducing  $T_1$  is enhanced. Estimations of the number of available binding sites as well as information on the type of site to which the various ions are bound, are thus obtained.



PART IIIFERROCENES

Ideally a paramagnetic probe which is to be used to explore the nature and positions of protons in a complicated molecule, through selective shifts or selective broadening of their resonance signals, should be bound to the molecule in a well-defined way so that the nature and geometry of the system is unambiguous. In this respect covalent attachment of the probe would seem to be superior to a metal-ligand complex formation since the stoichiometry and nature of complexes in solution is often uncertain.

A covalently attached probe based on the ferrocene nucleus appeared to offer particular advantages, not only because it seemed possible to introduce this nucleus in a variety of ways but also because the extent of oxidation to a ferricenium system, and hence the magnitude of the shifts and the broadening, can be controlled.

As reported in Part II, Section G(a), the N.M.R. spectra of a number of ferrocene-ferricenium systems have already been investigated but the potential of this system as a paramagnetic probe has not been explored. It was therefore decided to investigate the preparation of ferrocene derivatives of common functional groups and to study the N.M.R. spectra of such systems at various stages of oxidation.

Two types of derivatives were investigated. Esters of ferrocenoic acid were explored as derivatives formed from compounds containing a hydroxyl functional group and it was hoped that imine formation with ferrocenaldehyde



would provide a convenient derivative for primary amines. A number of other ferrocene derivatives were also investigated as model compounds.

## (A) EXPERIMENTAL

### (a) General

Except where otherwise stated the following instruments and procedures were used for all the systems studied.

#### (i) N.M.R. spectrometer

Two N.M.R. spectrometers were used in this work, a Perkin-Elmer R10 operating at 60 MHz at a probe temperature of 33.5°, and a Varian HA 100 operating at 100 MHz at a probe temperature of 28°. As accurate temperatures were not required for this work, these were checked only occasionally.

Use of the 60 MHz instrument was restricted almost entirely to preliminary work, and conditions of operation, such as scale factor and sweep rate were chosen as appropriate. Chemical shifts were obtained directly from the precalibrated chart paper.

Spectra on the 100 MHz instrument were in general recorded at sweep width 100 Hz, occasionally at 250 Hz. Linewidths were measured at half the peak height, normally an average of four sweeps, two in each direction, being taken. The position of the peak was determined by scanning the top region of the peak very slowly in both directions. The pen was then set on the position of maximum pen deflection and the chemical shift measured using the frequency counter, reading to 0.1 Hz.



Except for the saturation studies, the RF (radio-frequency) powers used were the maximum consistent with negligible saturation. This was explored by varying the RF powers over an appropriate range.

The Varian HA100 spectrometer requires a lock signal. In general tetramethylsilane (TMS) was used as an internal lock. Alternative lock signals and the special method of locking used in some of the saturation studies are discussed in the appropriate sections.

(ii) Solutions for N.M.R. spectra

Standard solutions were prepared in previously graduated 500 $\mu$ l volumetric flasks. These flasks, which were made by glass-blowing broken N.M.R. tubes, were graduated by filling with the correct mass of distilled water to give exactly 500 $\mu$ l volume, the mass being calculated from its density at a given temperature. The level was then marked.

All weighings were made using a Stanton one-pan four-decimal-place balance.

Volumes of additives were measured using Hamilton 10 $\mu$ l, 50 $\mu$ l, 100 $\mu$ l and 500 $\mu$ l syringes, as appropriate.

The preparation of the solutions varied for each system studied and is given in the appropriate sections. 0.5mm N.M.R. tubes were used.

(iii) Infra-red spectra and thin-layer chromatographs

Where required infra-red (I.R.) spectra were run of prepared compounds. The solids were run in spectroscopic grade carbon tetrachloride or chloroform solutions or as a Nujol mull, usually in that order of preference, according



to solubility. The spectra were obtained using a Unicam SP.200 I.R. Spectrophotometer.

Thin-layer chromatography (T.L.C.) was used to check the purity of some of the products. For coloured products, microscope slides covered with a thin layer of silica gel (Fisons) were used. For steroids, larger plates (20cm x 5cm) covered with Merck Kieselgel GF<sub>254</sub> were used. The spots were located under ultra-violet light and could be developed by spraying with a solution of concentrated sulphuric acid (5%) in ethanol, followed by drying on a hot plate.

#### (b) Preparation of compounds

##### (i) Ferrocene

Ferrocene (BDH) was purified by sublimation under reduced pressure at 100°. This was found to be more satisfactory than crystallisation from chloroform or light petroleum (b.p. 80-100°). After sublimation an appreciable (up to 5%) red-brown residue was left.

##### (ii) Acetyl ferrocene

This was prepared by acetylation of ferrocene with acetic anhydride, using phosphoric acid catalyst, the method of Herz<sup>213</sup>. The crude product was crystallised from n-hexane giving orange crystals, m.p. 84-85° (lit. 84-86°<sup>214</sup>), in 80% yield. The I.R. spectrum (Nujol mull) showed a carbonyl absorption at 1650cm<sup>-1</sup>. T.L.C., using 30:1 benzene: ethanol solvent, showed almost entire conversion to the monoacetyl compound.



(iii) Ferrocenoic acid

The acid was prepared from acetyl ferrocene using iodine in pyridine solution, the method of Weinmayr<sup>215</sup>. It was purified by Rinehart's method<sup>216</sup>, giving fluffy orange crystals in 32.6% yield, which decomposed at temperatures above 200° (lit. decomposition at 208.5°<sup>216</sup>). The I.R. spectrum ( $\text{CHCl}_3$  solution) showed the characteristic broad peak at 3100-2500 $\text{cm}^{-1}$  and a carbonyl absorption at 1670 $\text{cm}^{-1}$  with a small side-peak at 1700 $\text{cm}^{-1}$ . Other fairly strong peaks occurred at 1485, 1300, 1170 and 1110 $\text{cm}^{-1}$ .

(iv) Methyl ferrocenoate

The methyl ester was prepared by direct esterification of ferrocenoic acid with methanol and mineral acid catalyst<sup>217</sup>. The crude product did not crystallise satisfactorily and the best purification procedure comprised elution through a silica column using benzene (which brought through an orange band, leaving a deep red band at the top of the column) followed by crystallisation from light petroleum (b.p. 40-60°). After drying over phosphorus pentoxide in a desiccator, the orange crystals had a melting-point of 67-69° (lit. 70-71°).

(v) Ethyl ferrocenoate

The method of Weinmayr<sup>218</sup> was used to prepare the ethyl ester, by direct esterification. Crystallisation was not successful from ether, but was effected from 2:1 ethanol:water giving orange, fibrous crystals, m.p. 62-63° (lit. 63-64°<sup>219</sup>) in 75% yield. The I.R. spectrum (Nujol mull) showed a carbonyl absorption at 1710 $\text{cm}^{-1}$  and two



strong peaks at 1280 and  $1135\text{cm}^{-1}$ , the C-O stretching absorptions.

(vi) Ferrocenoyl chloride

Difficulties were encountered in the preparation of this compound, possibly due to polymerisation. Variations on three basic methods were investigated.

(1) The method of Kupchick and Kiesel<sup>220</sup> using phosphorous trichloride in benzene was used but yields were not very good, at best 60%, and the product contained unreacted acid, seen in both the T.L.C. and the I.R. spectrum. T.L.C. using 1:1 benzene:ether solvent gave two spots. The I.R. spectrum (Nujol mull) showed a strong carbonyl absorption at  $1755\text{cm}^{-1}$ , but also a smaller, broader peak at about  $1660\text{cm}^{-1}$  due to the acid. Elution of the mixture through a silica column using 1:1 benzene:ether converted all the acid chloride back to acid.

(2) Although no literature reference could be found in which thionyl chloride had been used, several preparations using the reagent in benzene solution were carried out, varying temperature, concentrations and reaction times. The best yield, 83%, was obtained under the following conditions.

Ferrocenoic acid (0.09g; 0.5 mmole) was dissolved in sodium-dried benzene (20ml) containing 1 drop pyridine and thionyl chloride (0.05ml). The solution was left standing at room temperature, with occasional swirling, for 4-5 hours, during which time the colour deepened. The benzene was evaporated and the deep red mass crystallised from n-hexane giving ferrocenoyl chloride (0.08g), m.p.  $47-48^{\circ}$  (lit.  $47-49^{\circ}$ <sup>220</sup>). The I.R. spectrum ( $\text{CHCl}_3$  solution) showed a strong carbonyl



absorption at  $1740\text{cm}^{-1}$  but smaller peaks also occurred at  $1710\text{cm}^{-1}$  and  $1670\text{cm}^{-1}$ , which were probably due to unreacted acid. Peaks at  $1450$  and  $1380\text{cm}^{-1}$  occurred in this spectrum but not in that of the pure acid, and were attributed to the acid chloride.

(3) Following the basic principles of Lee and Downie<sup>221,222</sup>, triphenyl phosphine and carbon tetrachloride were used as follows. Carbon tetrachloride was dried over calcium chloride, followed by distillation collecting the fraction distilling at  $74-76^{\circ}$ . Triphenyl phosphine was dried by dissolving in sodium-dried benzene which was then evaporated under reduced pressure. Triphenyl phosphine (1.1g; 4.2 mmole) was dissolved in carbon tetrachloride (10ml). Ferrocenoic acid (1.0g; 4.3 mmole) was added slowly with shaking and the mixture was boiled under reflux for 4 hours, T.L.C's, using 1:1 benzene:ether solvent, being run on samples from the reaction mixture at half-hour intervals. These showed an increase in acid chloride with time, very little acid remaining unreacted after 4 hours. The mixture was then evaporated to dryness under reduced pressure and the solid dissolved as far as possible in hot n-hexane. The deep red hot solution was decanted off a dark sludge and ferrocenoyl chloride (0.39g; 36%) crystallised from this solution. The I.R. spectrum ( $\text{CHCl}_3$  solution) showed carbonyl peaks of similar intensity at  $1750$ ,  $1710$  and  $1675\text{cm}^{-1}$  indicating that the product contained a considerable proportion of acid.

The thionyl chloride method was apparently the most satisfactory in yield and purity of product, but when it



was executed on ten times the scale, yields were greatly reduced, to 20-30%.

(vii) Menthyl ferrocenoate

Again difficulty in preparation was encountered and two methods were investigated.

(1) Menthol (0.33g; 2.1 mmole) was dissolved in pyridine (1ml, dried with barium oxide, redistilled and stored over potassium hydroxide pellets). Finely powdered ferrocenoyl chloride (0.26g; 1.05 mmole) was added slowly with constant shaking. It dissolved readily. After about 22 hours, water (1-2 drops) was added to decompose any unreacted acid chloride. The mixture was left for 30 minutes; then more water and chloroform were added. The chloroform layer was separated and washed several times with dilute sulphuric acid, sodium bicarbonate solution and finally water. The chloroform was evaporated under reduced pressure leaving a dark red oil which solidified. This was crystallised from benzene-light petroleum (b.p. 60-80°) giving menthyl ferrocenoate (0.09g; 28%). Ferrocenoic acid (0.09g; 38%) was retrieved by acidification of the sodium bicarbonate washings, showing that the esterification was incomplete.

(2) The method of Parish and Stock<sup>223</sup> was used. This is direct esterification under mild conditions using trifluoroacetic anhydride. Menthol (0.30g; 1.9 mmole) and ferrocenoic acid (.47g; 2.0 mmole), both dried in a desiccator over phosphorus pentoxide, were finely ground and mixed. Trifluoroacetic anhydride (1.5g; 7.2 mmole), prepared by distilling trifluoroacetic acid over phosphorus pentoxide and



taking the fraction boiling below  $41^{\circ}$ , was added and a rapid reaction took place, a deep blood-red solution forming. This was stirred for 20 minutes during which time the colour darkened to a deep red-brown. Benzene (approximately 10ml) was then added and the solution washed several times with 10% sodium hydroxide solution and then with water. After drying over magnesium sulphate, the solution was evaporated under reduced pressure, leaving a deep red oil.

The I.R. spectrum of the product ( $\text{CCl}_4$  solution) showed two carbonyl peaks ( $1770$  and  $1705\text{cm}^{-1}$ ) suggesting impurity. Peaks at  $1285$  and  $1160\text{cm}^{-1}$  suggested an ester was present.

The N.M.R. spectrum ( $\text{CCl}_4$  solution) showed the distinctive monosubstituted ferrocene pattern (that is, an up-field singlet for the unsubstituted ring protons and two lower field triplets for the substituted ring 2,5- and 3,4-protons, all in the region  $\tau 5-6$ ). The methinyl region was very similar to that of methinyl benzoate.

T.L.C. of the product using benzene solvent gave two distinct spots, an orange spot travelling faster than a red spot. The product was therefore eluted through a silica column, benzene bringing off an orange fraction and benzene-ether (10:1) a red fraction. Both were again oils. T.L.C. of the fractions as above showed the orange fraction to be free of the red product and only trace orange product to be present in the red fraction. The former fraction was the larger.



Orange fraction:

The I.R. spectrum ( $\text{CCl}_4$  solution) showed only one carbonyl peak, at  $1705\text{cm}^{-1}$ , and two strong bands at 1280 and  $1145\text{cm}^{-1}$  for the C-O stretching absorptions. The spectrum suggested reasonably pure ester.

The N.M.R. spectrum ( $\text{CCl}_4$  solution) showed the mono-substituted ferrocene pattern -

unsubstituted ring proton singlet:  $\tau 5.92$

substituted ring proton triplets:  $\tau 5.76, 5.32$

and a menthyl region very similar to that of menthyl benzoate. Integration gave the ratio of ferrocene:menthyl protons as 9:18 (theoretical 9:19).

It was hoped that the oil might crystallise, and no analysis was carried out. It seems, however, that the orange fraction was fairly pure, menthyl ferrocenoate.

Red fraction:

The I.R. spectrum ( $\text{CCl}_4$  solution) of this fraction was not dissimilar to that of the orange fraction, with peaks appearing at 1700, 1280 and  $1145\text{cm}^{-1}$ . The original peak at  $1770\text{cm}^{-1}$  appeared in neither spectrum.

The N.M.R. spectrum showed the usual ferrocene unsubstituted ring proton peak ( $\tau 5.86$ ), but four poorly resolved peaks replaced the normal two triplets for the substituted ring protons. The menthyl pattern was similar to that in the orange fraction except for an additional very strong singlet at  $\tau 8.71$  and a fairly small broad hump around  $\tau 6.5$ . Integration showed that the former corresponded to approximately half the protons in the methylene/methyl region and



so must be due to an impurity not present in the crude product. The latter peak could be due to the proton  $\alpha$  to the hydroxyl group in menthol, but observation of a hydroxyl signal to confirm the presence of menthol was not possible, perhaps due to the large signal at  $\tau$ 8.71 obscuring it.

This fraction thus contained several compounds, including two ferrocene derivatives and menthol either as the free alcohol or as an ester, or both.

The major component in the product prior to chromatography appeared to be menthyl ferrocenoate. A possible explanation for the carbonyl peak at  $1770\text{cm}^{-1}$  in the I.R. spectrum of the crude product is that it is due to menthyl trifluoroacetate, which would be expected to have a carbonyl peak in that region. A fluorine containing compound would also be expected to show a strong absorption in the  $1000\text{--}1200\text{cm}^{-1}$  region. The very intense, broad peak found at  $1140\text{--}1180\text{cm}^{-1}$  agrees with this. In the N.M.R. spectrum, the presence of this compound would appear only as an increase in the menthyl proton region.

(viii) Dihydrotestosterone ferrocenoate

The trifluoroacetic anhydride method used for the menthyl ester was again employed here, using ferrocenoic acid (0.43g; 1.9 mmole), dihydrotestosterone (0.5g; 1.7 mmole) and trifluoroacetic anhydride (2g; 9.5 mmole). The product, a thick orange oil, was eluted through a silica column, changing the solvent from benzene-light petroleum through benzene to benzene-ether, on the basis of the T.L.C. of the crude product. Three fractions were collected, the first



of which seemed most likely to be the ester.

The I.R. spectrum ( $\text{CCl}_4$  solution) of the first fraction showed two carbonyl peaks, at  $1710$  and  $1770\text{cm}^{-1}$ . The carbonyl peak in dihydrotestosterone is at  $1700\text{cm}^{-1}$  and, on the basis of the previous ferrocene esters studied, one would expect the ester carbonyl peak to occur in the region  $1700$ - $1710\text{cm}^{-1}$ . It would thus appear that the peak at  $1700\text{cm}^{-1}$  found here is due to one or both of these carbonyl groups, while the peak at  $1770\text{cm}^{-1}$  is due to the trifluoroacetic ester (see menthyl ferrocenoate section). Four peaks appeared in the region  $1100$ - $1300\text{cm}^{-1}$ , namely  $1135$ ,  $1160$ ,  $1225$  and  $1270\text{cm}^{-1}$ , of which the first and last were thought to be C-O stretching absorptions of the ferrocene ester. There was no indication of a hydroxyl peak in the  $3400$ - $3650\text{cm}^{-1}$  region.

The N.M.R. spectrum ( $\text{CCl}_4$  solution) of the first fraction showed the usual monosubstituted ferrocene pattern -

unsubstituted ring proton singlet:  $\tau 5.83$

substituted ring proton triplets:  $\tau 5.69$ ,  $5.26$ .

The steroid methylene hump was not diagnostically useful, only the C-18 and C-19 methyl groups being assignable with certainty, but the  $17\text{-}\alpha$  proton signal which appeared at  $\tau 6.35$  in the alcohol was no longer visible. Integration showed the ratio of ferrocene:dihydrotestosterone protons as  $9:33$  (theoretical  $9:28$ ), suggesting most of the steroid was present as the ferrocenoate rather than the trifluoroacetate.

The fraction was crystallised from n-hexane giving



orange crystals, m.p. 195-196°, in 13.8% yield.

Analysis:

found: C, 63.65; H, 6.21

requires: C, 71.71; H, 7.62.

The poor analysis figures and the extra carbonyl peak in the I.R. spectrum both cast doubts on the nature of the product obtained.

(ix) Cholesteryl ferrocenoate

The trifluoroacetic anhydride method was again used, with the addition of benzene to make a homogeneous solution. However, little or no reaction took place and most of the acid and alcohol were returned unchanged.

(x) Ferrocenaldehyde

The method of Rosenblum<sup>224</sup> was used, but, on account of the reaction mixture exploding on heating, the following modification was introduced. Stirring the mixture at room temperature for 72 hours in a nitrogen atmosphere replaced the heating at 65-70° for 2 hours in a nitrogen atmosphere. A deep red-purple solid was obtained. Part of this was crystallised from 2:1 ethanol:water giving orange-brown crystals with a metallic lustre, and part was crystallised from light petroleum (b.p. 40-60°) an easier procedure, giving red-purple plate-like crystals. Melting-points of both sets of crystals was 119-121° (lit. 120-121°<sup>225</sup>) so that these are the two crystalline forms of ferrocenaldehyde<sup>226</sup>, the latter being the lower temperature form. Interconversion of the two forms by recrystallisation from the



appropriate solvent was not satisfactory.

The N.M.R. spectrum ( $\text{CCl}_4$  solution) of the crystals from light petroleum showed the usual ferrocene pattern - unsubstituted ring proton singlet:  $\tau 5.80$   
substituted ring proton triplets:  $\tau 5.50, 5.29$   
and an aldehydic proton peak at  $\tau 0.13$ .

(xi) Attempted preparation of the aniline imine of ferrocen-aldehyde

Two variations of the basic method for formation of imines were tried. Both used ferrocen-aldehyde (1.0g; 4.7 mmole) and aniline (0.435g; 4.7 mmole). In the first case the two reactants were mixed and left overnight. In the second, they were dissolved in a small volume of benzene and glacial acetic acid (0.2ml) added, the mixture then being left for an hour. After purifying in the standard manner, both gave a deep red, plastic solid whose N.M.R. spectra showed that almost all the ferrocene was present as the aldehyde, and so the yield of imine was negligible.

It appears<sup>227</sup> that ferrocene imines are in fact very unstable and so not easily prepared.

(xii) p-Tolyl ferrocene

The method of Rosenblum<sup>228</sup> was used here, with diazotised p-toluidine and ferrocene. The crude product was chromatographed through neutral alumina, eluting with light petroleum (b.p.  $40-60^\circ$ ) changing through benzene to benzene-ether. Four fractions were collected, the N.M.R. spectra ( $\text{CCl}_4$  solution) of the first two showing at least two ferrocene derivatives to be present in each, and the two



fractions to be very similar. T.L.C. of these two fractions using light petroleum (b.p. 40-60°) showed up three spots, a brown spot moving very little, an orange spot moving more and a yellow spot moving fastest.

Chromatography of these two fractions on a silica column, eluting with light petroleum through benzene to ether, was then executed. (The third and fourth fractions from the alumina column contained trace amounts of a much darker material and were not further investigated.) The product separated readily into four fractions, of which the first two again were investigated. However, the N.M.R. spectrum (CCl<sub>4</sub> solution) of each of these again showed a mixture to be present, both fractions including ferrocene itself. The ferrocene was removed from the two fractions by sublimation under reduced pressure at 100° and the residue chromatographed again on alumina, light petroleum (b.p. 40-60°) eluting the largest fraction, a yellow-orange band which gave an orange crystalline solid whose N.M.R. spectrum indicated that it was reasonably pure p-tolyl ferrocene.

unsubstituted ring proton singlet:  $\tau$ 6.06

substituted ring proton triplets:  $\tau$ 5.82, 5.59

phenyl proton doublets:  $\tau$ 3.08, 2.94, 2.78, 2.65

methyl proton singlet:  $\tau$ 7.69.

The second band, also eluted with light petroleum (b.p. 40-60°) gave an orange solid whose N.M.R. spectrum suggested it to be 1,1'-di-p-tolyl ferrocene. It was not further investigated.

The p-tolyl ferrocene crystallised from light petroleum



(b.p.  $40-60^{\circ}$ ) as orange crystals, m.p.  $138^{\circ}$  (lit.  $139-140^{\circ}$ <sup>229</sup>), yield 7%. The best purification method, which should yield over 60% would appear to be removal of ferrocene by sublimation, followed by chromatography on alumina eluting with light petroleum, then crystallisation from light petroleum.

(xiii) 1-ferrocenyl-but-1-en-3-one

A sample of 1-ferrocenyl-but-1-en-3-one was kindly provided by P.L. Pauson.

(xiv) General conclusions

The simpler ferrocene derivatives, such as acetyl ferrocene, ferrocenoic acid and the methyl and ethyl esters, were fairly readily prepared, on the whole in reasonable yield. However considerable difficulty was encountered in the preparation of the more complex esters, with yields tending to be very low, and the imine was not obtained at all. Thus these two methods of inserting a ferrocene probe into a complex molecule are unlikely to be useful in practice unless the methods of preparation of these compounds can be improved. If the N.M.R. work on the oxidised solutions (see below) had proved more promising it would have been profitable to have investigated the preparative aspect further.

(c) Preparation of solutions

(i) Choice of oxidising agent and solvent

The limiting factor in the choice of oxidising agent and solvent arose from the fact that the ferrocene derivative, its ferricenium salt and the oxidising agent all had to be soluble in the chosen solvent.



The ferricenium salts were not soluble in deutero-chloroform but were soluble in deuteroacetone, and so, though rather more expensive and not so easy to handle, the latter was used. Iodine was rejected as oxidising agent as it was not strong enough to oxidise all the ferrocene derivatives. It did not oxidise either the acetyl ferrocene or the ethyl ferrocenoate, although ferrocene itself was oxidised. This is in contrast to the findings of Fritz and coworkers<sup>53b</sup> who oxidised various ferrocene derivatives, including acetyl ferrocene, using iodine. They found that with a five-fold excess of iodine complete oxidation could be achieved, even for acetyl ferrocene.

Silver perchlorate was finally chosen as oxidising agent, the deposition of silver ensuring that the reaction went to completion rather than stopping at an uncertain equilibrium position. However, the fact that silver metal was deposited and had to be removed by centrifugation was a disadvantage, particularly with rather volatile deuteroacetone. Other oxidising agents investigated were mercuric acetate, silver benzoate, periodic acid and lead tetraacetate, and solvents examined were benzene, dimethyl sulphoxide and hexachloroacetone, but all proved unsatisfactory.

#### (ii) Sample preparation

Two procedures were used for sample preparation.

- 1) A standard solution, usually either 0.1M or 0.2M, of the ferrocene derivative was prepared in a 0.5ml flask. A



second solution, the same molarity in ferrocene derivative, and either equimolar in silver perchlorate or with sufficient of the oxidising agent to give a known, fairly large degree of oxidation, was similarly made up, and centrifuged to remove the reduced silver. Only the approximate concentration of this solution could be known.

Aliquots of this second solution were then added to the first solution to give the approximate degree of oxidation required. The N.M.R. spectrum of the solution was then run as soon as possible (see section on stability below).

The accuracy of the method could be improved in two ways. Firstly, after centrifugation, the volume of the solution was increased to 0.5ml again by adding washings from the silver, thus making the molarity of the second solution more close to that of the first solution; and secondly, the second solution was as fully oxidised as possible so that aliquots of this solution, if of a different molarity to the first solution, changed the concentration of the resulting solution minimally.

2) Two equimolar solutions were prepared, the first, as above, containing the ferrocene derivative only, the second containing silver perchlorate only. Aliquots of the second solution were then added to the first as required, each resulting solution being centrifuged, then its spectrum run as soon as possible.

The first method was the better one for preparing a series of solutions of one derivative at various degrees of oxidation, while the second method was more economical with



the ferrocene derivative when only one solution was required.

The solvent used throughout was deuterioacetone (Ciba, 99 Atom % D) containing 3% tetramethylsilane (TMS) as internal standard for the R10 instrument or as lock for the HA 100 instrument. The solvent was stored in contact with oven-dried 4a molecular sieves in a stoppered bottle sealed with parafilm, in a desiccator over silica gel.

The silver perchlorate (BDH) was used without further purification.

Preliminary N.M.R. spectra were run using a Perkin-Elmer R10 (60 MHz) instrument, otherwise a Varian HA 100 (100 MHz) instrument was used.

#### (B) SHIFT STUDIES

The degree of oxidation of a solution could be known, at worst, to within 20%, although, by keeping the errors minimal as described above, it might be known to within 5%. Because of this uncertainty, comparisons of shift changes between different ferrocene compounds was rather tentative and more emphasis was placed on comparisons within each compound.

Shift changes, that is the difference in chemical shift in paramagnetic and diamagnetic solutions, were measured for increasing percentage oxidation for each derivative. It was immediately apparent that only low degrees of oxidations, up to about 5%, could be used as line-broadening was considerable and solutions with higher degrees of oxidation gave spectra with extensive overlap of peaks, or even



unobservably broad peaks, especially the ferrocene ring peaks.

Shift changes were rather small; typical values are shown in Table 1 for the shift changes in the unsubstituted ferrocene ring proton signal at the highest degree of oxidation measured. An upfield shift of the signal on oxidation is indicated by a positive sign, a downfield shift, negative.

Table 1. Displacement of unsubstituted ferrocene ring proton signal, in Hz, on oxidation of the ferrocene derivative, measured at 100 MHz.

Derivative	Degree of oxidation, as %	Displacement
FnCOMe	5	-85.3
FnCOOMe	5	-39.4
FnCOOEt	5	-33.0
FnCH=CHCOMe	3	-56.0
FnC <sub>6</sub> H <sub>4</sub> Me	4	-94.5

The ferrocene ring proton signals are considerably more shifted than the side-chain proton signals, which will thus have shifts much too small to be of use in distinguishing the side-chain protons.

Although the degree of oxidation is not known accurately, approximate figures for the shift displacement at 100% oxidation can be calculated from the above values. These are given in Table 2.



Table 2. Approximate displacement of unsubstituted ferrocene ring proton signal, in Hz, expected at 100% oxidation of various ferrocene derivatives.

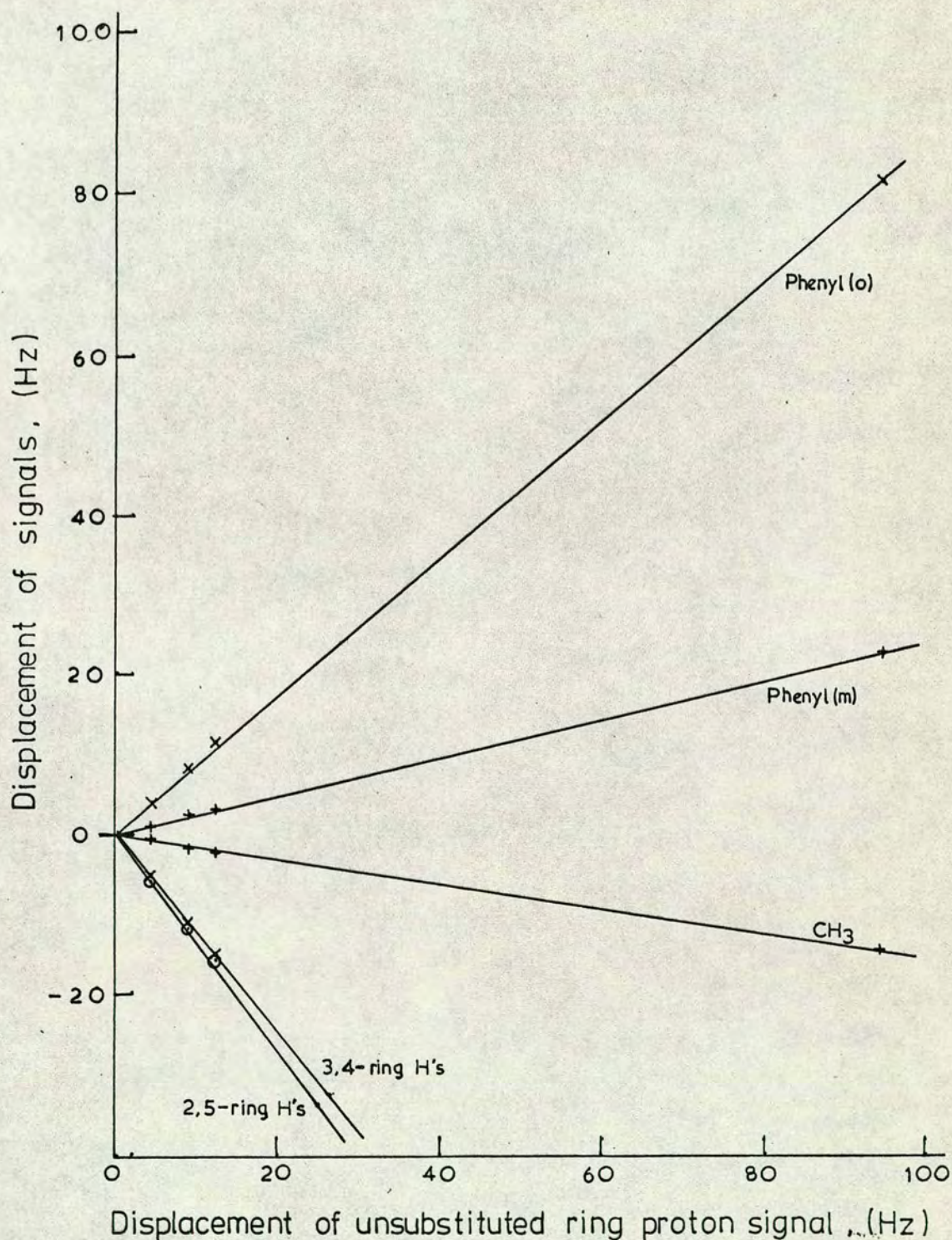
Derivative	Displacement
$\text{FnCOMe}$	-1710
$\text{FnCOOMe}$	-790
$\text{FnCOOEt}$	-660
$\text{FnCH=CHCOMe}$	-1870
$\text{FnC}_6\text{H}_4\text{Me}$	-2360

The value for acetyl ferrocene of -1710 Hz (-17.1 p.p.m) is in reasonably good agreement with the value of -16 p.p.m. measured by Fritz and coworkers<sup>53b</sup>.

Because the shift changes were so small, investigations were restricted to these simpler ferrocene systems. Graphs were plotted of the shifts of each proton-type in a given derivative against the shift of the unsubstituted ferrocene ring protons in that molecule. Good, straight lines through the origin resulted in almost every case, see Figure 1 for an example. Normalisation factors (see Part V for the origin of this concept) were calculated from the gradients taken as percentages, and thus represent the ratio of the shift of any proton to the shift of the unsubstituted ring protons. Peaks with upfield shifts relative to their diamagnetic position are taken to have positive values of shift change and positive normalisation factors, while peaks shifted downfield have negative values of both, irrespective of the direction of shift of the normalising peak.



Figure 1. Plot of shift displacements (Hz at 100 MHz) of the signals of *p*-tolyl ferrocene against the shift displacement of the signal of the unsubstituted ferrocene ring protons, at low degrees of oxidation.





All the ferrocene ring proton peaks moved downfield on oxidation, while almost all the side-chain proton peaks moved upfield. The methyl proton peak in *p*-tolyl ferrocene was an exception.

A typical set of spectra, those of ethyl ferrocenoate at different degrees of oxidation, is illustrated in Figure 2.

The normalisation factors are tabulated in Table 3.

Table 3. Normalisation factors (see text), expressed as percentages, for the protons in simple ferrocene derivatives, slightly oxidised.

Derivative	2,5-ring protons	3,4-ring protons	Side-chain protons
FnCOMe	-74.0	-63.2	COMe: +57.6
FnCOOMe	-77.5	-78	Me: +38.5
FnCOOEt	-64.3	-82.0	CH <sub>2</sub> : +41.3; CH <sub>3</sub> : +28.0
FnCH=CHCOMe	-110	-105	C <sub>α</sub> H: +64; C <sub>β</sub> H: +40.4* CH <sub>3</sub> : +28.4
FnC <sub>6</sub> H <sub>4</sub> Me	-186	-178	Ph(o): +86.5; Ph(m): +24.2;** CH <sub>3</sub> : -15.5

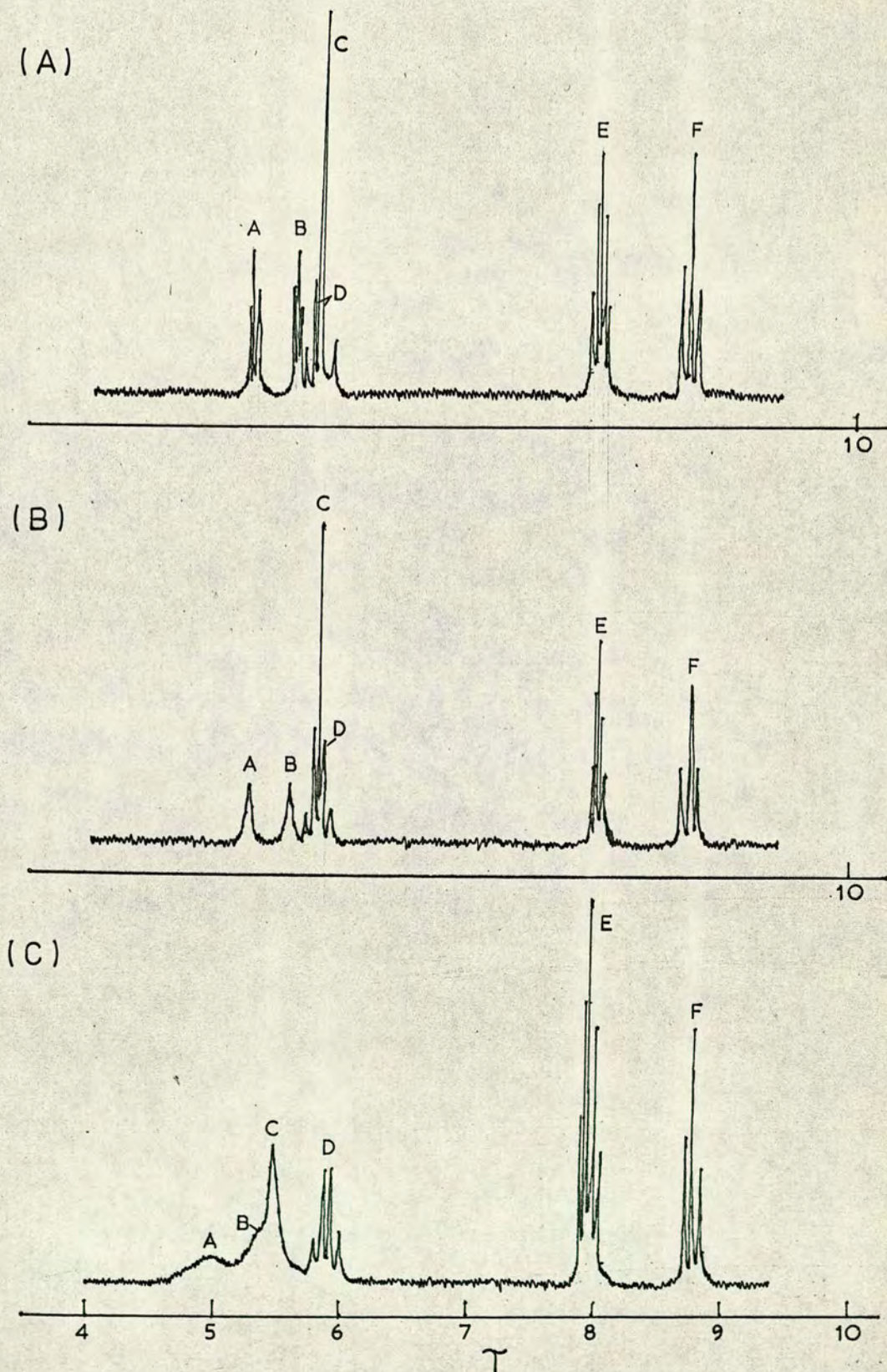
\* C<sub>α</sub>H and C<sub>β</sub>H: olefinic protons α and β, respectively, to the ferrocene ring.

\*\* Ph(o) and Ph(m): phenyl protons ortho and meta respectively, to the ferrocene ring.

The acetyl ferrocene has been examined by Fritz and co-workers (see above) apparently in the fully oxidised state. Only one peak is reported for the ring protons but the ratio of the shift of the methyl proton peak to that of this peak was 56%, in remarkably good agreement with the present work.



Figure 2. N.M.R. spectra of ethyl ferrocenoate in deuterioacetone solution at various degrees of oxidation: (A) 0%, (B)  $\frac{1}{2}$ %, (C) 5%.



A: 2,5-ring protons; B: 3,4-ring protons; C: unsubstituted ring protons;  
D:  $\text{CH}_2$ ; E: acetone; F:  $\text{CH}_3$ .



The assignment of the substituted ferrocene ring proton triplets was based on their diamagnetic line positions compared with those found in 2,5-dideuterated ferrocene derivatives<sup>230</sup>. Table 4 shows the diamagnetic positions of both ring and side-chain peaks at the concentrations of ferrocene derivative studied.

Confirmation of the assignments of the substituted ring proton signals was sought in the case of the conjugated ketone,  $\text{FcCH=CHCOMe}$ . The  $\alpha$  olefinic proton signal was broadened due to the coupling with the 2,5-ring protons. Irradiation of each ring triplet in turn should in the case of the 2,5-ring protons narrow this broadening. The narrowing observed confirmed the above assignment, but irradiation of the 3,4-ring proton signal also caused a small amount of narrowing, showing long-range coupling to be present.

The identical line positions found for ferrocene at two concentrations, see Table 4, would suggest that the diamagnetic positions are independent of concentration. This has been found independently to be true for comparably dilute solutions in deuteriochloroform, but a small concentration dependence was observed at higher concentrations<sup>231</sup>.

As mentioned in Part I, the usefulness of selective shifts in structure determination depends to a considerable extent on the shift changes being substantial while broadening is minimal. The ratio of the shift changes to the linewidth of any peak is thus a useful indicator of the potential of the system for shift studies. The shift to linewidth ratio here





**Table 4.** Diamagnetic line positions in simple ferrocene derivatives, expressed in Hz downfield from TMS, at 100 MHz.

Derivative	Molar- ity, M	Unsubstituted ring protons	2,5-ring protons	3,4-ring protons	Side-chain protons
FnCOMe	0.2	421.8	476.8	450.8	COMe: 234.7
FnCOOMe	0.1	420.2	475.3	442.7	Me: 375.1
FnCOOEt	0.2	419.8	475.6	441.6	CH <sub>2</sub> : 423.4; CH <sub>3</sub> : 131.4.
FnCH=CHCOMe	0.1	417.8	462.9	445.8	C <sub>α</sub> H: 748.5; C <sub>β</sub> H: 634.3; CH <sub>3</sub> : 222.4
FnH	0.1	414.2			
	0.2	414.2			
FnC <sub>6</sub> H <sub>4</sub> Me	0.1	400.0	467.8	427.9	Ph(o): 747.0, 738.7; Ph(m): 712.9, 704.8; CH <sub>3</sub> : 228.1



is less than 5, which is too low to enable ferrocene to be a useful "plug-in" shift reagent; however these shift studies produced some interesting results.

The diamagnetic line positions for the ferrocene unsubstituted ring protons were in the same order as the average positions of the substituted ring proton triplets, as can be seen in Table 5. Presumably both reflect mainly the electron-withdrawing ability of the substituent group.

Table 5. Diamagnetic line positions in ferrocene derivatives. Comparison of unsubstituted ring position with average substituted ring position, expressed in Hz downfield from TMS, and separation between triplets, in Hz, at 100 MHz.

Derivative	Unsubstituted ring protons	Average for substituted ring protons	Separation between triplets
FnCOMe	421.8	463.8	26.0
FnCOOMe	420.2	459.0	32.6
FnCOOEt	419.8	458.6	34.0
FnCHCHCOMe	417.8	454.4	17.1
FnC <sub>6</sub> H <sub>4</sub> Me	400.0	447.9	39.9

The separation of the substituted ring triplet signals did not fall in the same order, the p-tolyl derivative showing greatest separation while the conjugated ketone showed least. This could be indicative of a balance between inductive and conjugative effects, the variation from one substituent to another varying the distribution of the negative charge within the substituted ring, although the overall substituent effect is taken up by both rings. It



probably reflects also, the deshielding due to the diamagnetic anisotropy of the carbonyl group in the appropriate derivatives<sup>232</sup>.

In the paramagnetic systems, the strongly anisotropic  $g$ -factor in the ferricenium cations, for example, for  $\text{Fn}^+\text{H}$ ,  $g_{\parallel} = 4.35$ ,  $g_{\perp} = 1.26$ , and for  $\text{Fn}^+\text{COMe}$ ,  $g_{\parallel} = 3.62$ ,  $g_{\perp} = 1.76$ <sup>54b</sup>, will give rise to pseudocontact shifts. If the shifts found in the ferricenium cations were purely pseudocontact in nature and the cation were symmetrical as regards the rings and the iron atom, then all the ring protons would experience the same shift which was clearly not so. The Fe-ring bonds are weakened, and so lengthened, in the cation. If one were weakened more than the other, then the unsubstituted ring protons would experience a different shift to the substituted ring protons but the latter would be identical, which was not the case either. This suggested there was a Fermi contact contribution present, as in fact would be expected. Separation of pseudocontact and Fermi contact contributions is a doubtful procedure, even when  $g$ -factors are known.

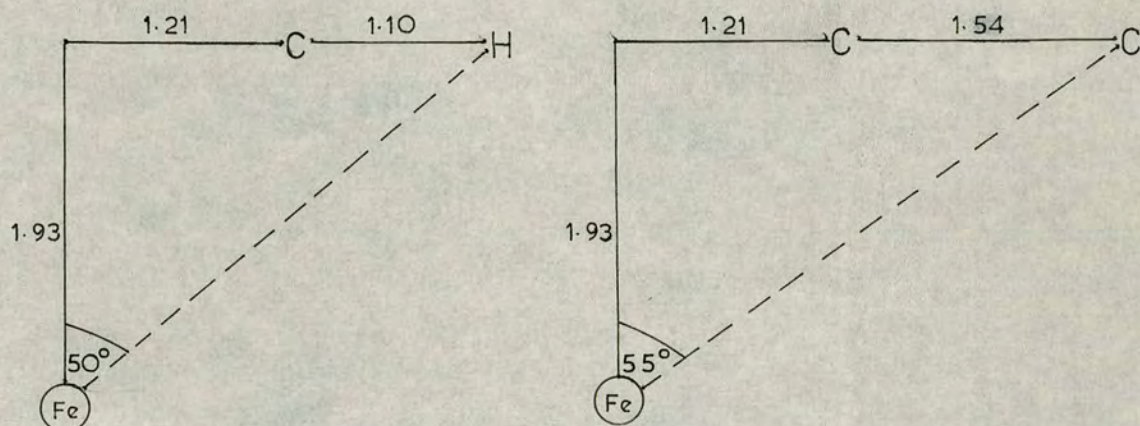
Fritz and coworkers<sup>53b</sup> concluded from their work that the pseudocontact contribution to the shifts and the  $g$ -factor anisotropy in the ferricenium cation were small, but Prins<sup>54b</sup> has pointed out the invalidity of their arguments and shown by his E.S.R. measurements the considerable  $g$ -factor anisotropy, mentioned above.

Some conclusions about the contact and pseudocontact shifts may be drawn from the normalisation factors here measured.



### Side-chain shifts

Taking a Fe-ring bond length of  $1.93 \times 10^{-10}$  m, the 'best value' calculated by Prins<sup>54b</sup>, and giving the other bond lengths the values: C-C (ring) 1.43; C-C (chain) 1.54; C-H  $1.10 \times 10^{-10}$  m, a change of sign of the pseudocontact shift, due to change in sign of the  $(3\cos^2\chi-1)$  factor with increasing  $\chi$ , would be expected between the ferrocene ring protons and the side-chain protons in all the derivatives studied here (see diagram).



The sign of the shift changes at  $\chi = 55^\circ$ .

The shifts did change in direction as predicted here, except for the methyl protons in *p*-tolyl ferrocene, where presumably the Fermi contact shift is greater in magnitude than the pseudocontact shift, and opposite in direction, i.e. negative, giving an overall negative shift. In the side-chain of this derivative, one would expect  $\pi$  delocalisation of spin on account of its aromatic nature. Thus, if the methyl signal exhibited a downfield contact shift, so also would the phenyl protons meta to the ferrocene, while the ortho proton signal would show an upfield contact shift. As suggested above, the pseudocontact shift for all



these three proton types is positive and approximate calculation of their relative magnitudes gave the ratio of their shifts as phenyl(o):phenyl(m):methyl 1.5:3.6:1.8. A linear combination of the two shift contributions can thus be envisaged which results in a substantial upfield shift for the ortho protons, a much smaller upfield shift for the meta protons (positive pseudocontact shift larger than absolute value of negative contact shift) and a small negative shift for the methyl protons as discussed above, in agreement with the shift values found experimentally. Incidentally, this situation requires the absolute value of the contact shift for the meta protons to be greater than that for the methyl group, as would in fact be expected.

#### Ring protons

These all had negative shifts. The three proton types would be expected to have the same pseudocontact contribution to their shift, assuming the ring geometry is undistorted by the substituent, and so their contact contribution must be different, showing an unequal distribution of spin density. This distribution would be expected to depend on the nature of the substituent.

#### (C) LINEWIDTH STUDIES

As mentioned above, the signals, particularly of the ring protons, were extensively broadened, even at low percentage oxidation. Although selective broadening was evident, it was not easy to measure as peaks overlapped considerably. Even the ring protons appeared to be



selectively broadened. To determine whether this was in fact the case, it was decided to examine the effect of saturation on the signals. A solution of very low percentage oxidation was most suitable for this. For the instrumentation and theory involved, see Part VIII.

Preliminary work was carried out on the R10 spectrometer, using 0.2M ethyl ferrocenoate solutions. The first solution was diamagnetic, the second approximately  $\frac{1}{2}\%$  oxidised, the third approximately 10% oxidised. Peak heights at varying radiofrequency (RF) powers were measured for all five proton types in each solution except the ring protons in the most oxidised solution where this was not possible. The results were treated graphically, first by plotting reciprocal peak height,  $h_s^{-1}$ , against the square of the RF power,  $V^2$ , (method 1), then by plotting  $h_s$  against  $h_s V^2$  (method 2). The former plots were fairly good straight lines but the distribution of points was such that it weighted the high RF points rather heavily. The latter plots gave poor straight lines for the diamagnetic solution, but the linearity improved with oxidation. For a discussion of the causes of non-linearity, see Part VIII. The gradient in both methods yielded a constant,  $c^2$ , where  $c^2 = \gamma^2 a^2 T_1 T_2$ , 'a' being a constant including instrumental conditions. Thus the gradient gave a direct comparison of the product of the relaxation times,  $T_1 T_2$ , of each peak. The  $c^2$  values are tabulated in Table 6.



Table 6.  $c^2$  values ( $\times 10^8$ ) obtained by saturation of three ethyl ferrocenoate solutions.

Percentage oxidation	Graphical method	$\text{CH}_3$	$\text{CH}_2$	$\text{C}_5\text{H}_5$	2,5- $\text{C}_5\text{H}_4$	3,4- $\text{C}_5\text{H}_4$
0	1	640	970	880	1,570	1,030
	2	550	370	930	910	590
$\leq \frac{1}{2}$	1	153	152	21	2.3	1.5
	2	207	142	26	7.5	6.0
$\sim 10$	1	9.3	2.8			
	2	8.7	2.5			

Although the error involved is sizeable, the results clearly indicate that the ease of saturation in the oxidised solutions is in the order



In the substituted ring, the 2,5-protons appear to saturate more readily than the 3,4- protons but this is far from certain.

During saturation, peaks decrease relatively in height and broaden. Peaks which are close to each other, as in multiplet signals, will thus add into each other, giving a falsely large measured peak height. Correction was made for this mathematically (see Part VIII). Four out of the five signals in ethyl ferrocenoate are multiplets and were thus affected. Correction to the methylene quartet and methyl triplet was made in the more oxidised solution. The corrected  $c^2$  values were

$$\begin{aligned} \text{for } \text{CH}_2 & (2.3 \pm 1.0) \times 10^{-8} \\ \text{CH}_3 & (9.7 \pm 1.5) \times 10^{-8} \end{aligned}$$



not greatly changed, and still indicating the quite definite differential saturation.

Corrections to the peak heights in the solutions of lower degree of oxidation were fairly small, at most 1%.

A second saturation series was carried out on the HAI00 instrument using methyl ferrocenoate solutions approximately  $\frac{1}{2}\%$  and 1% oxidised. This derivative was chosen partly for stability reasons (see below) and partly because the ferrocene ring proton signals could be more clearly seen. Peak heights were measured by "spotting" peak maxima and base-line, and graphs of  $h_s$  against  $h_s V^2$  (method 2) and  $\log h_s$  against  $\log V$  (method 3) were plotted. The values of  $c^2 = \gamma^2 a^2 T_1 T_2$  are tabulated in Table 7. N.B. "a" and "c" are different constants for the different instruments.

Table 7.  $c^2$  values ( $\times 10^8$ ) obtained by saturation of two methyl ferrocenoate solutions.

Percentage oxidation	Graphical method	$C_5H_5$	2,5- $C_5H_4$	3,4- $C_5H_4$
$\sim \frac{1}{2}$	2	2.5	0.24	0.26
	3	2.2	0.30	0.25
$\sim 1$	2	0.48	0.22*	0.10
	3	0.48	0.07	0.08

\* Very poor linearity.

Although the accuracy of these figures has increased with the improved technique, the errors involved are still considerable. However, the figures clearly show that the



unsubstituted ring protons are more readily saturated than the substituted ring protons, both pairs of which are saturated comparably, as was found with the ethyl ester.

The fact that the relaxation times in the substituted ring are shorter suggests that more of the unpaired spin is located in that ring. However the shifts for the unsubstituted ring were smaller than in the <sup>un</sup>substituted ring. Assuming identical pseudocontact shifts in the two rings, this could be explained if the contact and pseudocontact shifts act in opposite directions, the negative pseudocontact shift always being dominant. The protons with the larger contact shift will then have the smaller overall shift.

In the shift studies it was noted that the different shift changes in the substituted ring proton triplets arose most probably from unequal spin density at the two positions, the pseudocontact contribution being constant. These saturation results indicate approximately equal spin density at the two positions, but the shift difference was small for both esters, especially the methyl ester, and so the sizeable error involved in the saturation method could easily mask any difference.

#### (D) STABILITY OF FERRICENIUM CATIONS

It was noticed that in a partially oxidised acetyl ferrocene solution, after three hours a dark precipitate was settling out. The stability of the acetyl ferricenium solution was checked by making up a solution of low oxidation and running an N.M.R. spectrum of it at intervals over 24 hours. Even after a few hours the paramagnetic shifts



were substantially reduced, and another peak developed under the acetone peak. Obviously the acetyl ferricenium cation is not very stable under these conditions. Addition of acid did not improve the stability.

Solutions of methyl and ethyl ferrocenoate and p-tolyl ferrocene, similarly examined, also proved unstable but to a lesser degree, the p-tolyl ferrocene being the most stable. This is in accordance with Prins<sup>54b</sup> who states that ferrocene derivatives with electron-withdrawing groups are less readily oxidised, and that the formed cations are rather unstable.

#### (E) CONCLUSION

The aim of this work was to investigate the possibilities of the ferrocene system either for selective shifts or for selective broadening. The relatively small shifts and small shift to linewidth ratios ruled out the former as the basis of a method of general utility, while overlap of peaks and difficulty in linewidth measurement ruled out the latter. Selective saturation proved the most satisfactory method in some ways, but the low accuracy and the tedious procedure involved limited its applicability. The instability of these systems and the difficulty in preparing suitable derivatives were also severe disadvantages from a practical point of view.



PART IVFREE RADICALS.

In the search for a "plug-in" paramagnetic probe which might provide useful structural information, it seemed of interest to investigate the potential of free radicals, particularly for selective broadening. A nitroxide system was chosen since nitroxide free radicals have been widely used as probes in E.S.R. spectroscopy<sup>233,234</sup>, and since their chemistry has been explored in some detail<sup>235</sup>.

As already mentioned in Part II, section G(e), N.M.R. studies of free radicals to date have been dependent on the line-narrowing produced in concentrated solutions of radicals, either the radical under investigation being very concentrated, or the solvent being a free radical.

However, for selective broadening studies, dilute solutions must be used, as it is only the intramolecular broadening which is significant from a structural point of view, and all effects outside the molecule, that is the intermolecular broadening, must be eliminated. The linewidth will then reflect the distance of the proton from the centre of unpaired spin in the molecule; more precisely, for the more distant protons, it depends on the decrease in  $A^2$  or in  $r^{-6}$  depending on whether the linewidth is dominated by scalar or dipolar relaxation processes (see Part II, section D).

It was therefore of interest to explore whether intermolecular broadening could be eliminated without reducing the concentration to such an extent as to make the spectra

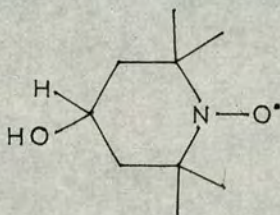


unobservable and, if this could be achieved, to show that selective intramolecular broadening was in fact observable.

(A) EXPERIMENTAL

(a) Preparation of compounds

(i) 2,2,6,6-tetramethyl-4-piperidinol nitrogen oxide  
(alcohol nitroxide)

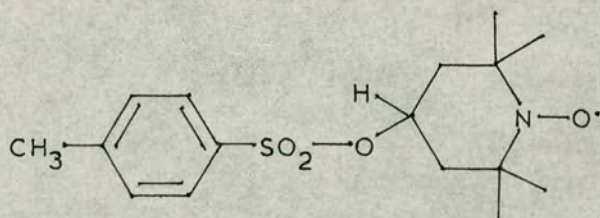


The nitroxide was prepared from the amine by the method of Rassat<sup>236</sup>, using tetramethylpiperidinol (5g; 0.032 mole), phosphotungstic acid (50mg), hydrogen peroxide (30%)(12.5ml) and water solvent (45ml). The reaction mixture was left overnight. It was worked up as described by Rassat except that very little acid (6ml N H<sub>2</sub>SO<sub>4</sub>) was used in washing out the unreacted amine as the nitroxide was also found to be soluble in acid. The resulting product was crystallised from light petroleum (60-80°) to give an orange solid, m.p. 66-68° (lit. 72°) in 43.6% yield.

The N.M.R. spectrum showed that the product still contained unreacted amine. This appeared as a relatively sharp peak at approximately  $\tau$ 8.8 which was attributable to the methyl protons. The amine was removed by eluting the mixture through an alumina column using benzene with increasing proportions of ether. With 1:1 benzene:ether, the majority of the product was eluted. It had m.p. 68-71° and the N.M.R. spectrum showed that it contained no residual amine.



(ii) 2,2,6,6-tetramethylpiperidine-4-p-toluene sulphonate  
nitrogen oxide (tosylate nitroxide)



Alcohol nitroxide (2.0g; 0.012 mole) was dissolved in dry pyridine (20ml). The solution was cooled to  $0^{\circ}$  in a stoppered flask, then toluene-p-sulphonyl chloride (3.3g; 0.018 mole) was added in small portions, the mixture being shaken after each addition to ensure complete solution. The reaction mixture was left to stand overnight at room temperature. Water (1.5ml) was added and the solution left for 30 minutes to destroy unreacted toluene-p-sulphonyl chloride. After evaporation of the pyridine under reduced pressure, excess water was added to the residue. The solid which separated was then filtered off, dried and crystallised from light petroleum ( $80-100^{\circ}$ ) to give the tosylate nitroxide, a pinkish-red solid, m.p.  $111-112^{\circ}$  (lit.  $115^{\circ}$ <sup>237</sup>) in 64% yield.

(b) Preparation of solutions for N.M.R. measurements

For each solvent used a standard solution was prepared of the tosylate nitroxide in that solvent with 3% TMS. The solution was more concentrated than the most concentrated solution required. A series of solutions was then prepared using aliquots of the standard solution to give the exact molarity of nitroxide required. 25  $\mu$ l dioxan was added to



each solution to provide a lock signal, and the solutions were made up to 0.5ml with the appropriate solvent containing no TMS. In this way the ratio of nitroxide to TMS could be held constant, and exact molarities of nitroxide achieved. This technique was more satisfactory than the preparation of individual solutions by direct weighing.

Solutions of the following molarities were prepared:

In  $\text{CDCl}_3$ , 0.01, 0.02, 0.05, 0.1, 0.2, 0.5 and 1.0M

In  $(\text{CD}_3)_2\text{CO}$ , similarly up to 0.5M

In  $\text{CCl}_4$ , similarly up to 0.2M.

The solutions containing methanol (see below) were prepared by direct weighing of the tosylate nitroxide into a 0.5ml flask, adding the appropriate volume of AnalaR methanol using a Hamilton 10 $\mu$ l syringe and making up to the mark with carbon tetrachloride containing 3% TMS for the lock signal.

Preliminary work was carried out on the R10 instrument, probe temperature 33.5 $^\circ$ , otherwise the HA 100 instrument, probe temperature 28 $^\circ$ , was used. The HA 100 instrument was operated at a non-saturating RF power level of 24dB, modulation amplitude 1 mG (approximately RF field .04 mG, see Part VIII for measurement details). The linewidths were measured, where possible, at sweep width 100 Hz, the broader peaks being measured at sweep width 250 Hz, or, for the broadest phenyl peaks, at 1000 Hz. The average linewidth from four scans of the signal was taken. The phenyl peaks for the most dilute solutions (0.01 and 0.02M) were recorded using a Varian C 1024 Time Averaging computer accumulating approximately 200 scans. The phenyl signals in the 0.02M



solution in  $\text{CDCl}_3$  were also recorded directly and, although the spectrum was very noisy, the linewidths agreed fairly well, within 8%, with the values from the "CAT" spectrum.

For other experimental details see Part III, section A(a).

## (B) PRELIMINARY INVESTIGATIONS

### (a) Alcohol nitroxide

An approximately 0.2M solution of the alcohol in carbon tetrachloride containing TMS gave a N.M.R. spectrum showing two broad signals about 32 p.p.m. apart. The lower field peak was the sharper of the two, the higher field peak being very broad, linewidth about 1,500 Hz. Dilution of the solution sharpened the lower field peak while the other broadened. Addition of further TMS to the solution substantiated that the sharper peak was due to TMS. This peak narrowed on dilution since it is broadened by intermolecular interaction with the nitroxide. The broader peak can be assigned to the alcohol nitroxide; here intramolecular broadening is dominant and the increase in linewidth on dilution can be ascribed to an increase in the electron relaxation time.

The first samples of the alcohol nitroxide were contaminated with the amine from which it was prepared. The methyl signal of this appeared as an additional peak in the spectrum, just downfield of TMS. It was noticed that the TMS signal saturated more easily than this methyl signal, on increasing the RF power, which suggested the nitroxide was associating selectively with the amine, although the



difference could arise from different correlation times in the two cases. It seemed likely that this association was due to hydrogen bonding, and this chance observation suggested that it might be possible to explore hydrogen bonding involving nitroxide radicals by the selective broadening of N.M.R. signals. This possibility was further investigated as described later using a much simpler system, namely methanol and tosylate nitroxide.

(b) Tosylate nitroxide

As the spectrum of the alcohol nitroxide showed only one very broad peak, it was decided to extend the molecule by forming the tosylate to see whether more distant protons would give narrower, distinct signals.

An approximately 0.5M solution of the tosylate nitroxide in 5:2 carbon tetrachloride:deuteriochloroform mixed solvent, with TMS, was prepared. The N.M.R. spectrum of this solution at 60 MHz showed three peaks, A, B and C having half-widths of 60 Hz, 30 Hz and ca. 15 Hz respectively. C was verified as being the TMS peak by addition of more TMS to the solution. Taking the TMS peak to be at  $\tau$ 10.0 then peak A was at  $\tau$ 2.45 and peak B at  $\tau$ 7.5, suggesting A could be the phenyl protons and B the tosylate methyl protons.

There was an indication of two other very broad peaks lying under these peaks, which could have been due to protons closer to the centre of unpaired spin. These peaks disappeared on dilution of the solution.

Dilution of the solution caused all three peaks, A, B and C, to narrow. The TMS peak, broadened solely by intermolecular inter-



actions would be expected to sharpen. The fact that the other two peaks also decreased in linewidth indicated that intermolecular broadening of these peaks was at least as great as broadening due to intramolecular interactions. Dilution also revealed that peak A was in fact two peaks, in accordance with its assignment as arising from the phenyl protons.

The effect of saturating the tosylate nitroxide and TMS peaks by increasing the RF power is shown in Table 8. The measured peak heights were corrected for the varying sensitivities used, then divided by the RF power used, to give a normalised peak height,  $Z$ . Each value of  $Z$  was divided by the normalised peak height,  $Z_0$ , of the same peak in the same solution, run at the lowest RF power, that expressed as  $2 \times 10^3$  mV. The relative decreases in this ratio,  $Z/Z_0$ , indicate the relative susceptibility of the peaks to saturation.

**Table 8.** Relative decreases in normalised peak heights of tosylate nitroxide and TMS signals on increasing the RF power, operating at 60 MHz.

RF power, expressed in mV	$Z/Z_0$	0.22M nitroxide			0.11M nitroxide		
		A	B	C	A	B	C
$2 \times 10^3$		1	1	1	1	1	1
$4 \times 10^3$		0.98	0.93	0.71	0.96	0.93	0.75
$1 \times 10^4$		0.87	0.73	0.43	0.77	0.67	0.36
$2 \times 10^4$		0.78	0.58	0.25	0.65	0.41	0.18



Although the peak heights were not measured with great accuracy, these figures clearly show the ease of susceptibility to saturation to be  $A < B < C$ . This is also in accordance with the signal assignment above since the TMS peak (C) has no intramolecular factor and the methyl protons (B) are further removed from the centre of unpaired spin than are the phenyl protons (A).

(C) MORE DETAILED STUDY OF THE CONCENTRATION EFFECT FOR THE TOSYLATE NITROXIDE

For these studies the 100 MHz instrument was used, the first series of solutions having concentrations from 1.0M to 0.01M of tosylate nitroxide in deuteriochloroform solution.

The linewidths of the TMS, the methyl and the two phenyl peaks, where sufficiently separated, were measured at each concentration of tosylate nitroxide. The relationship between linewidth and the nitroxide molarity is shown in Figures 3(a) and 3(b). The appearance of the spectra at various nitroxide concentrations is shown in Figure 4. A chloroform peak, just upfield of the phenyl peaks, was observed only in solutions in deuteriochloroform.

At high concentrations, the signals are broadened both due to intramolecular effects within the free radical molecule and intermolecular effects between the molecules in solution. At any concentration, only the latter will be operative in the case of the TMS. Extrapolation to infinite dilution should give the linewidth due to intramolecular broadening only. For TMS, this is its normal instrumental linewidth of 0.6 Hz. For the nitroxide signals, the closer



Figure 3. Plot of linewidth (Hz) against molarity of tosylate nitroxide in deuteriochloroform solution: (A) Methyl and TMS signals, (B) Phenyl signals.

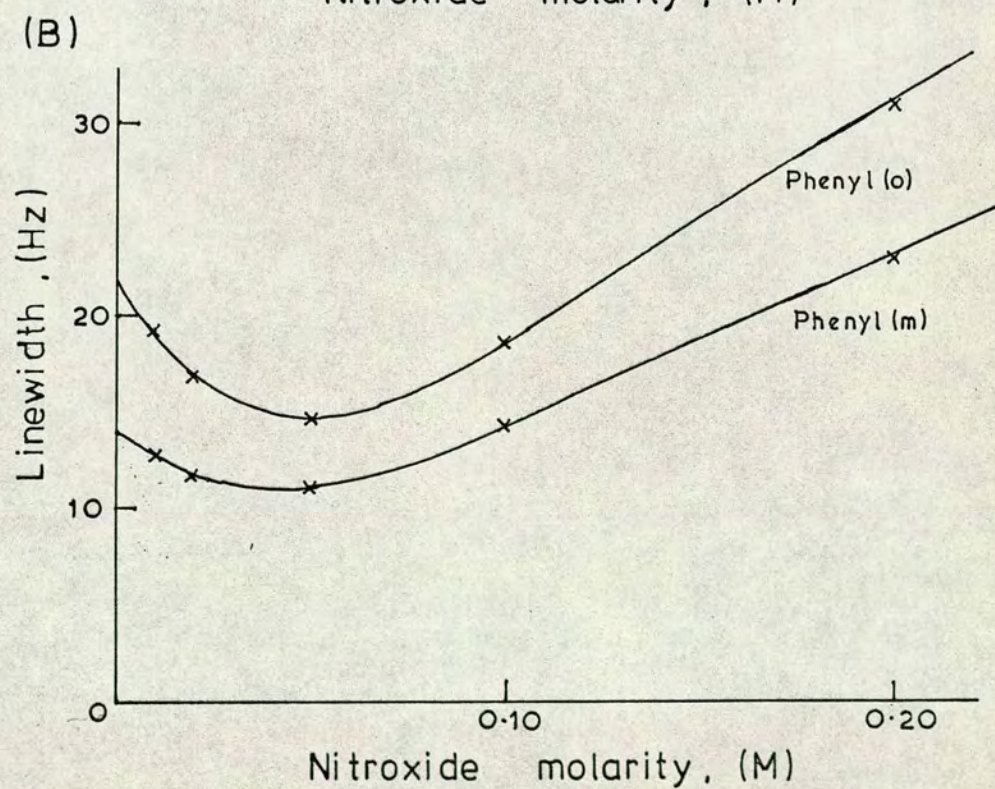
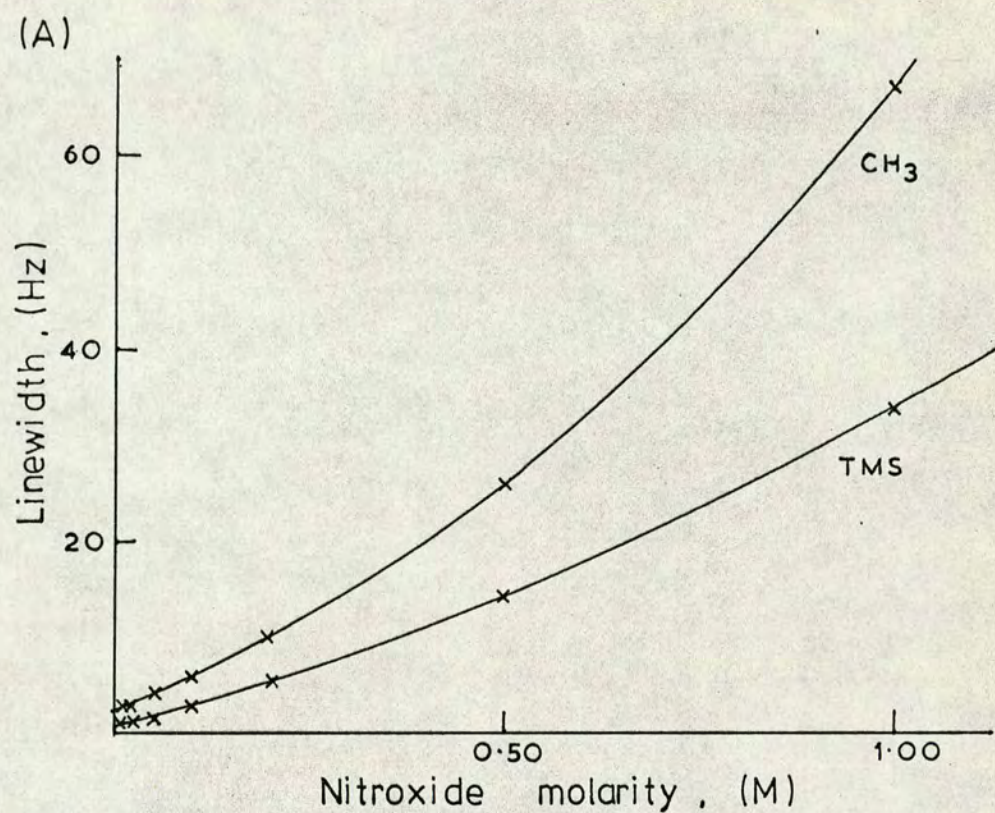
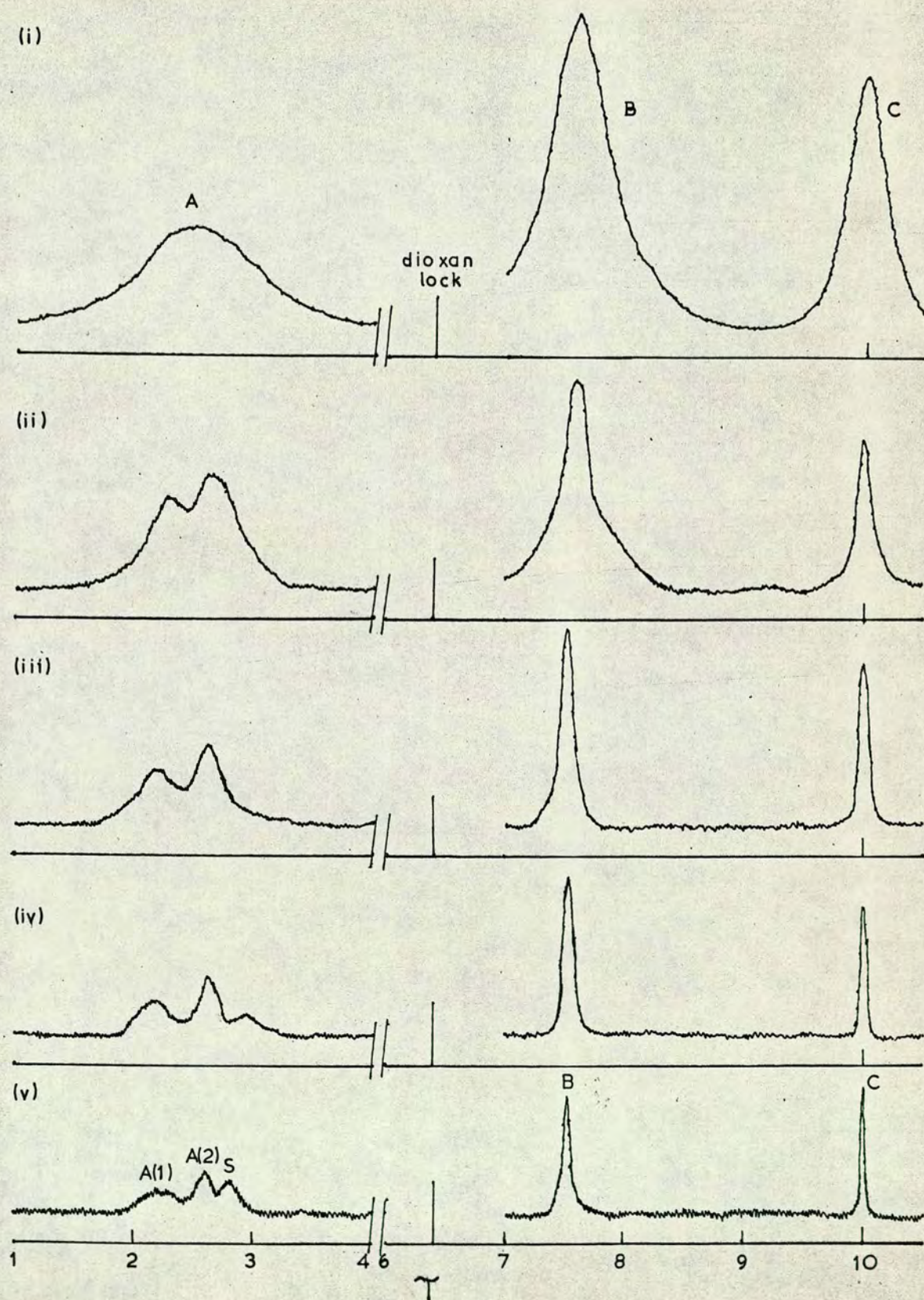




Figure 4. N.M.R. spectra of tosylate nitroxide at various concentrations in deuteriochloroform solution: (i) 1.0M, (ii) 0.5M, (iii) 0.2M, (iv) 0.1M, (v) 0.05M.



A(1): Ph(o) ; A(2): Ph(m) ; B: Me ; C: TMS ; S:  $\text{CHCl}_3$ .



the protons were to the centre of unpaired spin, the larger was the linewidth at all concentrations, that is phenyl (ortho,  $\tau 2.2$ ) > phenyl(meta,  $\tau 2.6$ ) > methyl( $\tau 7.5$ ). The assignments of the two phenyl peaks are based on those in methyl toluene-*p*-sulphonate which appear at  $\tau 2.25$  and  $\tau 2.65$  as two rough doublets. The higher field doublet is further split by coupling with the methyl protons and so arises from the protons meta to the sulphonyl group. The coupling constant between the phenyl protons is ca. 8 Hz, but this coupling was not observed in the nitroxide tosylate, see Figure 4.

The apparent increase in linewidth of the two phenyl peaks at the lowest concentrations is remarkable. This can be explained as follows. The peaks due to each pair of the phenyl protons in the nitroxide tosylate would be expected to be a doublet by analogy with methyl toluene-*p*-sulphonate described above. In the tosylate nitroxide this coupling is not resolved but it is thought to contribute to the linewidth at the lowest concentrations. The apparent narrowing of the peaks at intermediate concentrations can then be explained by postulating that "spin-decoupling", brought about by intermolecular relaxation, is occurring.

A second possible explanation was investigated graphically. Two identical curves were "added together" for increasing linewidths maintaining a constant separation between them. The measured overall linewidths showed a consistent increase such that the apparent linewidth changed from the sum of an individual linewidth plus the coupling



constant, when the lines were fairly narrow, to an individual linewidth only when the lines were very broad. However this theory did not explain the decrease in the linewidths found at intermediate concentrations of nitroxide. It was therefore assumed that spin-decoupling was occurring.

If the intermolecular broadening for each proton were the same, then the "slopes of the curves" (Figure 3) would be the same. This did not seem to be the case. The "gradients" appeared to increase in the order TMS < methyl < phenyl(meta) < phenyl(ortho), which suggested selective intermolecular interaction. It is possible that this is due to weak hydrogen bonds between the hydrogens in the nitroxide and the oxygen of the nitroxide in another molecule. Morishima<sup>200,201</sup> has investigated chemical shifts in various compounds (see Part II, section G(e)) in carbon tetrachloride solutions containing dimethyl or di-*t*-butyl nitroxide, which he ascribed to hydrogen bonds (see also section E of this part).

Alternatively, the differences could be due to differences in the correlation times for the dipolar interactions between the various protons.

One aim of the present work was to observe how low a concentration of nitroxide was required to eliminate intermolecular effects and to reveal the intramolecular effects. The results indicate that these conditions are effectively reached only at concentrations as low as 0.01M to 0.02M. The signal to noise ratios in these solutions were so small that the spectra had to be obtained using the Time Averaging



Computer, approximately 200 scans being required. Under these circumstances, the use of a nitroxide probe to produce selective broadening is clearly not a practicable proposition as a tool in structure determination.

#### (D) VISCOSITY EFFECT WITH TOSYLATE NITROXIDE

A decrease in the viscosity of the solvent would be expected to reduce the intermolecular contribution to the broadening by increasing the tumbling rate of the molecules. If the intermolecular broadening could be thus reduced without simultaneously reducing the intramolecular factor, then by using a suitable solvent it might be possible to eliminate the intermolecular contribution at higher concentrations.

To investigate this, two further series of tosylate nitroxide solutions were run, one series in deuterioacetone which has lower viscosity, the other in carbon tetrachloride, which has higher viscosity.

Graphs of linewidth with respect to nitroxide molarity were again plotted for each peak and were very similar in shape to those of the deuteriochloroform solutions, see Figure 5(a-d). Extrapolation to infinite dilution, gave the intramolecular broadened linewidths as tabulated in Table 9.

Table 9. Intramolecular broadened linewidths, in Hz, of the signals of tosylate nitroxide in three solvents.

Solvent	TMS	Methyl	Phenyl (meta)	Phenyl (ortho)	Viscosity of non- deuterated sol- vent at 30°, in mP
$(\text{CD}_3)_2\text{CO}$	0.6	2.1	14	17	2.95
$\text{CDCl}_3$	0.6	2.5	15	22	5.14
$\text{CCl}_4$	0.7	2.3	14	26(?)	8.45



Figure 5. Comparative plots of linewidth (Hz) against molarity of tosylate nitroxide for three different solvents.

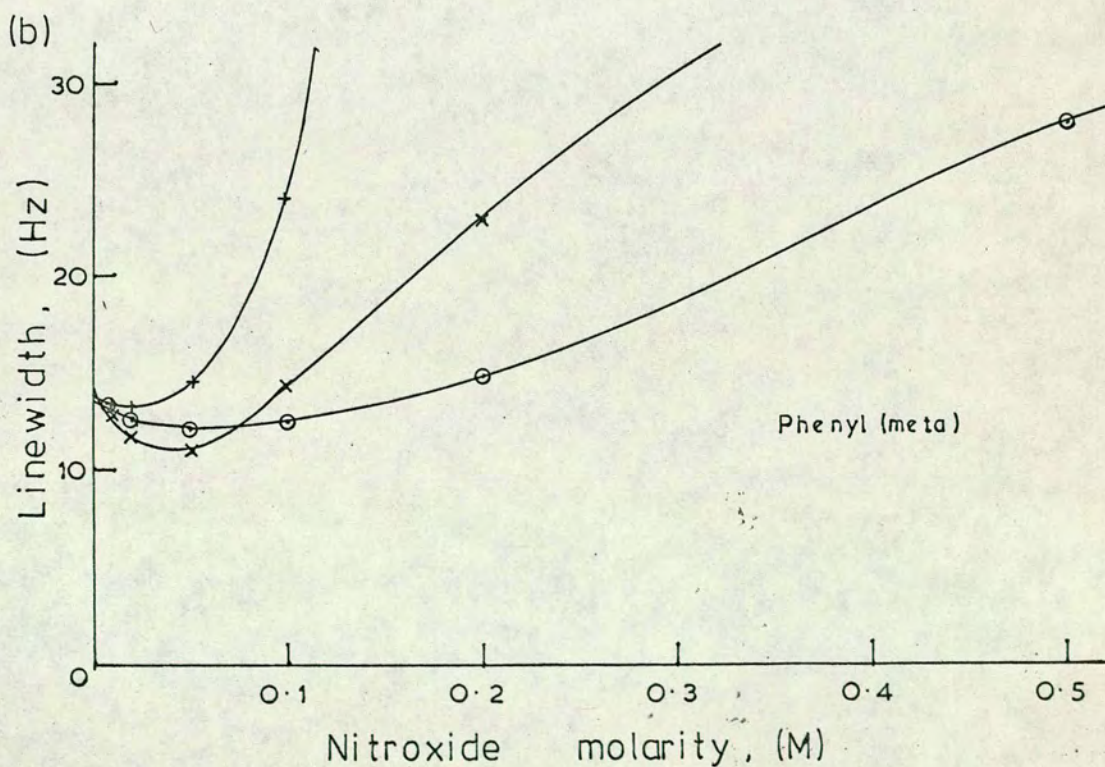
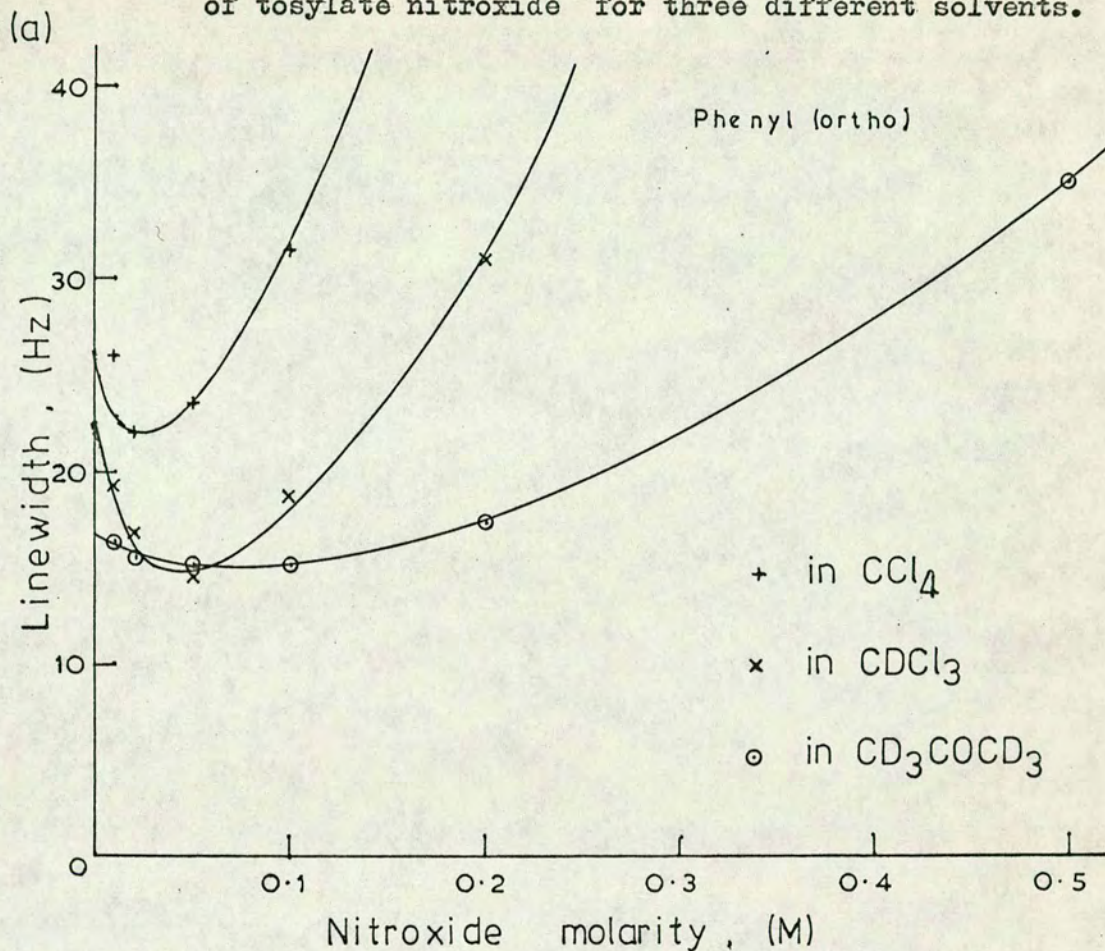
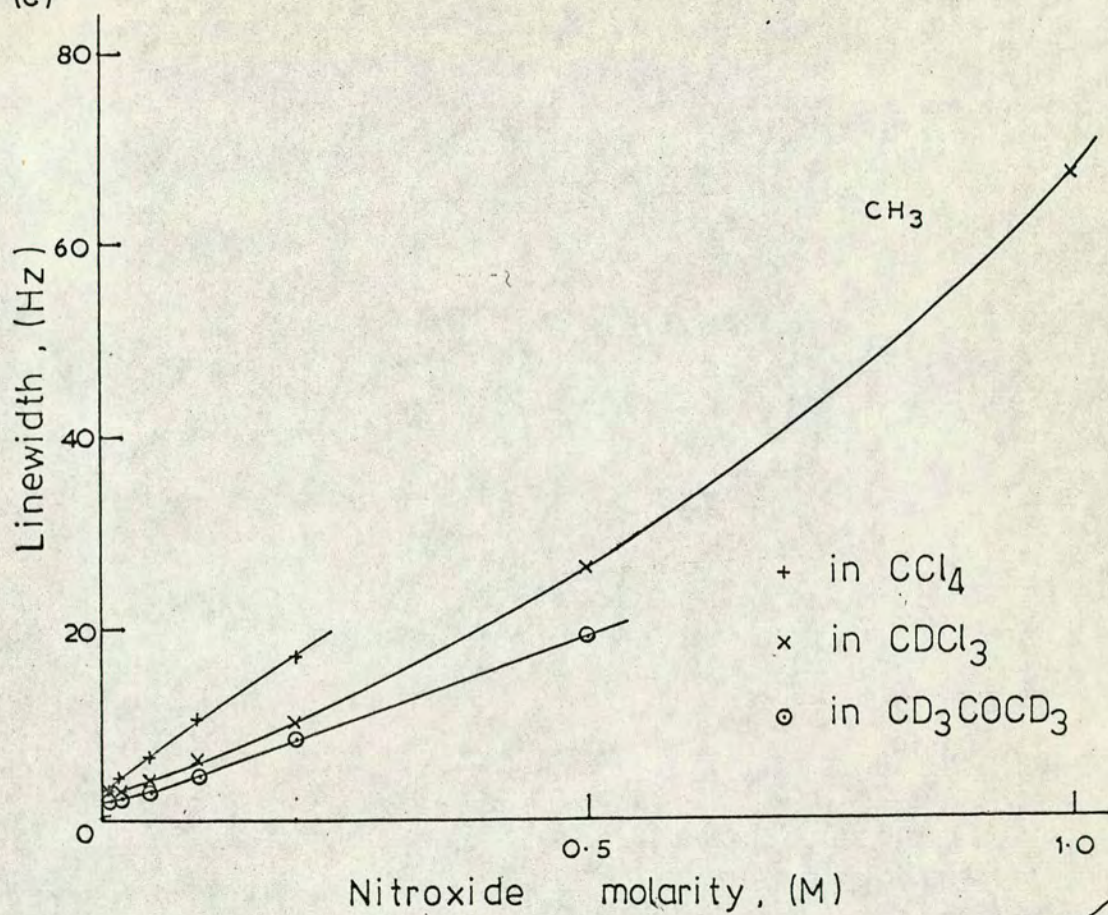


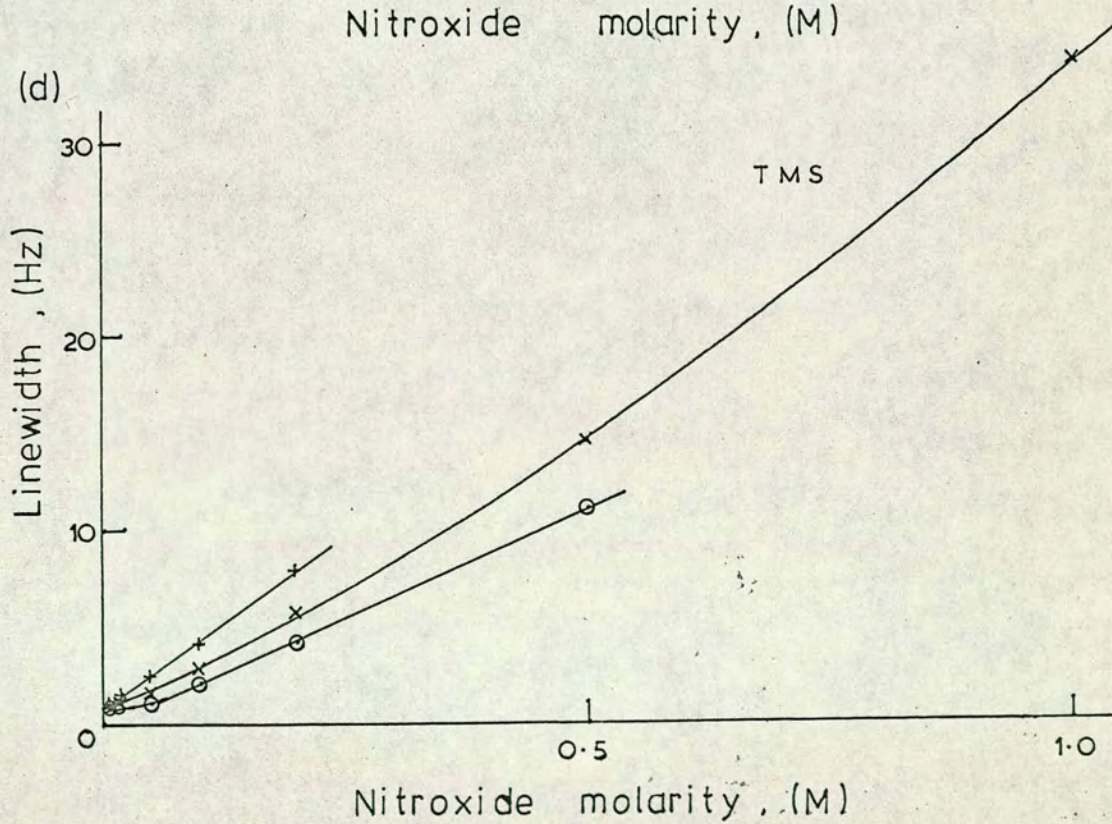


Figure 5. (cont.)

(c)



(d)





These figures showed that the intramolecular broadening was only very slightly dependent on viscosity.

The "gradients" of the plots, see Figures 5(a-d), indicated that the intermolecular effect had a much greater dependence on viscosity. Thus a solvent of low viscosity is definitely advantageous.

However, though the acetone solutions were superior, they still required too low a concentration of nitroxide for the method to be of any great value. It may be that Fourier transform instruments, with their much greater sensitivity, will solve this problem and establish this technique as a useful tool in organic chemistry.

#### (E) SELECTIVE BROADENING ARISING FROM INTERMOLECULAR ASSOCIATION

It was noted in the sample of alcohol nitroxide contaminated with amine that the amine methyl peak was less readily saturated by increasing the RF power than was the TMS, suggesting that selective association may be taking place in the solution.

The previous work has shown that plugging a nitroxide into a molecule was not of practical utility as a selective broadening agent and so the possibilities of selective association were probed, methanol being used as a model compound.

Two series of spectra were run:

(1) at constant nitroxide molarity varying the methanol concentration, thus keeping the intermolecular broadening constant unless there is selective association



(ii) at constant methanol molarity, the progress of the methanol peaks being observed at various low concentrations of nitroxide.

(i) constant nitroxide molarity

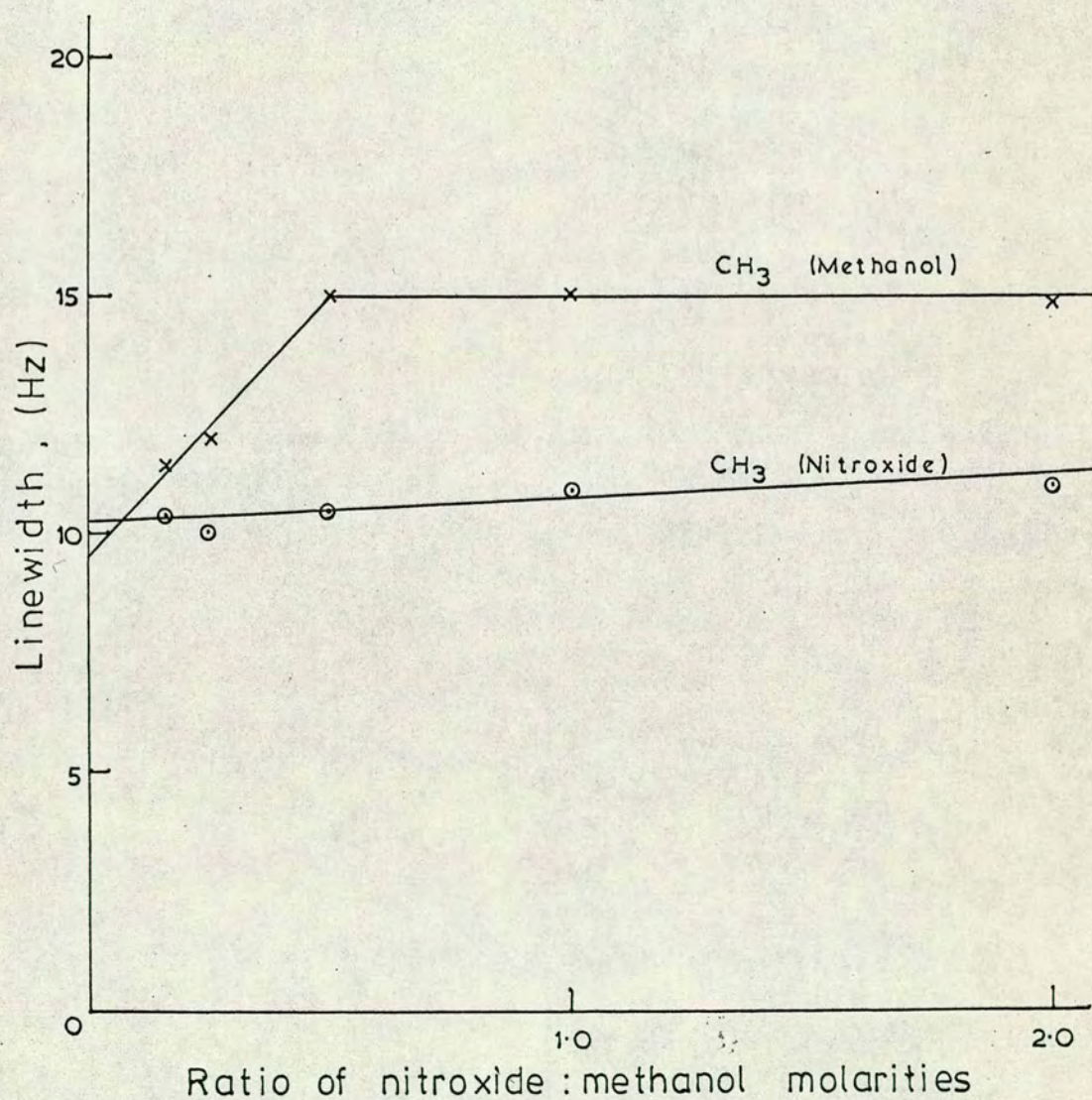
All solutions were 0.1M in nitroxide, and contained 0.05, 0.1, 0.2, 0.4 and 0.6M (ca. 2.5%) methanol. The graph of the linewidths of the methanol methyl and the tosylate methyl with respect to the nitroxide:methanol molarity ratio is shown in Figure 6. The tosylate methyl gave a fairly straight line which showed the linewidth increased very slightly with decreasing methanol concentration. The linewidth of the methanol methyl appeared to increase rapidly with decreasing methanol concentration until the ratio of nitroxide to methanol was 0.5 and then remain constant. This suggested that at this ratio of nitroxide to methanol, all the methanol was bound to nitroxide, whereas at lower ratios, that is with more methanol, there was an equilibrium between bound and free methanol, thus reducing the overall linewidth. However, further investigation of this would be required to substantiate these findings.

The gentle increase of the tosylate methyl linewidth could be the result of increased association between the nitroxide molecules as the methanol concentration decreases, or it could be due to small changes in the viscosity resulting from the changing percentage of methanol present.

There was thus strong evidence that there is interaction between the methanol and nitroxide molecules, and some evidence for a species involving one nitroxide and two



Figure 6. Plot of linewidth (Hz) of methyl signals of tosylate nitroxide and methanol against nitroxide: methanol molarity ratio.





methanol molecules, rather than one of each. The magnitude of the methanol methyl linewidth suggested a fairly close association.

(ii) constant methanol molarity

With a methanol molarity of 0.4M, the nitroxide molarity was increased from 0.001M to 0.1M, by which concentration the hydroxyl peak was no longer observable. Significant changes were found in the chemical shifts of the two peaks; these are given in Table 10.

Table 10. Displacement of methanol peaks, in Hz, on addition of tosylate nitroxide.

Conc. nitroxide, <u>M</u>	CH <sub>3</sub>	OH
.001	-0.3	+6.9
.005	-1.7	+26.1
.01	-2.7	+27.3
.1	-26.1	

The methyl peak showed a linear increase of shift with nitroxide molarity but the hydroxyl peak did not.

As was found independently by Morishima<sup>201</sup>, studying the effect of increasing concentrations of di-*t*-butyl nitroxide on methanol in carbon tetrachloride solution, the hydroxyl peak experienced an upfield shift; however the methyl peak moved downfield only in neat methanol solution, remaining almost unaffected in carbon tetrachloride solution. The hydroxyl peak shift change was at least ten times the magnitude of the methyl shift change here, whereas Morishima,



using a solution of  $1 \times 10^{-4}M$  nitroxide in neat methanol, found a ratio of shift displacements of about 5. In his solutions in carbon tetrachloride solvent, the methyl peak did not appear to be displaced, although shifts of up to 60 Hz were observed for the hydroxyl peak. Thus, although the different nitroxides and/or the different concentrations used show up certain differences, the two systems are rather similar.

It would appear that the intermolecular association observed here is indeed due to hydrogen bonding.

#### (F) CONCLUSION

Without more sensitive N.M.R. instruments, the dilution of the radical required to eliminate intermolecular broadening made the system of little worth in structure determination. Information is obtainable by extrapolation to infinite dilution, but this was not ideal. Choice of a low viscosity solvent, though helpful, was not adequate.

The selective association type of system might be capable of development as a useful tool but requires much deeper investigation.



PART VCOBALT COMPLEXES.

In an attempt to find a system in which selective paramagnetic shifts could be used in structure determination of organic molecules, complexing with cobalt(II) was investigated. Cobalt(II) was chosen as the paramagnetic species as it appeared to be the most favourable transition metal ion in producing sizeable shift changes while retaining fairly narrow lines<sup>238</sup>. Cobaltous acetylacetonate has been considerably used with some degree of success, see Part II, section G(c), but it was thought that other cobalt(II) systems might prove superior.

Addition of a commercially available cobalt salt to a solution containing a potential ligand has the advantage of simplicity in preparation of samples; however, most cobalt salts are not soluble in organic solvents while most organic compounds are not soluble in aqueous solution. Cobalt perchlorate, however, is soluble in acetone, as are many organic compounds, and so this system was chosen for study.

Since different ligands complex to different extents, it would be useful, as with the ferrocene system, to have a reference proton in the ligand molecule with which the shifts of the other protons could be compared<sup>239</sup>. It was therefore decided to investigate first the potential of complex formation of ligands containing the group  $\text{CH}_2\text{CN}$  with cobalt salts. This group seemed to have three desirable features:



- (1) it contains a readily distinguishable methylene signal capable of being used for normalisation
- (2) the group would appear suitable as a "plug-in ligand" (e.g. complex alcohols could be converted to their cyanoacetates).
- (3) experience in this Department with simple alkyl cyanides showed that complexing of these with cobalt(II) gave fairly large shifts without excessive broadening<sup>240</sup>.

Cyanides have not been greatly studied to date<sup>101</sup>.

The value of using a reference proton in the ligand for "normalisation" of the shifts depends on the extent to which the "normalisation factor", that is the ratio of the displacement of the shift of a given proton to that of the reference proton, measured as a percentage, stays constant, independent of ligand and cobalt concentrations and preferably also of the presence of water and the nature of the solvent.

Preliminary work was therefore carried out with ethyl cyanoacetate and also with propionitrile, two simple ligands both containing a  $\text{CH}_2\text{CN}$  group and representing two types of cyanides. Organic molecules of known structure were then used to test the applicability of the system. Difficulties encountered in the preparation of cyanoacetates then led to an investigation of other ligand types, principally alcohols and amides. Finally, some of these ligands were investigated using cobaltous acetylacetonate for comparison of the two paramagnetic systems.



## (A) EXPERIMENTAL

(a) Preparation of compounds

First are detailed the preparations of various cyanoacetates and other ligands and purification of samples where required, then the preparations of the cobalt reagents are given. Those ligands not described were commercial or departmental samples used without further purification.

(i) Menthyl cyanoacetate

The preparation of menthyl cyanoacetate was investigated in some detail. Esterification, using the acid chloride under different conditions, was unsuccessful. The acid chloride, prepared by stirring the acid in thionyl chloride, appeared to be formed, but reaction of it with menthol in dried pyridine was very vigorous, the product after purification being a red oil containing no cyanoacetate. Use of dried benzene as solvent and maintaining the temperature below  $0^{\circ}$  during the addition of the alcohol to the acid chloride, did not improve the preparation.

Direct esterification<sup>241</sup>, using trace toluene-*p*-sulphonic acid as catalyst in benzene solvent, was used. The product, shiny, white crystals, was obtained in 35% yield (lit. 55%), m.p.  $83-84^{\circ}$  (lit. m.p.  $83-84^{\circ}$ ). I.R. spectrum ( $\text{CCl}_4$  solution) showed a strong carbonyl absorption at  $1730\text{cm}^{-1}$ , a cyanide absorption at  $2300\text{cm}^{-1}$  and many strong peaks in the region  $1460-860\text{cm}^{-1}$ .

The direct esterification method was improved by using ethylene dichloride solvent under the following conditions. Menthol (1g; 6.4 mmole), cyanoacetic acid (1.1g; 13.0 mmole)



and a trace of toluene-p-sulphonic acid in 40ml ethylene dichloride were heated together on a boiling-water bath for 50 hours, using a Dean and Stark apparatus. No water visibly separated in the Dean and Stark column, but on cooling two layers formed in the flask. On further standing white crystals formed. The mixture was poured into water (white crystals redissolved), and extracted with ether. The ether layer was washed with sodium bicarbonate solution, then water, dried over magnesium sulphate and evaporated under reduced pressure to give 1.34g (94%) white solid whose N.M.R. spectrum was consistent with that expected for menthyl cyanoacetate. Crystallisation from a small volume of benzene-methanol gave white crystals, m.p. 82-84°. This method was thus the most satisfactory.

(ii) Cholesteryl cyanoacetate

Variations on the direct esterification methods used for the menthyl ester were tried here, the best method again using ethylene dichloride as solvent and the same concentrations of reactants. Although this method gave the purest product, melting-point 173-177° prior to chromatography (lit. m.p. 182-183°), the yield was rather low (28%). The product was purified by eluting through a silica column with light petroleum-benzene through benzene to benzene-chloroform, the ester being eluted with the benzene and having a melting-point of 190°.

(iii) Dihydrotestosterone cyanoacetate (cyanoacetate of 5 $\alpha$ -androstan-17 $\beta$ -ol-3-one).

The direct esterification in ethylene dichloride was



again the method used here. The product contained a considerable amount of unreacted alcohol although excess acid had been used, and separation of alcohol and ester proved difficult. Crystallisation resulted in the compounds co-crystallising, and column chromatography, using either silica or neutral alumina columns, caused hydrolysis of the ester.

Three consecutive preparations were therefore carried out, returning the product of each preparation for further reaction with more acid. This greatly increased the ratio of ester to alcohol, and T.L.C. of the final product showed very little alcohol. The ester was crystallised, with some difficulty, from a large volume of light petroleum (b.p. 40-60°) giving a fine, white, crystalline solid, which after drying over phosphorus pentoxide under reduced pressure, had a melting-point of 135-137° and N.M.R. spectrum consistent with dihydrotestosterone cyanoacetate.

(iv) p-acetamidotoluene

This amide was prepared by the standard method from p-toluidine and glacial acetic acid as white needles, m.p. 149-151°, or pale grey plates, m.p. 150-152°, mixed m.p. 148-151° (lit. m.p. 146.5-147.5°<sup>242</sup>). The N.M.R. spectrum showed water to be present in the amide even after 24 hours in a dessicator over phosphorus pentoxide under reduced pressure.

(v) N-methyl-p-acetamidotoluene

This was prepared by methylation of p-acetamidotoluene. Initially this was attempted by the method of Johnson and



Riggs<sup>243</sup> using purified and dried methyl iodide in xylene. The sodium salt was formed quite satisfactorily but methylation did not take place.

The method of Mills and Kelham<sup>244</sup> was then investigated. It was found that the volume of dimethyl sulphate used was critical as separation of the product from it was not easy. The best conditions were as follows.

Sodium metal (0.16g; 6.9 mmole), cut into small pieces, and p-acetamidotoluene (1g; 6.7 mmole) were boiled together under reflux for 2½ hours in sodium-dried, redistilled toluene, a white solid of sodium salt forming. After cooling, dimethyl sulphate (0.64ml; 6.7 mmole) was added slowly, a little heat being evolved. The heating was continued for 1½ hours, the white solid going into solution fairly quickly leaving a whitish gel of sodium sulphate at the foot of the flask. After cooling again, water (3ml) was added and the two layers were separated. The toluene layer was dried over magnesium sulphate and evaporated under reduced pressure, leaving an orange-brown oil which crystallised on standing. The whitish crystals were recrystallised from light petroleum giving colourless, rod-like crystals in 27% yield, m.p. 78-79° (lit. m.p. 79.5°<sup>243</sup>). The N.M.R. spectrum indicated pure N-methyl-p-acetamidotoluene.

The following compounds were available without preparation and were purified as follows.

(vi) Cholesterol

Commercial cholesterol was purified by forming the dibromide then reducing it back to cholesterol with zinc dust<sup>245</sup>.



A 60% yield was obtained, m.p.  $148^{\circ}$  (lit. m.p.  $149.5-150^{\circ}$ ). The cholesterol was dried by dissolving in sodium-dried benzene which was then removed by evaporation under reduced pressure, then in a drying pistol at  $100^{\circ}$ , and was stored in a desiccator over phosphorus pentoxide.

(vii) Methyl 4,6-O-benzylidene- $\alpha$ -D-glucopyranoside

The sugar diol was crystallised from 1:1 ethanol:water, m.p.  $163-165^{\circ}$  (lit. m.p.  $163-164^{\circ}$  <sup>246</sup>).

(viii) Penta-O-acetyl- $\alpha$ -D-glucopyranose

The ester was crystallised from 1:1 ethanol:water, m.p.  $105-108^{\circ}$  (lit. m.p.  $112-113^{\circ}$  <sup>247</sup>).

(ix) Methyl 2,3,4,6-tetra-O-acetyl- $\alpha$ -D-galactopyranoside

This was also crystallised from 1:1 ethanol:water, m.p.  $83-85^{\circ}$  (lit. m.p.  $86-87^{\circ}$  <sup>248</sup>).

(x) Menthol

The menthol was dried by storing in a desiccator over phosphorus pentoxide, after being finely powdered.

(xi) Testosterone (Androst-4-en-17 $\beta$ -ol-3-one)

This was crystallised from 1:1 ethanol:water, m.p.  $151-153^{\circ}$  (lit. m.p.  $155^{\circ}$  <sup>249</sup>).

(xii) Cholestan-3-one

This was crystallised from acetone, m.p.  $126-127^{\circ}$  (lit. m.p.  $129^{\circ}$  <sup>250</sup>).

The remaining ligands were used without further purification.



(xiii) Dehydrated cobalt perchlorate

Cobalt perchlorate,  $\text{Co}(\text{ClO}_4)_2 \cdot 6\text{H}_2\text{O}$  (Fluka), was dried over phosphorus pentoxide in a drying pistol heated by boiling water, for several weeks. Zinov'ev and Naumova<sup>251</sup> have found that drying under these conditions gives the dihydrate salt, and Hathaway and coworkers<sup>252</sup> have found that in the dihydrate salt, the two perchlorate groups are covalently bound through two of their oxygen atoms, the water binding axially in the remaining two sites of the six-coordinated cobalt. Loss of weight on drying the salt and N.M.R. investigation, by measuring the increase in the water peak in a  $\text{D}_2\text{O}$  solution on addition of the dried salt, both confirmed that the dried salt was the dihydrate. The salt was stored over phosphorus pentoxide under reduced pressure, and showed no subsequent gain in weight.

(xiv) Cobaltous acetylacetonate

A stock sample of cobaltous acetylacetonate was crystallised from methanol. The solvated complex was dried over boiling carbon tetrachloride in a drying pistol for several days prior to use.

(b) Preparation of solutions for N.M.R.(i) Solvents

Deuteroacetone (Ciba, 99 atom % D) solvent was used for all the cobalt perchlorate solutions, for solubility reasons. The N.M.R. spectrum of the deuteroacetone showed a very small water peak which could be due either to a small trace of  $\text{H}_2\text{O}$  or to HOD in which case rather more water might have been present as  $\text{D}_2\text{O}$ . The presence of water was critical



in these solutions and so this was further investigated.

To distinguish between the two possibilities, some methanol was added. The N.M.R. spectrum of the solution showed a second-order methanol peak pattern, and so the solution was run at higher temperatures to separate the two signals and thus create a first order spectrum. The integral then showed the ratio of methanol:hydroxyl protons as 3:0.7 whereas it should have been 3:1, showing that the hydroxyl peak had been partially deuterated and so the deuterioacetone contained  $D_2O$  as well as  $H_2O$ .

The spectra of these methanol solutions showed distinct HOD and  $H_2O$  signals, the latter a singlet, the former a broadened 1:1:1 triplet. A similar isotope effect has been observed by Gold and Tomlinson<sup>253</sup>.

To remove both  $H_2O$  and  $D_2O$ , the deuterioacetone was stored in contact with oven-dried 4a molecular sieves, as described in Part III, Section A(c)(ii).

Deuteriochloroform (NMR Ltd., > 98.8% D) used in the steroid solutions and all cobaltous acetylacetonate work, was similarly dried over oven-dried 4a molecular sieves.

#### (ii) Sample preparation

Solutions were prepared by direct weighing of the cobalt salt into the graduated 0.5ml flasks. Solid ligands were similarly weighed into the flasks, while liquid ligands were added using a Hamilton syringe of suitable volume. The solutions were then made up to the mark with the deuterioacetone which contained 3% TMS for an internal reference.

The steroids were not sufficiently soluble in deuterio-



acetone and 0.2ml of deuteriochloroform containing 3% TMS was added before making up to the mark with deuterioacetone. In solutions which gave spectra with signals close to the TMS signal, AnalaR benzene (25  $\mu$ l), added before making up to 0.5ml with deuterioacetone containing no TMS, was used as locking signal, a trace of TMS then being added as reference signal.

Solutions using cobaltous acetylacetonate were prepared in the same way as with the cobalt salt, but deuteriochloroform containing 3% TMS was used as solvent throughout.

(c) Instrumental conditions

All spectra were recorded using a Varian HA 100 (100 M Hz) spectrometer at probe temperature of 28°. Shifts were measured on sweep width 100 Hz by setting the recorder pen on the maximum pen deflection for the peak and reading the position of it relative to the lock on a frequency counter. Linewidths were measured as described in Part III, Section A(a)(i).

(B) DETAILED INVESTIGATION OF SIMPLE MODEL COMPOUNDS: ETHYL CYANOACETATE AND PROPIONITRILE.

(a) Ethyl cyanoacetate

AnalaR ethyl cyanoacetate was used without further purification.

Investigations were carried out using solutions which were 1.0M, 0.5M and 0.1M in cyanide, CN, and 0.1M, 0.2M and 0.5M in cobalt(II) perchlorate.

Line positions in the absence of Co(II), which will be



referred to here as the "diamagnetic line positions", are given in Table 11. The acetone peak is a quintet arising predominantly from the species  $\text{CD}_3\text{COCD}_2\text{H}$  giving a proton signal coupled to two deuteriums ( $I=1$ ).

**Table 11.** Diamagnetic line positions, in Hz downfield from TMS, of signals in ethyl cyanoacetate.

Solvent	Conc. ligand, <u>M</u>	$\text{CH}_2\text{CN}$	$\text{CH}_2$	$\text{CH}_3$	Acetone
A	1.0	376.9	421.8	126.4	205.2
A	0.5	377.9	421.7	126.4	205.0
A	0.1	378.7	421.7	126.2	204.8
A/C	1.0	366.5	423.5	129.4	209.2

A: deuterioacetone;

A/C: 1:1 deuterioacetone:deutero-chloroform.

The concentration of cyanide has a small effect on the position of the  $\text{CNCH}_2$  peak but the ethyl peak positions are essentially constant. The change of solvent has a greater effect.

Displacements of the signals on the addition cobalt(II) perchlorate are given in Table 12, in Hz relative to the signal position in the diamagnetic solution at the same cyanide concentration. Acetone displacements are also given.

All the shifts are to higher fields (positive sign), and, as expected, they decrease in magnitude in the order  $\text{CH}_2\text{CN} > \text{CH}_2 > \text{CH}_3$ .

Table 12 shows that the shift changes are sufficiently large to be diagnostically useful.



Table 12. Displacements (all positive) in Hz, of signals in ethyl cyanoacetate on addition of cobalt(II) perchlorate.

Conc. ligand, <u>M</u>	Conc. Co(II), <u>M</u>	CH <sub>2</sub> CN	CH <sub>2</sub>	CH <sub>3</sub>	Acetone
1.0	0.10	193.8	25.6	15.4	13.9
	0.20	389.8	51.1	30.8	28.3
	0.50	920.5	118.2	70.0	71.3
0.5	0.10	211.3	28.2	17.4	16.1
	0.20	421.6	55.9	34.4	33.8
	0.50	983.4	127.8	76.0	85.1
0.1	0.10	238.0	32.1	20.0	18.8
	0.20	458.2	61.5	37.9	39.3
	0.50	1054.0	137.4	82.9	99.6

Although the results for 0.1M and 0.2M cobalt(II) suggest that the displacements of the signals are proportional to the cobalt molarity, the results at 0.5M cobalt(II) show a significant departure from linearity. The proportionality was best with higher cyanide concentrations.

The normalisation factors for the ester peaks relative to the CNCH<sub>2</sub> peaks, calculated from individual shift changes, are given in Table 13.

Table 13. Normalisation factors, expressed as percentages, for the ester peaks of ethyl cyanoacetate.

Conc. Co(II), <u>M</u>	1.0M CN		0.5M CN		0.1M CN	
	CH <sub>2</sub>	CH <sub>3</sub>	CH <sub>2</sub>	CH <sub>3</sub>	CH <sub>2</sub>	CH <sub>3</sub>
0.1	13.2	7.95	13.4	8.24	13.5	8.40
0.2	13.1	7.90	13.2	8.16	13.4	8.27
0.5	12.8	7.61	13.0	7.73	13.0	7.86



The normalisation factors were adequately constant to distinguish between neighbouring protons using only one solution. The fact that plots of the shifts of the protons against that of the reference protons, the normalisation plots, are essentially straight lines whose gradients give the normalisation factors (Figure 6') will be useful in the assignment of signals in spectra of more complicated molecules in the presence of cobalt(II) perchlorate.

The average normalisation factors calculated from Figure 6 were

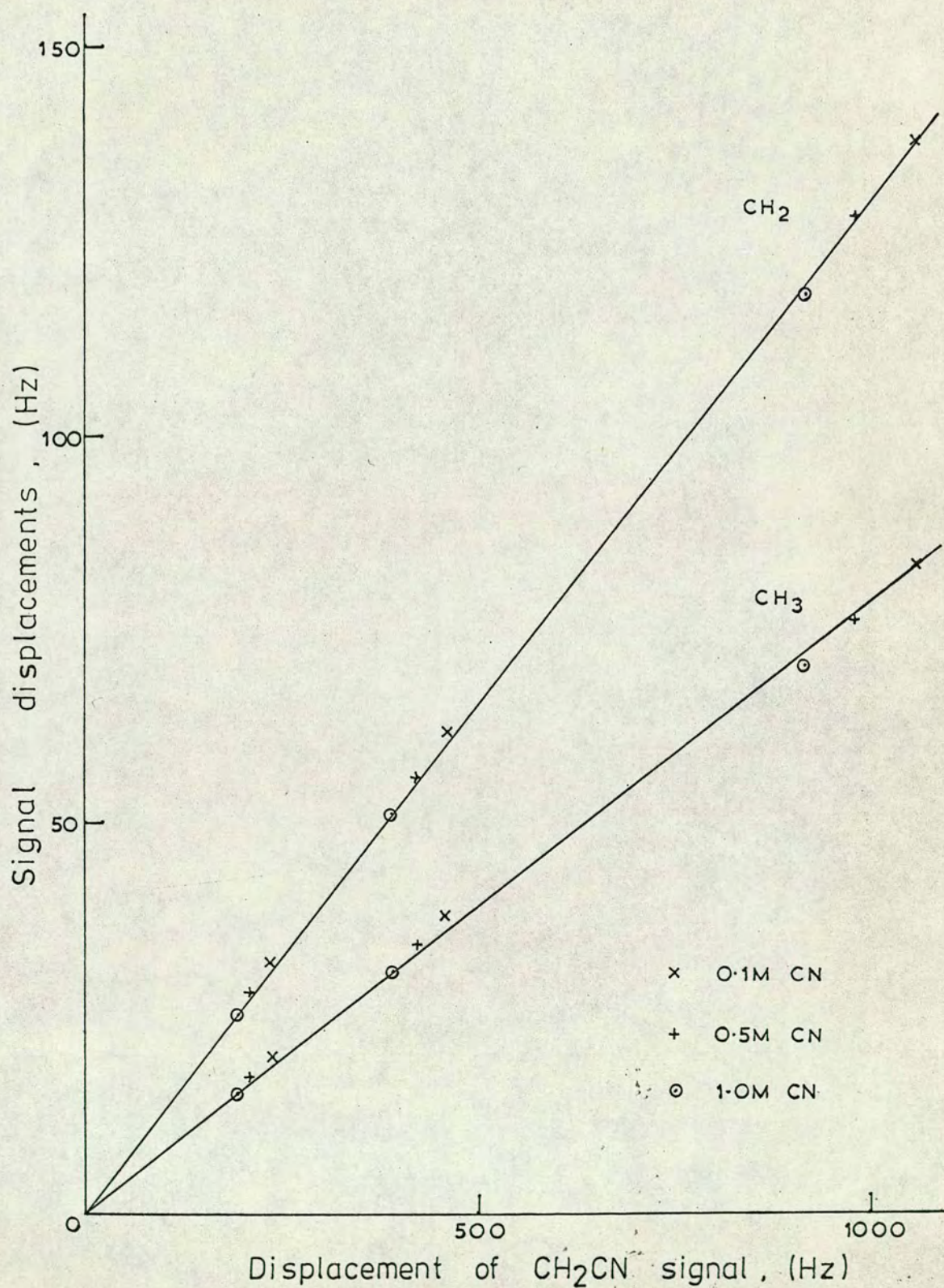
$$\text{CH}_2: 13.0\% ; \text{CH}_3: 8.0\%.$$

Close examination shows that the normalisation factors increased slightly both with decreasing cyanide and decreasing cobalt concentrations.

Decreasing the ligand concentration increased the shift changes observed. This effect provides quite a useful monitor of the strength of the complex being formed, provided that other factors, such as a change in nature of the complex, are not also affecting the shifts. In a solution containing excess ligand, if the complex formation is very strong then the shifts for a given cobalt concentration will be inversely proportional to the ligand concentration,  $S \propto 1/L$ , or  $S_1/S_2 \times L_1/L_2 = 1$  where  $L_1$  and  $L_2$  are the first and second concentration of ligand having shift displacements of  $S_1$  and  $S_2$  respectively. On the other hand, if complexing is very weak, then the shift changes are effectively independent of ligand concentration and  $S_1/S_2 = 1$  for all values of  $L_1$  and  $L_2$ . To compare the degree of complexing occurring with different ligands, it would be useful to have a numerical scale



Figure 6'. Normalisation plots for ethyl cyanoacetate on addition of cobalt(II) perchlorate.





to express this, such that 1 (or 100%) represents very strong complexing and 0 (or 0%) represents very weak complexing. One can therefore use the expression,  $E = (1 - S_1/S_2)(1 - L_2/L_1)^{-1}$ , as an approximate measure of the strength of complexing, this expression being 0 when  $S_1/S_2 = 1$  and 1 when  $S_1/S_2 = L_2/L_1$ . This expression will give values representative of the degree of complexing occurring but these values have no absolute chemical significance, purely forming a scale.

In the case of ethyl cyanoacetate, the expression had a value from 12% to 20% indicating that complexing was rather weak.

The shift to linewidth ratios of the  $\text{CH}_2\text{CN}$  peak, where measurable, are presented in Table 14.

Table 14. The ratio of the shift displacement, in Hz, to the linewidth at half peak-height, in Hz, for the  $\text{CH}_2\text{CN}$  peak of ethyl cyanoacetate.

Conc. cyanide, <u>M</u>	Conc. Co(II), <u>M</u>	Linewidth, $\frac{\Delta\nu_{1/2}}{\text{Hz}}$	Shift: line- width ratio
1.0	0.50	33	27.9
0.5	0.10	8.9	23.7
0.5	0.50	32	30.6
0.1	0.10	9.2	25.9
0.1	0.50	29	36.4

The values, which increased with increasing displacement, were quite acceptable for selective shift studies.

Increasing the temperature caused a definite decrease in both the shifts and the linewidths. The shift to line-



width ratio for the  $\text{CH}_2\text{CN}$  singlet in a solution 1.0M in cyanide and 0.5M in cobalt(II) increased to 44.0 at  $50^\circ$ . The normalisation factors stayed fairly constant throughout.

Since it is very difficult to keep N.M.R. solutions completely free of water without using very sophisticated techniques and it is equally difficult to know exactly how much water is indeed present, the effect of water on the shifts was investigated.

The presence of water had a profound effect on the cyanide shift values. Tables 15 and 16 show the results of additions of small volumes of heavy water,  $\text{D}_2\text{O}$ , to two ethyl cyanoacetate/cobalt solutions. The presence of water had only a very small effect on the diamagnetic line positions, as can be seen in Table 17.

**Table 15.** Displacements, in Hz, of signals of 1.0M ethyl cyanoacetate in presence of 0.1M cobalt(II) perchlorate, and normalisation factors, as percentages, on addition of water ( $9 \mu\text{l} \equiv 1\text{M}$ ).

$\mu\text{l D}_2\text{O}$ added	Displacements (all +ve)				Normalisation factors	
	$\text{CH}_2\text{CN}$	$\text{CH}_2$	$\text{CH}_3$	acetone	$\text{CH}_2$	$\text{CH}_3$
0	196.0	25.9	15.6	14.2	13.2	8.0
2	151.7	20.1	11.4	17.3	13.2	7.5
4	117.8	15.8	9.0	15.6	13.4	7.6
6	98.3	13.1	7.5	13.5	13.3	7.6
9	75.5	10.4	5.9	10.7	13.8	7.8
18	41.9	6.5	3.7	5.9	15.5	8.8



Table 16. Displacement, in Hz, of signals of 1.0M ethyl cyanoacetate in presence of 0.5M cobalt(II) perchlorate, and normalisation factors, as percentages, on addition of water.

$\mu\text{l D}_2\text{O}$ added	Displacement (all +ve)				Normalisation factors	
	$\text{CH}_2\text{CN}$	$\text{CH}_2$	$\text{CH}_3$	acetone	$\text{CH}_2$	$\text{CH}_3$
0	897.4	116.4	67.0	68.1	13.0	7.5
2	880.3	111.7	64.6	74.3	12.7	7.3
4	821.2	104.0	58.9	84.2	12.7	7.2
6	811.4	100.8	58.6	86.8	12.4	7.2
9	723.7	90.8	51.0	87.4	12.5	7.1
18	551.3	69.7	39.3	70.6	12.6	7.1

Table 17. Diamagnetic line positions, in Hz relative to TMS, of 1.0M ethyl cyanoacetate on addition of water.

$\mu\text{l H}_2\text{O}$ added	$\text{CH}_2\text{CN}$	$\text{CH}_2$	$\text{CH}_3$
0	377.4	421.7	126.4
2	377.6	421.4	126.1
4	378.0	421.8	126.6
6	378.2	421.8	126.5
9	379.0	421.9	126.3
18	379.8	422.3	126.8

Normalisation plots, that is plots of the displacements of the  $\text{CH}_2$  and  $\text{CH}_3$  peaks against that for the  $\text{CH}_2\text{CN}$  peak, for these two families of solutions were straight lines through the origin giving the average normalisation factors as:



for 0.1M Co(II),  $\text{CH}_2$ : 13.2%;  $\text{CH}_3$ : 7.7%

for 0.5M Co(II),  $\text{CH}_2$ : 12.7%;  $\text{CH}_3$ : 7.2%.

Dilution of the deuterioacetone with an equal volume of deuteriochloroform caused a considerable (about 60%) increase in the shift changes, but normalisation factors were not affected, being

$\text{CH}_2$ : 13.3%;  $\text{CH}_3$ : 8.3%.

It thus appeared that though the actual magnitude of the shift displacement was strongly dependent on cobalt molarity and varied with cyanide molarity, solvent, temperature and the presence of water, the normalisation factors with respect to the  $\text{CH}_2\text{CN}$  protons, remained reasonably constant throughout. The shift to linewidth ratios were also quite acceptable in size, and so, the cyanide/cobalt perchlorate system would appear to have potential as a system for selective shift studies.

#### (b) Nature of the complex and solution

The nature of the complex is difficult to establish since several species are undoubtedly involved, cyanide, acetone and water molecules and perchlorate ions in addition to the cobalt ions. However it was possible to establish some characteristics.

The cobalt salt was dissolved in deuterioacetone to give a solution 0.5M in cobalt (II), that is with a ratio of cobalt ions to acetone molecules of 1:27.3. This gave an acetone shift displacement of +101.0 Hz. When the cobalt salt is dissolved in the acetone, the perchlorate groups will be displaced by acetone ligands<sup>254</sup>. The two water molecules may



also be displaced, perhaps in part. Thus each cobalt would be expected to coordinate between four and six acetone molecules.

If each cobalt coordinated to four acetone molecules, then the shift displacement of a bound acetone molecule would be +689 Hz, whereas if each cobalt coordinated to six acetones, it would be +460 Hz.

In a similar way, the cobalt salt was dissolved in neat ethyl cyanoacetate to form a solution with the ratio of cobalt ions to cyanide molecules 1:127. The  $\text{CH}_2\text{CN}$  proton peak displacement was +48.8 Hz.

If each cobalt coordinated to four cyanide molecules, then the shift displacement of a bound acetone molecule would be +1550 Hz, whereas if each cobalt coordinated to six cyanides, it would be +1035 Hz.

It should now be possible in each solution containing both acetone and cyanide molecules to calculate the number of acetone and cyanide ligands coordinated to a cobalt ion.

This is provided that various conditions are fulfilled:

- (1) the axial positions are occupied by water molecules only
- (2) the conformation of a ligand in the complex is unaffected by the nature of the other ligands
- (3) the  $g$ -factor anisotropy is independent of the nature of the ligands.

These conditions are unlikely to be fulfilled; indeed the fact that the normalisation factors for the  $\text{CH}_2$  and  $\text{CH}_3$  signals in neat ethyl cyanoacetate are +0.2% and -2.5% respectively shows that they are not fulfilled for the ethyl signals although they may be for the  $\text{CH}_2\text{CN}$  signal.



Although subject to these reservations, the results in Table 18 are interesting. This table shows the number of ligands bound to each cobalt in the various solutions. They are calculated as indicated above, assuming that two water molecules remain coordinated throughout. (If no water is coordinated, the resulting ratios should be multiplied by 1.5).

Table 18. Number of cyanide and acetone ligands per cobalt ion in solutions of ethyl cyanoacetate.

Conc. cya- nide, <u>M</u>	Conc. Co(II), <u>M</u>	* Sol- vent	CH <sub>2</sub> CN Displace- ment	No. of CN lig- ands per Co ion	Acetone Dis- place- ment	No. of acetone ligands per Co ion	No. of CN plus acetone ligands per Co ion
1.0	0.10	A	193.8	1.22	13.9	2.70	3.92
	0.20		389.8	1.24	28.3	2.76	4.00
	0.50		920.5	1.19	71.3	2.82	4.01
0.5	0.10		211.3	0.68	16.1	3.18	3.86
	0.20		421.6	0.68	33.8	3.34	4.02
	0.50		983.4	0.63	85.1	3.36	3.99
0.1	0.10		238.0	0.15	18.8	3.72	3.87
	0.20		458.2	0.15	39.3	3.88	4.03
	0.50		1054.0	0.14	99.6	3.93	4.07
1.0	0.10	A'	146.5	0.95	15	2.96	3.91
	0.10	A'/C	235.6	1.52	15.3	1.51	3.03

\* See Table 11

A': undried deuterioacetone.

The calculations assumed a constant acetone molarity of 13.6M although this must have varied slightly from solution to solution.



Despite the large inaccuracies involved the resulting ratio of cobalt ions to acetone plus cyanide ligand molecules is very close to 1:4.00, the theoretical value, in every case.

The results from two further solutions are shown at the foot of Table 18. The first was similar to those above but was prepared with undried deuterioacetone. As expected the number of cyanide ligands complexed has decreased but the number of acetones has apparently increased giving a falsely high ratio of 1:3.91. The reason for this apparent increase is given below (Addition of water) and shows that the required conditions for these calculations are not satisfied. The second solution was in 1:1 deuterioacetone: deuteriochloroform solvent but otherwise identical to the first solution. The apparently low ratio of 1:3.03 can be explained by the fact that the deuterioacetone was undried and so some cyanide and acetone ligands were replaced by water. However, little weight can be put on this ratio for the same reason as for the first solution.

#### Addition of water

It should be possible by observing the acetone shift changes produced by addition of small volumes of water to a solution of cobalt perchlorate in acetone, ~~by observing the acetone shift changes,~~ to estimate the number of acetone molecules coordinated and hence the number of water molecules displacing the acetones at any given water concentration.



Table 19. Displacements, in Hz, of acetone signal on addition of water to a solution 0.5M cobalt(II) perchlorate in deuterioacetone (9  $\mu$ l water = 1M)

$\mu$ l H <sub>2</sub> O added	-	2	4	6	9	18	27
Acetone displacement (all +ve)	101.0	109.0	114.5	114.4	110.8	85.9	65.7

However, as Table 19 shows, the acetone displacements first increased before decreasing showing that the shifts were being affected by the nature of the complex. This finding was analogous to the observations of Horrocks and co-workers<sup>255</sup> who found that when some ligands were introduced into aqueous solutions of cobalt(II), the water shift increased rather than decreased although water was being replaced by ligand molecules. They interpreted their results in terms of an increased pseudocontact contribution to the total observed shift.

Because of this increase it was not possible to estimate the number of water molecules coordinated. This increase in the shift changes could also explain the apparently high ligand to cobalt ratio found in the undried acetone solution (Table 18), the closeness of the other ratios to 1:4.00 being remarkable.

This maximum in the acetone shift changes was also observed during water additions to solutions containing cyanide ligands in the presence of cobalt(II), see Tables 15 and 16. The maxima in the shift displacements occurred at



a cobalt:added water ratio of 1:1.5-2.0 when 1.0M cyanide was present but at a ratio of 1:1.1-1.3 when no cyanide was present. This could be indicative of the different complexes present in the two cases or could be due to a greater percentage of water being required to displace cyanide from the complex than to displace only acetone which is less firmly held.

The fact that both the cyanide shifts and, eventually, the acetone shifts decreased on addition of water showed that the water replaced both ligands. Since the decreases were gradual, this must be an equilibrium situation. It is possible that, in the absence of added water, the two water molecules already present with each cobalt were also to some extent replaced by acetone or cyanide ligands but axial ligands may be more strongly held and so an equilibrium situation may not necessarily apply to them also.

In conclusion, the nature of the complex is rather variable. Probably in the solutions here studied, between four and five sites were occupied by cyanide and acetone, their exact ratio depending on the various concentrations in solution. The remaining one to two sites were occupied by water, and additional water readily, though not irreversibly, replaced both cyanide and acetone ligands. The changing nature of the complex could thus account very easily for the small variations in the normalisation factors, their relatively good concordancy being perhaps remarkable.

### (c) Propionitrile

Propionitrile (Koch-Light) was used without further purification. Drying over oven-dried 4a molecular sieves



had no effect on the results, so the cyanide was assumed water-free.

Investigations were carried out using solutions that were 1.0M, 0.5M and 0.1M in cyanide and 0.1M, 0.2M and 0.3M in cobalt(II). Displacements of the N.M.R. signals on addition of cobalt(II) were measured in Hz relative to the signal position in the cobalt-free solution (Table 20) at the same cyanide concentration. All displacements were to higher fields. Table 21 gives the displacements of the cyanide and acetone signals and the normalisation factors of the  $\text{CH}_3$  peak with respect to the  $\text{CH}_2\text{CN}$  peak.

Table 20. Diamagnetic line positions, in Hz downfield from TMS, of the signals in propionitrile.

Conc. ligand, <u>M</u>	$\text{CH}_2\text{CN}$	$\text{CH}_3$	Acetone
1.0	242.5	122.2	204.8
0.5	242.9	122.3	204.7
0.1	243.2	122.8	204.7

Table 21. Displacements of N.M.R. peaks of propionitrile, in Hz, and normalisation factors of  $\text{CH}_3$  peak, as percentages, on addition of cobalt(II) perchlorate.

Conc. ligand, <u>M</u>	Conc. Co(II), <u>M</u>	Displacements (all +ve)			Normalisation factor for $\text{CH}_3$
		$\text{CH}_2\text{CN}$	$\text{CH}_3$	Acetone	
1.0	0.10	368.0	113.3	1.7	30.8
	0.20	743.8	239.7	5.4	32.2
	0.30	1068.8	342.8	10.9	32.1
0.5	0.10	501.5	165.4	8.3	32.0
	0.20	934.0	308.5	19.4	33.1
	0.30	1295.1	423.6	31.8	32.7
0.1	0.10	641.4	217.1	16.4	33.8
	0.20	1137.7	383.0	35.6	33.6



The shift changes in this case were nearly twice as great as those of comparable solutions of ethyl cyanoacetate, perhaps due to stronger complexing.

The plots of the shift changes against the cobalt molarity showed much greater curvature than for ethyl cyanoacetate (as would be expected for a greater degree of complexing), the curves being most pronounced at lower cyanide concentrations.

The normalisation factors were fairly concordant although they increased slightly with decreasing cyanide molarity. The average normalisation factor for each cyanide concentration, calculated from the gradient of normalisation plots, were 31.9% (for 1.0M CN), 32.9% (for 0.5M CN) and 33.7% (for 0.1M CN).

The shifts were considerably more dependent on cyanide concentration here than with the cyanoester, again suggesting a greater degree of complexing. The expression  $(1 - S_1/S_2)(1 - L_2/L_1)^{-1}$  gives the range of "strength of complexing" here to be from 34% to 54%.

Estimation of the number of cyanide molecules complexed to each cobalt ion was not possible here as the cobalt salt, when dissolved in the neat cyanide gave a green precipitate. It was obvious, however, see Table 21, that the acetone peak displacements were much smaller in this case suggesting more cyanide was complexed.

Individual shift to linewidth ratios for the propionitrile were not readily measured as the  $\text{CH}_2\text{CN}$  signal was a quartet and the  $\text{CH}_3$  a triplet. The average ratio was calculated,



from the gradient of the plot of shift change against linewidth (Figure 7) to be  $3/4$ , which is quite acceptable.

As in the case of ethyl cyanoacetate<sup>ta</sup>, the shifts are greatly affected by the addition of water but normalisation factors are reasonably independent.

Thus, the propionitrile shifts were found to be greater, and more strongly dependent on cyanide concentration, than those of the ethyl cyanoacetate, and again the presence of water had a profound effect, but, as with the ester, the normalisation factors with respect to the  $\text{CH}_2\text{CN}$  peak displacement remained reasonably constant and the shift to linewidth ratio was again acceptable.

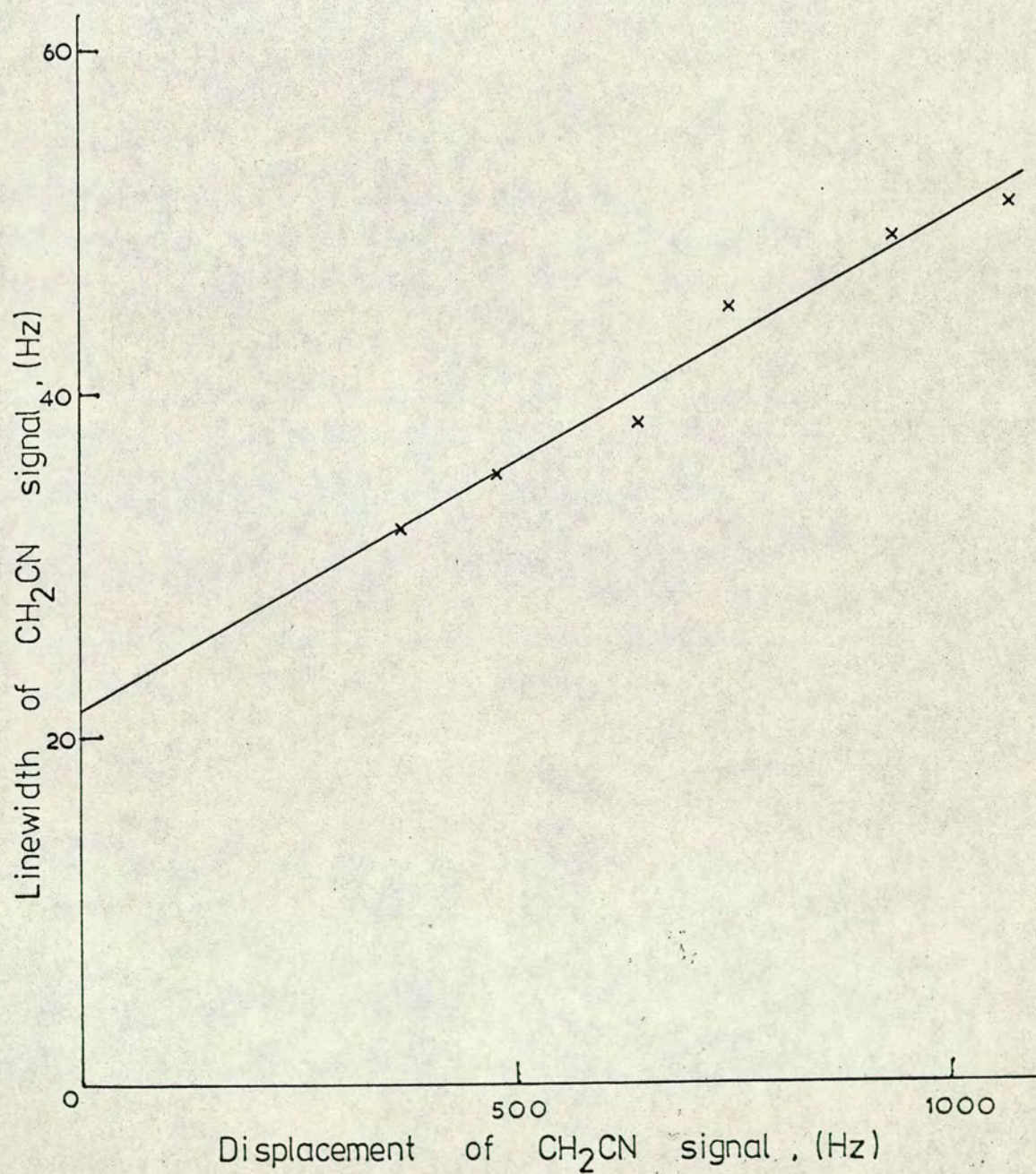
(d) Shifts in the absence of complex formation, ("non-complexing shifts").

In the propionitrile solutions, the substantial upfield movement of the signals on addition of cobalt(II) caused the peaks to move through the TMS signal thus making it unsuitable for a locking signal. Benzene would seem to be a more suitable lock provided the signal remained unmoved on addition of cobalt.

Shifts unrelated to complex formation did in fact occur, as was shown by the displacement of cyclohexane relative to TMS on addition of cobalt. The displacement was small, about 0.5 Hz with 0.2M Co(II) and 0.5M cyclohexane in deuteroacetone, and was water independent. Ethyl benzene also showed small shifts which seemed to be made up of two parts, one water dependent, the other water independent. With 0.2M Co(II) and 0.5M ethyl benzene, the latter was found to be 2.0 Hz for



Figure 7. Plot of linewidth (Hz) against shift displacement (Hz) for  $\text{CH}_2\text{CN}$  signal of propionitrile on addition of  $^{59}\text{Co}(\text{II})$  perchlorate.





the aromatic protons, 1.2 Hz for the  $\text{CH}_2$  and 0.6 Hz for the  $\text{CH}_3$ . The water dependent shifts were smaller.

Care would thus need to be taken in the choice of internal standard. The TMS itself might well be subject to shifts caused by interactions with the paramagnetic species but since this molecule is non-polar and highly symmetrical, the effects might be expected to be small. The best procedure would thus seem to be to have at least a small signal of TMS in every spectrum to act as an internal reference when an alternative locking signal is used, and this was done in the work described here whenever benzene was used as an auxiliary lock.

In a related study, the possibility that ethyl cyanoacetate might be complexing at more than one site was investigated by examining the behaviour of ethyl acetate. Small shifts, 9.8 Hz for the acetyl  $\text{CH}_3$ , were found for 1.0M ethyl acetate with 0.1M  $\text{Co(II)}$ . This is probably due to weak complexing at the carbonyl group, borne out by the smaller displacements found for the more distant protons, 2.4 Hz for the ester  $\text{CH}_2$ , the ester  $\text{CH}_3$  being unchanged. These shifts were water dependent, suggesting again they arose from definite complexing with the cobalt. They could also be present in the ethyl cyanoacetate, but would change the results very little.



### (C) INVESTIGATION OF MORE COMPLEX MOLECULES

The detailed study of ethyl cyanoacetate and propionitrile ligands with cobalt(II) perchlorate has shown that this type of system may well be suitable for use in selective shift studies. Although having the disadvantage of involving complexes of variable and unspecifiable composition, this did not seem to remove the effectiveness of the system and was well compensated by the ease of preparation of N.M.R. samples. If the system were equally applicable to other ligands, then its scope would be greatly broadened and preparative difficulties in formation of cyanoacetates would be circumvented.

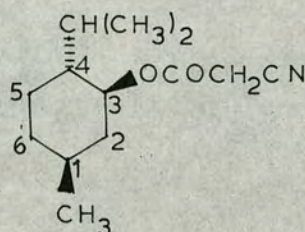
It thus remained to ascertain the applicability of the method with more complex cyanide ligands of known structure. It also seemed of interest to investigate its utility with other ligand types such as alcohols and amides.

In each case, assignment of signals was made as far as possible from the diamagnetic spectrum, then further assignments were made on the basis of the paramagnetic shifts. The size of the shifts and their proportionality with respect to the cobalt molarity were observed and normalisation factors were calculated when molecules contained protons appropriate for this. Where possible, the effect of ligand concentration, of changing the temperature and of adding water were investigated. Shift to linewidth ratios were measured where there were suitable singlets.



(a) Cyanide ligands

Three cyanoacetates, of known structure but with complex N.M.R. spectra, as well as two other simpler cyanides were investigated.

(i) Menthyl cyanoacetate

Diamagnetic spectrum: The diamagnetic line positions of the assignable signals are given in Table 22.

Table 22. Diamagnetic line positions, in Hz downfield from TMS, at 100 MHz, of the assignable signals in menthyl cyanoacetate.

Conc. cya- nide, <u>M</u>	CH <sub>2</sub> CN	Isopropyl methyl(1)		Isopropyl methyl(2)		C <sub>1</sub> - methyl		H <sub>3</sub>
0.5	379.1	73.1	80.0	86.4	93.4	88.6	95.0	473.9
0.2	380.4	73.2	80.1	86.5	93.5	88.8	94.9	474.0

The methyl doublets were assigned by spin-decoupling by irradiating progressively through the methylene hump. Irradiation at 145 Hz collapsed one doublet ( $J = 6.2$  Hz) which was therefore assigned as the C<sub>1</sub>-methyl signal, the H<sub>1</sub> signal presumably occurring around 145 Hz. Irradiation at 188 Hz collapsed the other two doublets ( $J = 6.9$  and  $7.0$  Hz) which were therefore assigned as the isopropyl methyls, the



isopropyl proton being around 188 Hz. This assignment was in agreement with the observed coupling constants. The  $H_3$  signal was a sextet as would be expected for an axial proton coupled to two axial and one equatorial proton. The  $CH_2CN$  signal was a distinct singlet.

**Addition of cobalt:** Investigations were carried out with solutions 0.5 and 0.2M in cyanide. On addition of cobalt(II) perchlorate the  $CH_2CN$  shift changes were very similar in magnitude to those of the ethyl ester. The displacements of the peaks, which are all upfield relative to their diamagnetic position in solutions of the same cyanide concentration, are given in Table 23.

Table 23. Displacements (all positive) in Hz, of peaks of menthyl cyanoacetate on addition of cobalt(II) perchlorate.

Cya- nide conc. <u>M</u>	Co(II) conc. <u>M</u>	$CH_2CN$	Isopropyl methyl(1)		Isopropyl methyl(2)		$C_1$ -Methyl		$H_3$
0.5	0.11	220.0	16.9	17.0	9.0	9.0	5.9	6.4	33.0
	0.20	420	32.4	32.9	16.9	17.0	12.2	12.3	63.9
	0.38	785.3	59.7		27.2		22.4	23.3	117.7
0.2	0.20	383.4	32.6	32.8	17.9	18.2	13.5	13.5	64.8
	0.41	776.1	65.7		30.4		25.9		126.8

The shifts were proportional to the cobalt molarity, suggesting a low degree of complexing was occurring.

The normalisation factors, with respect to the  $CH_2CN$  peak, are given in Table 24 and were reasonably concordant



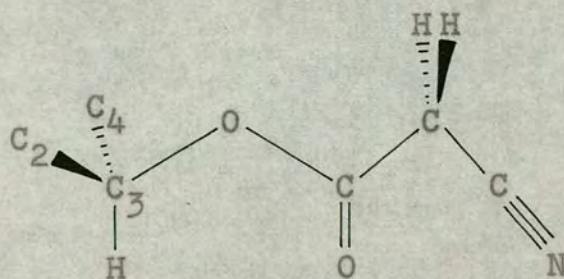
for each ligand molarity. They increased slightly on decreasing the ligand molarity.

Table 24. Normalisation factors (all positive), as percentages, for signals of menthyl cyanoacetate with respect to  $\text{CH}_2\text{CN}$  signal.

Cyanide conc., <u>N</u>	Co(II) conc., <u>M</u>	Isopropyl methyl(1)	Isopropyl methyl(2)	$\text{C}_1$ -methyl	$\text{H}_3$
0.5	0.11	7.7	4.1	2.8	15.0
	0.20	7.8	4.0	2.9	15.2
	0.38	7.6	3.5	2.9	15.0
0.2	0.20	8.5	4.7	3.5	16.9
	0.41	8.5	3.9	3.3	16.3

The three methyl doublets gave different normalisation factors, one isopropyl methyl value being over twice the value of the other, and both being greater than the lone methyl. These methyl protons are all ten bonds removed from the cobalt and the different shifts can therefore be ascribed to different pseudocontact shifts arising from different geometric factors.

Geometric factors were not readily estimated as the cyanoacetate group is very flexible. The most probable conformation for it might be

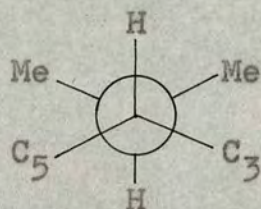




but accurate measurement of the geometric factors based on this would not be justified without further evidence.

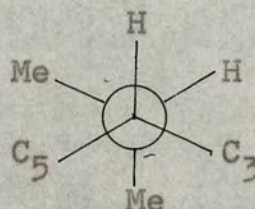
The isopropyl group too could have two conformations, (the third conformation is improbable because of interaction between the methyls and the cyanoacetate group),

(a)



or

(b)



In both cases one methyl would be closer than the other to the complexed cobalt.

Changing the ligand concentration had very little effect on the shifts; if anything decreasing the concentration decreased the CH<sub>2</sub>CN shift.

The shift to linewidth ratio, where measurable for the CH<sub>2</sub>CN peak, was quite reasonable at 23-25.

Water additions were made to a solution 0.5M in cyanide and 0.1M in cobalt(II). This solution contained 100  $\mu$ l AnalaR chloroform for locking signal and the deuterioacetone solvent was not dried. Displacements of the signals and the normalisation factors with respect to the CH<sub>2</sub>CN peak are given in Table 25. Again water had a profound effect on the shifts but the normalisation factors were fairly consistent.

It is thus seen that this more complicated cyanoacetate behaved very similarly to the ethyl cyanoacetate. Addition of cobalt(II) did not enable more signal assignments to be



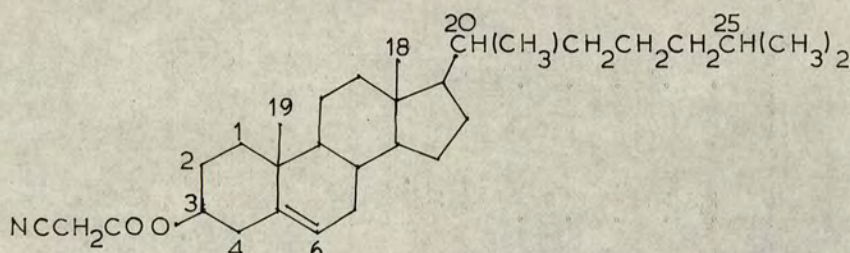
**Table 25.** Displacements of peaks, in Hz, and normalisation factors, as percentages, for menthyl cyanoacetate in presence of cobalt(II), on addition of water.

Water added in $\mu$ l	Displacements (all +ve)					Normalisation factors					
	$\text{CH}_2\text{CN}$	Isop.	Me(1)	Isop.	Me(2)	$\text{C}_1\text{-Me}$	$\text{H}_3$	Isop. Me(1)	Isop. Me(2)	$\text{C}_1\text{-Me}$	$\text{H}_3$
-	138.5	12.0	11.9	5.9	6.0	4.6	4.7	8.6	4.3	3.4	16.9
3	90.0	7.6	7.6	3.8	3.8	3.1	3.0	8.4	4.2	3.4	16.6
6	56.0	4.9	4.8	2.5	2.4	2.0	2.0	8.7	4.4	3.6	16.3
9	37.5	3.3	3.5	1.8	1.7	1.4	1.5	9.1	4.7	3.9	16.8
18	16.8	1.8	1.6	1.1	1.0	0.9	0.8	10.1	6.2	5.1	17.3



made, such as the ring proton signals, but it did confirm the pairing of the methyl peaks into doublets which had been established by spin-decoupling.

(11) Cholesteryl cyanoacetate



**Diamagnetic spectrum:** The diamagnetic line positions of the assignable peaks are given in Table 26. The two equivalent  $C_{25}$ -methyl groups give rise to a single doublet. The mixed solvent was used as the steroid was sparingly soluble in acetone.

Table 26. Diamagnetic line positions, in Hz downfield from TMS, at 100 MHz, of the assignable signals in cholesteryl cyanoacetate (0.1M).

Solvent*	$CH_2CN$	C-18 Me	C-19 Me	$C_{20}-Me$		$C_{25}-Me's$		$H_3$	$H_6$
A/C	368.0	72.1	105.2	90.5	97.7	84.2	90.5	460	539
A/B	349.8	67.3	96.5	91.5	98.1	84.8	91.5	460.7	533.5

\* Solvent A/C: Solution contains 0.2ml  $CDCl_3$

A/B: Solution contains 0.2ml  $C_6H_6$  (AnalaR).

The methyl peaks were assigned on the basis of their expected positions<sup>256</sup>, coupling constants and relative heights.

**Addition of cobalt:** Investigations were carried out using solutions 0.1M in cyanide. 0.2ml  $CDCl_3$  or 0.2ml AnalaR  $C_6H_6$



was added to each solution before making up to 0.5ml with  $(\text{CD}_3)_2\text{CO}$ . The benzene was used as a lock signal, but TMS was always used as standard.

Direct comparison of shift sizes with those of the previously studied cyanides was not possible because of the mixed solvent.

The displacements of the peaks, which are all upfield relative to their diamagnetic positions are given in Table 27.

Table 27. Displacements, in Hz, of peaks of cholesteryl cyanoacetate on addition of cobalt(II) perchlorate.

Solvent*	Conc. Co(II), <u>M</u>	CH <sub>2</sub> CN	C-18 Me	C-19 Me	C <sub>20</sub> -Me	C <sub>25</sub> -Me's	H <sub>3</sub>	H <sub>6</sub>		
A/C	0.10	546	5.0	16.0	1.3	3.8	1.4	1.3	83	23
	0.24	1064	9.7	32.3	5	6.8	1.8	1.7	168	45
	0.30	1301	11.0	38.6	**	**	1.8	1.9	204	53
A/B	0.11	380.4	2.7	11.5	**	1.6	-0.2	0.5	61	15

\* See Table 26.

\*\* peak not observable.

The shifts were not so linear with respect to the cobalt molarity in this case suggesting a slightly higher degree of complexing, but the effect of varying the ligand concentration was not investigated to substantiate this.

The normalisation factors, with respect to the  $\text{CH}_2\text{CN}$  signal, are given in Table 28.



Table 28. Normalisation factors, as percentages, for signals of cholesteryl cyanoacetate with respect to  $\text{CH}_2\text{CN}$  signal.

Solvent*	Conc. Co(II), $\frac{\text{M}}{\text{M}}$	C-18 Me	C-19 Me	C <sub>20</sub> -Me	C <sub>25</sub> -Me's	H <sub>3</sub>	H <sub>6</sub>
A/C	0.10	0.9	2.9	0.7	0.25	15.2	4.2
	0.24	0.9	3.0	0.6	0.16	15.8	4.2
	0.30	0.8	3.0		0.14	15.7	4.1
A/B	0.11	0.7	3.0			16.0	3.9

\* See table 26.

The concordancy of the normalisation factors is fairly good, even with the change of solvent. Although the  $\text{C}_{25}$ -methyls are very far removed from the cobalt, they do show shift displacements. The normalisation factors are in the order of magnitude expected on the basis of the distance of the protons from the cobalt. It seems likely that the more distant protons, indeed perhaps all the ring protons, would be expected to have only a pseudocontact contribution to their shift.

The acetone-benzene solvent was used for two reasons, first to see the effect on the shifts and normalisation factors of a change in solvent, and second, because the benzene provided a useful low field lock so that signals passing through the region of the TMS could be observed.

The shift to linewidth ratio for the  $\text{CH}_2\text{CN}$  signal was approximately 24, similar to those for the other cyanoacetates.

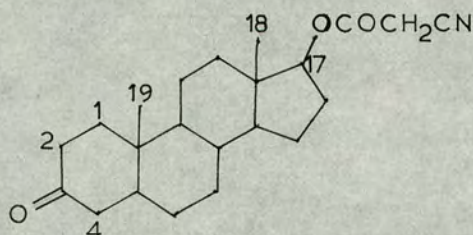
A series of water additions was not possible as water



caused an emulsion to form, but exploratory experiments, for which undried acetone was used, showed much smaller shifts, 77% in the acetone-benzene case and 44% in the acetone-chloroform case, which showed that water had a considerable effect on the shifts, particularly with the chloroform solution. Normalisation factors, however, remained very similar.

Thus the effect of adding cobalt(II) perchlorate to cholesteryl cyanoacetate is similar to the effect observed with the other esters and the shifts are such as to distinguish the various methyl resonances and give an indication of their distance from the cobalt ion.

(iii) Dihydrotestosterone cyanoacetate



Diamagnetic spectrum: The diamagnetic line positions of the assignable proton signals are given in Table 29.

Table 29. Diamagnetic line positions, in Hz downfield from TMS, at 100 MHz, of the assignable signals in dihydrotestosterone cyanoacetate (0.07M) in chloroform-acetone solvent.

CH <sub>2</sub> CN	H <sub>17</sub>	C-18 Me	C-19 Me
370.2	466.2	86.4	106.7



Addition of cobalt: Investigations were carried out with solutions 0.07M in cyanoacetate, each solution containing 0.2ml  $\text{CDCl}_3$ .

The peak displacements, all upfield, and the normalisation factors are given in Table 30.

Table 30. Displacements, in Hz, and normalisation factors, as percentages, of peaks of dihydrotestosterone cyanoacetate on addition of cobalt(II) perchlorate.

Conc. Co(II), <u>M</u>	Displacements (all +ve)				Normalisation factors		
	$\text{CH}_2\text{CN}$	$\text{H}_{17}$	C-18 Me	C-19 Me	$\text{H}_{17}$	C-18 Me	C-19 Me
0.11	475.8	78.9	52.2	9.2	16.5	11.0	1.9
0.21	922.4	151.2	*	14.5	16.4		1.6
0.32	1300**	212.0	140.1	17.8	16.5	10.9	1.4

\* Signal obscured by TMS

\*\* Value extrapolated from linearity with  $\text{H}_{17}$  shifts, for use in calculation of normalisation factors.

The  $\text{CH}_2\text{CN}$  peak shift was a little smaller than that of the cholesteryl ester, and again, the linearity of the shifts with respect to the cobalt molarity was not perfect.

Although insufficient displacements were measured for certainty, it would appear that the normalisation factors for  $\text{H}_{17}$  and C-18 Me signals were fairly constant while that for the C-19 Me decreased somewhat with increasing cobalt molarity. This might be due to a small amount of complexing at the  $\text{C}_3$  carbonyl group, but on the basis of the results with cholestan-3-one (see Section d(i)) this would seem to be unlikely to be a significant factor here.

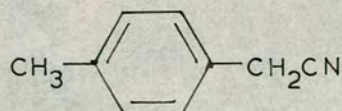


Another signal moved downfield out of the methylene hump on addition of cobalt(II). Its movement was linear with respect to the  $\text{CH}_2\text{CN}$  signal movement, the gradient and intercept of the normalisation plot giving a normalisation factor of -13.5% and a diamagnetic line position of 186 Hz. All cyanoacetate displacements with cobalt(II) have been up-field as yet and so this shift in the opposite direction was surprising. The shift was rather large, almost as great as that of the  $\text{H}_{17}$  peak. With the expected conformation of the cyanoacetate group, no proton lies outside the pseudocontact cone ( $\chi > 55^\circ$ ) so that this would not appear to be a satisfactory explanation for the negative shifts. Nor does it seem likely to be the result of complexing at the carbonyl group for the same reason as given above. A third possibility, that the peak is an impurity peak would seem to be the only satisfactory explanation.

No other signals separated out on addition of cobalt.

The shift to linewidth ratio for the  $\text{CH}_2\text{CN}$  peak was about 26, similar to the previous values.

(iv) p-methyl benzyl cyanide



Diamagnetic spectrum: The diamagnetic line positions are shown in Table 31.



Table 31. Diamagnetic line positions, in Hz downfield from TMS, at 100 MHz, of the signals in p-methyl benzyl cyanide.

Conc. cyanide, <u>M</u>	CH <sub>2</sub> CN	Phenyl (o & m)	CH <sub>3</sub>
1.0	384.9	721.9	230.7
0.5	385.3	722.2	231.2

The phenyl signals appeared as a very close doublet, whose average position is given in the table, with very small side peaks.

Addition of cobalt: Investigations were carried out using solutions 1.0 and 0.5M in cyanide. The peak displacements are again all upfield. The phenyl signals separated into two doublets on addition of cobalt. The positions of the doublets were plotted with respect to the CH<sub>2</sub>CN peak displacement, see Figure 8, and gave straight lines extrapolating back to diamagnetic positions of 722 Hz (presumed ortho protons) and 717 Hz (meta protons) for both cyanide molarities, which gave an average position of 719.5 Hz slightly upfield of the average positions found. These extrapolated positions were used to calculate the phenyl peak displacements. The peak displacements, all upfield, and the normalisation factors are given in Table 32.

The shifts were not completely linear with respect to cobalt molarity.



Figure 8. Plot of position (Hz) of phenyl signals against shift displacement (Hz) of  $\text{CH}_2\text{CN}$  signal for *p*-methyl benzyl cyanide on addition of  $^{59}\text{Co}(\text{II})$  perchlorate.

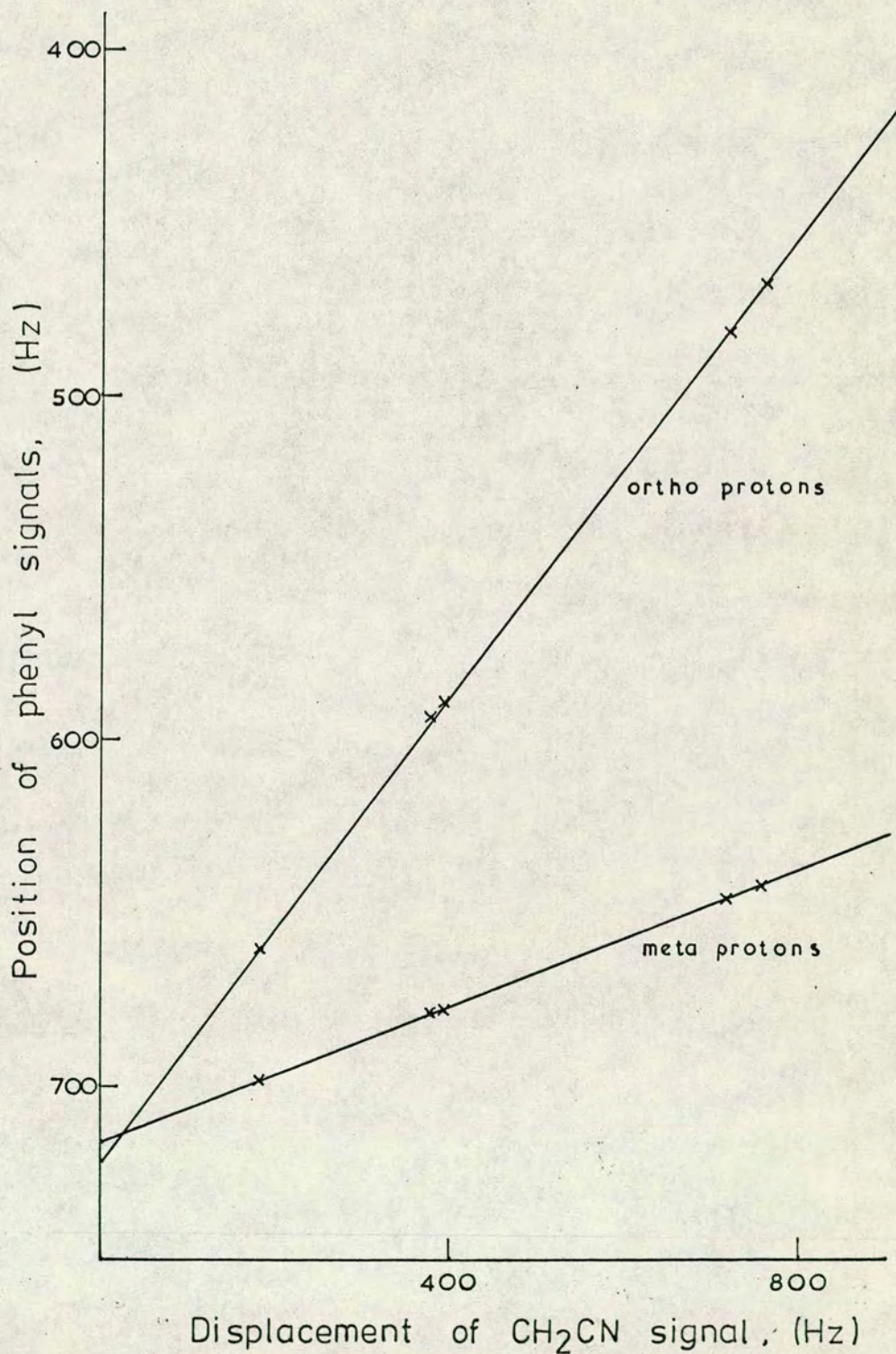




Table 32. Displacements, in Hz, and normalisation factors, as percentages, of peaks in *p*-methyl benzyl cyanide, on addition of cobalt(II) perchlorate.

Conc. cya- nide, <u>M</u>	Conc. Co(II), <u>M</u>	Displacements (all +ve)				Normalisation factors		
		CH <sub>2</sub> CN	Ph(o)	Ph(m)	CH <sub>3</sub>	Ph(o)	Ph(m)	CH <sub>3</sub>
1.0	0.05	184.0	61	17	9.7	33.2	9.2	5.3
	0.10	380	128	37	18.2	33.7	9.7	4.8
	0.20	720	240	70	33.3	33.4	9.7	4.6
0.5	0.10	396	133	38	19.0	33.6	9.6	4.8
	0.20	761	254	73	34.7	33.4	9.6	4.6

The normalisation factors were in good agreement. In a phenyl ring, one would expect  $\pi$  delocalisation of spin density and hence contact shifts of alternating sign. The fact that all the shifts were positive suggested that either spin density is not distributed through the  $\pi$  system or, more likely, that the pseudocontact contribution is the larger and determining factor here. It was not possible to distinguish the two possibilities on the basis of the approximate ratios calculated for the pseudocontact shifts.

The average shift to linewidth ratio for the CH<sub>2</sub>CN peak was 20, slightly lower than the cyanoacetates but still acceptable.

Decreasing the cyanide concentration increased the shift changes only slightly, the "strength of complexing" expression evaluating at 8-10%.

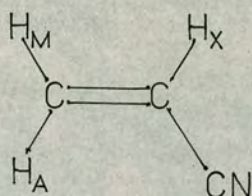
On heating, both the shift changes and the linewidths decreased. The shift to linewidth ratio showed a marked



improvement, increasing to 49 at 55°.

It would thus appear that aromatic cyanides of this type are also suitable for selective shift studies.

(v) Acrylonitrile



Diamagnetic spectrum: From the second order spectrum, the approximate signal centres and coupling constants were calculated (as from a first order spectrum) to be

$H_X$ centre at 582.8 Hz	$J_{AX} = 17.2$ Hz
$H_M$ 614.6 Hz	$J_{MX} = 11.5 - 11.6$ Hz
$H_A$ 625.2 Hz	$J_{AM} = 1.8$ Hz.

The purpose of this study was to compare the figures obtained by measurement and extrapolation of the cobalt data with the above figures calculated approximately from the second-order spectrum.

Addition of cobalt: Investigations were carried out using solutions 1.0M in acrylonitrile, each solution containing 0.2ml  $CDCl_3$ .

The peak positions are given in Table 33.

The relationship between the peak positions for the three signals is shown in Figure 9. The three diamagnetic line positions are interdependent but not unique. Taking  $H_X$  to be at the above value of 583 Hz, then  $H_M$  is centred at 614 Hz and  $H_A$  at 625 Hz in reasonably good agreement with the above figures.



Figure 9. Plot of position (Hz) of  $H_A$  and  $H_M$  signals against position (Hz) of  $H_X$  signal of acrylonitrile on addition of cobalt(II) perchlorate.

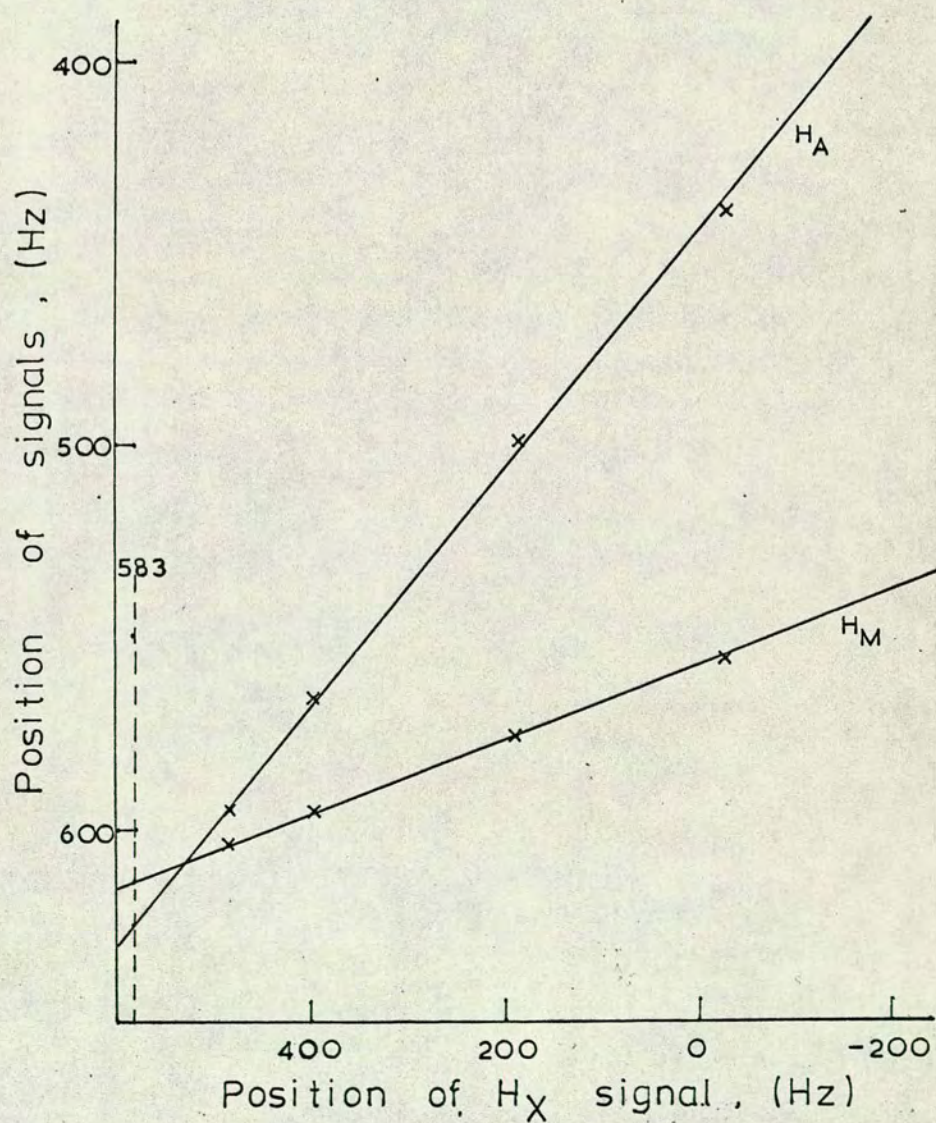




Table 33. Peak positions, in Hz downfield from TMS, at 100 MHz, for acrylonitrile signals, on addition of cobalt(II) perchlorate.

Conc. Co(II), <u>M</u>	$H_A$		$H_M$		$H_X$			
0.05	603.7	586.1	610.5	599.1	498.0	486.4	480.3	468.7
0.10	575.8	558.0	602.2	590.4	409.0	369.9	391.6	380.0
0.20	509.9	492.5	581.8	570.5			183.6	
0.30	447.8	431.5	562.5	551.8			-29	

The normalisation factors with respect to the  $H_X$  (CHCN) proton were calculated from the gradients to be

$$H_A + 30.8\%; \quad H_M + 9.4\%.$$

If the paramagnetic shifts were purely pseudocontact in nature, then, assuming that the  $C \equiv N$  is colinear with the principal axis of the complex and that the Co-N bond length is  $1.7 \times 10^{-10}$  cm, all other bond lengths and angles taking their normal values, then normalisation factors, on the basis of the geometric factor  $(3 \cos^2 \chi - 1)r^{-3}$ , would be

$$H_A \quad 79\%; \quad H_M \quad 54\%.$$

The much lower values found here indicated that contact shifts were also contributing, particularly to the  $H_X$  shift.

Two coupling constants were immediately available from the first order spectra,

$$J_{AX} = 17.6 \text{ Hz}; \quad J_{MX} = 11.4 \text{ Hz},$$

in reasonable agreement with the diamagnetic spectrum.

It would thus appear that unknown diamagnetic line positions and coupling constants can be fairly accurately



determined (the former to within 1 Hz, the latter to within 0.5 Hz) by addition of cobalt(II) to expand the spectrum.

(vi) Conclusion

All the cyanides investigated proved suitable for selective shift studies. The normalisation factor is a more reliable structural parameter than the slope of the plot of the shift of a signal against the cobalt molarity, the latter being sensitive to ligand and cobalt concentration, to the nature of the solvent, changes in temperature and the presence of water. The shift to linewidth ratios were similar for all the cyanides and were acceptable in magnitude. They did however limit the usefulness of the system in that only protons fairly close to the complexing site were shifted sufficiently to be separated out from protons with similar diamagnetic positions before broadening became too excessive.

(b) Alcohol ligands

Cyanides have proved suitable ligands for cobalt shift studies. However, organic compounds containing a cyanide functional group are not all that common, nor are they always readily prepared, as the above work showed (Section A). It would be helpful if other ligands, particularly alcohols, would complex with cobalt(II) producing a similarly suitable system. The investigation of alcohols as ligands was therefore undertaken.

Firstly, the analogous alcohols to the above cyanides (excluding acrylonitrile) were investigated, then a diol was studied.



(i) Menthol

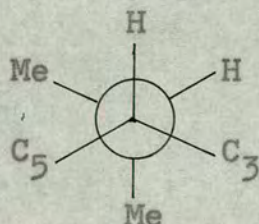
Diamagnetic spectrum: This was similar to that of the cyanoacetate. The diamagnetic line positions are given in Table 34.

Table 34. Diamagnetic line positions, in Hz downfield from TMS, at 100 MHz, for assignable signals in menthol.

Sol- <sup>*</sup> vent	Conc. alco- hol, <u>M</u>	Isopropyl methyl (1)		Isopropyl methyl (2)		C <sub>1</sub> -methyl		H <sub>3</sub>	OH	Iso- pro- pyl H
A	0.5	75.0	81.9	85.9	93.0	85.9	91.6	330.9	330.9	227.9
A	0.2	75.0	82.0	85.9	93.1	85.9	91.7	328.4	328.4	227.4
A/C	0.5	75.8	82.7	87.0	94.1	87.0	92.8	331	325.5	227.1

\* Solvent: A (CD<sub>3</sub>)<sub>2</sub>CO; A/C (CD<sub>3</sub>)<sub>2</sub>CO/CDCl<sub>3</sub> (see below).

With the alcohol, the isopropyl hydrogen signal was visible just downfield of the methylene hump. It was a septet ( $J \sim 6.9$  Hz), each line of which was split into a doublet ( $J \sim 1.8$  Hz). That this signal was the isopropyl hydrogen was confirmed by spin-decoupling from the isopropyl methyls. The coupling with H<sub>4</sub> was too small for trans diaxial splitting and so the preferred conformation of the isopropyl group must have been



The upfield shift of the isopropyl hydrogen signal of about 40 Hz, from 228 Hz to 188 Hz, on formation of the cyano-



acetate from the alcohol could have been due to the resulting proximity of the proton to the cyanoacetate group or could be the result of a different conformation of the isopropyl group in the two cases.

Addition of cobalt: Investigations were carried out with solutions 0.5 and 0.2M in alcohol. The peak displacements on addition of cobalt(II) are given in Table 35.

Table 35. Displacements of peaks, in Hz, for menthol on addition of cobalt(II) perchlorate.

Conc. alcohol, <u>M</u>	Conc. Co(II), <u>M</u>	Isopropyl methyl(1)	Isopropyl methyl(2)	C <sub>1</sub> -methyl	H <sub>3</sub>	Isopropyl hydrogen
0.5	0.10	+17.4	-28.5	-14.6	-364.7	-90.2
	0.20	+32.1	-54.3	-29.3	-657	-171.7
	0.30	+45.9	-77.1	-42.5	-937	-243.2
0.2	0.10	+20.0	-33.7	-17.3	-423	-91
	0.30	+51.5	-85.8	-50.0	-1060	-274

All the signals, with the exception of one isopropyl methyl doublet, moved downfield, and shifts were considerably greater than those with the cyanides. The hydroxyl proton signal was not observable after cobalt had been added. The shifts were not completely proportional to the cobalt molarity, the proportionality being worse at the lower alcohol concentration.

Normalisation factors were calculated with respect to the H<sub>3</sub> shift (by convention, the sign of the shift of the proton used for normalisation is disregarded, the denominator being taken as positive), and are shown in Table 36.



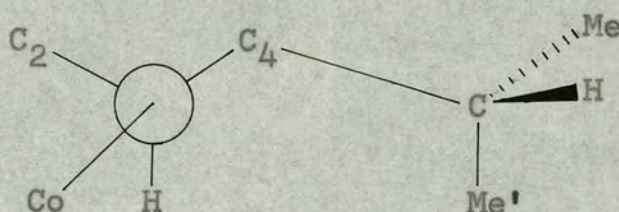
Table 36. Normalisation factors, as percentages, for menthol signals on addition of cobalt(II) perchlorate.

Conc. alcohol, <u>M</u>	Conc. Co(II), <u>M</u>	Isopropyl methyl(1)	Isopropyl methyl(2)	C <sub>1</sub> -methyl	Isopropyl hydrogen
0.5	0.10	+4.8	-7.8	-4.0	-24.7
	0.20	+4.9	-8.3	-4.5	-26.1
	0.30	+4.9	-8.2	-4.5	-25.9
0.2	0.10	+4.7	-8.0	-4.1	*
	0.30	+4.9	-8.1	-4.7	-25.8

\* peak overlapped.

The values were reasonably concordant.

The fact that almost all the shift displacements were negative suggested that the pseudocontact shifts within the cone,  $\chi < 55^\circ$ , were negative, and the contact shifts, if significant, were also negative. This would mean that one isopropyl methyl lay outside the cone, which is in fact true of the methyl labelled Me' (in diagram) if one assumes a preferred conformation of



This would be expected to be the most favourable conformation.

Three further peaks moved downfield out of the methylene hump on addition of cobalt. Their paramagnetic positions are given in Table 37.

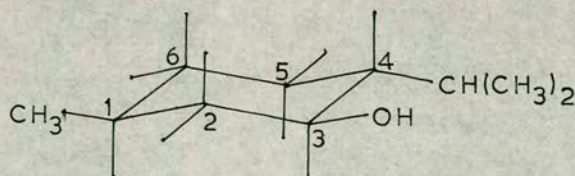


Table 37. Paramagnetic positions, in Hz downfield from TMS, of unassigned signals in menthol, on addition of cobalt(II) perchlorate.

Conc. alcohol, <u>M</u>	Conc. Co(II), <u>M</u>	A	B	C
0.5	0.10	290.8	251.9	282.4
	0.20	452.6	399.6	399.6
	0.30	592.3	513.5	502.3
0.2	0.10	318	282	318
	0.30	647	570	550

Their positions were plotted with respect to the  $H_3$  peak displacement, see Figure 10, and three lines drawn through them included each signal observed. The gradients of these lines gave the normalisation factors A: - 52.4%; B: -45.8%; C: -38.7%, and extrapolation to zero  $H_3$  displacement gave their diamagnetic positions to be A: 100 Hz; B: 88 Hz; C: 142 Hz, which were all acceptable values.

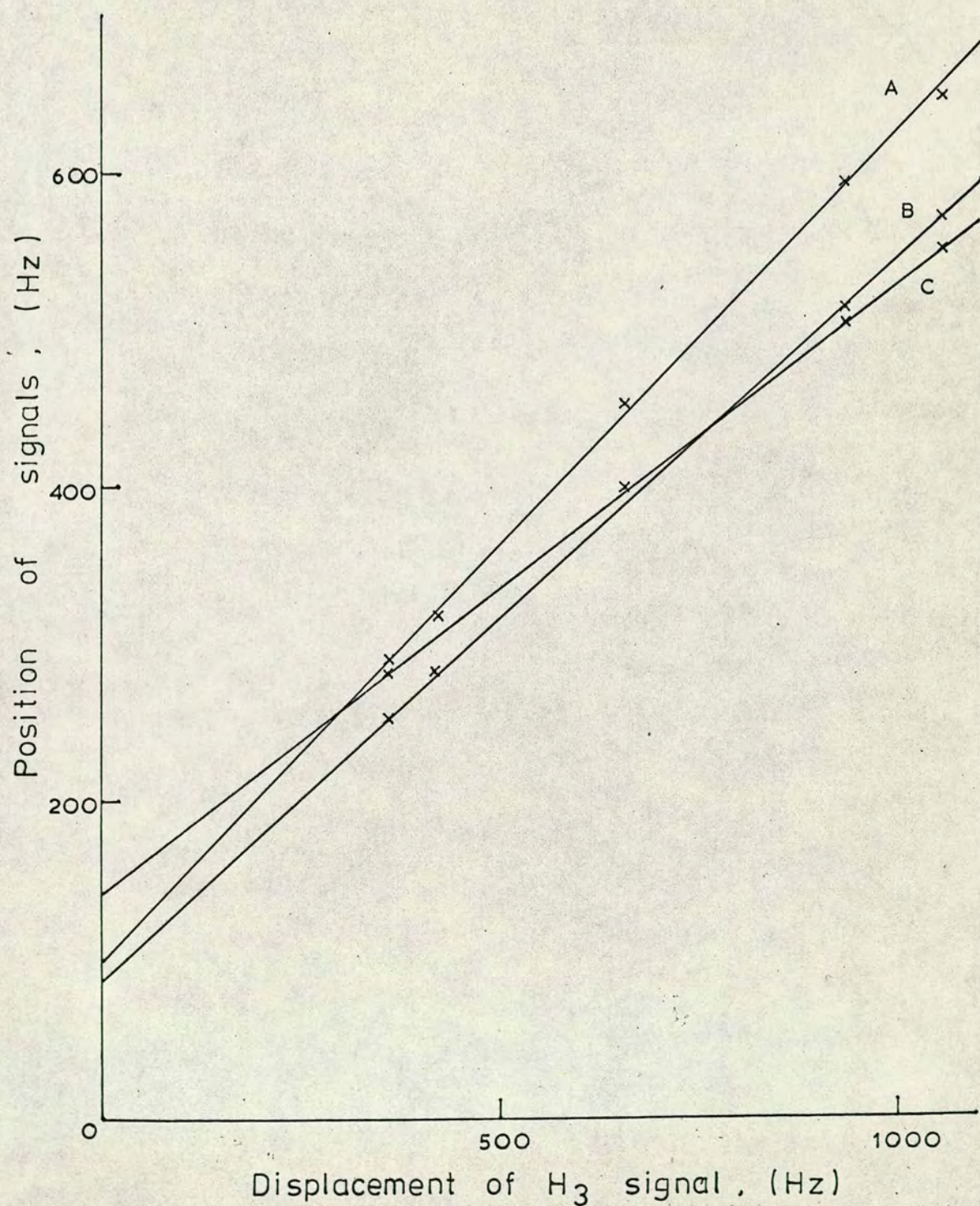
These were the signals of ring protons, which, by their large normalisation factors, were close to the cobalt. Diamagnetic line positions suggested that A and B were axial protons and C was equatorial.



The most likely protons would be the  $H_4(ax)$ ,  $H_2(ax)$  and  $H_2(eq)$ . Thus C would be  $H_2(eq)$ . The two axial protons are symmetrically placed with respect to the oxygen of the hydroxyl



Figure 10. Plot of position (Hz) of peaks A, B and C against shift displacement (Hz) of  $H_3$  signal of menthol on addition of cobalt(II) perchlorate.





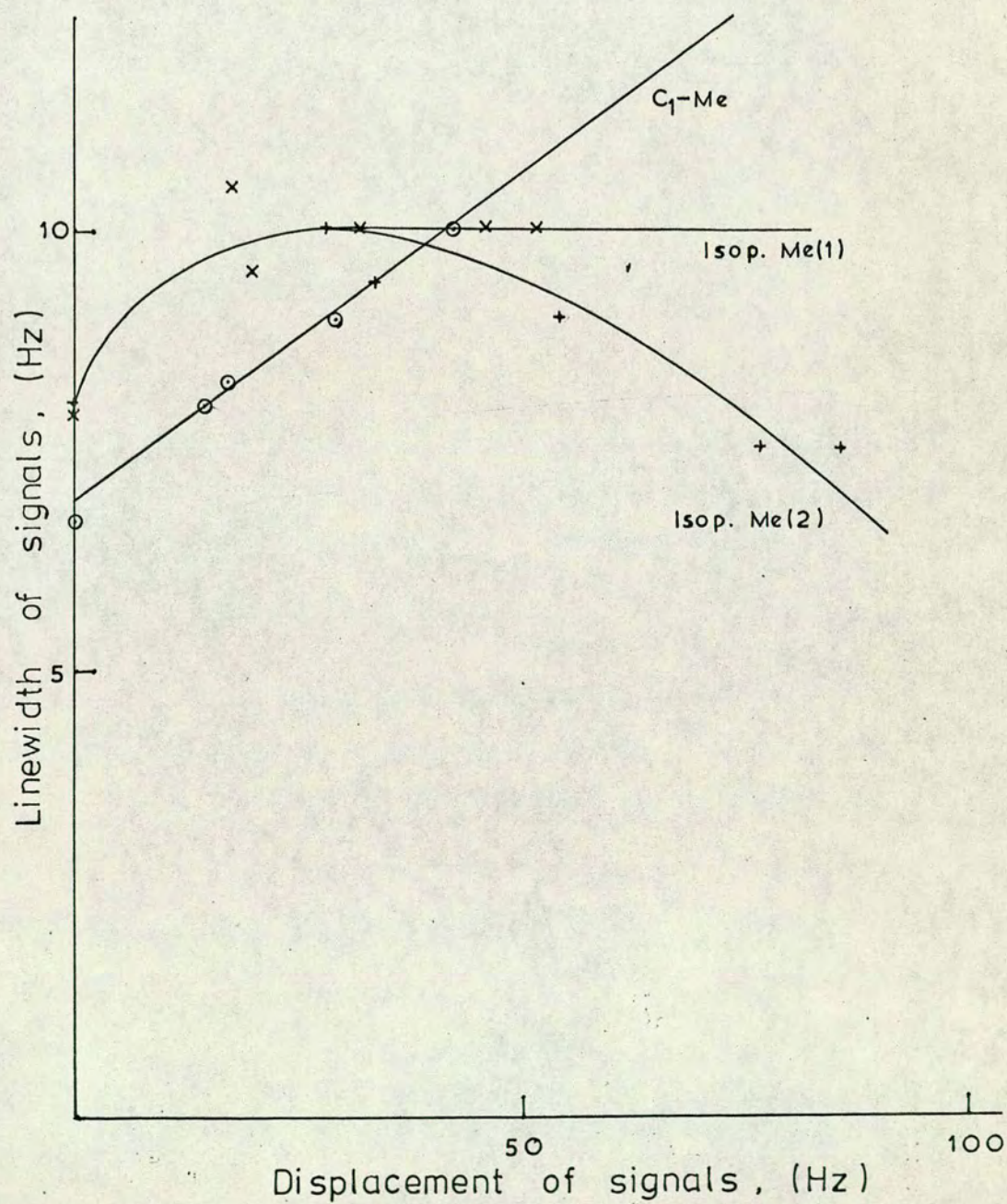
group. The fact that the normalisation factors, though similar, were not identical supported the proposition made above that the cobalt ion was not symmetrically placed.

Assignment of the two axial protons can only be tentative. Both are coupled to two axial protons but  $H_2$  also has a large vicinal coupling while  $H_4$  has a small coupling to the isopropyl hydrogen and so would be the slightly narrower peak overall. The narrower peak was in fact A. Support for its assignment as  $H_4$  came from its slightly larger normalisation factor. Assuming the above conformation for the cobalt, the  $H_4$  proton would have the larger pseudocontact shift. Thus a reasonable assignment of these signals is: A is  $H_4(ax)$ , B is  $H_2(ax)$  and C is  $H_2(eq)$ .

The overall linewidths of the methyl doublets were measured and the relationship between their shift changes and linewidths is shown graphically in Figure 11. The  $C_1$ -methyl gave a linear plot yielding a shift to linewidth ratio of 14.5 which is not very good when compared with those for the cyanides. The isopropyl methyl linewidths first increased then decreased, suggesting that spin-decoupling from the isopropyl hydrogen was occurring at higher cobalt concentrations. With the conformation of the isopropyl group suggested above, the hydrogen lies very close to the cobalt ion (its sizeable normalisation factor supports this) and so chemical spin-decoupling was quite possible. Although the two doublets must have been spin-decoupled to the same extent, doublet (1) gave a smaller shift to linewidth ratio than doublet (2), that is, was more broadened. This presumably arose from the fact that for the former the angle factor in the pseudocontact



Figure 11. Plot of overall linewidth (Hz) against shift displacement (Hz) for methyl signals of menthol on addition of cobalt(II) perchlorate.





expression was smaller ( $\chi$  estimated at ca.  $60^\circ$  and  $35^\circ$  respectively) while in fact the group lay closer to the cobalt.

The shifts were dependent on the ligand concentration, the "strength of complexing" factor being about 22%, a little greater than for the cyanoacetates, but smaller than for propionitrile.

Water was added to a solution 0.5M in menthol and 0.2M in cobalt(II). The shifts were greatly reduced (Table 38).

Table 38. Displacements of peaks, in Hz, for menthol in presence of cobalt, on addition of water.

water added, $\mu$ l	Iso-propyl methyl (1)	Iso-propyl methyl (2)	C <sub>1</sub> -methyl	H <sub>3</sub>	Iso-propyl hydrogen	H <sub>4</sub>	H <sub>2</sub> (ax)	H <sub>2</sub> (eq)
-	+30.7	-52.4	-28.2	-635	*	-338	-302	-248
2	+6.8	-39.6	-21.9	-463	*	*	-220	-190
4	-4.8	-30.7	-16.8	-337	-93	*	-166	-144
6	-9.2	-23.5	-12.8	-248	-71	*	-125	*
9	-9.5	-16.7	-9.1	-165	-52	*	*	*
18	-7.2	-8.6	-4.5	-78	-23	*	*	*

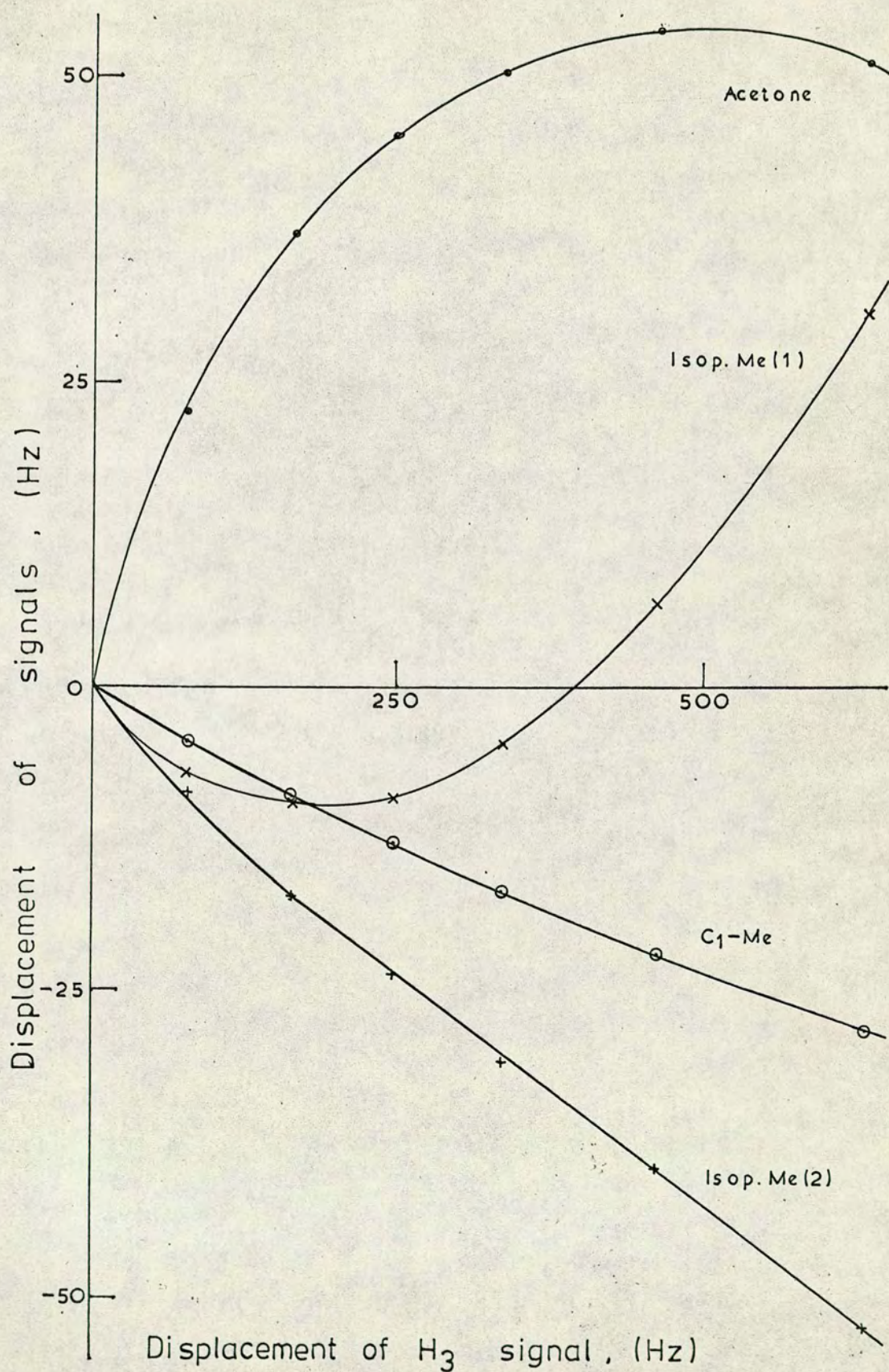
\* peak position not measurable due to overlap.

The normalisation plots for the methyls, Figure 12, were not straight lines. The C<sub>1</sub>-methyl and isopropyl methyl(2) gave gentle curves, while the isopropyl methyl (1) moved dramatically downfield to give negative displacements, then curved back to zero.

The normalisation plots for the signals of the observable protons showed fairly straight lines in each case, but the



Figure 12. Normalisation plots for methyl signals of menthol in presence of cobalt(II) perchlorate on addition of water.





lines did not pass through the origin.

It was thus obvious that normalisation was not good in the presence of water. There were various possible explanations for this. It could have been that substitution of acetones and/or menthol ligands in the complex by water changed the magnitude of the g-factor term for the pseudo-contact shift. If this were the case then all the more distant protons (negligible contact contribution) would experience the effect proportionately the same, which was not the case.

A second possibility was that water in some way changed the conformation of the isopropyl group. This would affect only those three signals, which was not the case.

It could be that the replacement of the ligands by water caused a change in direction of the principal axis of the complex thus changing the angle factor for all the protons. Similarly, it could be that changing the ligands caused a change in the position of the cobalt relative to the menthol. In either case, all the protons would be affected, but the effect would be greatest for protons lying near the cone ( $\chi = 55^\circ$ ), that is the isopropyl methyl(1), which was found. Either explanation would thus seem to be satisfactory. In the latter case, negative shifts for the isopropyl methyl(1) protons would arise if the cobalt ion moved further away from the isopropyl group.

A further series of solutions was investigated. These were 0.5M in menthol and 0.1 and 0.2M in cobalt(II), each solution containing 0.2ml  $\text{CDCl}_3$  and made up to 0.5 ml with



undried acetone. This series was to examine the effect of changing the solvent.

The peak displacements relative to a diamagnetic solution of the same menthol molarity in the same solvent, are given in Table 39.

Table 39. Displacement of peaks, in Hz, for menthol on addition of cobalt(II) perchlorate in chloroform-acetone solution.

Conc. Co(II), <u>M</u>	Isopropyl methyl(1)	Isopropyl methyl(2)	C <sub>1</sub> -methyl	H <sub>3</sub>	Isopropyl hydrogen
0.1	+3.4	-20.1	-9.0	-210	-62.3
0.2	+7.4	-36.7	-17.1	-385.5	-112.6

Again all the signals move downfield except the isopropyl methyl(1) signal. Normalisation factors with respect to the H<sub>3</sub> signal are shown in Table 40.

Table 40. Normalisation factors, as percentages, for menthol signals on addition of cobalt(II) perchlorate in chloroform-acetone solution.

Conc. Co(II), <u>M</u>	Isopropyl methyl(1)	Isopropyl methyl(2)	C <sub>1</sub> -methyl	Isopropyl hydrogen
0.1	+1.6	-9.6	-4.3	-29.6
0.2	+1.9	-9.5	-4.4	-29.2

Only the C<sub>1</sub>-methyl signal had the same normalisation factor as in the pure acetone solutions, although those for



the isopropyl methyl(2) and isopropyl hydrogen were not greatly different. This was probably due to a slightly different cobalt position either because of the presence of chloroform or because the water content of the solution had changed.

In conclusion, it would appear that using the alcohol directly rather than preparing and using the cyanoacetate has some advantages and some disadvantages. Shifts were greater with the alcohol and so more proton signals were observable and more information could be obtained. However shift to linewidth ratios did not seem as good and the effect of water was much greater, normalisation breaking down. However this latter factor may not be true for all alcohols and, though care would need to be taken in this respect, the drawback may not prove very severe.

It could be that information from both ligand types may be complementary, not least because the shifts are in general in opposite directions.

#### (ii) Cholesterol

Diamagnetic spectrum: The same signals were recognisable as in the cyanoacetate spectrum. It was found to be impossible to eliminate all trace of water. The diamagnetic line positions are given in Table 41.

Table 41. Diamagnetic line positions, in Hz downfield from TMS, at 100 MHz, of the assignable signals in cholesterol (0.2M) in chloroform-acetone solvent.

C-18 Me	C-19 Me	C <sub>20</sub> -Me	C <sub>25</sub> -Me's	H <sub>3</sub>	H <sub>6</sub>	OH
71.4	102.1	90.5 97.3	84.2 90.5	342	531.1	352.5



Addition of cobalt: Investigations were carried out with solutions 0.2M in alcohol, each solution containing 0.2ml  $\text{CDCl}_3$ .

Peak displacements on addition of cobalt are given in Table 42.

Table 42. Displacements, in Hz, of peaks of cholesterol on addition of cobalt(II) perchlorate.

Conc. Co(II), $\frac{\text{M}}{\text{M}}$	C-18 Me	C-19 Me	C <sub>20</sub> -Me		C <sub>25</sub> -Me's		H <sub>3</sub>	H <sub>6</sub>
0.06	-12.0	-79.2	-4.0	-3.4	-0.1	-0.3	-824	+7
0.10	-19.4	-126.2	-6.1	-5.3	-0.7	-0.3	-1291	+8.6
0.20	-31.3	-202.9	**	-9.2	-1.6	-1.7	-2075*	+9.7

\* value extrapolated from linearity with C-19 methyl shifts for normalisation purposes.

\*\* peak not observable.

Even allowing for the mixed solvent, the displacements were much greater than those for menthol. All the shifts, except for the H<sub>6</sub> olefinic proton, were downfield. The shift changes were not very linear with respect to the cobalt molarity.

Table 43 gives the normalisation factors calculated with respect to the H<sub>3</sub> proton signal.

Table 43. Normalisation factors, as percentages, for signals of cholesterol with respect to H<sub>3</sub> signal.

Conc. Co(II), $\frac{\text{M}}{\text{M}}$	C-18 Me	C-19 Me	C <sub>20</sub> -Me	C <sub>25</sub> -Me's	H <sub>6</sub>
0.06	-1.5	-9.6	-0.45	-0.02	+0.85
0.10	-1.5	-9.8	-0.44	-0.04	+0.67
0.20	-1.4	-9.8	-0.42	-0.08	+0.45



Concordancy was good except for the olefinic proton and the  $C_{25}$ -methyls. The shifts of the latter were too small to be significant.

As with the isopropyl methyl protons of menthol, it was assumed that the olefinic proton here lay outside the pseudocontact cone ( $\chi > 55^\circ$ ), so having an upfield pseudocontact shift. Assuming the cobalt lay on average in the conformation where it eclipsed  $H_3$ , then  $H_6$  would be the only proton of those observed whose pseudocontact angle was greater than  $55^\circ$ . The fact that with this conformation, the proton lies rather close to the cone would be the reason for its poor normalisation, since small changes in the average cobalt position would greatly affect its shifts.

Three other signals moved downfield out of the methylene hump on addition of cobalt, one of which was a doublet in general appearance. Their positions are given in Table 44.

Table 44. Paramagnetic positions, in Hz downfield from TMS, of unassigned signals in cholesterol, on addition of cobalt(II) perchlorate.

Conc. Co(II), <u>M</u>	Doublet	A	B
0.06	358	545	459
0.10	459	742	642
0.20	622	1045	933

The peak positions gave straight line plots with respect to the  $H_3$  shift change, from which normalisation factors and diamagnetic line positions were calculated:



Doublet	-20.5%;	193 Hz
A	-40.2%;	220 Hz
B	-38.0%;	150 Hz.

These calculated positions were all possible peak positions and in fact there was a peak at 220 Hz visible. The large normalisation factors suggested that they arose from protons fairly close to  $H_3$ , probably  $H_2$  or  $H_4$  protons.

The diamagnetic line positions suggested that the doublet and peak A were due to equatorial protons and peak B to an axial proton. Thus an axial and an equatorial proton moved at about the same rate while a second axial proton moved at about half the rate. There are altogether four  $H_2$  and  $H_4$  protons and yet there was no sign of a fourth peak and so it presumably moved very slowly, suggesting it is near the pseudocontact cone.

As with the cyanoacetate it was not possible to make water additions to these solutions, but in undried acetone the shifts were found to be 30% smaller, showing that again water had a considerable effect.

The greater shifts of cholesterol over its cyanoacetate were advantageous in that they pulled out more proton signals from the methylene hump, but normalisation would appear to be a little less certain, and poorer shift to linewidth ratios were certainly disadvantageous.

### (iii) Dihydrotestosterone

Diamagnetic spectrum: The diamagnetic line positions of the assignable peaks are given in Table 45.



Table 45. Diamagnetic line positions, in Hz downfield from TMS, at 100 MHz, of the assignable signals in dihydrotestosterone, (0.2M) in chloroform-acetone solvent.

C-18 Me	C-19 Me	H <sub>17</sub>	OH
76.8	106.1	360.5	338.0

Addition of cobalt: Investigations were carried out using solutions 0.2M in alcohol, each solution containing 0.2ml CDCl<sub>3</sub>. The peak displacements on addition of cobalt, and the normalisation factors for the methyl signals with respect to H<sub>17</sub> signal, are given in Table 46.

Table 46. Displacements, in Hz, and normalisation factors, as percentages, of peaks in dihydrotestosterone on addition of cobalt(II) perchlorate.

Conc. Co(II), <u>M</u>	Displacements (all-ve)			Normalisation factors	
	C-18 Me	C-19 Me	H <sub>17</sub>	C-18 Me	C-19 Me
0.07	106.8	3.6	304	35.1	1.2
0.09	159.2	5.7	452.4	35.2	1.3
0.19	277.6	8.6	792	35.0	1.1
0.31	393	13.6	1135	34.6	1.2

The magnitude of the shift changes was smaller than was the case for cholesterol, presumably due to steric hindrance, but appeared to be larger, allowing for the mixed solvent, than those with menthol. The dependence of the shifts on cobalt concentration showed significant departures from linearity



indicating a moderate degree of complexing was occurring. The normalisation factors for the two methyls were reasonably concordant, that for the C-18 methyl being quite considerable in size.

Another peak moved very rapidly downfield out of the methylene hump. Its peak positions are given in Table 47.

Table 47. Paramagnetic positions, in Hz downfield from TMS, of unassigned signal in dihydrotestosterone, on addition of cobalt(II) perchlorate.

Conc. Co(II), <u>M</u>	A
0.07	304.6
0.09	382.5
0.19	560.3
0.31	740

This peak normalised very well yielding a normalisation factor of -52.4% and a diamagnetic line position of 146 Hz. It would seem likely that this peak is an  $H_{16}$  proton signal, probably the  $H_{16}(\beta)$ .

At least six further proton signals moved downfield out of the methylene hump at a much slower rate. Their signals were much overlapped and so very difficult to follow. An estimate of normalisation factors less than 15% for all the protons was made. These were probably signals of protons near to the site of complexing, in the D or C rings. If broadening had not been so great their progress could almost certainly have been traced quite readily.



Although there could have been complexing at the C<sub>3</sub> carbonyl group, there was no sign of this, the C-19 methyl shifts being fairly small and normalising reasonably.

This alcohol thus supports the findings with the previous alcohols that, although shift sizes are good allowing more protons to be observed than with the cyanoacetates, the broadening is such as to produce severe limitations.

(iv) Testosterone

This alcohol was studied for comparison with the above alcohol.

Diamagnetic spectrum: The diamagnetic line positions of the assignable peaks are given in Table 48.

Table 48. Diamagnetic line positions, in Hz downfield from TMS, at 100 MHz, for assignable signals in testosterone (0.2M) in chloroform-acetone solvent.

C-18 Me	C-19 Me	H <sub>17</sub>	OH	H <sub>4</sub>
79.8	123.0	359.5	347.0	564.4

Addition of cobalt: Investigations were carried out using solutions 0.2M in alcohol, each solution containing 0.2ml CDCl<sub>3</sub>. The peak displacements on addition of cobalt and the normalisation factors with respect to the H<sub>17</sub> signal are given in Table 49.

The H<sub>17</sub> shift change was slightly smaller here than with dihydrotestosterone and the proportionality with cobalt molarity was slightly better, suggesting a lesser degree of complexing.



**Table 42.** Displacements, in Hz, and normalisation factors, as percentages, of signals in testosterone, on addition of cobalt(II) perchlorate.

Conc. Co(II), $\bar{M}$	Displacements				Normalisation factors				
	C-18 Me	C-19 Me	H <sub>17</sub>	OH	H <sub>4</sub>	C-18 Me	C-19 Me	OH	H <sub>4</sub>
0.008	-10.1	-1.4	-32.9	-94.2	+18.2	-30.4	-4.3	-283	+55.4
0.02	-23.0	-4.2	-68.9	-210.9	+34.8	-33.4	-6.1	-306	+50.5
0.05	-66.8	-13.4	-200.4	-654	+75.7	-33.4	-6.7	-326	+37.8
0.07	-87.6	-19.5	-267.3	-833	+92.4	-32.8	-7.3	-312	+34.6
0.11	-145.3	-35.6	-436.3	*	+123.0	-33.2	-8.2		+28.2
0.18	-224.4	-55.1	-678.0	*	+159.3	-33.1	-8.2		+23.4

\* signal not observable.



The normalisation factors showed poor concordancy, the hydroxyl proton (surprisingly visible in this compound) and the C-18 methyl protons having the most consistent factors. The factors for  $H_4$  proton decrease and those for C-19 methyl increase with increasing cobalt concentration. These observations, and the fact that the  $H_4$  peak had a very considerable, and upfield, shift, suggested that some complexing was occurring at the carbonyl group. No such complexing was found in the dihydro derivative and so it can be assumed that only conjugated ketones complex strongly enough to give significant shifts (see also Section (d)).

If the proportion of complexing at each site remained constant, then one would expect the normalisation factors to be fairly constant which was not the case except for protons far removed from the carbonyl group. The decrease in the  $H_4$  factors suggested that the relative extent of complexing at the two sites varied with the composition of the solution, possibly because complexes containing two cobalt ions may make a significant contribution at higher cobalt concentrations. Alternatively, complexing at the different sites may involve different stoichiometries.

Two further peaks moved downfield out of the methylene hump, one of which appeared to be a doublet. Also a multiplet, possibly a pentet, appeared at higher fields than the methylene hump. The normalisation plots for these signals were straight lines whose gradients and intercepts gave the normalisation factors and diamagnetic line positions shown in Table 50.



Table 50. Normalisation factors, as percentages, and diamagnetic line positions, in Hz downfield from TMS, at 100 MHz, for unassigned signals in testosterone.

	A(doublet)	B	C(upfield peak)
Normalisation factor	-64	-50.4	-4.3
Diamagnetic line position	216	145	95.7

Peak B was assigned as  $H_{16}(\beta)$  on the basis of the peak in dihydrotestosterone (Section (iii)) which had a very similar diamagnetic position (146 Hz) and normalisation factor (-52.4%).

There was no corresponding signal in dihydrotestosterone to peak A here, and so it was assumed that it could not arise from any proton close to the hydroxyl group. It had however a very considerable shift and so it must have arisen from a proton very close to the carbonyl group, that is one of the  $H_2$  protons. Of the two  $H_2$  protons, the  $\alpha$  proton would be expected to be a broad doublet, the  $\beta$  proton a broad triplet, and so the doublet here was assigned tentatively as  $H_2(\alpha)$ . Further evidence for this assignment came from studies with cholest-4-en-3-one (see Section d(ii)).

Shift to linewidth ratios for the C-18 methyl were approximately 20, comparable with the other alcohols, but for the C-19 methyl peak they were smaller, presumably due to opposing shifts, resulting from the two complexing sites.

Thus these two very similar alcohols behave rather



differently due to the fact that cobalt complexes significantly with conjugated ketones but not with unconjugated ones.

(v) p-methyl benzyl alcohol

Diamagnetic spectrum: The diamagnetic line positions are presented in Table 51.

Table 51. Diamagnetic line positions, in Hz downfield from TMS, at 100 MHz, for signals of p-methyl benzyl alcohol.

Conc. alcohol, <u>M</u>	OH	CH <sub>2</sub>	Phenyl	CH <sub>3</sub>
1.0	413.3	456.0	716.1	227.6
0.5	406.7	456.7	717.0	228.6

The CH<sub>2</sub> signal was a doublet and the OH signal a triplet,  $J = 5.3$  Hz, showing that the hydroxylic proton exchange was relatively slow. The phenyl signals consisted of four peaks whose weighted average position is given in the table. Their positions and relative heights (1.0M solution) were 726.6 Hz (1.0); 718.6 Hz (3.1); 713.0 Hz (2.8); 705.0 Hz (0.86) and the peaks showed further splitting. The signals were thus approximately two doublets of coupling constant 8.0 Hz.

Addition of cobalt: Investigations were carried out on solutions 1.0 and 0.5M in alcohol. On addition of cobalt all the peaks moved downfield, and the phenyl multiplet became one singlet. The shift changes and the normalisation factors with respect to CH<sub>2</sub> signal are given in Table 52.



Table 52. Displacements, in Hz, and normalisation factors, as percentages, of signals in p-methyl benzyl alcohol on addition of cobalt(II) perchlorate.

Conc. alcohol, <u>M</u>	Conc. Co(II), <u>M</u>	Displacements (all -ve)				Normalisation factors		
		OH	CH <sub>2</sub>	Ph	CH <sub>3</sub>	OH	Ph	CH <sub>3</sub>
1.0	0.08	1027	596	11.1	17.8	172	1.9	3.0
	0.11	1415	836	16.5	24.7	169	2.0	3.0
	0.21	*	1595	35.6	47.5		2.2	3.0
0.5	0.05	743	457.9	8.9	13.2	162	1.9	2.9
	0.10	*	992	21.8	28.7		2.2	2.9

\* Signal not observable.

The linearity of the shift changes with respect to cobalt molarity was fairly good though not perfect.

The methylene and hydroxyl peak shifts were very large, much greater than for the corresponding peaks of any of the other alcohols, but the phenyl and methyl peak shifts were small, as is displayed by their very low normalisation factors.

The normalisation factors were reasonably concordant. The fact that the phenyl signals first coalesced to a singlet, of linewidth less than 8.0 Hz, and then moved as a singlet on addition of cobalt was very strange. Confirmation of the fact that the singlet did arise from four rather than just two protons was obtained by integration. The signals of the two pairs of protons were obviously being shifted at very similar rates.

The unusual shifts found here may be explained as follows. The contact contribution to the shifts would be expected to be similar in pattern to those found in the benzylamine (bz)



complex with nickel(II). Fitzgerald and Drago<sup>14</sup> found the shifts for the complex  $\text{Ni}(\text{bz})_6(\text{BF}_4)_2$  to be  
 $\text{NH}_2$ : +6330 Hz;  $\text{CH}_2$ : -2060 Hz; Ph(ortho): +88 Hz;  
 Ph(meta): -85 Hz; Ph(para): +93 Hz.

The pseudocontact shifts would be expected to have a negative sign for all the protons since they all lie within the cone with  $\chi = 55^\circ$ . These shifts will decrease in magnitude with distance, the angle dependence being fairly small.

We thus have the resultant shifts as shown in Table 53.

Table 53. Descriptive evaluation of contact and pseudocontact contributions and resultant shifts for p-methyl benzyl alcohol in presence of cobalt(II) perchlorate.

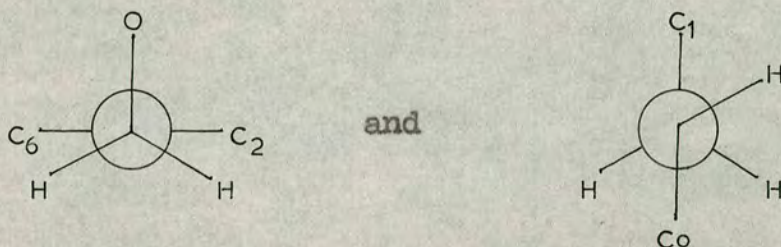
Protons	Contact shift	Pseudocontact shift	Resultant shift
OH	med. large +ve	very large -ve	large -ve
$\text{CH}_2$	fairly large -ve	large -ve	large -ve
Ph(o)	very small +ve	small -ve	small -ve
Ph(m)	very small -ve	very small -ve	small -ve
$\text{CH}_3$	extremely small -ve	very small -ve	small -ve

It was assumed that the hydroxyl peak would be similarly shifted to the amino peak. The pseudocontact contribution must be greater in general than the contact contribution to give the resultant observed shifts. The methyl peak shift is the only one not very satisfactorily explained. As both its pseudocontact and contact contributions to the shift should be smaller than those for the meta phenyl protons, and



all these shifts are negative, its overall shift should be smaller, which was not the case.

The conformation assumed to be the most likely here was that involving the configurations



The shift changes were strongly dependent on ligand concentration, the "strength of complexing" expression having a value of around 50%. This was perhaps surprising considering the reasonably good proportionality found between the shifts and the cobalt concentration.

The shift to linewidth ratio for the  $\text{CH}_2$  peak was 7.4 which was not very good.

Heating from  $28^\circ$  to  $50^\circ$  decreased both the shift change and the linewidth, but improved the ratio of the two, to 17.3 at  $50^\circ$ .

The solutions for this series were prepared using undried deuterioacetone. Three further solutions in dried deuterioacetone were also investigated and the shifts were found to have increased about 12% showing that again water had a considerable effect. The normalisation factors were not greatly affected.

The *p*-methyl benzyl alcohol and *p*-methyl benzyl cyanide molecules are very similar with only the functional group for complexing different. In both, the pseudocontact contribution to the shifts was dominant, for the former in a down-

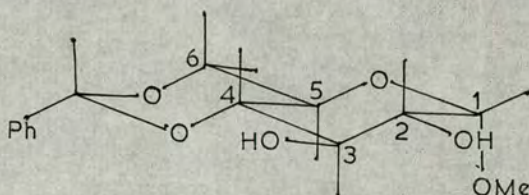


field direction, for the latter upfield. Combined with the contact shifts, the overall shifts found in the cyanide were more satisfactory as they distinguished between the phenyl protons and gave shifts of a reasonable size for all the protons. The shift to linewidth ratios too were greater and the dependence on the ligand concentration less, both factors making the cyanide system more acceptable.

However, useful results can obviously be obtained from alcohols of this type in general and probably can give complementary information to the cyanides.

(vi) Methyl 4,6-O-benzylidene- $\alpha$ -D-glucopyranoside

This diol was investigated to see whether diols would give stronger complexes and whether they too would be amenable to normalisation procedures and, if so, under what conditions.



Diamagnetic spectrum: The diamagnetic line positions of the distinguishable peaks are given in Table 54.

Table 54. Diamagnetic line positions, in Hz downfield from TMS, at 100 MHz, of assignable signals in methyl 4,6-O-benzylidene- $\alpha$ -D-glucopyranoside (0.2M).

OMe	H <sub>1</sub>	benzylic H	Quartet	Phenyl
339.4	472.0	556.8	420.1	729 - 757



The aromatic proton signals appeared as a multiplet. The  $H_1$  signal was a doublet of coupling constant 3.8 Hz. It was assigned on the basis of its position (505 Hz) and coupling constant (3.5 Hz) found in pyridine solution<sup>257</sup>. The irregular quartet at 420.1 Hz with coupling constants of approximately 10 and 5 Hz was thought to be the signal of  $H_6(eq)$  which would have a large geminal coupling with  $H_6(ax)$  and a moderate vicinal coupling with the axial  $H_5$ . The remaining ring protons and hydroxyl protons lay in the region 340-440 Hz. Addition of cobalt: Investigations were carried out using solutions 0.2M in diol. The phenyl peaks (two fairly broad peaks), the benzylic proton and the methoxy group signals were the only signals assignable with certainty, and their paramagnetic positions or displacements, as appropriate, are given in Table 55.

**Table 55.** Displacements, in Hz, or paramagnetic positions, in Hz downfield from TMS, of assignable signals in methyl 4,6-O-benzylidene- $\alpha$ -D-glucopyranoside, on addition of cobalt(II) perchlorate.

Conc. Co(II), <u>M</u>	Displacement		Paramagnetic position	
	OMe	benzylic H	Phenyl	
0.02	+16.3	-26.2	741.7	731.9
0.05	+31.4	-44.7	737.6	726.2
0.16	+71.4	-60.1	704.8	
0.33	+78.2	-52.8	691.8	

The shift changes of the methoxy and benzylic proton signals, when plotted with respect to the cobalt molarity, gave very



distinct curves; in fact showed a maximum shift, occurring when the cobalt and diol were approximately equimolar.

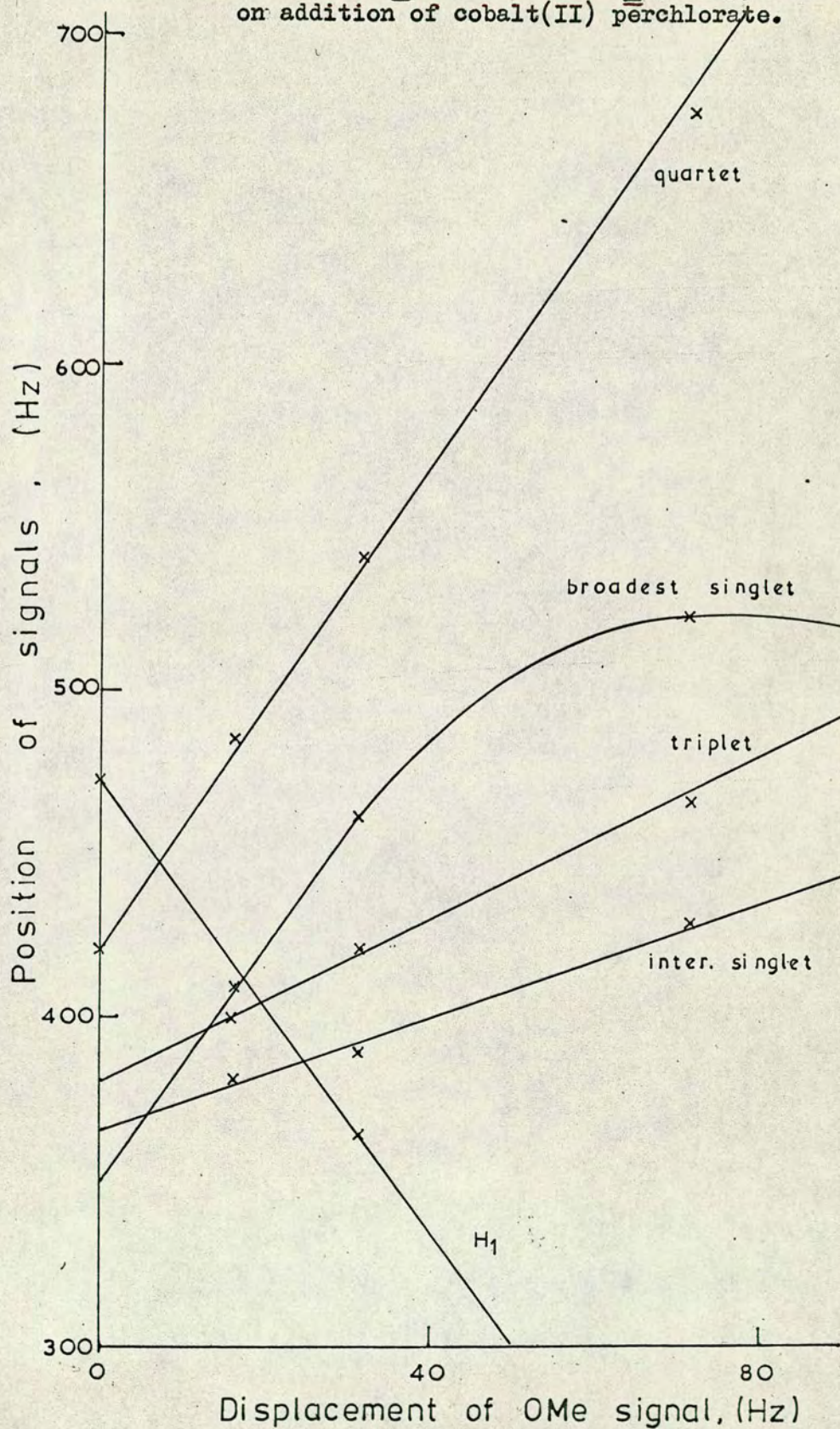
At the lowest concentrations of cobalt, 0.02 and 0.05M, five signals, each corresponding to one proton, became apparent as broad peaks moving downfield. Since there are nine protons remaining to be assigned, seven ring and two hydroxylic, the other four protons must have shifted very rapidly on addition of cobalt, so rapidly that even at 0.02M cobalt no peak was visible between  $\tau$  -10 to 20 at increased RF powers. It could be that these four signals were too broad to be visible but that would seem to be less likely.

Assuming that the "missing" four protons are the two hydroxylic protons and  $H_2$  and  $H_3$ , the remaining five peaks can be attributed to  $H_1$ ,  $H_4$ ,  $H_5$  and two  $H_6$ 's. One was a triplet, one a doublet and the remaining three variously broadened singlets in general appearance. Unfortunately there was no ideal signal to which the signals could be normalised. Of the two possible signals, the methoxy proton signal was chosen rather than the benzylic proton since its shift changes always increased with increasing cobalt molarity and it was also closer to the complexing site.

The peak positions were plotted with respect to the methoxy shift changes (Figure 13). Although there was considerable uncertainty in the peak positions, straight lines could be drawn for four out of the five signals, the "left-over" points giving a curve for the broadest "singlet". From the gradients, normalisation factors with respect to the methoxy signal were calculated to be



Figure 13. Normalisation plots (with respect to OMe signal) for signals in methyl 4,6-O-benzylidene- $\alpha$ -D-glucopyranoside on addition of cobalt(II) perchlorate.





triplet	-120%
doublet	-370%
narrowest singlet	+350%
intermediate singlet	-86%
broadest singlet curve (-ve)	

The "doublet" extrapolated back to the diamagnetic position of the quartet (420 Hz; see Table 54) while the narrowest "singlet" extrapolated back to the diamagnetic position of  $H_1$  (472 Hz), thus assigning that signal. The remaining three peaks extrapolated back to 380 Hz (triplet), 365 Hz (intermediate singlet) and approximately 350 Hz (broadest singlet).

Assignment of the signals was not possible with any certainty. The magnitude of the shifts indicated that considerable complexing was occurring, the possibility of chelation remaining unconfirmed. Complexing of the diol with cobalt(II) was not further investigated but shifts on addition of lanthanides are reported later.

#### (vii) Conclusion

The alcohols studied above have shown that they too are suitable ligands for complexing with cobalt for shift studies. On the whole, however, they are not as consistent in their behaviour as were the cyanides, perhaps because the closer position of the cobalt makes variation in the pseudo-contact angle more influential, but the results from them often yield complementary information which may prove valuable in certain situations.



(c) Amide ligands

Although various studies<sup>258-260</sup> have shown that amides complex with cobalt(II) and other paramagnetic ions giving substantial shifts, the studies were conducted from a physical/inorganic point of view and so the potential of these ligands in giving selective shifts useful in structural work was unexplored. Acetamido compounds seemed of particular interest since the acetamido methyl could provide a normalising signal.

Two aromatic and one aliphatic amide were first investigated fairly extensively and then two sugar acetamides were examined in less detail, with a view to the ease of assignment of the signals.

(i) p-acetamidotoluene

Diamagnetic spectrum: The signals were all readily assigned in the diamagnetic spectrum and their positions are given in Table 56.

Table 56. Diamagnetic line positions, in Hz downfield from TMS, at 100 MHz, for signals in p-acetamidotoluene (0.2M).

COMe	NH	Ph(ortho)	Ph(meta)	ArMe
204.3	903	749.8	707.0	225.1

The phenyl signals appeared as clear doublets of coupling constant 8.6 Hz. The NH peak was small and very broad. Addition of cobalt: Investigations were carried out with 0.2M amide solutions. Much lower molarities of cobalt(II)



were required in this case than with either the cyanides or the alcohols to give considerable shift displacements.

The NH peak disappeared very rapidly on addition of cobalt, but the other peaks were readily followed. The shift displacements are given in Table 57.

Table 57. Displacements (all negative), in Hz, of signals of p-acetamidotoluene, and linewidth of ArMe signal, on addition of cobalt(II) perchlorate.

Conc. Co(II), <u>M</u>	COMe	Ph(o)	Ph(m)	ArMe	Linewidth of ArMe, <u>Hz.</u>
0.02	5.8	62.7	0.5	4.9	3.2
0.05	42	212.4	8.1	16.2	2.6
0.10	110	347	16.8	26.2	2.2

The shift changes were not linear with respect to the cobalt molarity for any of the signals although they all increased consistently with increasing molarity.

Normalisation was not attempted since the ratios of the shifts of the various peaks were inconsistent, except for the ratio between the shifts of the ortho phenyl and aromatic methyl signals which remained fairly constant (12.8, 13.1 and 13.2). The acetamido methyl which it was hoped to use for normalisation behaved particularly anomalously (see below).

There were only two singlet peaks available for measurement of the ratio of shift to linewidth. The aromatic methyl linewidth first increased then decreased with cobalt concentration and so no consistent ratio could be measured from it. The acetamido methyl linewidth was very broad, in



the order of 50 Hz in the 0.10M cobalt solution, and clearly did not provide a typical measure of the shift to linewidth ratio for this type of compound.

As mentioned above, the acetamido methyl signal shifts were anomalous. In a series of solutions of increasing cobalt molarity (amide molarity 0.2M) in undried acetone, the signal showed an upfield shift instead of the downfield shift observed in the dried acetone solutions. Further, the shifts did not increase consistently with cobalt concentration, being smaller at 0.07M than at 0.04M.

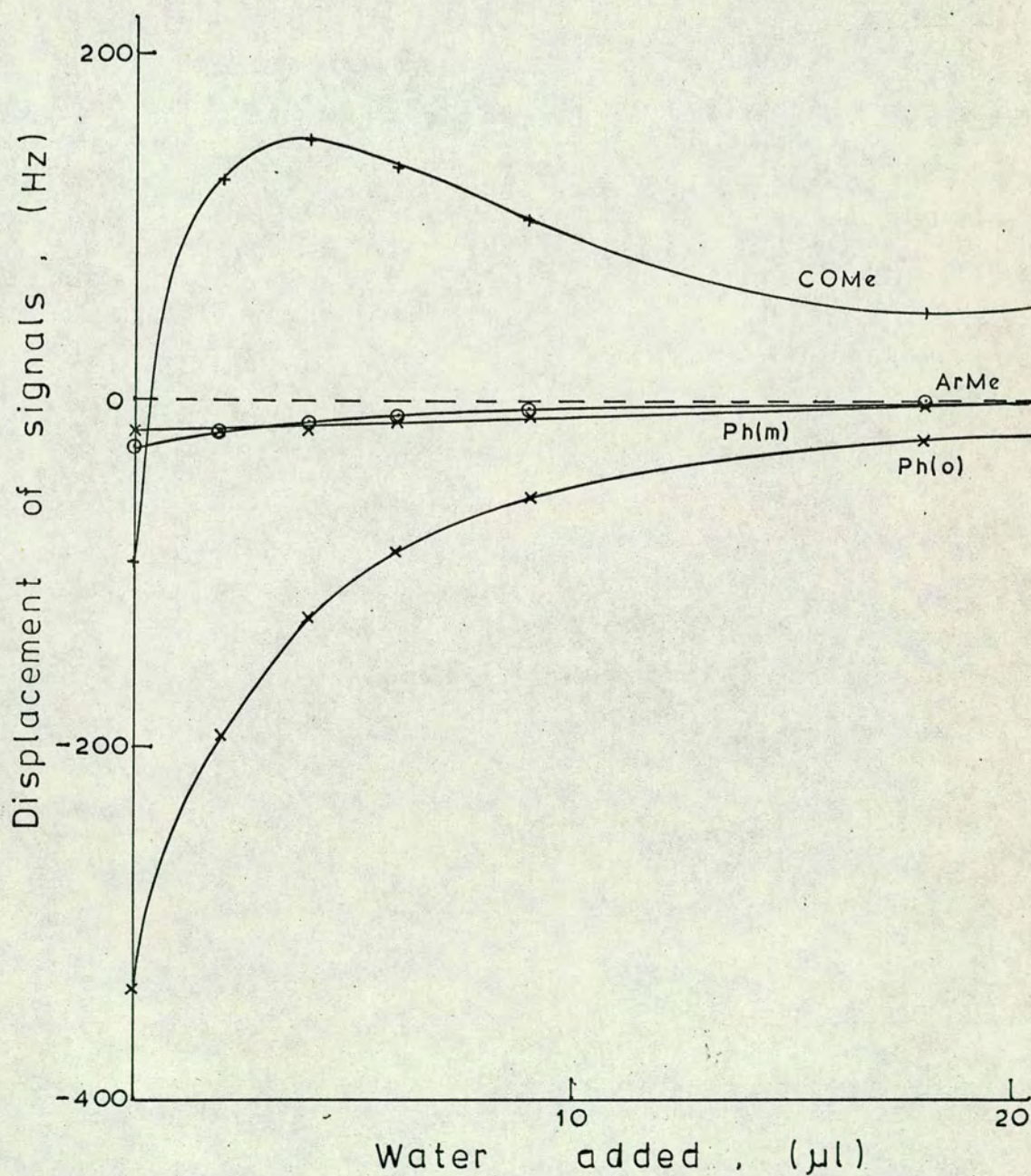
To investigate this, water was added to a solution in dried acetone (with 0.1M cobalt) and the effect of heat at various stages in the water addition examined. On addition of water, all the shifts decreased except the acetamido methyl which moved from a downfield shift to an upfield shift then returned towards its diamagnetic position (Figure 14). None of the shift ratios remained constant and normalisation was clearly out of the question. The shifts of the acetamido methyl were consistent with the observations in the undried acetone solutions.

Although the acetamido methyl shifts increased in the opposite direction before returning to zero, the linewidths systematically decreased with increasing water concentration.

The effect of heat on three solutions was investigated, the first with no added water, the second with 2  $\mu$ l water and the third with 9  $\mu$ l (approx. 1M) water. The direction of movement of the peaks on heating was unpredictable, the ortho phenyl and acetamido methyl peaks being the most consistent. The shift of the former in each case decreased,



Figure 14. Plot of shift displacement (Hz) of signals of p-acetamidotoluene in presence of cobalt(II) perchlorate with respect to volume of water added ( $\mu$ l).





and the latter showed a downfield movement independent of whether its initial shift was upfield or downfield. The remaining two peaks sometimes moved upfield, sometimes downfield and sometimes one then the other, but in each case the shift changes were small.

In conclusion, the behaviour of *p*-acetamidotoluene shows that for this type of amide, complexing with cobalt is unlikely to be useful as a structural tool. In particular, the anomalous behaviour of the acetamido methyl shifts make these quite unsuitable for normalisation and even the shift ratios of the other peaks were dependent on the cobalt concentration and particularly on the presence of water.

In an attempt to explain this anomalous behaviour, further amides were examined.

(ii) N-methyl p-acetamidotoluene

This amide not only provides an additional useful signal for study, but, more importantly, has an alternative preferred configuration in the diamagnetic state. Two configurations exist for these amides, the *cis* configuration (phenyl group *cis* to carbonyl group) being more normal but the *trans* configuration being preferred when the nitrogen is alkylated<sup>261,262</sup>. If this configurational equilibrium is responsible for the anomalous behaviour of *p*-acetamidotoluene, then the N-methylated derivative should show rather different behaviour, indeed may be amenable to normalisation and shift studies.

Diamagnetic spectrum: The diamagnetic line positions are given in Table 58.



Table 58. Diamagnetic line positions, in Hz downfield from TMS, at 100 MHz, for signals of N-methyl p-acetamidotoluene (0.2M).

COMe	NMe	Ph(o)	Ph(m)	ArMe
175.6	315.7	717.8	724.5	235.1

The three methyl peaks were assigned on the basis of their shifts compared with those in  $\text{CDCl}_3$  solution<sup>261</sup>. The heights of these peaks are all different although each is due to three protons. Their relative heights are ArMe:NMe:COMe 2.2:1.9:1.0 while the linewidths respectively are 1.3 Hz, 1.3 Hz and 2.5 Hz. Each linewidth is broader than the instrumental linewidth (approx. 0.6 Hz). The ArMe signal is broadened due to coupling with the phenyl protons closest to it (meta phenyl). The NMe signal is broadened due to the quadrupolar relaxation and possibly coupling arising from the nitrogen. The COMe signal may be broadened due to exchange between cis and trans configurations. If this were the case, then increasing the temperature should increase the rate of exchange and so narrow the peak. A diamagnetic solution of the amide was heated from 28° to 60° at which temperature the COMe linewidth had decreased to 1.3 Hz. The NMe linewidth also decreased slightly (to 1.1 Hz) but the ArMe linewidth remained constant as would be expected.

In the diamagnetic solution, the phenyl signals appeared as a close doublet with many small side peaks. The average positions for each of the two sets of protons was calculated as the weighted average of the appropriate peaks.



Addition of cobalt: Investigations were carried out using solutions 0.2M in amide. The shift displacements and the normalisation factors calculated with respect to the NMe signal are given in Table 59.

Table 59. Displacements, in Hz, and normalisation factors, as percentages, with respect to NMe signal, for N-methyl p-acetamidotoluene on addition of cobalt(II) perchlorate.

Conc. Co(II), <u>M</u>	Displacements (all -ve)					Normalisation factors			
	COMe	NMe	Ph(o)	Ph(m)	ArMe	COMe	Ph (o)	Ph (m)	ArMe
0.014	86	242.1	90.8	52.0	27.1	35.5	37.5	21.5	11.2
0.03	153.6	466.0	172.7	99.1	53.5	32.9	37.0	21.3	11.5
0.07	339.0	905.6	342.2	192.7	105.1	37.4	37.8	21.3	11.6
0.10	473.3	1195.3	459.6	252.9	139.1	39.6	38.4	21.2	11.6
0.11	520.2	1263.6	487.1	268.4	147.1	41.1	38.5	21.2	11.6

The methyl peaks were assigned in each spectrum by plotting their positions with respect to the cobalt molarity which gave gentle curves for each peak. A plot of the shift of the ortho phenyl protons (assumed to be displaced more by cobalt) against that of the meta protons gave a straight line which confirmed the assignment of these protons in the diamagnetic spectrum (Table 58), the alternative assignment being inconsistent with this line.

Normalisation was carried out with respect to the NMe signal as it was the most shifted and the COMe signal had proved unreliable in the p-acetamidotoluene studies. As Table 59 shows, normalisation was good, and even the COMe



signal gave fairly consistent normalisation factors. All the peaks were shifted downfield, including the COMe peak, as were the peaks for the unmethylated amide in dried acetone solution. However the sizes of the displacements were very different from one proton type to another in the two amides, the methylated derivative having the larger shifts overall.

The effect of ligand concentration on the shifts was investigated by examining a solution 0.5M in amide and 0.10M in cobalt(II). All the peaks gave the same normalisation factors as with the 0.2M solutions except the COMe peak which had a normalisation factor of -17.8%, considerably different. Shift sizes were greatly decreased, the "strength of complexing" expression having a value of 80%.

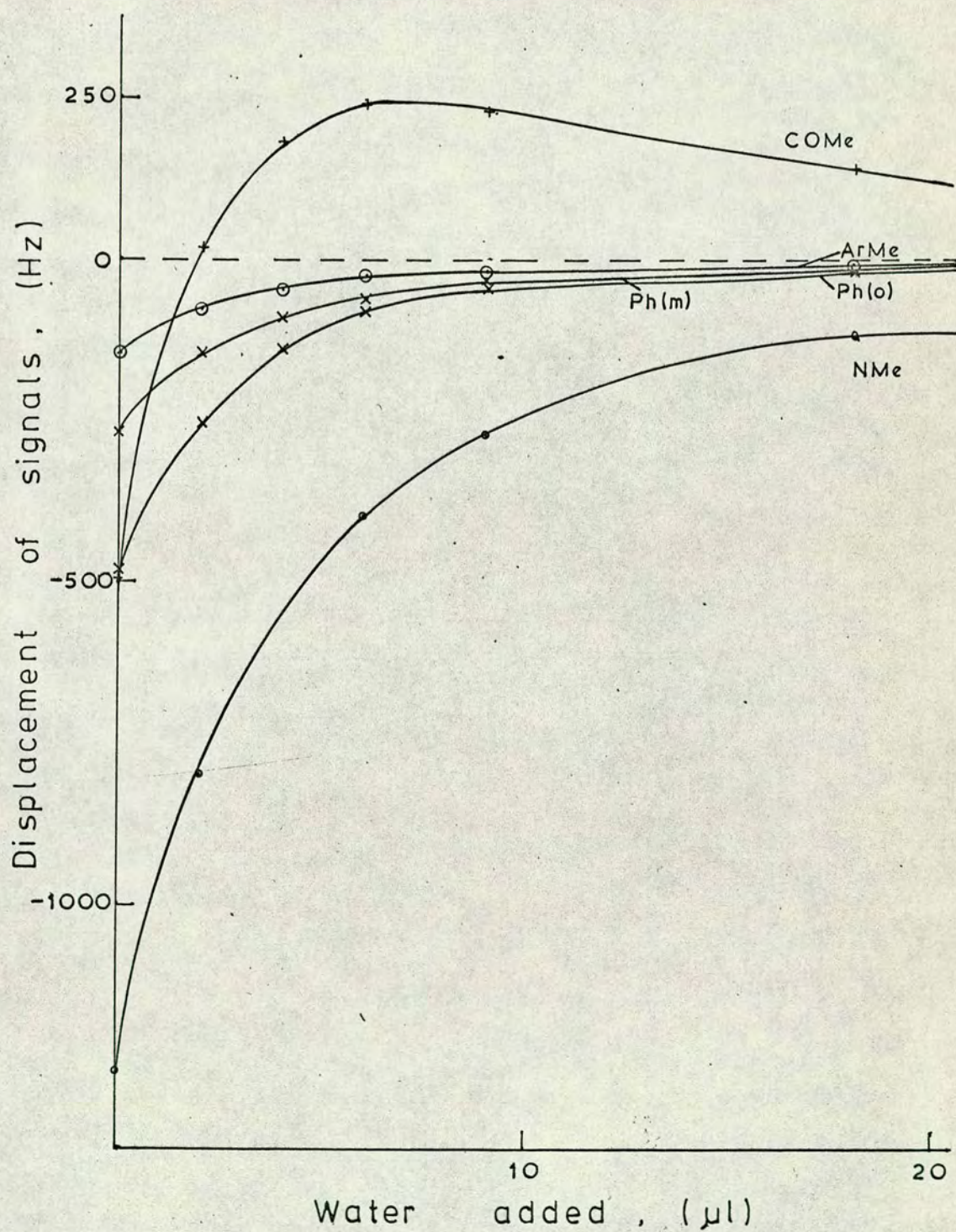
Shift to linewidth ratios were about 30 for the NMe signal which was quite acceptable. The value was much lower ( $< 10$ ) for the COMe peak and the ArMe linewidth first increased then decreased, with increasing cobalt concentration, by an amount too great ( $> 2$  Hz) to be accounted for by decoupling from the phenyl protons. The phenyl peaks also appeared to narrow after an initial increase in linewidth. The latter could be due to decoupling from each other.

The effect of adding water was examined with a solution 0.2M in amide and 0.11M in cobalt(II) (Figure 15). Shifts were greatly affected, and, as with the unmethylated derivative, the COMe peak moved rapidly upfield beyond its diamagnetic position before returning to it.

On addition of water, the NMe linewidth decreased



Figure 15. Plot of shift displacement (Hz) of signals of N-methyl p-acetamidotoluene in presence of cobalt(II) perchlorate, with respect to volume of added water ( $\mu$ l).





considerably, the shift to linewidth ratio of 29 being little changed. The ArMe linewidth first increased then decreased, while the COMe linewidth where measurable appeared to decrease consistently.

Three solutions were examined for the effect of increasing the temperature, the first with no added water, the second with 1  $\mu$ l water and the third with 18  $\mu$ l water. As with *p*-acetamidotoluene the peaks moved inconsistently in direction. The COMe peak again always moved downfield. In the first and second solutions, decreases in the shift change were observed for all the other peaks, but an increase was found for all the peaks in the third solution. Except for the COMe peak, normalisation factors were not greatly affected by heating.

The methylated and unmethylated amides clearly behave similarly in some respects, particularly with regard to the effect of water on the COMe shift. It therefore seems unlikely that their anomalous behaviour can be ascribed to the conformational equilibrium mentioned above. Examination of *N,N*-dimethylacetamide (next section) helped considerably to clarify the problem and more detailed discussion is therefore deferred.

(iii) *N,N*-dimethylacetamide

The diamagnetic spectrum consisted of three methyl signals whose positions and linewidths are given in Table 60. The highfield peak was readily assigned as the COMe peak; the NMe peaks were assigned on the basis of literature figures for  $\text{CCl}_4$  solution<sup>263</sup>:



Table 60. Diamagnetic line positions, in Hz downfield from TMS, at 100 MHz, and linewidths, in Hz, of signals in N,N-dimethylacetamide (0.2M).

	COMe	NMe (cis)	NMe (trans)
Line position	196.4	283.3	300.5
Linewidth	1.2	1.35	0.8

COMe  $\tau$ 8.02; NMe (cis to carbonyl)  $\tau$ 7.17;

NMe (trans)  $\tau$ 7.00.

Addition of cobalt: Investigations were carried out using solutions 0.2M in amide. The solutions were purple in colour, a bluer purple at low cobalt concentrations and a pinker purple at higher concentrations. (The two previous amides both gave pink solutions.) Since the tetrahedral complex is normally blue and the octahedral pink, this suggested the presence of both types of complex in this system.

The shift displacements and the normalisation factors with respect to the COMe signal are given in Table 61.

Table 61. Displacements, in Hz, and normalisation factors, as percentages, with respect to COMe signal, for signals in N,N- dimethylacetamide on addition of cobalt(II) perchlorate.

Conc. Co(II), <u>M</u>	Displacements (all -ve)			Normalisation factors	
	COMe	NMe(cis)	NMe(trans)	NMe(cis)	NMe(trans)
0.01	84.7	261.2	321.2	308	379
0.03	197.9	567.2	665.0	286	336
0.05	395.5	1018.9	1123.0	258	284
0.06	499.4	1216.9	1317.4	244	264



The plot of the peak positions with respect to cobalt molarity was linear for the COMe peak and sufficiently linear for the NMe peaks to enable assignment of them (cis and trans) in the paramagnetic spectra.

The NMe shift changes here were greater than those for the N-methyl p-acetamidotoluene.

Normalisation was not very good and the NMe signals do not normalise with respect to each other either.

The linewidths of the three peaks were noticeably different; the shift to linewidth ratios were calculated graphically to be NMe(cis) 43; NMe(trans) 120; COMe ca. 6. Again the COMe peak was exceptionally broad. The trans NMe peak had a very high ratio, much greater than those encountered previously with cobalt.

As water was added to the solution containing 0.06M cobalt, the colour grew pinker. The NMe peaks were moved very similarly, though not identically, back towards their diamagnetic positions. The COMe peak moved very rapidly upfield then turned and moved back towards its diamagnetic position, as for the two previous amides studied.

The COMe linewidth decreased consistently with added water, irrespective of the direction or magnitude of shift.

A solution with 0.05M cobalt(II) was heated to 50°. The NMe shift changes both decreased but again the COMe peak moved downfield, thus increasing its shift.

Finally, a solution of 0.10M cobalt in neat amide (ratio of cobalt:amide  $\approx$  1:100) was prepared. The shift changes observed are tabulated in Table 62.



Table 62. Displacements, in Hz, and normalisation factors, as percentages, for signals in N,N-dimethylacetamide for 0.10M cobalt(II) perchlorate in neat amide.

Displacements			Normalisation factors	
COMe	NMe(cis)	NMe(trans)	NMe(cis)	NMe(trans)
+11.9	-21.1	-49.2	-177	-414

Assignment of the peaks was necessarily tentative, based on the peak positions and the linewidths assuming similarity with the acetone solutions. It can be seen that the normalisation factors were completely different to those in the acetone solutions, the COMe peak showing an upfield shift.

### Discussion

Amides have been shown<sup>258,259</sup> to coordinate with cobalt(II) ions predominantly through the carbonyl oxygen, with the Co-O-C angle less than  $180^\circ$ . Both four-coordinated tetrahedral and six-coordinated octahedral complexes have been isolated for N,N-dimethylacetamide<sup>259</sup> and six-coordinated complexes with N,N-dimethylformamide<sup>258</sup> and with benzamide<sup>260</sup> have been reported.

In the present work with dimethylacetamide, purple solutions were obtained suggesting a tetrahedral complex might be present. Shift changes have been evaluated<sup>259</sup> for the tetrahedral and the octahedral complexes of this ligand and are presented in Table 63.



Table 63. Shift displacements, in Hz relative to diamagnetic position, at 60 MHz, in four- and six-coordinated complexes of N,N-dimethylacetamide with cobalt(II)<sup>259</sup>.

Complex	COMe	NMe(cis)	NMe(trans)	Solvent
Co(DMA) <sub>6</sub> (ClO <sub>4</sub> ) <sub>2</sub>	+44	-262	-649	DMA
Co(DMA) <sub>4</sub> (ClO <sub>4</sub> ) <sub>2</sub>	-342	-1021	-1017	CH <sub>2</sub> Cl <sub>2</sub>

Two qualitative features of these results are of interest in relation to the present work.

(i) for the four-coordinated species the ratio of the shifts of the cis methyl to the trans methyl is approximately 1 while for the six-coordinated species it is less than 0.5.

(ii) the shift of the COMe is negative in the four- and slightly positive in the six-coordinated species.

Thus in a solution containing both species, the ratio (cis/trans) of the NMe shifts and the relative magnitude and sign of the COMe shift will give a measure of the proportion of each form present. Although the numerical values shown in Table 63 will not be strictly relevant to the acetone solutions studied in the present work, (an additional complication being the presence of two water molecules in the perchlorate) it is interesting to use these data for a qualitative examination of our results.

#### 1) concentration of cobalt

The ratio (cis/trans) of the NMe shifts (0.8-0.9) and the fairly high negative displacement of the COMe signal suggests a strong predominance of the four-coordinated species. This



is borne out by the purple colour of the solutions. Increasing the cobalt concentration gave an increase in the ratio suggesting an increase in the amount of four-coordinated species, which would be expected on increasing the cobalt: amide ratio.

2) addition of water

Rapid decrease in the negative displacement of the COMe shift to a positive value suggests an increase in the proportion of the six-coordinated species. This was supported by the increasing pink colour of the solutions. However the ratio (cis/trans) of the NMe shifts unexpectedly increased on addition of water.

3) effect of heat

The increased negative displacement of the COMe peak suggests more four-coordinated species, supported by an increase in the shift ratio.

4) cobalt in neat amide

In this case an upfield COMe displacement was observed suggesting a six-coordinated species predominant. This was supported by a low ratio (0.43) for the NMe shifts. With the large amide:cobalt ratio in this solution, a six-coordinated species would be expected to predominate.

It would thus appear that the equilibrium between tetrahedral and octahedral complexes is sufficient to explain the dimethylacetamide results obtained in this work at least qualitatively without recourse to other possible explanations. The discrepancy in the water addition results is not surprising in view of the changing nature of the complex with water replacing amide ligands.



It seems very likely that the anomalous behaviour of the two aromatic amides is also accounted for, at least to a considerable extent, by an equilibrium between four- and six-coordinated species (although the consistently pink colour of the solutions suggests that the octahedral complex either predominates or absorbs more intensely). Thus, for both aromatic amides, the upfield shift of the COMe peak on addition of water can be ascribed to an increase in the proportion of the octahedral species and the downfield shift on heating to an increase in the proportion of tetrahedral species. The non-linearity with cobalt concentration of the COMe shifts for *p*-acetamidotoluene (both in dry and undried acetone) can be ascribed to an increase in the proportion of tetrahedral species at higher cobalt concentration. The effect of amide concentration on the COMe shift of the *N*-methyl compound (lower negative normalisation factor at higher amide concentration) also becomes explicable. Finally, the relatively small shift to linewidth ratios ( $< 10$ ) for the COMe signal in both amides is consistent with the interpretation that two species with shifts of opposite sign are involved. It was originally thought that the small values of this ratio indicated that the methyl group lay near the "pseudocontact cone" and that the anomalies occurred because it crossed the cone when one of the other ligands in the species was altered. The possibility of cancellation between pseudocontact and contact shifts was also considered. However, the tetrahedral-octahedral equilibrium discussed above appears to provide a more satisfactory and consistent explanation of the anomalies.



(iv) 2-acetamido-1,3,4,6-tetra-O-acetyl-2-deoxy- $\alpha$ -D-glucopyranose

Diamagnetic spectrum: The diamagnetic line positions, where measurable, are given in Table 64.

Table 64. Diamagnetic positions, in Hz downfield from TMS, at 100 MHz, for distinguishable signals in 2-acetamido-1,3,4,6-tetra-O-acetyl-2-deoxy- $\alpha$ -D-glucopyranose (0.15M).

$C_1$ -OAc	NHAc	OAc(A)	OAc(B)	OAc(C)	$H_1$	NH
215.7	184.2	195.8	199.6	200.7	611.6	716

The  $C_1$ -acetyl and acetamido signals were assigned on the basis that acetamido peaks absorb at higher fields than primary or equatorial acetyl peaks, which absorb at higher fields than axial acetyl peaks<sup>264</sup>. Horton and coworkers<sup>265</sup>, by deuteration studies, established the following acetyl peak shifts ( $\tau$ ) for acetone- $d_6$  solutions at 60 MHz:

$C_1$ -OAc: 7.90; NHAc: 8.20;  $C_6$ -OAc: 8.05;  $C_3$ -OAc and  $C_4$ -OAc: 8.05 and 8.09, not differentiated.

These assignments substantiate the tabulated assignments but do not enable specific assignment of peaks A, B and C to be made, except that OAc(A) is not  $C_6$ -OAc. The  $C_1$ -OAc assignment was also confirmed by the changed position of this peak in the  $\beta$  isomer.

The ring protons, except  $H_1$ , appeared in two groups, four protons in the region 390 - 460 Hz (downfield from TMS) and two protons at 510 - 530 Hz.



Addition of cobalt: Investigations were carried out with solutions containing 0.15M amide.

On addition of cobalt, the ring proton signals separated out. Spin-decoupling of a solution with 0.075M cobalt(II) (undried acetone) enabled total assignment of these signals, as indicated in Table 65.

Table 65. Assignment of ring proton signals by spin-decoupling, in a solution of 2-acetamido-1,3,4,6-tetra-O-acetyl-2-deoxy- $\alpha$ -D-glucopyranose with 0.075M cobalt(II) perchlorate.

Signal position, Hz	Signal multiplicity	Effect of irradiation at -			Assignment
		723Hz	547Hz	480Hz	
723	Doublet		Doublet to singlet	-	H <sub>3</sub>
547	Triplet	Triplet to doublet		Triplet to doublet	H <sub>4</sub>
480	Doublet	-	Doublet to singlet		H <sub>5</sub>
440	Quartet	-	-	Quartet to doublet	H <sub>6</sub>
415	Quartet	-	-	Quartet to doublet	H <sub>6</sub>
775	Broad peak	-	-	-	H <sub>1</sub>
985	Broad peak	-	-	-	H <sub>2</sub>

The assignments are unambiguous for H<sub>3</sub>, H<sub>4</sub>, H<sub>5</sub> and H<sub>6</sub>'s, the multiplicities being as expected except that H<sub>5</sub> appears as a broad doublet instead of an octet, the small couplings with



the  $H_6$ 's, though present, not being observable. Also,  $H_3$  appears as a doublet rather than a triplet (if  $J_{23} \sim J_{34}$ ) or a quartet. This, and the fact that no narrowing was observed on irradiation of the  $H_2$  peak, suggested that  $H_2$  and  $H_3$  are chemically spin-decoupled. Similarly  $H_1$  and  $H_2$  would be decoupled. The diamagnetic position of  $H_1$  is known, thus confirming the  $H_2$  assignment.

By observation of the signals as they were separated out by the cobalt, coupling constants could be determined in every case:

$J_{12} = 3.7$  Hz;  $J_{23} \approx 9$  Hz (decoupled by 0.05M Co(II));

$J_{34} = 7.7$  Hz;  $J_{45} = 9.4$  Hz;  $J_{56} = 3.7$  and  $2.4$  Hz;

$J_{66} = 12.5$  Hz.

The inequality of the two  $J_{56}$  coupling constants shows the asymmetric disposition of the  $H_6$  protons with respect to  $H_5$ , probably due to a rapid exchange between the two most favoured conformations, the staggered conformation in which the  $C_4$ - and  $C_6$ -acetyls are eclipsed being negligibly populated<sup>266</sup>.

The peak displacements on addition of cobalt are given in Table 66 for the signals whose diamagnetic positions were known, and the peak positions of the remaining signals are given in Table 67.

The  $H_2$  signal was chosen as the basis for normalisation, since the work with the previously studied amides suggested that the acetamido peak would be unsuitable. However the  $H_2$  diamagnetic line position was not known. It was determined from the intercept of the linear plot of the  $H_2$  peak position with respect to the  $H_1$  shift change.



Table 66. Displacements, in Hz, for signals in 2-acetamido-1,3,4,6-tetra-O-acetyl-2-deoxy- $\alpha$ -D-glucopyranose on addition of cobalt(II) perchlorate.

Conc. Co(II), $\frac{M}{M}$	C <sub>1</sub> -OAc	NHAc	OAc(A)	OAc(B)	OAc(C)	H <sub>1</sub>	H <sub>2</sub> *
0.014	-17.4	-58.6	-8.8	-5.0	+11.2	-56.4	-187
0.03	-36.0	-132.5	-18.0	-10.3	+22.5	-118.0	-379
0.05	-48.9	-170.8	-22.2	-14.2	+30.0	-166.4	-553
0.11	-87.3	-336	-40.6	-25.9	+52.7	-291	-969
0.16	-108.6	-459	-51.6	-32.7	+64	-354	-1164

\* extrapolated diamagnetic line position used (see text)

Table 67. Paramagnetic signal positions, in Hz downfield from TMS, for signals in 2-acetamido-1,3,4,6-tetra-O-acetyl-2-deoxy- $\alpha$ -D-glucopyranose, on addition of cobalt(II) perchlorate.

Conc. Co(II), $\frac{M}{M}$	H <sub>3</sub>	H <sub>4</sub>	H <sub>5</sub>	H <sub>6</sub>	H <sub>6</sub>
0.014	599.3	522.6	*	*	*
0.03	674.1	534.8	462.6	427.5	409.4
0.05	733.9	544.8	482.0	431.3	412.6
0.11	891.8	571.4	534.1	440.0	418.7
0.16	966	584	560	449	421

\* signal position not measurable.

The normalisation plots with respect to the H<sub>2</sub> signal were all good straight lines except for the acetamido signal for which the shifts were more negative at higher cobalt concentrations than would be expected from a linear relationship.



This is consistent with a change of equilibrium towards the tetrahedral form at higher cobalt concentrations.

The diamagnetic positions of the proton signals, obtained from the intercepts of their normalisation plots, are given in Table 68, where they may be compared with literature values<sup>267</sup> in  $\text{CDCl}_3$  solution obtained approximately by spin-decoupling.

Table 68. Diamagnetic line positions, measured from normalisation graphs, and compared with literature values<sup>267</sup>, for ring proton signals in 2-acetamido-1,3,4,6-tetra-O-acetyl-2-deoxy- $\alpha$ -D-glucopyranose.

Proton	Calculated value		Literature value
	Hz	$\tau$	$\tau$
H <sub>2</sub>	441	5.59	5.56
H <sub>3</sub>	530	4.70	$\sim$ 4.8
H <sub>4</sub>	511	4.89	$\sim$ 4.9
H <sub>5</sub>	413	5.87	$\sim$ 6.1
H <sub>6</sub> 's	404; 420	5.96; 5.80	*

\* not given.

The correspondence, allowing for the different solvent, is good. These calculated positions also fit into the two groups of signals observed in the diamagnetic spectrum.

The normalisation factors, calculated from the gradients of the graphs, are shown in Table 69.

If one assumes the conformation is that in which the amide oxygen eclipses the H<sub>2</sub> proton<sup>268</sup> and that the Co-O bond lies in the plane of the amide group and represents the



Table 69. Normalisation factors, as percentages, of signals in 2-acetamido-1,3,4,6-tetra-O-acetyl-2-deoxy- $\alpha$ -D-glucopyranose.

C <sub>1</sub> -OAc	NHAc	OAc(A)	OAc(B)	OAc(C)	H <sub>1</sub>	H <sub>3</sub>	H <sub>4</sub>	H <sub>5</sub>	H <sub>6</sub> 's
-9.1	-31	-4.2	-2.7	+5.5	-30.0	-37.5	-6.2	-12.5	-1.6;-2.1

principal axis of the complex, then the calculated normalisation factors for the ring protons fit only qualitatively. Such a conformation would give rise to larger shifts for H<sub>1</sub> than for H<sub>3</sub> and larger shifts for H<sub>4</sub> than for H<sub>5</sub>. However a slightly different position for the amide group would be sufficient to explain the discrepancies.

Although the ring protons have been fairly confidently assigned, only the C<sub>1</sub>-acetyl and acetamido signals have been assigned with any certainty. On the basis of the conformation suggested above (with the acetamido group slightly towards C<sub>3</sub>-acetyl, to account numerically for the ring proton shifts), the C<sub>3</sub>-acetyl would lie outside the pseudocontact cone, the C<sub>4</sub>-acetyl fairly close to it and the C<sub>6</sub>-acetyl within it. This would suggest that OAc(C) is the C<sub>3</sub>-acetyl, and since OAc(A) is not the C<sub>6</sub>-acetyl (see above) it must be the C<sub>4</sub>-acetyl and OAc(B) the C<sub>6</sub>-acetyl.

These acetyl signals gave very different shift to linewidth ratios: C<sub>1</sub>-acetyl: 38; OAc(A): 8; OAc(B): 19; OAc(C): 28; NHAc: 4. Poor shift to linewidth ratios could arise if

- 1) the protons lie near the pseudocontact cone
- 2) the shifts of the tetrahedral and octahedral complexes have opposite sign and so cancel.



3) there is slow exchange either between two conformations or between the tetrahedral and octahedral species.

In the first two cases, the relaxation times,  $T_1$  and  $T_2$ , should be affected comparably, whereas, in the third case,  $T_2$  should be selectively decreased. Measurement of  $T_2$  from linewidths and  $T_1$  by progressive saturation (see Part VIII) should therefore distinguish the cases.

Two solutions were used for this, one containing 0.029M cobalt(II) and the other 0.16M cobalt(II), and the distinct (non-overlapping) peaks were examined. The HA 100 instrument was used, spotting peak maxima and baseline for increasing RF powers. Plots of  $h_s$  v.  $h_s V^2$  and of  $\log h_s$  v.  $\log V$  were made and an average value of  $c^2 T_1 T_2 = \gamma^2 a^2 T_1 T_2$  taken,  $T_1 T_2$  being calculated assuming  $c^2 = 3.63^2 \times 10^{-8}$ . (see Part VIII for details of instrumentation, method and accuracy).

The results are given in Table 70.

Table 70. Relaxation times for acetyl peaks in 2-acetamido-1,3,4,6-tetra-O-acetyl-2-deoxy- $\alpha$ -D-glucopyranose, in presence of cobalt(II) perchlorate.

Conc. Co(II), <u>M</u>	Peak	$T_1$ , <u>sec.</u>	$T_2$ , <u>sec.</u>	$T_1/T_2$	Normal- isation factor $\times T_1$	Normal- isation factor $\times T_2$
0.029	C <sub>1</sub> -OAc	0.359	0.245	1.47	3.3	2.2
	OAc(C)	0.402	0.276	1.46	2.2	1.5
	NHAc	0.192	0.012	15.9	~6.0	~0.4
0.16	C <sub>1</sub> -OAc	0.274	0.095	2.89	2.5	0.9
	OAc(A)	0.262	0.042	6.25	1.1	0.2



The acetamido signal has a very high  $T_1/T_2$  ratio suggesting that there is slow exchange occurring. The high value for OAc(A) also suggests exchange.

The results from a preliminary series of solutions using undried acetone suggest this exchange could be, at least in part, exchange between the four- and six-coordinated species. The signals which are most broadened by such an exchange will be those for which the chemical shifts of the two species are most different. Since addition of water causes a change in the equilibrium position (towards the six-coordinated species), these signals will also be the ones which show the greatest change in normalisation factor with different amounts of water present. With the undried solutions, the acetamido signal showed an upfield shift, with non-concordant normalisation factors, and the normalisation factors for OAc(A) increased from 0% at low cobalt molarity to -2.8% at high cobalt molarity. The remaining acetyl signals had concordant normalisation factors, not dissimilar to those in the dried acetone:  $C_1$ -OAc: -8.3% (cf. -9.1%); B: -2.8% (cf. -2.7%); C: +5.1% (cf. +5.5%). It would thus appear that in the four-coordinated complex, the acetamido peak has a large negative shift while in the six-coordinated species the shift is positive, and OAc(A) has negative shift in the former and a smaller negative, or possibly positive shift in the latter, while the remaining three acetyl peaks have very similar shifts in both species.

If the shift sizes are small due to the protons being close to the pseudocontact cone or due to cancelling shifts



from the two complexes, then the product of normalisation factor  $\times T_1$  (and normalisation factor  $\times T_2$  if exchange is excluded) will be relatively small. This is true for peak A, which was thought to lie near the cone (see above).

An alternative method for indicating the presence of broadening due to slow exchange is the effect of heat, which, by increasing the exchange rate, causes narrowing of the lines. Thus if one acetyl signal sharpens more quickly than the others on heating, it would suggest that exchange is taking place.

A solution containing 0.17M cobalt(II) was heated from 28° to 55° and the linewidths of the  $C_1$ -acetyl and peaks A, B and C measured. Although no peak narrowed markedly more than the rest, OAc(A) and the  $C_1$ -acetyl appeared to narrow most (8.5 to 6.0 Hz and 4.2 to 2.8 Hz, respectively), then OAc(C) (4.0 to 3.2 Hz) while OAc(B) remained almost unchanged. However these results are not very conclusive.

The shift changes were also measured, but again gave rather inconclusive results. All the shift changes decreased:  $C_1$ -acetyl by 7.4%, OAc(A) by 16.8%, OAc(B) by 10.7% and OAc(C) by 10.8%. Again OAc(A) appears to show the greatest change.

In conclusion, complexing this sugar amide with cobalt has enabled total assignment of the ring protons to be made, both diamagnetic line positions and coupling constants being evaluated fairly accurately. However, although the acetyl peaks can be followed with no difficulty, the assignment of three of them was only tentative. Possible reasons for the widely different shift to linewidth ratios have been



put forward, further work to substantiate them being desirable.

(v) 2-acetamido-1,3,4,6-tetra-O-acetyl-2-deoxy- $\beta$ -D-glucopyranose

Diamagnetic spectrum: The diamagnetic peak positions, where measurable, are given in Table 71.

Table 71. Diamagnetic positions, in Hz downfield from TMS, at 100 MHz, for distinguishable signals in 2-acetamido-1,3,4,6-tetra-O-acetyl-2-deoxy- $\beta$ -D-glucopyranose (0.075M).

C <sub>1</sub> -OAc	NHAc	OAc(A)	OAc(B)	OAc(C)	H <sub>1</sub>	NH
204.9	182.8	194.9	198.9	200.5	586.5	708.7

The H<sub>1</sub> coupling of 8.9 Hz was greater here than in the  $\alpha$  isomer, and a NH coupling of 9.3 Hz was visible. The acetyl signals were labelled by comparison with the  $\alpha$  isomer. The ring protons, except H<sub>1</sub>, appeared in two groups, four protons at 380-440 Hz and two protons at 490-540 Hz.

Addition of cobalt: Investigations were carried out with solutions containing 0.075M amide, the lower molarity being chosen because of poor solubility.

The shift displacements of the signals whose diamagnetic positions are known are given in Table 72 and the peak positions of the remaining signals are given in Table 73.

As the H<sub>2</sub> signal position was not very certain, normalisation plots were made with respect to the H<sub>1</sub> signal. Since the H<sub>2</sub> normalisation plot was linear, the "normalisation factors" calculated with respect to the H<sub>1</sub> signal were divided by the "H<sub>2</sub> normalisation factor" to give normalisation factors



Table 72. Displacements, in Hz, for assignable signals in 2-acetamido-1,3,4,6-tetra-O-acetyl-2-deoxy- $\beta$ -D-glucopyranose, on addition of cobalt(II) perchlorate.

Conc. Co(II), $\underline{M}$	C <sub>1</sub> -OAc	OAc(A)	OAc(B)	OAc(C)	NHAc	H <sub>1</sub>
0.006	+1.2	+4.5	-0.5	+4.9	-62.3	-66
0.01	+1.8	+6.4	-0.7	+6.9	-88	-95
0.02	+2.9	+13.3	-1.0	+14.9	-186	-203
0.05	+4.1	+25.4	-1.9	+27.3	-336	-387
0.11	+3.5	+36	-2.5	+41.1	-509	-562

Table 73. Paramagnetic signal positions, in Hz downfield from TMS, for signals in 2-acetamido-1,3,4,6-tetra-O-acetyl-2-deoxy- $\beta$ -D-glucopyranose on addition of cobalt(II) perchlorate.

Conc. Co(II), $\underline{M}$	H <sub>2</sub>	H <sub>3</sub>	H <sub>4</sub>	H <sub>5</sub>	H <sub>6</sub> 's
0.006	546	593	513	*	*
0.01	597	617	519	*	*
0.02	773	718	537	*	427
0.05	*	886	567	463	430
0.11	1417	1046	598	488	436

\* signal position not measurable.

with respect to the H<sub>2</sub> signal. The ring protons were assigned by comparison with the  $\alpha$  isomer, the fine structure of the signals being almost identical. The quartets from the two H<sub>6</sub> protons could be seen but separate measurement was not possible.

All the ring protons gave linear normalisation plots



from which diamagnetic line positions could be obtained.

These are given in Table 74, along with literature values<sup>267</sup> for  $\text{CDCl}_3$  solution.

Table 74. Diamagnetic line positions, measured from normalisation graphs, and compared with literature values<sup>267</sup>, for ring proton signals in 2-acetamido-1,3,4,6-tetra-O-acetyl-2-deoxy- $\beta$ -D-glucopyranose.

Proton	Calculated value		Literature value
	Hz	$\tau$	$\tau$
H <sub>2</sub>	436	5.64	5.56
H <sub>3</sub>	533	4.67	4.8
H <sub>4</sub>	502	4.98	4.9
H <sub>5</sub>	409	5.91	6.1
H <sub>6</sub> 's	422	5.78	*

\* not given.

All the acetyl signals, including the acetamido signal, gave straight line normalisation plots, except the C<sub>1</sub>-acetyl which gave a distinct curve (factors decreased with increasing cobalt molarity). The normalisation factors, with respect to the H<sub>2</sub> signal, calculated from the gradients, are given in Table 75.

Table 75. Normalisation factors, as percentages, of signals in 2-acetamido-1,3,4,6-tetra-O-acetyl-2-deoxy- $\beta$ -D-glucopyranose.

C <sub>1</sub> -OAc	OAc(A)	OAc(B)	OAc(C)	NHAc	H <sub>1</sub>	H <sub>3</sub>	H <sub>4</sub>	H <sub>5</sub>	H <sub>6</sub> 's
$\approx +1$	+3.8	-0.3	+4.2	-51.7	-57.2	-52.2	-9.8	-8.1	-1.4



As with the  $\alpha$  isomer, all the ring protons showed a downfield shift. Three of the acetyl signals showed an upfield shift, the  $C_1$ -acetyl, OAc(A) and OAc(C), while the other two moved downfield. The  $C_1$ -acetyl group, now equatorial, might well be placed just outside the pseudocontact cone, giving it a small positive shift. OAc(A) is the only other peak whose shift direction has changed. In the  $\alpha$  isomer, this signal was tentatively assigned as the  $C_4$ -acetyl, which lies fairly close to the cone, in which case a change in shift direction is not improbable.

As with the  $\alpha$  isomer, shift to linewidth ratios were very different, average values for each acetyl signal being 30 for OAc(C), 4.6 for acetamido peak, 1.5 for OAc(B) and very approximately 5 for OAc(A) and 2 for  $C_1$ -acetyl.

Again progressive saturation was used to attempt to clarify the situation. Peaks A and C in a solution containing 0.10M cobalt were investigated in the same manner as with the  $\alpha$  isomer. The results are shown in Table 76.

Table 76. Relaxation times for acetyl peaks in 2-acetamido-1, 3,4,6-tetra-O-acetyl-2-deoxy- $\beta$ -D-glucopyranose, in presence of cobalt(II) perchlorate.

Peak	$T_1$ , <u>sec.</u>	$T_2$ , <u>sec.</u>	$T_1/T_2$	Normal- isation factor $\times T_1$	Normal- isation factor $\times T_2$
OAc(A)	0.202	0.163	1.24	0.77	0.62
OAc(C)	1.12	0.374	2.99	4.70	1.57

Unfortunately the linewidth of peak C (0.85 Hz) was very little greater than its diamagnetic linewidth and so the



calculated relaxation times for that peak probably contain a considerable error. However, two facts do emerge from these results. The low  $T_1/T_2$  ratio for OAc(A) suggests that exchange broadening is not occurring, and the lower products of normalisation factor  $\times T$  for OAc(A) than for OAc(C) suggest that the protons of the former may lie near the pseudocontact cone. The alternative explanation, that the shifts arising from the tetrahedral and octahedral complexes are cancelling, is less likely since there is no exchange broadening. However, exchange could be more rapid with this isomer.

As with the  $\alpha$  isomer, a solution (containing 0.01M cobalt) was heated from 28° to 55° in an attempt to detect exchange broadening. The acetyl peaks overlapped too much for accurate measurements to be made of linewidths, but it appeared that OAc(A) sharpened while OAc(C) broadened. However, little weight can be put on these results.

It has thus not been possible, from this work with the  $\beta$  isomer, to substantiate the acetyl assignments suggested for the  $\alpha$  isomer. However, the results do not conflict with the assignments.

In conclusion, although these two isomers are chemically very similar, only the stereochemistry at  $C_1$  being different, their behaviour on addition of cobalt was remarkably different. This could be due to a different placing of the amide group in the two cases, or a changed equilibrium position between four- and six-coordinated species.

These studies have shown that the cobalt perchlorate/amide system can give shifts which are usable for signal



assignments, but that results must be treated with great caution as the system is very complex and shift magnitudes may not bear a close relationship to the distance of the protons from the cobalt ion.

(vi) Conclusion

Studies on the above amides have shown that they are less reliable as ligands for complexing with cobalt(II) perchlorate for structural purposes than either the cyanides or the alcohols, mainly because of the equilibrium which exists between tetrahedral and octahedral species, which is very sensitive to conditions especially to the presence of water. However, if due care is taken and results are interpreted with caution, this system can yield useful information and so should not be discarded. For example, with the sugar amides, the diamagnetic positions of the ring protons and coupling constants between them are far more easily established by this technique than by the analysis of the second-order spectra, and no doubt further work on related compounds would enable confident assignment of the acetyl signals to be made.

(d) Ketone ligands

In general ketones have not been found to complex very strongly with transition metal ions, and so it was not so much to explore their potential as ligands in their own right but to establish to what extent complexing does occur at a carbonyl site in a bifunctional molecule, such as testosterone, that the following two compounds were studied. The first contains a simple carbonyl group, the second a conjugated carbonyl group.



(i) 5 $\alpha$ -cholestan-3-one

Diamagnetic spectrum: In the diamagnetic spectrum, the only distinguishable peaks were those of the methyls and their positions are given in Table 77 assignment being made by comparison with cholesterol.

Table 77. Diamagnetic line positions, in Hz downfield from TMS, at 100 MHz, of methyl peaks in cholestan-3-one (0.2M) in chloroform-acetone solvent.

C-18 Me	C-19 Me	C <sub>20</sub> -Me	C <sub>25</sub> -Me's		
71.6	105.2	90.3	96.3	84.1	90.3

Addition of cobalt: Solutions 0.2M in ketone and 0.15 to 0.28M in cobalt(II), with 0.2ml CDCl<sub>3</sub> for solubility, were investigated, but the maximum shift changes observed were all less than 2 Hz and normalisation was not attempted.

It would thus appear that non-conjugated ketones complex very little indeed and so the presence of such a group in a bifunctional molecule can effectively be ignored with regard to cobalt-induced shifts.

(ii) Cholest-4-en-3-one

Diamagnetic spectrum: In the diamagnetic spectrum the methyl peaks were again assigned by comparison with cholesterol, and the C<sub>4</sub> olefinic proton was also readily distinguished. Their positions are given in Table 78.



Table 78. Diamagnetic line positions, in Hz downfield from TMS, at 100 MHz, of assignable signals in cholest-4-en-3-one (0.15M) in chloroform-acetone solvent.

C-18 Me	C-19 Me	C <sub>20</sub> -Me	C <sub>25</sub> -Me's	H <sub>4</sub>
75.0	122.4	90.6	97.2	84.2
				90.6
				563.9

Addition of cobalt: Investigations were carried out using solutions 0.15M in ketone, each solution containing 0.2ml CDCl<sub>3</sub>. It was immediately apparent that the shift changes were not insignificant in this case, in fact were about one fifth those found for cholesterol. The shift changes and the normalisation factors with respect to H<sub>4</sub> signal, the most suitable signal for normalisation, are given in Table 79.

Table 79. Displacements, in Hz, and normalisation factors, as percentages, for signals in cholest-4-en-3-one on addition of cobalt(II) perchlorate.

Conc. Co(II), <u>M</u>	Displacements					Normalisation factors				
	C-18 Me	C-19 Me	C <sub>20</sub> -Me	C <sub>25</sub> -Me's	H <sub>4</sub>	C-18 Me	C-19 Me	C <sub>20</sub> - Me	C <sub>25</sub> - Me's	
0.065	-5.6	-25.6	-2.4	-2.4	-0.7	-0.7	+59.7	-9.4	-42.9	-4.0
0.11	-8.4	-37.9	-3.7	-3.3	-1.2	-1.0	+84.4	-10.0	-44.9	-4.2

The normalisation factors showed reasonable concordancy. Another peak moved rapidly out from the methylene hump, with a normalisation factor of approximately -360% and diamagnetic position of around 210 Hz. It was a broad doublet with a coupling of about 11 Hz. This signal would appear to be the same as the signal found in testosterone with diamagnetic position 216 Hz, which was there tentatively assigned as



$H_2(\alpha)$ . It is interesting that the equatorial proton at  $C_2$  shows a considerable shift, over three times the shift of the olefinic proton, while the axial proton is not shifted sufficiently to be observed clear of the methylene hump.

The results with this ligand thus substantiate the findings with testosterone and dihydrotestosterone, that while ketones themselves complex very little, conjugated ketones complex very considerably and so may not be ignored if present in bifunctional systems. The degree of complexing is in fact large enough to be utilised in its own right in molecules which contain a conjugated keto group as the only functional group.

#### (e) Ester ligands

In the preliminary work, it was seen that ethyl acetate gave very small shift changes in the presence of cobalt(II), and it is probably true that all esters give negligible shifts. However, in the study of sugar alcohols and amides, it would be advisable to try to confirm that no complexing occurred at the acetate functions, particularly since binding might be enhanced by chelation. For this reason, two sugar esters were investigated, the first containing only ester functional groups, the second containing ester groups and one methoxy group.

##### (i) Penta-O-acetyl- $\alpha$ -D-glucopyranose

Diamagnetic spectrum: Four of the acetyl signals occurred in two six-proton peaks, one at 198.2 Hz and the other at 200.7 Hz, while the fifth acetyl was at lower field, 217.8 Hz,



and so was assumed the axial  $C_1$ -acetyl signal. The  $H_1$  signal was also visible at 627.1 Hz while the remaining ring proton signals occurred in two groups of three, which were not assignable.

Addition of cobalt: Investigations were carried out with solutions containing 0.1M acetate. The shift changes are given in Table 80.

Table 80. Displacements, in Hz, of assignable signals in penta-O-acetyl- $\alpha$ -D-glucopyranose, on addition of cobalt(II) perchlorate.

Conc. Co(II), <u>M</u>	$C_1$ -Ac	A C E T Y L S				$H_1$
		A	B	C	D	
0.10	-1.9	-0.7	-3.2	-2.8	+4.9	+4
0.20	-3.4	-1.4	-7.2	-4.7	+10.1	+7.9
0.50	-6.8	-3.7	-18.1	-15.6	+25.4	+21

It can be seen that shift changes were very small, a maximum of 25 Hz at 0.5M cobalt. Some signals were shifted upfield, some downfield.

(ii) Methyl 2,3,4,6-tetra-O-acetyl- $\alpha$ -D-galactopyranoside

Diamagnetic spectrum: In the diamagnetic spectrum, the acetyl peaks were all separate, and the  $C_4$ -acetyl (axial) was tentatively assigned as the lowest field signal (212.6 Hz); the remaining three signals (192.8, 199.6 and 201.7 Hz) were not assigned. The methoxy signal was easily distinguished at 341.0 Hz but none of the ring protons were distinct, appearing in a low field group of four protons and a higher



field group of three protons.

Addition of cobalt: Investigations were carried out with solutions containing 0.2M ester. The shift changes are shown in Table 81.

Table 81. Displacements, in Hz, of assignable signals in methyl 2,3,4,6-tetra-O-acetyl- $\alpha$ -D-galactopyranoside, on addition of cobalt(II) perchlorate.

Conc. Co(II), <u>M</u>	C <sub>4</sub> -Ac	A C E T Y L S			OMe
		E	F	G	
0.10	-0.6	+0.5	+2.4	-1.0	-2.0
0.20	-1.3	+0.9	+5.3	-2.1	-4.1
0.50	-4.0	+4.5	+15.1	-5.2	-11.3

The shift changes were all very small, less than 16 Hz even at 0.5M cobalt. As with the previous ester, they varied in direction. The methoxy signal showed no greater shift than the acetyl signals and so there is no selective complexing at that site.

It would thus seem safe to assume that any complexing at ester sites can be ignored in sugar derivatives which contain functional groups such as alcohols or amides.

#### (f) Conclusion

Molecules involving five different functional groups have been investigated in the above studies, to see their relative potentials as ligands for complexing with cobalt(II) perchlorate to give shifts of useful magnitude for spectral simplification and assignment. Assessment of their usefulness was based not only on the shift magnitudes, but on the



shift to linewidth ratios and the behaviour of the shifts, particularly with regard to normalisation, on varying cobalt concentration, ligand concentration, in the presence of water and on changing the temperature.

The results have shown that the amides gave the largest shifts for a given cobalt concentration but that these gave very variable shift to linewidth ratios and were highly sensitive to conditions, particularly to the presence of water, and so not very predictable in their behaviour.

Alcohols showed the next largest shifts and had reasonably good shift to linewidth ratios in general but, although much more predictable than amides under varying conditions, they tended not to give very concordant normalisation factors in the presence of varying amounts of water.

Cyanides were the best behaved of all the ligands and in this respect would be the ligand of choice, but the shifts tended to be smaller, although still of a useful size.

The esters and ketones proved to have negligible shifts except in the case of conjugated ketones, whose shifts were large enough to be utilised.

These results show that cobalt perchlorate in acetone can give useful results as a "shift reagent"; however, it is inferior to the rare-earth chelates recently studied both because the shift to linewidth ratios are generally poorer and because the nature and geometry of the complexes involved are less certain.



## (D) COBALTOUS ACETYLACETONATE COMPLEXES

Cobaltous acetylacetonate<sup>at</sup>,  $\text{Co}(\text{AA})_2$ , has been used as a shift reagent with amines, alcohols and furans (see Part II Section G(c)). It would be of considerable interest to see how it compares with the cobalt perchlorate-acetone system as a shift reagent. For this purpose, four of the ligands investigated above, one cyanide, two alcohols and one amide, were examined in the presence of  $\text{Co}(\text{AA})_2$  in deuterochloroform solution, and the shifts produced were assessed and compared with those in the corresponding cobalt perchlorate-acetone system.

(i) p-methyl benzyl cyanide

Diamagnetic spectrum: The diamagnetic line positions are given in Table 82.

Table 82. Diamagnetic line positions, in Hz downfield from TMS, at 100 MHz, of signals in p-methyl benzyl cyanide.

Conc. cyanide, <u>M</u>	$\text{CH}_2\text{CN}$	Phenyl	Me
1.0	363.7	715.7	232.1
0.5	366.9	717.5	233.4

The phenyl signals appeared as one singlet with very small side peaks.

Addition of  $\text{Co}(\text{AA})_2$ : Investigations were carried out using solutions 1.0 and 0.5M in cyanide and 0.05 and 0.10M in  $\text{Co}(\text{AA})_2$ . The shift changes and normalisation factors with



respect to the  $\text{CH}_2\text{CN}$  signal are given in Table 83.

Table 83. Displacements, in Hz, and normalisation factors, as percentages, for signals of p-methyl benzyl cyanide on addition of  $\text{Co}(\text{AA})_2$ .

Conc. cya- nide, <u>M</u>	Conc. $\text{Co}(\text{AA})_2$ <u>M</u>	Displacements (all +ve)				Normalisation factors		
		$\text{CH}_2\text{CN}$	Ph(o)	Ph(m)	Me	Ph(o)	Ph(m)	Me
1.0	0.05	+73.4	+25.8	+10.6	+5.3	+35.2	+14.5	+7.2
	0.10	+137.1	+49.7	+17.3	+8.8	+36.2	+12.6	+6.4
0.5	0.05	+78.1	+26.2	+10.4	+4.7	+33.6	+13.3	+6.0
	0.10	+187.1	+65.1	+21.4	+10.8	+34.8	+11.4	+5.8

The shift sizes for the  $\text{CH}_2\text{CN}$  peak were around a third of those for the cobalt perchlorate-acetone system.

The normalisation factors are fairly constant and not dissimilar to those in the cobalt perchlorate-acetone system.

The effect of changing the ligand concentration on the shift sizes indicated a moderate degree of complexing.

The shift to linewidth ratios were very variable, ranging from 45 to 70 for  $\text{CH}_2\text{CN}$  peak, which is very good, but having the much poorer value of 5 for methyl peak.

Thus in general the cobalt perchlorate-acetone system is the better one but the  $\text{Co}(\text{AA})_2$ -chloroform system is obviously usable.

#### (ii) Menthol

Diamagnetic spectrum: The diamagnetic line positions are given in Table 84.



Table 84. Diamagnetic line positions, in Hz downfield from TMS, at 100 MHz, for signals in menthol.

Conc. alcohol, <u>M</u>	Isopropyl methyl (1)	Isopropyl methyl (2)	C <sub>1</sub> -methyl	H <sub>3</sub>	OH	Isopro- pyl H
0.5	77.5 84.5	89.2 96.3	88.0 94.2	340.1	153.5	218.0
0.2	77.8 84.8	89.2 96.5	88.3 94.4	341.2	135.6	217.2

Addition of Co(AA)<sub>2</sub>: Investigations were carried out using solutions 0.5 and 0.2M in alcohol and 0.05 and 0.10M in Co(AA)<sub>2</sub>, each solution containing 0.1ml AnalaR chloroform for lock signal.

The shift changes are shown in Table 85.

Table 85. Displacements, in Hz, for signals in menthol on addition of Co(AA)<sub>2</sub>.

Conc. alcohol, <u>M</u>	Conc. Co(AA) <sub>2</sub> , <u>M</u>	Isopropyl methyl (1)	Isopropyl methyl (2)	C <sub>1</sub> -methyl	H <sub>3</sub>
0.5	0.05	+17.6	+41.0	+39.4	-44.2
	0.10	+39.1	+68.3	+66.6	-107.5
0.2	0.05	+19.0	+43.9	+42.4	-56.7

The methyl assignments were only tentative as there was so much broadening that the peaks were difficult to follow. If the assignments are correct, it would appear that the isopropyl methyls may be decoupled to singlets.

It is noticeable that, while all the methyl signals had an upfield displacement, the proton H<sub>3</sub> moved downfield.

Various peaks appeared above the TMS signal but these were not distinct enough to follow. The methyl shift



changes were not linear with respect to the change in shift of  $H_3$  signal.

The shifts were strongly dependent on ligand concentration, the "strength of complexing" expression for  $H_3$  evaluating in the range 31% to 64%.

It was obvious that this system compared very unfavourably with the cobalt perchlorate-acetone system. The shift to linewidth ratios were very poor and shifts were not large, less than a third those with the same concentration of cobalt perchlorate.

(iii) p-methyl benzyl alcohol

Diamagnetic spectrum: The diamagnetic peak positions are given in Table 86.

Table 86. Diamagnetic line positions, in Hz downfield from TMS, at 100 MHz, for signals of p-methyl benzyl alcohol.

Conc. alcohol, $\frac{M}{M}$	$CH_2$	Phenyl	Me	OH
1.0	451.6	714.2	231.2	259.4
0.5	457.5	717.3	233.0	209.2

The phenyl signals in the diamagnetic spectra are a very close doublet surrounded by tiny peaks. The doublets are at 714.9 and 713.5 Hz for 1.0M alcohol and 718.4 and 716.1 Hz for 0.5M alcohol, the centre of the doublets being given in the Table.

Addition of  $Co(AA)_2$ : Investigations were carried out using



solutions 1.0 and 0.5M in alcohol. The peak displacements of the  $\text{CH}_2$  and Me signals are given in Table 87. The hydroxyl signal was not visible in the paramagnetic solution spectra.

Table 87. Displacements, in Hz, and peak positions, in Hz downfield from TMS, for signals of p-methyl benzyl alcohol.

Conc. alcohol, <u>M</u>	Conc. $\text{Co}(\text{AA})_2$ , <u>M</u>	Displacements		Peak positions	
		$\text{CH}_2$	$\text{CH}_3$	Ph(o)	Ph(m)
1.0	0.05	-135.2	+4.8	672.8	695.4
	0.10	-273.7	+9.5	629.6	681.1
	0.17	-483.0	+16.4	567.3	658.9
0.5	0.05	-218	+8.4	632.1	685.9
	0.11	-511.7	+18.2	527.5	652.8

The  $\text{CH}_2$  peak displacement gave a linear plot with  $\text{Co}(\text{AA})_2$  concentration for each ligand concentration.

The normalisation plots with respect to the  $\text{CH}_2$  signal were also straight lines for each ligand concentration, giving the normalisation factors shown in Table 88. The phenyl plots extrapolated to give diamagnetic line positions of 712.8 and 709.5 Hz for 1.0M alcohol and 710.0 and 711.0 Hz for 0.5M alcohol, which are in only fair agreement with the positions in the diamagnetic spectra.

Table 88. Normalisation factors, as percentages, calculated from normalisation graphs for p-methyl benzyl alcohol.

Conc. alcohol, <u>M</u>	Phenyl (o)	Phenyl (m)	Me
1.0	+30.5	+10.5	+3.5
0.5	+35.6	+11.4	+3.7



The normalisation factors were totally different from those found in the cobalt perchlorate-acetone system. As with menthol, all the shifts were upfield except the  $\alpha$  proton shift. The shift sizes were considerably smaller for the  $\text{CH}_2$  signal in this system, but normalisation was so different that this did not apply to the other signals.

Changing the ligand concentration had a considerable effect on the shifts, the "strength of complexing" expression having a value of about 80%. The ligand concentration also changed the normalisation factors slightly.

The shift to linewidth ratio for the  $\text{CH}_2$  signal (about 10) was rather poorer than with the cobalt perchlorate-acetone system.

Thus with this alcohol ligand, shifts were considerable, (probably because there is less steric hindrance than with menthol), and, with a constant ligand molarity, were amenable to normalisation, although perhaps normalisation is not necessary if the shifts are proportional to the  $\text{Co}(\text{AA})_2$  concentration as would appear to be the case. Shift to linewidth ratios were not as good but the larger normalisation factors obtained with this system were an advantage. However, relatively low solubility of  $\text{Co}(\text{AA})_2$  (ca. 0.2M) sets a limit to the shift changes which can be achieved.

It would thus appear that for alcohols in general, the cobalt perchlorate-acetone system is superior.

#### (iv) p-acetamidotoluene

Diamagnetic spectrum: The diamagnetic line positions are given in Table 89.



Table 89. Diamagnetic line positions, in Hz downfield from TMS, at 100 MHz, for signals in p-acetamidotoluene (0.2M).

COMe	NH	Ph(o)	Ph(m)	Me
212.5	756	736.9	708.5	229.9

Addition of  $\text{Co}(\text{AA})_2$ : Investigations were carried out using solutions 0.2M in amide. Difficulty was encountered in achieving complete solution of 0.2M  $\text{Co}(\text{AA})_2$ .

The shift changes are given in Table 90.

Table 90. Displacements, in Hz, of signals of p-acetamidotoluene on addition of  $\text{Co}(\text{AA})_2$ .

Conc. $\text{Co}(\text{AA})_2$ , <u>M</u>	COMe	Ph(o)	Ph(m)	Me
0.1	+93.0	+54.2	+9.3	+0.3
<0.2	+156.8	+91.1	+10.3	-2.6

The shifts did not appear to be linear with respect to the  $\text{Co}(\text{AA})_2$  molarity, nor were they linear with respect to each other.

Shift to linewidth ratios for the COMe peak were around 11 which is not very good, and the shift sizes were much smaller than with the cobalt perchlorate-acetone system, about one fifth the size for the ortho phenyl signal.

Although this ligand did not give ideal results in the cobalt perchlorate-acetone system, it is obvious that they were much better than the results obtained from this system with  $\text{Co}(\text{AA})_2$ .



(v) Conclusion

Although rather too few ligands have been studied with  $\text{Co}(\text{AA})_2$ , it would appear that the cobalt perchlorate-acetone system is much superior to the previously used  $\text{Co}(\text{AA})_2$ -chloroform system, although for certain situations, the latter may prove valuable.



PART VILANTHANIDE COMPLEXES

While the work described in Part V using cobalt(II) as a shift reagent was being undertaken, lanthanide shift reagents appeared in the literature, as reviewed in Part II, Section G(d). In particular, the trisdipivalomethanato [2,2,6,6-tetramethylheptanedionato] complexes of europium(III) and praseodymium(III) were found to be especially effective in producing large paramagnetic shifts while causing very little broadening.

It was therefore decided to investigate the shifts produced by these complexes in some of the ligands studied previously with cobalt(II), for comparison of the two systems.

Although it was not long after their discovery as shift reagents before the complexes were readily available commercially, preparation of them was undertaken to ascertain the simplicity of the procedure.

A further study was carried out using the europium(III) and praseodymium(III) nitrates as shift reagents in acetone solution. As with the cobalt(II) perchlorate-acetone system, this should have the advantage of greater ease of preparation of samples and it was hoped that better shift to linewidth ratios might be achieved.



## (A) EXPERIMENTAL

(a) Preparation of shift reagents(i) Trisdipivalomethanato-praseodymium(III),  $\text{Pr}(\text{DPM})_3$ .

The method of Eisentraut and Sievers<sup>269</sup> was used to prepare the complex. Commercial praseodymium nitrate pentahydrate (Koch-Light) was available, and the reaction was carried out in a nitrogen atmosphere rather than in vacuo. An 82% yield of unsublimed product was obtained, m.p. 196-197°. After sublimation at 190° under reduced pressure and crystallisation from aqueous methanol, the green complex had m.p. 215-217° (lit. m.p. 222-224°). It was stored over phosphorus pentoxide in a desiccator and resublimed prior to use.

(ii) Trisdipivalomethanato-europium(III),  $\text{Eu}(\text{DPM})_3$ .

The same method was used again for this complex, but sublimation of the crude product proved difficult due to the considerable amount of water present. Satisfactory removal of this water before sublimation was not achieved.

Rather than persevere with this preparation, a commercial sample (BDH) of the complex was used for the shift studies. This sample was also found to contain water, and was dried over phosphorus pentoxide in a vacuum pistol at 60°. The loss in weight on drying corresponded to 1.6 molecules water per molecule complex. The dried complex was stored over phosphorus pentoxide in a desiccator.

(iii) Praseodymium nitrate monohydrate,  $\text{Pr}(\text{NO}_3)_3 \cdot \text{H}_2\text{O}$ .

Praseodymium nitrate pentahydrate (Koch-Light) was dried<sup>270</sup> over phosphorus pentoxide in a vacuum pistol,



gradually raising the temperature from room temperature to 140° (boiling xylene) over a period of ten days. The green crystals became much paler and the decrease in weight (all occurring under 60°) corresponded to five molecules water per molecule nitrate. It was assumed that the monohydrate rather than the anhydrous salt was obtained since the literature<sup>270</sup> suggested that a temperature of 155° was required to form the latter, and also, spectra of these solutions showed a water peak corresponding to approximately one molecule. The dried salt was very hygroscopic so that all solutions were prepared with freshly dried product.

(iv) Europium nitrate dihydrate,  $\text{Eu}(\text{NO}_3)_3 \cdot 2\text{H}_2\text{O}$ .

Europium nitrate hexahydrate (Rare Earth Products Ltd.) was dried over phosphorus pentoxide in a vacuum pistol for three days at room temperature, followed by ten days at 75°. The white crystals turned very pale pink and "hardened". Loss of weight corresponded to 4.5 molecules water per molecule nitrate. The product was assumed to be the dihydrate. Integration of the water peak in solutions containing the dried nitrate suggested from 1.5 to 2.0 molecules water.

(b) Preparation of solutions for N.M.R.

The solutions were prepared in the same way as for the cobalt work, all weighings being made as quickly as possible because of the hygroscopic nature of the rare-earth compounds. The solutions containing lanthanide complex were prepared using dried deuterochloroform (containing 3% TMS) as solvent, while the lanthanide nitrate solutions were



prepared using dried deuterioacetone (containing 3% TMS).

Freshly prepared solutions were used in all cases. Instrumental details were the same as for the cobalt work.

(B) TRISDIPIVALOMETHANATO-LANTHANIDE(III) SHIFT STUDIES

(a) Trisdipivalomethanato-europium(III)

One cyanide ligand and three alcohol ligands were investigated with this complex. The diamagnetic assignments and line positions of those ligands run under the same conditions (concentration and solvent) during the cobalt work were given in Part V and are not repeated.

(i) p-methyl benzyl cyanide

Investigations were carried out using solutions 1.0 and 0.5M in cyanide. The shift displacements on addition of the  $\text{Eu(DPM)}_3$  are given in Table 91.

Table 91. Displacements (all negative), in Hz, of signals of p-methyl benzyl cyanide on addition of  $\text{Eu(DPM)}_3$ .

Conc. ligand, <u>M</u>	Conc. $\text{Eu(DPM)}_3$ , <u>M</u>	$\text{CH}_2$	Ph(o)	Ph(m)	Me
1.0	0.008	-0.9	-0.3	-0.3	-0.1
	0.024	-10.0	-3.7	-3.7	-1.0
	0.074	-58.2	-42.4	-27.9	-27.2
0.5	0.012	-2.0	-0.6	-0.6	0
	0.037	-21.5	-12.1	-2.1	-1.7

It can be seen that the shift changes were small compared with the cobalt perchlorate-acetone system. They were all to lower fields and were not very linear with respect to the



$\text{Eu}(\text{DPM})_3$  molarity. Normalisation was very poor. Decreasing the ligand concentration appeared to increase the shifts considerably. The shift to linewidth ratio seemed very good, at least 50 and probably nearer 100.

(ii) Menthol

Investigations were carried out using solutions 0.5 and 0.2M in alcohol.

The  $\text{H}_3$  signal was a regular septet with a coupling of about 5 Hz.  $\text{H}_3$  has a large coupling ( $J \sim 11-12$  Hz) with  $\text{H}_2(\text{ax})$  and  $\text{H}_4$ , and a smaller coupling with  $\text{H}_2(\text{eq})$  and OH. The  $\text{H}_3\text{-OH}$  coupling was 5.4 Hz. A septet would arise if the coupling with  $\text{H}_2(\text{eq})$  was also about 5.4 Hz, while the two larger couplings were both about twice that figure.

The shift displacements of the assignable signals on addition of  $\text{Eu}(\text{DPM})_3$  are given in Table 92.

Table 92. Displacements (all negative), in Hz, of assignable signals in menthol, on addition of  $\text{Eu}(\text{DPM})_3$ .

Conc. ligand, <u>M</u>	Conc. $\text{Eu}(\text{DPM})_3$ , <u>M</u>	$\text{Isop.Me}(1)$	$\text{Isop.Me}(2)$	$\text{C}_1\text{-Me}$	$\text{H}_3$	OH	Isop. H			
0.5	~0.004	5.1	5.2	4.1	3.9	1.7	1.7	20.2	70.7	13.4
	~0.008	11.6	11.4	8.8	8.8	4.0	3.8	46.4	165.3	31.6
	~0.02	30.9	31.0	24.3	24.0	10.8	10.3	125.3	455.5	85.4
	0.046	54.5	53.9	42.3	42.1	18.6	18.7	221.4	806.5	150.1
0.2	~0.004	9.7	9.6	7.8	7.4	3.3	2.6	37.3	131.0	26.0
	0.063	175.9	175.7	135.4	135.1	60.4	60.8	724.2	?	484.9

The shift sizes, again all downfield, were quite considerable and the normalisation factors with respect to the  $\text{H}_3$



signal, given in Table 93, were reasonably concordant.

Table 93. Normalisation factors (all negative), expressed as percentages, for assignable signals in menthol.

Conc. ligand, <u>M</u>	Conc. Eu(DPM) <sub>3</sub> , <u>M</u>	Isop.Me(1)	Isop.Me(2)	C <sub>1</sub> -Me	OH	Isop. H
0.5	~0.004	-25.4	-19.8	-8.4	-350	-66.3
	~0.008	-24.8	-19.0	-8.4	-356	-68.0
	~0.02	-24.7	-19.3	-8.4	-364	-68.0
	0.046	-24.5	-19.1	-8.4	-364	-67.8
0.2	~0.004	-25.9	-20.4	-7.9	-351	-69.8
	0.063	-24.3	-18.7	-8.4	?	-67.0

Two other signals separated out, one a multiplet (basically a doublet with  $J \sim 12$  Hz) and the other a quartet ( $J = 11.2$  Hz). Their peak positions where visible are given in Table 94.

Table 94. Paramagnetic positions, in Hz downfield from TMS, of unassigned signals in menthol on addition of Eu(DPM)<sub>3</sub>.

Conc. ligand, <u>M</u>	Conc. Eu(DPM) <sub>3</sub> , <u>M</u>	Multiplet	Quartet
0.5	~0.004	208.4	*
	~0.008	224.5	*
	~0.02	271	*
	0.046	328.5	245.1
0.2	~0.004	219.4	*
	0.063	628.0	581.0

\* not observable.



The normalisation plot for the multiplet was linear giving a normalisation factor of -59.4% and a diamagnetic line position of 197 Hz, suggesting an equatorial proton close to  $H_3$ . The most likely proton would be  $H_2(eq)$ . This proton would have a large coupling with  $H_2(ax)$  and smaller couplings with  $H_3$  and  $H_1$ .

The quartet was visible in only two of the spectra and these positions gave a normalisation line yielding a normalisation factor of -67% and a diamagnetic position of about 98 Hz, suggesting an axial proton close to  $H_3$ . There are two such axial protons,  $H_2(ax)$  and  $H_4(ax)$ . The former, with three large couplings, might be expected to be a quartet, while the latter would probably appear as a triplet or sextet or just a multiplet. The quartet was therefore assigned as  $H_2(ax)$ .

A third peak, a hump, was just visible. This would most likely be  $H_4$ .

The shifts were strongly dependent on ligand concentration and appeared to be almost proportional to the  $Eu(DPM)_3$ :ligand ratio.

The shift to linewidth ratios were not measurable, but were obviously very good.

Thus this alcohol ligand gave very satisfactory shifts with the europium complex. Normalisation and the shift to linewidth ratios were good. No further assignments were made than were made with the cobalt perchlorate-acetone system. The limiting factor was not resolution but the solubility of the complex, apparently a severe drawback to the system.



(iii) p-methyl benzyl alcohol

Investigations were carried out using solutions 1.0 and 0.5M in alcohol. The peak displacements and the normalisation factors with respect to  $\text{CH}_2$  signal, on addition of  $\text{Eu}(\text{DPM})_3$ , are given in Table 95.

Table 95. Displacements (all negative), in Hz, and normalisation factors, expressed as percentages, for signals of p-methyl benzyl alcohol, on addition of  $\text{Eu}(\text{DPM})_3$ .

Conc. ligand, <u>M</u>	Conc. $\text{Eu}(\text{DPM})_3$ <u>M</u>	Displacements					Normalisation factors			
		$\text{CH}_2$	Ph (o)	Ph (m)	Me	OH	Ph (o)	Ph (m)	Me	OH
1.0	0.012	28.6	13.7	3.7	2.4	109.9	48.0	12.9	8.4	384
	0.022	55.0	26.3	7.0	4.7	214.0	47.8	12.6	8.6	389
	0.051	131.4	62.6	16.8	11.4	515.7	47.6	12.8	8.7	392
0.5	0.011	48.3	22.7	7.2	3.9	173.7	47.0	14.9	8.1	359
	0.021	95.1	44.0	13.7	7.8	359.2	46.3	14.4	8.2	378
	0.047	230.3	106.2	33.5	18.9	885.8	46.1	14.5	8.2	384

The diamagnetic phenyl positions were calculated, by extrapolation of the straight line normalisation plots, to be for 1.0M alcohol: Ph(o) 716.4; Ph(m) 712.4

0.5M alcohol: Ph(o) 720.4; Ph(m) 714.3.

The centres of the phenyl "doublets" in the diamagnetic spectra are at 714.2 Hz and 717.3 Hz for 1.0 and 0.5M alcohol solutions respectively, in good agreement. These diamagnetic positions were used to calculate the displacements and normalisation factors.

The table shows that the shifts were quite sizeable, and they were linear with respect to the lanthanide concentration for each ligand concentration. The shifts were very



nearly proportional to the  $\text{Eu(DPM)}_3$ :ligand ratio. The normalisation factors were consistent, varying very slightly with the different ligand concentrations.

The shift to linewidth ratio was not easily measured as the  $\text{CH}_2$  signal was a doublet which was gradually decoupled and the methyl was not greatly displaced. The ratio was obviously good, at least 60 and possibly as high as 100.

Although the effect of water could not be fully investigated as it is immiscible with chloroform, 2  $\mu\text{l}$  water was added to the solution with 1.0M alcohol and 0.05M  $\text{Eu(DPM)}_3$ . This caused a 37% decrease in the shift sizes, but normalisation remained the same except for the hydroxyl signal whose normalisation factor appeared to increase to -500%, possibly as a result of averaging of hydroxyl and water peaks.

Thus, with this aromatic alcohol also, good shifts were obtained, with good normalisation and shift to linewidth ratios. It would appear that  $\text{Eu(DPM)}_3$  is a quite satisfactory shift reagent with alcohol ligands in general, as indeed has been widely found (see Part II, Section G(d)). It seemed interesting to investigate if it would be equally satisfactory with diols.

(iv) Methyl 4,6-O-benzylidene- $\alpha$ -D-glucopyranoside

Diamagnetic spectrum: In addition to those signals assigned in the acetone solution, two doublets were visible which were removed by shaking with  $\text{D}_2\text{O}$  and so were assigned as hydroxyl signals. The diamagnetic line positions are given in Table 96.



Table 96. Diamagnetic line positions, in Hz downfield from TMS, of assignable signals in methyl 4,6-O-benzylidene- $\alpha$ -D-glucopyranoside (0.2M).

OCH <sub>3</sub>	benzylic H	H <sub>1</sub>	quartet	OH	OH	Phenyl (most intense peak)
340.8	549.2	471.7	426.1	273.8	332.0	737.0

Addition of Eu(DPM)<sub>3</sub>: Investigations were carried out using solutions 0.2M in diol. The shift changes are given in Table 97.

Table 97. Displacements (all negative), in Hz, of assignable signals in methyl 4,6-O-benzylidene- $\alpha$ -D-glucopyranoside on addition of Eu(DPM)<sub>3</sub>.

Conc. Eu(DPM) <sub>3</sub> , <u>M</u>	OCH <sub>3</sub>	benzylic H	H <sub>1</sub>	quartet	Phenyl (most intense peak)
0.008	0.5	0.3	1.4	0	0.3
0.016	1.5	0.9	2.6	1	0.5
0.030	3.1	2.0	4.7	2	0.9
0.043	5.4	4.2	10.7	3	1.4

The shift changes, again all downfield, were very small. Except with the strongest solution, the shifts were linear with respect to the Eu(DPM)<sub>3</sub> concentration.

Normalisation with respect to the H<sub>1</sub> signal was not very good.

Thus, although Eu(DPM)<sub>3</sub> seemed to be a good shift reagent for alcohols, this was not the case for this diol. This is probably due to steric hindrance, a close approach



of the bulky rare-earth complex to the considerably hindered diol not being possible.

(b) Trisdipivalomethanato-praseodymium(III)

With the praseodymium complex, the two ligands which gave promising results with the europium complex were investigated, and then an amide was examined.

(i) Menthol (with F.A.K. Maclean)

Investigations were carried out using solutions 0.5M in alcohol.

The shift changes are given in Table 98.

Table 98. Displacements (all positive), in Hz, of assignable signals in menthol, on addition of  $\text{Pr(DPM)}_3$ .

Conc. $\text{Pr(DPM)}_3$ , <u>M</u>	Isop.Me(1)	Isop.Me(2)	$\text{C}_1\text{-Me}$
0.006	15.3	13.3	4.1
0.036	45.6	36.9	17.0
0.10	137.1	111.5	46.2

All the shift changes were upfield and were quite sizeable, but unfortunately the  $\text{H}_3$  signal moved into the methylene hump and could not be followed, thus making normalisation with respect to it impossible. The methyl doublets normalised well with respect to each other and, giving the isopropyl methyl(1) signal a normalisation factor of 24.4% as in the europium complex case, then isopropyl methyl(2) had a normalisation factor of 19.8% and  $\text{C}_1\text{-methyl}$  8.4%, which



compares very well with the europium system with 18.7% and 8.4% respectively.

Various other signals could be seen moving upfield out of the methylene hump but it was very difficult to follow their progress due to obscuring of the signals by the TMS signal and the t-butyl signal of the complex.

The shift to linewidth ratios were again good, ranging between 25 and 140 for the methyls.

Thus, this alcohol also complexes readily with  $\text{Pr}(\text{DPM})_3$ , the only disadvantage being that the upfield direction of the shifts causes an increase in overlap of the signals, so assignment is not facilitated.

(ii) p-methyl benzyl alcohol (with F.A.K. Maclean)

Investigations were carried out using solutions 0.6 and 0.2M in alcohol. The shift displacements and the normalisation factors with respect to the  $\text{CH}_2$  signal are given in Table 99.

Table 99. Displacements (all positive), in Hz, and normalisation factors, expressed as percentages, for signals of p-methyl benzyl alcohol on addition of  $\text{Pr}(\text{DPM})_3$ .

Conc. ligand, <u>M</u>	Conc. $\text{Pr}(\text{DPM})_3$ , <u>M</u>	Displacements				Normalisation factors		
		$\text{CH}_2$	Ph (o)	Ph (m)	Me	Ph (o)	Ph (m)	Me
0.6	0.027	158.2	69.1	28.1	14.0	43.7	17.8	8.9
	0.034	181.7	79.9	32.5	16.5	44.0	17.9	9.1
	0.11	627.1	281.6	103.2	56.2	44.9	16.5	9.0
0.2	0.034	338.8	148.6	57.5	29.0	43.9	17.0	8.6
	0.095	1152.8	514.0	179.3	96.9	44.6	15.6	8.4
	0.10	1205.5	538.8	187.7	100.9	44.7	15.6	8.4



The hydroxyl signal was not visible after addition of  $\text{Pr}(\text{DPM})_3$ . All the shifts were upfield and were large. They were linear with respect to the  $\text{Pr}(\text{DPM})_3$  molarity for each ligand concentration. Normalisation was moderately good and the factors were similar, although not identical, to those with the europium complex.

The shifts were strongly dependent on the ligand concentration but not inversely proportional to it.

The shift to linewidth ratio for all the signals was over 100 and for the  $\text{CH}_2$  signal was about 500, which is extremely good. This appears to be better than with the europium complex.

Two aliquots of 0.5  $\mu\text{l}$  water were added to a solution with 0.2M alcohol and 0.034M  $\text{Pr}(\text{DPM})_3$ , and the shift changes and normalisation factors are given in Table 100.

Table 100. Displacements, in Hz, and normalisation factors, as percentages, for signals of *p*-methyl benzyl alcohol in presence of  $\text{Pr}(\text{DPM})_3$ , on addition of water (9  $\mu\text{l}$   $\equiv$  1M).

Water added, <u><math>\mu\text{l}</math></u>	Displacements (all +ve)				Normalisation factors		
	$\text{CH}_2$	Ph(o)	Ph(m)	Me	Ph(o)	Ph(m)	Me
-	338.8	148.6	57.5	29.0	43.9	17.0	8.6
0.5	329.1	143.9	55.9	28.1	43.7	17.0	8.5
1.0	265.2	116.4	50.2	24.1	44.0	18.9	9.1

The shifts were water dependent and the normalisation factors appeared to increase slightly, though not very significantly.



The praseodymium complex would appear the better shift reagent of the two provided that upfield shifts do not obscure rather than clarify the signals.

(iii) p-acetamidotoluene (with F.A.K. Maclean)

Investigations were carried out using solutions 0.2 and 0.3M in amide.

The shift changes and normalisation factors with respect to the ortho phenyl signal are given in Table 101.

Table 101. Displacements (all positive), in Hz, and normalisation factors, as percentages, for signals of p-acetamidotoluene on addition of  $\text{Pr}(\text{DPM})_3$ .

Conc. ligand, <u>M</u>	Conc. $\text{Pr}(\text{DPM})_3$ , <u>M</u>	Displacements				Normalisation factors		
		COMe	Ph(o)	Ph(m)	Me	COMe	Ph(m)	Me
0.2	0.1	378.0	336.4	63.2	28.7	112.2	18.8	8.5
0.3	0.1	298.3	266.0	51.6	24.3	112.1	19.4	9.1

The shift changes, all upfield, are again considerable. The normalisation factors vary slightly for the two ligand concentrations (except for COMe signal).

The ligand concentration obviously had a substantial effect on the shift sizes.

The shift to linewidth ratios were good, about 40 for ArMe and about 150 for COMe. Normalisation appears satisfactory, judging from only two solutions, and complexing between amides and these shift reagents may therefore be of interest for further study.



## (C) LANTHANIDE NITRATE SHIFT STUDIES

(a) Europium nitrate dihydrate

An alcohol and a diol were investigated with europium nitrate in acetone solution.

(i) p-methyl benzyl alcohol

Investigations were carried out using solutions 1.0 and 0.5M in alcohol.

The shift displacements for the  $\text{CH}_2$ ,  $\text{CH}_3$  and OH signals and the peak positions for the phenyl signals are given in Table 102.

Table 102. Displacements, in Hz, or peak positions, in Hz downfield of TMS, of signals in p-methyl benzyl alcohol on addition of  $\text{Eu}(\text{NO}_3)_3 \cdot 2\text{H}_2\text{O}$ .

Conc. ligand, <u>M</u>	Conc. $\text{Eu}(\text{NO}_3)_3$ , <u>M</u>	Displacements (all-ve)					Peak positions
		$\text{CH}_2$	Me	OH	Ph(o)	Ph(m)	
1.0	0.13	26.2	0.8	127.0	723.3	713.5	
	0.34	53.6	1.6	268.4	744.5	716.4	
0.5	0.11	25.4	0.8	119.7	732.6	714.4	
	0.33	57.7	1.8	284.6	747.2	717.3	

The shift changes, all downfield, were relatively small and not strictly linear with respect to the europium molarity. A further signal which increased in size with increasing europium molarity was assumed to be due to water and its positions are not given.

The normalisation factors for the Me and OH signals with respect to the  $\text{CH}_2$  signal are given in Table 103, as are



the phenyl signal factors, calculated graphically.

Table 103. Normalisation factors (all negative), as percentages, for signals of p-methyl benzyl alcohol on addition of  $\text{Eu}(\text{NO}_3)_3 \cdot 2\text{H}_2\text{O}$ .

Conc. ligand, <u>M</u>	Conc. $\text{Eu}(\text{NO}_3)_3$ , <u>M</u>	Me	OH	Ph(o)	Ph(m)
1.0	0.13	3.1	485	44.8	10.6
	0.34	3.0	501		
0.5	0.11	3.1	472	42.2	8.0
	0.33	3.1	493		

They are fairly concordant. The phenyl normalisation plots yielded the diamagnetic positions given in Table 104 where they are compared with the weighted average positions in the diamagnetic spectra.

Table 104. Diamagnetic positions, in Hz downfield from TMS, of phenyl signals in p-methyl benzyl alcohol.

Conc. ligand, <u>M</u>	Calculated graphically			Weighted average from spectra
	Ph(o)	Ph(m)	centre	
1.0	720.6	710.7	715.7	716.1
0.5	721.9	712.4	717.2	717.0

They are in good agreement.

The shifts were slightly dependent on ligand concentration, the "strength of complexing" expression being about 22%.



The shift to linewidth ratios were not measurable as the  $\text{CH}_2$  signal was gradually decoupled, but were obviously good.

Thus the shifts with europium nitrate were not as large as those with the europium complex, although much higher concentrations of europium could be attained. However, the system did prove usable and in some circumstances may be preferable, for example for alcohol ligands soluble in acetone but not in chloroform.

(ii) Methyl 4,6-O-benzylidene- $\alpha$ -D-glucopyranoside

Investigations were carried out using solutions 0.2M in diol. It was immediately obvious that shifts were sufficiently large to be of assistance in signal assignment.

The peak displacements of the assignable signals are given in Table 105.

Table 105. Displacements (all negative), in Hz, of assignable signals in methyl 4,6-O-benzylidene- $\alpha$ -D-glucopyranoside, on addition of  $\text{Eu}(\text{NO}_3)_3 \cdot 2\text{H}_2\text{O}$ .

Conc. $\text{Eu}(\text{NO}_3)_3$ , <u>M</u>	OMe	benzylic H	$\text{H}_1$
0.044	12.9	11.7	38.7
0.092	20.5	19.2	63.1
0.191	31.6	30.0	99.0
0.446	43.8	43.1	142.4

All shifts were to lower fields.

Five more broadened peaks, one of which increased in size with increasing paramagnetic molarity and so was a



water peak, were fairly readily observed in each spectrum and their positions (except for the water peak) are given in Table 106 along with the positions of the most intense peak in each of the two phenyl multiplets. The multiplets, consisting of two and three protons, changed very little in shape so that the most intense peak in each remained the same.

Table 106. Paramagnetic positions, in Hz downfield from TMS, of "fast moving" signals in methyl 4,6-O-benzylidene- $\alpha$ -D-glucopyranoside, on addition of  $\text{Eu}(\text{NO}_3)_3 \cdot 2\text{H}_2\text{O}$ .

Conc. $\text{Eu}(\text{NO}_3)_3$ , $\frac{\text{M}}{\text{M}}$	A	B	C	D	Ph (2 H's)	Ph (3 H's)
0.044	451.8	487.4	611.1	540.8	750.9	740.0
0.092	507.7	549.8	721.0	643.8	754.5	741.3
0.191	598.4	640.8	888.5	815	759.9	743.6
0.446	704.9	746	1101.9	988.6	767.0	745.8

Four further peaks moved downfield at a much slower rate and were difficult to follow as they passed through each other. Their positions, where visible, are given in Table 107.

Table 107. Paramagnetic positions, in Hz downfield from TMS, of "slow moving" signals in methyl 4,6-O-benzylidene- $\alpha$ -D-glucopyranoside, on addition of  $\text{Eu}(\text{NO}_3)_3 \cdot 2\text{H}_2\text{O}$ .

Conc. $\text{Eu}(\text{NO}_3)_3$ , $\frac{\text{M}}{\text{M}}$	E	F	G	H
0.044	*	*	429.9	*
0.191	*	*	*	406.2
0.446	497.1	471.9	454.4	421.8

\* position not measurable.



Normalisation was carried out with respect to the  $H_1$  signal, the benzylic H giving an excellent straight line and the OMe signal being linear except for the last point.

The positions of the four "fast moving" signals also gave good linear plots, yielding diamagnetic positions: A: 355 Hz; B: 390 Hz; C: 424 Hz; D: 370 Hz. These positions agreed with the range of signals observed in the diamagnetic spectrum. Two of these peaks (C and D) moved very much faster than the other two and these were assigned as hydroxyl signals. The other two peaks (A and B) were assumed to be  $H_2$  and  $H_3$ . A was approximately a doublet and B a triplet.  $H_2$  would have a large coupling with  $H_3$  and smaller couplings with  $H_1$  and OH(2), which would make it a doublet of triplets, and  $H_3$  would have large couplings with  $H_2$  and  $H_4$  and a smaller coupling with the OH(3), which would make it a triplet of doublets. Thus from the overall appearances, peak A was  $H_2$  and peak B  $H_3$ .

For the four "slow moving" signals there were insufficient points for graphs to be made. However, by comparing the multiplicities of these signals with the signals observed using praseodymium nitrate (see below) and then using the diamagnetic positions determined there, it was possible to draw graphs, and the groups of signals found in each spectrum agreed well with the graphically interpolated signal positions.

Thus normalisation factors with respect to  $H_1$  signal were calculated for all the proton types in the molecule, and these are given in Table 108.



Table 108. Normalisation factors (all negative), as percentages, for signals in methyl 4,6-O-benzylidene- $\alpha$ -D-glucopyranoside, on addition of  $\text{Eu}(\text{NO}_3)_3 \cdot 2\text{H}_2\text{O}$ .

OMe	benzy- lic H	Ph (o)	Ph (m & p)	H <sub>2</sub> (A)	H <sub>3</sub> (B)	H <sub>4</sub> (E)	H <sub>5</sub> (F)	H <sub>6</sub> (eq) (G)	H <sub>6</sub> (ax) (H)	OH's (C & D)
32	30.2	15.4	5.7	253	245	102	69	24	33	474; 434

The shift to linewidth ratios were very variable for the singlets, OMe and benzylic H, and so were not readily calculated. They were obviously good as the retention of fine structure in the ring proton signals showed.

Thus, although alcohols proved to be rather unrewarding in the results with europium nitrate, this diol has yielded very good results, much superior to those with the europium complex,  $\text{Eu}(\text{DPM})_3$ . It is most probable that chelation is occurring assisting complex formation. It may be also that chelation gives a complex with a larger g factor anisotropy thus giving larger shift to linewidth ratios.

(b) Praseodymium nitrate monohydrate

With the praseodymium nitrate representatives of each of the ligand types were examined, that is, a cyanide, an aromatic and an alicyclic alcohol, a diol and an amide.

(i) p-methyl benzyl cyanide

Investigations were carried out using solutions 1.0 and 0.5M in cyanide.

The shift changes and the normalisation factors with respect to  $\text{CH}_2\text{CN}$  signal are given in Table 109.



Table 109. Displacements (all negative), in Hz, and normalisation factors, as percentages, for signals of p-methyl benzyl cyanide on addition of  $\text{Pr}(\text{NO}_3)_3 \cdot \text{H}_2\text{O}$ .

Conc. ligand, <u>M</u>	Conc. $\text{Pr}(\text{NO}_3)_3$ , <u>M</u>	Displacements			Normalisation factors	
		$\text{CH}_2$	Ph	Me	Ph	Me
1.0	0.15	3.9	1.9	1.4	48.7	35.9
	0.23	6.1	2.6	2.2	42.6	36.1
	0.69	9.6	2.7	3.7	28.2	38.6
0.5	0.21	8.0	3.7	2.8	46.2	35.0
	0.38	10.1	4.4	4.2	43.6	41.6

The shifts, surprisingly all negative whereas they were positive with all ligand types with the praseodymium complex,  $\text{Pr}(\text{DPM})_3$ , were very small, and normalisation was poor. The phenyl signals, a close doublet with small side peaks in the diamagnetic spectrum, became one singlet.

The effect of ligand concentration was difficult to assess because of the poor normalisation, but decreasing the concentration obviously increased the shift sizes.

It thus appears that praseodymium nitrate is not suitable as a shift reagent for cyanides.

(ii) Cholesterol (with F.A.K. Maclean)

Investigations were carried out using solutions 0.2 and 0.1M in alcohol.

The shift changes of the assignable peaks and the normalisation factors with respect to  $\text{H}_3$  signal are given in Table 110.



Table 110. Displacements (all positive), in Hz, and normalisation factors, as percentages, of assignable signals in cholesterol on addition of  $\text{Pr}(\text{NO}_3)_3 \cdot \text{H}_2\text{O}$ .

Conc. ligand, $\frac{\text{M}}{\text{M}}$	Conc. $\text{Pr}(\text{NO}_3)_3$ , $\frac{\text{M}}{\text{M}}$	Displacements				Normalisation factors										
		$\text{H}_3$	C-18 Me	C-19 Me	C <sub>20</sub> -Me	C <sub>25</sub> -Me's	H <sub>6</sub>	OH	C-18 Me	C-19 Me	C <sub>20</sub> - Me	C <sub>25</sub> - Me's	H <sub>6</sub>	OH		
0.2	0.10	55	2.1	6.3	1.3	1.7	1.0	1.3	5	89.6	3.8	11.5	12.7	2.1	9.1	163
0.1	0.07	64	3.0	8.6	1.7	2.0	1.5	1.7	6.3	103.5	4.7	13.4	2.9	2.5	9.8	162

Table 111. Displacements (all positive), in Hz, or peak positions, in Hz downfield from TMS, and normalisation factors, as percentages, for signals of p-methyl benzyl alcohol on addition of  $\text{Pr}(\text{NO}_3)_3 \cdot \text{H}_2\text{O}$ .

Conc. ligand, $\frac{\text{M}}{\text{M}}$	Conc. $\text{Pr}(\text{NO}_3)_3$ , $\frac{\text{M}}{\text{M}}$	Displacements			Peak positions		Normalisation factors		
		$\text{CH}_2$	$\text{CH}_3$	OH	Ph(o)	Ph(m)	$\text{CH}_3$	$\text{CH}_3$	OH
1.0	0.12	63.2	3.9	145.7	700.3	700.3	6.2	230	-
	0.28	122.2	7.1	284.3	676.4	695.7	5.8	232	-
	0.37	153.9	8.7	356.5	664.6	692.6	5.7	232	-
	0.57	222.7	12.2	515.6	638.5	685.4	5.5	232	-
0.5	0.11	68.2	4.3	156.1	699.6	699.6	6.3	229	-
	0.33	169.3	9.8	*	659.4	691.8	5.8	-	-

\* peak not observable.



The shift changes, all upfield, were small, and normalisation was not very good. The  $C_{25}$ -methyls had a surprisingly large normalisation factor, comparable with that of the  $C_{20}$ -methyl.

Decreasing the alcohol concentration increased the shift quite considerably.

Again praseodymium nitrate seemed unsuitable as a shift reagent for this alicyclic alcohol, although there was some doubt whether the nitrate used for this series was fully dehydrated to the monohydrate, and the shifts may therefore be somewhat larger than found here.

(iii) p-methyl benzyl alcohol

Investigations were carried out using solutions 1.0 and 0.5M in alcohol.

The shift changes for the  $CH_2$ ,  $CH_3$  and OH signals, the peak positions for the phenyl signals and the normalisation factors for  $CH_3$  and OH with respect to  $CH_2$  signal are given in Table 111. Another signal which increased in size with increasing praseodymium concentration was almost certainly due to water and its positions are not given.

The shift changes, all upfield, were appreciable though not very large. The  $CH_3$  normalisation factors were acceptably concordant while those of OH signal were remarkably good. The phenyl normalisation plots yielded factors of +37.9% for phenyl(o) and +10.3% for phenyl(m) for both alcohol concentrations, and diamagnetic line positions:

at 1.0M alcohol, Ph(o):722.7 Hz; Ph(m): 708.4 Hz

at 0.5M alcohol, Ph(o): 723.3 Hz. Ph(m): 709.3 Hz.



These are in reasonable agreement with the positions found in the diamagnetic spectra.

The shift changes were fairly linear with respect to the praseodymium concentration for each ligand concentration, and were dependent on the ligand concentration, the "strength of complexing" expression evaluating at 35-40%.

As the  $\text{CH}_2$  signal became decoupled, shift to linewidth ratios were not easy to measure, but were obviously good, greater than 50 and perhaps nearer 300.

Water was added to one paramagnetic solution. This caused a definite decrease in the shifts but normalisation remained almost constant.

Thus this alcohol gives quite an acceptable system for shift studies. The shift sizes are adequate and shift to linewidth ratios good. The apparent independence of the normalisation factors to varying conditions, including addition of water, is a great advantage.

(iv) Methyl 4,6-O-benzylidene- $\alpha$ -D-glucopyranoside

Investigations were carried out using solutions 0.2M in diol. As with  $\text{Eu}(\text{NO}_3)_3 \cdot 2\text{H}_2\text{O}$ , addition of  $\text{Pr}(\text{NO}_3)_3 \cdot \text{H}_2\text{O}$  caused considerable peak movement and separation, the peaks already assigned from the diamagnetic spectrum being easily followed, while four signals moved rapidly upfield leaving four slower moving peaks with fine structure quite visible.

The shift changes of the assigned peaks and the paramagnetic positions of the other peaks are given in Table 112.



Table 112. Displacements, in Hz, or peak positions, in Hz downfield from TMS, of signals in methyl 4,6-O-benzylidene- $\alpha$ -D-glucopyranoside, on addition of  $\text{Pr}(\text{NO}_3)_3 \cdot \text{H}_2\text{O}$ .

Conc. Pr(NO <sub>3</sub> ) <sub>3</sub> M	Displacements		Peak positions									
	OMe	ben- zylic H <sub>H</sub>	H <sub>1</sub>	Ph (2H's)(3H's)	Tri- plet	Quar- tet	Sex- tet	Broad Tri- plet	P	Q	R	S
0.053	+47.4	+38.6	+95.0	726.0	333.5	384.4	281.2	233.9	94.9	94.9	115	94.9
0.113	+80.9	+66.8	+162.1	710.7	304.5	358.2	216	153.8	*	*	*	*
0.285	+117.6	+99.8	+243.3	688.0	269.7	326.4	138.7	54.6	-286.7	-329.1	-388.6	-388.6
0.462	+128.6	+111.2	+272.1	678.9	257.2	313.9	110.0	*	-344.9	-420.8	-492.8	-492.8
0.536	+129.8	+112.2	+276.0	677.0	255.5	311.4	103.1	*	-350.5	-429.8	-514.6	-490.7

\* peak position not measurable.

Table 113. Normalisation factors (all positive), as percentages, and diamagnetic line positions, in Hz downfield from TMS, calculated graphically, for signals in methyl 4,6-O-benzylidene- $\alpha$ -D-glucopyranoside.

OMe	benz- ylic H	Ph(o)	Ph(m & p)	Tri- plet $\text{H}_6(\text{ax})$	Quar- tet $\text{H}_6(\text{eq})$	Sex- tet $\text{H}_5$	broad trip- let, $\text{H}_4$	"fast moving" peaks				
								P	Q	R	S	S
Normalisation factors	49.7	41.2	28.2	3.4	43.3	38.7	96.3	121	252	289	344	330
Line positions					375	420.0	373	351	336	371	444	411



Again the phenyl signals were in two groups, one of two protons, one of three, and the position of the most intense peak was noted. The slower moving signals were readily followed as their multiplicity was visible, but the positions of the four faster moving signals had to be determined from the normalisation plots.

The shift sizes were quite reasonable and all shifts were upfield in direction. They were not very linear with respect to the praseodymium molarity. Comparison of the shift sizes with those of the europium system could not be made accurately because of this non-linearity, but the praseodymium shifts are 1.5-3.0 times as great as the europium shifts.

The normalisation plots with respect to  $H_1$  signal were straight lines except for the OMe signal which curved very slightly and the "fast moving" peaks for which the peak positions were a little uncertain. Normalisation factors calculated from the gradients are given in Table 113, as are the diamagnetic line positions evaluated graphically.

The four "fast moving" peaks were almost certainly the two hydroxyl peaks and  $H_2$  and  $H_3$ , although which is which could not be determined with certainty as normalisation factors were rather similar. It was assumed that the two faster moving peaks were the hydroxyl signals.

The four "slow moving" peaks were assigned on the basis of their multiplicity and speed of movement.

The  $H_4$  signal, coupled twice trans diaxially, was a triplet with  $J \sim 8.5-10$  Hz. Of the four signals, it was the most broadened and moved fastest.



The  $H_5$  signal, coupled twice trans diaxially and once axial-equatorially, was a sextet with  $J_{\text{trip}} \sim 9.8$  Hz,  $J_{\text{doub}} \sim 4.8$  Hz. It was the peak which was the next most shifted.

The  $H_6(\text{eq})$  signal, coupled geminally ( $J = 10.2$  Hz) and vicinally (axial-equatorial,  $J = 4.8$  Hz), was a quartet. The signal moved the slowest of the four.

The  $H_6(\text{ax})$  signal, coupled geminally and vicinally (trans diaxial) was a triplet (actually a quartet with the central peaks very close together).  $J_{\text{gem}}$  was 10.2 Hz and  $J_{\text{vic}}$  was around 10 Hz. The signal moved at a very similar rate to the equatorial  $H_6$  signal.

These assignments all appeared to be quite satisfactory.

The shift to linewidth ratios were good, but decreased at the higher praseodymium concentrations where the shifts increased very little with increasing concentration while linewidths continued to increase. At low praseodymium concentration a ratio of 130 was found for the benzylic proton signal and a rather lower ratio for the methoxy signal.

It is thus apparent that of all the shift reagents examined, praseodymium nitrate produces the best spectral clarification for this diol. The results from the europium nitrate system were to some extent complementary. Full signal assignment has been made possible with diamagnetic signal positions and most coupling constants being determined with a good degree of accuracy.

The calculated diamagnetic line positions and the normalisation factors evaluated using these two nitrates



are compared in Table 114.

Table 114. Comparison of diamagnetic line positions and normalisation factors for methyl 4,6-benzylidene- $\alpha$ -D-glucopyranoside with  $\text{Eu}(\text{NO}_3)_3 \cdot 2\text{H}_2\text{O}$  and  $\text{Pr}(\text{NO}_3)_3 \cdot \text{H}_2\text{O}$ .

Proton(s)	Diamagnetic position		Normalisation factor	
	Eu	Pr	Eu	Pr
$\text{H}_1$			-100	+100
$\text{H}_2$	355	371; 336	-253	+289; +252
$\text{H}_3$	390		-245	
$\text{H}_4$	*	351	-102	+121
$\text{H}_5$	*	373	-69	+96.3
$\text{H}_6(\text{eq})$	*	420.0	-33	+43.3
$\text{H}_6(\text{ax})$	*	375	-24	+38.7
OH's	424, 370	444; 411	-474; -434	+344; +330
Ph(o)			-15.4	+28.2
Ph(m & p)			-5.7	+3.4
OMe			-32	+49.7
benzylic H			-30.2	+41.2

\* assumed to be the same as for  $\text{Pr}(\text{NO}_3)_3$  in the calculation of normalisation factors.

The normalisation factors form a similar pattern in each case but are quite distinctly different in absolute values. This shows that changing from one metal ion to the other involves more than simply changing the g-factor anisotropy in an axially symmetric complex since this would result in



the same shift ratios (see Part II, Section G(d)). The geometry of the complex may have altered slightly or the complex may not be axially symmetric. Alternatively, the complexes may even be different in stoichiometry because of the different amount of water present. A change in contact contribution to the shifts would affect the ratio of the shifts of the closer protons but not the more distant ones; this, however, was not the case.

The diamagnetic positions for the  $H_2$ ,  $H_3$  and hydroxyl signals in the two cases did not agree very well, but in the praseodymium case these were determined very approximately (due to considerable overlap of the peaks) and so the europium values may be assumed to be the more accurate.

(v) p-acetamidotoluene (with F.A.K. Maclean)

Investigations were carried out using solutions 0.2M in amide.

The shift displacements and the normalisation factors with respect to the ortho phenyl signal are given in Table 115.

Table 115. Displacements, in Hz, and normalisation factors, as percentages, for signals of p-acetamidotoluene on addition of  $Pr(NO_3)_3 \cdot H_2O$ .

Conc. $Pr(NO_3)_3$ <u>M</u>	Displacements					Normalisation factors			
	COMe	NH	Ph (o)	Ph (m)	Me	COMe	NH	Ph (m)	Me
0.09	-77.3	-142	+68.7	+24.6	+11.6	-107	-207	+35.8	+16.9
0.34	-168.9	-272	+77.3	+33.2	+17.3	-218	-352	+43.0	+22.4



Although shift displacements were appreciable, normalisation was very poor. The NH, surprisingly, was visible even after addition of praseodymium, and it and the COMe signal moved downfield while the other signals moved upfield.

The linearity of the shifts with praseodymium concentration was very poor; it is possible that in some of these exploratory experiments the nitrate had not been dried sufficiently.

Shift to linewidth ratios were good, about 100 for the COMe signal, but rather less for the ArMe signal.

Two solutions were run using the same molarity of amide but 0.06 and 0.28M  $\text{Pr}(\text{NO}_3)_3 \cdot 6\text{H}_2\text{O}$ . The shift displacements and normalisation factors with respect to the ortho phenyl signal for these solutions are given in Table 116.

Table 116. Displacements, in Hz, and normalisation factors, as percentages, for signals of p-acetamidotoluene on addition of  $\text{Pr}(\text{NO}_3)_3 \cdot 6\text{H}_2\text{O}$ .

Conc. $\text{Pr}(\text{NO}_3)_3$ $\frac{\text{M}}{3}$	Displacements					Normalisation factors			
	COMe	NH	Ph (o)	Ph (m)	Me	COMe	NH	Ph (m)	Me
0.06	-39.9	-87	+57.2	+13.1	+8.0	-69.9	-152	+22.9	+14.0
0.28	-81.5	-161	+87.2	+25.4	+14.4	-93.5	-185	+29.2	+16.5

The shifts of some of the signals increased with the additional water while those of others decreased, and normalisation was very poor. The only consistency appeared to be in the direction of the shift changes. Obviously normalisation has totally broken down in the presence of varying amounts of water.



Thus, this amide gives very poor shift results with the praseodymium nitrate shift reagent. Although complexing obviously occurs, as shown by the reasonable size of shifts, normalisation is quite impossible, making the system of little value.

#### (D) CONCLUSION

Of the four shift reagents studied each was found to have a different potential. The ligands with which they were found to be most useful varied and results were sometimes complementary. A full comparison will be made in the next Part.



## PART VII

### COMPARISONS OF SHIFT REAGENTS

In the last two parts, Parts V and VI, the results from work with six different shift reagents has been described. The value of each shift reagent with a variety of cyanide, alcohol and amide ligands has been assessed and these results will now be gathered together for comparison of the relative merits and potentials of each shift reagent system.

Although a considerable number of ligands has been examined, these represent only a small sample of the possible ligand types and so, although generalisations will be made, these will necessarily be tentative.

Comparisons will primarily be made to establish which shift reagents are suitable for each ligand type and, of those, which is the most satisfactory. Then the shift reagents will be compared with a view to ease of preparation of N.M.R. samples and cost of reagents.

Since interchange of europium and praseodymium in each of the lanthanide systems caused very little change in the results apart from direction of shifts, the two ions will be considered together, comparisons being made only when relevant.

#### (A) CYANIDE LIGANDS

##### (i) Cobalt perchlorate-acetone system

All the cyanides investigated proved suitable ligands for selective shift studies with cobalt perchlorate. Normalisation was good and shift to linewidth ratios were in the range 20 - 40. Shift sizes were reasonable, the  $\text{CH}_2\text{CN}$  signal



being displaced 200 - 500 Hz with 0.1M cobalt(II), the shifts being slightly dependent on ligand concentration.

(ii) Co(AA)<sub>2</sub> - chloroform system

The one ligand investigated, *p*-methyl benzyl cyanide, proved a suitable ligand for this system. Normalisation was reasonable. Shift to linewidth ratios were very variable, from 5 to 70, while shift sizes were smaller than with cobalt perchlorate, the CH<sub>2</sub>CN signal being displaced 140 - 190 Hz with 0.1M Co(AA)<sub>2</sub>, the shifts being noticeably dependent on ligand concentration.

(iii) Ln(DPM)<sub>3</sub> - chloroform system

The results with *p*-methyl benzyl cyanide and Eu(DPM)<sub>3</sub> indicated that this shift reagent was unsuitable for this ligand. Shift displacements were very small, the CH<sub>2</sub>CN signal being displaced only 58 Hz with 0.07M Eu(DPM)<sub>3</sub>, and normalisation was very poor. Shift to linewidth ratios however were good, in the range 50 - 100.

(iv) Lanthanide nitrate-acetone system

The results with *p*-methyl benzyl cyanide and Pr(NO<sub>3</sub>)<sub>3</sub>·H<sub>2</sub>O showed that this shift reagent was not suitable for this ligand. Shift changes were very small, the CH<sub>2</sub>CN signal being displaced only 3.9 Hz with 0.15M Pr(NO<sub>3</sub>)<sub>3</sub>, and normalisation was poor.

(v) Conclusion

For cyanide ligands, by far the best system is the cobalt perchlorate-acetone system, the Co(AA)<sub>2</sub>-chloroform system taking second place. Although the shift to linewidth



ratios of the former are not very high, they are adequate to give satisfactory results in at least the simpler cases.

## (B) ALCOHOL LIGANDS

The alcohols will be considered in two groups, first the simple monofunctional alcohols and second the diol.

### (a) Simple alcohols

#### (i) Cobalt perchlorate-acetone system

Although not quite as satisfactory as for the cyanides, this system proved suitable for all the simple alcohols investigated. Normalisation was in general good. Shift to linewidth ratios were in the range 10-30, not so good as with cyanides, but shift sizes were greater, the  $\alpha$ -CH being displaced from 350-1200 Hz with 0.1M cobalt(II). The shifts were noticeably dependent on ligand concentration.

#### (ii) Co(AA)<sub>2</sub>-chloroform system

The results for the two ligands studied, menthol and *p*-methyl benzyl alcohol, were not very satisfactory, especially those for the former. The aromatic alcohol gave usable results. Normalisation was possible but shift changes were not very large, the  $\alpha$ -CH signal being displaced 270 Hz with 0.1M Co(AA)<sub>2</sub>. Shift to linewidth ratios were very poor, in the region of 10.

#### (iii) Ln(DPM)<sub>3</sub>-chloroform system

Both menthol and *p*-methyl benzyl alcohol with both Eu(DPM)<sub>3</sub> and Pr(DPM)<sub>3</sub> gave very good results. In each case normalisation was good and shift to linewidth ratios were very good, around 100 for the europium complex and greater for the



praseodymium complex. Shift sizes were satisfactory; for 0.5M ligand and 0.05M complex, shift changes of the  $\alpha$ -CH of *p*-methyl benzyl alcohol were 220-230 Hz for  $\text{Eu}(\text{DPM})_3$  and around 300 Hz for  $\text{Pr}(\text{DPM})_3$ . The shifts were strongly dependent on ligand concentration. Of the two complexes,  $\text{Pr}(\text{DPM})_3$  was the better, but choice of complex would be dependent mainly on the direction of shifts required, as dictated by the distribution of signals in the spectrum.

(iv) Lanthanide nitrate-acetone system

Although cholesterol appeared to give rather poor results with  $\text{Pr}(\text{NO}_3)_3 \cdot \text{H}_2\text{O}$ , *p*-methyl benzyl alcohol gave satisfactory results with both nitrates. Normalisation was good as were the shift to linewidth ratios. The shifts were not very large however, about 25 Hz for  $\alpha$ -CH with 0.1M  $\text{Eu}(\text{NO}_3)_3$  and 60-70 Hz with 0.1M  $\text{Pr}(\text{NO}_3)_3$ . They were noticeably dependent on ligand concentration.

(v) Conclusion.

The best shift reagents for simple alcohols are clearly the lanthanide complexes,  $\text{Ln}(\text{DPM})_3$ . A second choice would depend on whether large shifts or good resolution was more important, cobalt perchlorate giving the former and the lanthanide nitrates the latter. The  $\text{Co}(\text{AA})_2$ -chloroform system is not satisfactory.

(b) Diols

Only one sugar diol was investigated and further investigation of such compounds would be of particular interest.

(i) Cobalt perchlorate-acetone system

This system did not give very good results with the diol.



Normalisation was not very good and assignment of signals was hampered by poor shift to linewidth ratios of less than 10.

(ii) Co(AA)<sub>2</sub> - chloroform system

This system was not studied.

(iii) Ln(DPM)<sub>3</sub> - chloroform system

This system did not prove satisfactory either. Shift changes were very small and normalisation was poor.

(iv) Lanthanide nitrate-acetone system

Both nitrates gave very good results enabling total assignment of the signals to be made. Normalisation in both cases was good and so were the shift to linewidth ratios. Shift sizes, though not very large, were quite adequate; for 0.1M nitrate, H<sub>1</sub> was displaced about 70 Hz for Eu(NO<sub>3</sub>)<sub>3</sub> and about 150 Hz for Pr(NO<sub>3</sub>)<sub>3</sub>.

(v) Conclusion

Clearly the only system of any value with this diol is the lanthanide nitrate-acetone system which gave very satisfactory results.

(C) AMIDE LIGANDS

(i) Cobalt perchlorate-acetone system

Although the results in this case had to be treated with great caution due to the presence of an octahedral-tetrahedral complex equilibrium, the system was quite acceptable. Shift changes were quite substantial, the ortho phenyl signal in p-acetamidotoluene being displaced about 350 Hz with 0.1M cobalt(II).



(ii) Co(AA)<sub>2</sub> - chloroform system

This system gave poor results. Shift changes were small, the ortho phenyl signal in p-acetamidotoluene being displaced 54 Hz with 0.1M Co(AA)<sub>2</sub>, and normalisation was poor. Shift to linewidth ratios also were low.

(iii) Ln(DPM)<sub>3</sub> - chloroform system

This system appeared suitable although very little work was done with it. Normalisation was reasonable and shift changes quite considerable, the ortho phenyl signal of p-acetamidotoluene being displaced 250-350 Hz with 0.1M complex.

(iv) Lanthanide nitrate-acetone system

Pr(NO<sub>3</sub>)<sub>3</sub>·H<sub>2</sub>O with p-acetamidotoluene gave a very poor system for shift studies. Although complexing obviously occurred since shifts were of reasonable size (ortho phenyl signal displaced around 75 Hz with 0.1M Pr(NO<sub>3</sub>)<sub>3</sub>), normalisation was very poor, especially with varying amounts of water. Shift to linewidth ratios, however, were quite acceptable.

(v) Conclusion

Of the four systems studied, two proved to be of little use with amides - the Co(AA)<sub>2</sub> and the lanthanide nitrate systems - while of the other two, the Ln(DPM)<sub>3</sub> system appeared to be the more satisfactory although insufficient results were obtained to substantiate this. The extensive studies with the cobalt perchlorate system, however, showed it to be a system with considerable potential.



#### (D) SUMMARY

Within the limited range of ligands which has been examined, it is clear that different shift reagents are the most effective for different ligand types. The cobalt perchlorate-acetone system is the shift reagent of choice for cyanides and is possibly the most satisfactory with amides. The lanthanide nitrate-acetone system is the best for the diol, while  $\text{Ln}(\text{DPM})_3$ -chloroform is the system of choice for simple alcohols and possibly amides. Only the  $\text{Co}(\text{AA})_2$ -chloroform system was consistently less satisfactory.

It would thus appear that although the  $\text{Ln}(\text{DPM})_3$  complexes have been accepted with great acclaim as shift reagents, there are situations in which more satisfactory reagents can be found. This may also be true for the  $\text{Ln}(\text{fod})_3$  reagents which, although producing greater shifts due to greater degrees of complexing, would be expected to behave rather similarly to the non-fluorinated complexes in other respects.

#### (E) EXPERIMENTAL COMPARISON

Although the most important factor in evaluating a shift reagent is the effectiveness of the reagent in selective shift studies as described above, the ease of preparation of N.M.R. solutions and the cost of using the reagent are also important factors, and will now be discussed and compared.

##### (a) Ease of preparation of solutions

The ease of preparation of the N.M.R. solutions depends on the need for purification or dehydration of the commercial



reagent, the ease of handling the reagent, the ease of handling the solvent and the stability of the resulting solutions. The solubility of the reagent in the solvent is also an important factor.

(i) Cobalt perchlorate-acetone system

Cobalt perchlorate hexahydrate was dried to the dihydrate, a process requiring several weeks. The resulting solid was easily handled and did not pick up water very readily during weighing. The deuterioacetone was dried over molecular sieves and had to be stored in a well sealed bottle to prevent loss by evaporation. There was no problem in measuring accurate volumes. The prepared solutions appeared quite stable but, if kept, they required to be carefully sealed to prevent evaporation of acetone and absorption of water. Concentrations of cobalt(II) up to at least 0.5M were readily attained.

(ii) Co(AA)<sub>2</sub>-chloroform system

The reagent required to be dried for several days but did not pick up water again very rapidly and was easy to handle. The deuteriochloroform solvent required the same treatment as the acetone solvent above. The solutions appeared reasonably stable but high concentrations of reagent could not be achieved, about 0.2M being the greatest.

(iii) Ln(DPM)<sub>3</sub>-chloroform system

The reagents required to be dried for several days. They appeared to pick up water readily if transfers involved in weighing were not executed fairly rapidly, but were otherwise easy to handle. The solutions did not appear to be very



stable and were always freshly prepared for running their N.M.R. spectrum. The complexes were not very soluble, concentrations over 0.1M being difficult to attain.

(iv) Lanthanide nitrate-acetone system

Both nitrates required to be dehydrated, a process requiring up to two weeks. The praseodymium salt was the easier of the two to dehydrate. Both nitrates went "hard" on drying and were not easily handled as they were very hygroscopic and became sticky. The solutions appeared to be quite stable and concentrations up to 0.7M were readily prepared.

(v) Conclusion

There is not much to choose between the solvents, the deuteriochloroform perhaps being slightly easier to store. Of the reagents, the complexes only required to be dried whereas the salts required removal of water of crystallisation, a slower and slightly more difficult process. The cobalt perchlorate was the most easily handled. The greatest paramagnetic concentrations could be achieved in the acetone solutions, low solubility being a restriction in both chloroform systems. Thus each system has its advantages and disadvantages.

(b) Cost of solutions

In costing the various solutions, it was assumed that no reagent or solvent would be retrieved. Although in theory it is possible to recover some of the starting materials, in practice this proves to be very time consuming, and the purity of the products is not adequate for their reuse. Typical



weights of reagents required for the N.M.R. solutions will be compared, using the prices relevant at the time of these studies.

The results are shown in Table 117.

Table 117. Price comparison for typical solutions of each cobalt and lanthanide shift reagent.

System	Cost of 0.5 ml solvent, p	Typical mass of reagent reqd., g	Cost per gram of reagent, p	Cost per required mass re- agent, p	Approx. cost per sample, p
Co(II)-acetone	32	0.03	1.5	0.05	32.1
Co(AA) <sub>2</sub> - chloroform	5	0.015	5.2	0.08	5.1
Ln(DPM) <sub>3</sub> - chloroform	5	0.01	450	4.5	9.5
Eu(NO <sub>3</sub> ) <sub>3</sub> -acetone	32	0.04	10	0.4	32.4
Pr(NO <sub>3</sub> ) <sub>3</sub> -acetone	32	0.04	72	2.9	34.9

It is immediately apparent that the major contribution to the cost of a solution is the cost of the deuterated solvent, which makes the acetone solutions by far the more expensive.

#### (F) CONCLUSION

In choosing the best shift reagent to use, the most important factor is which reagent is the most effective for selective shift studies with the given ligand. As discussed above this varies from one ligand to another and so an appropriate choice must be made. There is not much to choose between the reagents as regards experimental factors, but, everything else being equal, the use of deuteriochloroform as solvent and so Ln(DPM)<sub>3</sub> as shift reagent, is preferable on the basis of cost.



PART VIIIPROGRESSIVE SATURATION STUDIES

## (A) INTRODUCTION

During the work on the ferrocene system (Part III), it was noticed that selective broadening of side-chain signals and probably also of ferrocene ring proton signals was occurring, but studies of this by linewidth measurement proved difficult due to extensive overlap of peaks. An alternative approach appeared to be by means of progressive saturation.

A nucleus of spin  $I = \frac{1}{2}$  in a magnetic field will absorb energy from a RF field,  $H_1$ , of appropriate frequency causing transitions between the lower and the upper energy spin states. The energy absorbed will depend on the excess population of the lower energy spin state,  $n$ , and the transition probability,  $P$ , given by

$$P = \frac{1}{4} \gamma^2 H_1^2 g(\nu)$$

where  $g(\nu)$  is the line shape function (see Part II, section D).

Absorption of energy reduces the excess spin population in the lower state and so less energy is then absorbed and the signal intensity is reduced. This effect is known as "Saturation". Eventually the spin populations in the two states would equalise and no signal would be observed, but for the fact that spin-lattice relaxation tends to restore the equilibrium Boltzmann distribution of nuclei in the spin states. Under the influence of these two opposing effects, the signal intensity is reduced by a factor,

$$Z = \frac{1}{1 + \frac{1}{2} \gamma^2 H_1^2 T_1 g(\nu)} ,$$



known as the saturation factor. At the signal maximum  $g(\nu) = 2T_2$  and therefore

$$Z = \frac{1}{1 + \gamma^2 H_1^2 T_1 T_2}.$$

Thus, as the RF field increases, the degree of saturation increases, the effect being most pronounced for long relaxation times.

It is therefore possible by observing the ease of saturation of different proton signals to evaluate their relaxation times.

Various, basically similar, approaches can be made in progressive saturation studies.

Geet and Hume<sup>271</sup> plotted  $\log \gamma^2 J_1^2 H_1^2 T_1 T_2 = \log (Z^{-1} - 1)$  against  $\log J_1 H_1$  which gave straight lines of gradient 2 whose intercepts on the  $Z^{-1} - 1 = 1$  axis gave  $\log (1/\gamma T)$  where  $T^2 = T_1 T_2$ .  $J_1$  is a factor introduced to account for the modulation of the RF field.

They used three alternative methods for determining  $Z$ : measurement as a function of  $H_1$  of

- (1) peak height (proportional to  $Z$ )
- (2) peak area (proportional to  $Z^{\frac{1}{2}}$ )
- (3) linewidth (proportional to  $Z^{-\frac{1}{2}}$ ).

They also studied cases where there was inhomogeneity broadening. This did not affect method (2) and could be corrected for in method (3), but provided an alternative method of evaluating  $T$  in method (1). To obtain good results in this last case, they had to offset the homogeneity controls purposely so that the inhomogeneity linewidth,  $\Delta\nu_{\frac{R}{2}}$ , was about 100 times the natural linewidth,  $\Delta\nu_{\frac{1}{2}}$ , and then the peak height is



proportional to  $Z^{\frac{1}{2}}$ . Of these methods, peak height measurement with negligible inhomogeneity proved the most satisfactory.

They obtained absolute values of  $(T_1 T_2)^{\frac{1}{2}}$  by determining  $J_1 H_1$  for various settings of the RF voltage using a standard copper sulphate solution of known relaxation times.

Finer and Harris<sup>272</sup> evaluated  $T_1$  by a similar method. The saturation equation they used was

$$E \propto \frac{H_1 g(\nu) Q}{1 + \frac{1}{2} \gamma^2 H_1^2 g(\nu) Q T_1},$$

where  $Q$  is the square of the matrix element of the shift operator, given by  $Q = \frac{1}{2}(I + m')(I - m + 1)$ , which for protons ( $I = \frac{1}{2}$ ,  $m' = m + 1 = \frac{1}{2}$ ), gives

$$E \propto \frac{H_1 g(\nu)}{1 + \frac{1}{2} \gamma^2 H_1^2 g(\nu) T_1}.$$

$E$  is the e.m.f. of the measured signal. At the peak maximum,  $E = E(0)$  and  $g(\nu) = g(0)$ ,

thus

$$\frac{H_1}{E(0)} = \frac{\gamma^2 H_1^2 T_1}{2B} + \frac{1}{Bg(0)}$$

where  $B$  is a constant of proportionality containing instrumental factors and the concentration of nuclei in the sample.

Finer and Harris plotted  $H_1/E(0)$  against  $H_1^2$  which gave a straight line of gradient  $\gamma^2 T_1/2B$ . Absolute values of  $T_1$  were produced by calibrating the instrument with a sample of known  $T_1$ .

In the present work, peak heights,  $h$ , were measured over a range of RF voltages,  $V$ . A standardised peak height,  $h_s$ , was calculated by dividing the measured peak height by the



RF voltage and the recorder sensitivity, S;  $h_s = \frac{h}{V x S}$ .

The constant value of  $h_s$  under non-saturating conditions is  $h_u = kg(0) = 2kT_2$ , where  $k$  is a constant containing instrumental conditions and concentration of nuclei.

Now,

$$h_s = \frac{h_u}{1 + \gamma^2 H_1^2 T_1 T_2}$$

$$\text{or } h_s = \frac{h_u}{1 + \gamma^2 a^2 V^2 T_1 T_2} \quad \text{where } H_1 = aV.$$

$V$  is the reading of the applied RF voltage (Perkin-Elmer R10) or the setting of the RF attenuator (Varian HA 100) and " $a$ " is a constant for each instrument under constant instrumental conditions (" $a$ " includes the modulation factor,  $J$ ).

The saturation equation can be expressed in two ways, for graphical purposes:

$$h_s = h_u - \gamma^2 a^2 T_1 T_2 \cdot h_s V^2$$

$$\text{or } \frac{1}{h_s} = \frac{1}{h_u} + \frac{\gamma^2 a^2 T_1 T_2}{h_u} \cdot V^2$$

Thus, a plot of  $h_s$  against  $h_s V^2$  has a gradient of  $-\gamma^2 a^2 T_1 T_2$ , and a plot of  $h_s^{-1}$  against  $V^2$  has a gradient of  $\gamma^2 a^2 T_1 T_2 h_u^{-1}$  from which  $\gamma^2 a^2 T_1 T_2$  can be calculated using the intercept ( $h_u^{-1}$ ). The latter plot is analogous to that used by Finer and Harris, except that in their method the quantity  $h_u/T_2$  ( $=2k$ ) is determined by calibration.

The former plot was found to be more satisfactory as it gave a more even "spread" of points.

Absolute values of  $T_1 T_2$  can be obtained by evaluating  $\gamma^2 a^2$  using a sample of known  $T_1 T_2$ . To evaluate  $T_1$  directly,



k must be known, which may prove difficult since k contains the concentration (which may not be easy to control in a volatile solvent such as acetone) and also depends on the sensitivity of the detector and recording system (which may vary from day to day). Alternatively  $T_1$  can be evaluated if  $T_2$  is known from linewidths. Linewidths will not give accurate  $T_2$  values unless the inhomogeneity broadening is small,  $\Delta\nu_{\frac{R}{2}} \ll \Delta\nu_{\frac{1}{2}}$ . Also linewidths may be extremely difficult to measure in broadened multiplets or where there is considerable overlap of signals.

We thus have a method involving measurement of peak heights as a function of RF voltage which should readily yield relative values of  $T_1 T_2$  for different proton signals, and, provided calibration is satisfactory, give absolute values to the product. Evaluation of the two individual relaxation times may prove possible if experimental conditions are favourable but may be subject to large errors.

Before discussing the experimental details, the effect of peak overlap on peak heights will be examined.

#### Peak height correction for overlap of multiplet peaks

Although peak heights are much more readily measured than linewidths in spectra with considerable overlap of peaks, the heights are affected by the "adding in" of other peaks. However, it is possible to correct for this.

The general expression for the shape of a single line under conditions with some saturation is

$$g(\nu) = \frac{kT_2 Z}{1 + 4\pi^2 (\nu_0 - \nu)^2 T_2^2 Z}.$$



If we have  $n$  peaks in a multiplet of coupling constant,  $J$ , and peak height ratios  $k_1:k_2:---:k_s:---:k_n$ , then the peak height measured for the  $m$ 'th peak is given by

$$\sum_{s=1}^n \frac{k_s T_2 Z}{1 + 4\pi^2 (s-m)^2 J^2 T_2^2 Z}$$

(assuming that the relaxation times are the same for all the peaks in the multiplet)

or, since  $T_2 Z^{\frac{1}{2}} = 1/\pi \Delta \nu_{\frac{1}{2}}$

$$h_{\text{meas}}(\text{peak } m) = T_2 Z \sum_{s=1}^n \frac{k_s}{1 + 4(s-m)^2 J^2 / \Delta \nu_{\frac{1}{2}}^2}$$

Now, the correct peak height of the  $m$ 'th peak alone is

$$h_{\text{corr}}(\text{peak } m) = k_m T_2 Z$$

so that

$$h_{\text{corr}}(\text{peak } m) = \frac{\sum_{s=1}^n \frac{k_m}{k_s}}{\sum_{s=1}^n \frac{1}{1 + 4(s-m)^2 J^2 / \Delta \nu_{\frac{1}{2}}^2}} \times h_{\text{meas}}(\text{peak } m)$$

In the general case of peak overlap (not multiplets), the expression is not readily simplified.

The expression requires measurement of the linewidth which may not always be easy. When the linewidth is small it is usually fairly readily measured, although inhomogeneity error is greater in this case. When the lines are broad, overlap makes accurate linewidth measurement difficult; however the error in this case is less significant in the results. Care must also be taken that a broadened multiplet has not been spin-decoupled, which would give a considerably different peak height.

Initially individual peak heights were corrected for peak



overlap using the above expression, but then, a simpler procedure became applicable and it is described in the appropriate section.

## (B) EXPERIMENTAL

Full instrumental details are discussed below in the sections appropriate to each instrument. The details of individual N.M.R. solutions, which were prepared by the standard methods previously described, are given also in the appropriate sections. Reagents, other than those previously used, are now detailed.

The cobalt(II) solutions were prepared using cobalt perchlorate hexahydrate (Fluka), and the copper(II) solutions using AnalaR copper sulphate pentahydrate (BDH) or the pentahydrate dried at  $100^{\circ}$  for 1-2 days and assumed to be the trihydrate on the basis of weight loss, although exact water content is not important.

Absolute ethanol was used for the cobalt-ethanol solutions. The deuterium oxide solvent was 99.7% (Norsk Hydro).

## (C) PROGRESSIVE SATURATION USING THE R10 INSTRUMENT

### (a) Instrumental conditions and accuracy checks

#### (i) Accuracy of the sensitivity control and linearity of the slide-wire

Using a power pack to introduce a voltage and a digital voltmeter (DVM) to measure its magnitude, the deflection of the recorder pen was measured for given voltages for each setting



of the sensitivity control. This showed the sensitivity control to be accurate to 99.5%. The linearity of the slide-wire was similarly checked at three different sensitivity values and found to be as good as the readability of the chart.

(ii) H<sub>1</sub> control

This was investigated using a solution approximately 0.3M copper sulphate in water, which gave a very broad singlet signal of suitable peak height, which did not saturate over the range of RF powers to be investigated (shown by constant linewidths). Measurements were made at scale factor 60 as the peak was very broad. The ratio  $\frac{\text{measured peak height}}{\text{sensitivity} \times \text{RF reading}}$  should stay constant if the RF control is accurate. This was not found to be so. In fact the RF attenuators are not precision components and so accurate values would not be expected. It was suggested<sup>273</sup> that replacement of the H<sub>2</sub> inlet (on the junction box between the attenuator and the probe) with a 50  $\Omega$  . non-inductive screened resistor might improve the values, but in fact this changed the relative RF values insignificantly, although decreasing the peak heights by decreasing the overall RF power. However, it did improve the bridge-balance, and so calibration and all subsequent work was carried out with the resistor inserted.

The calibrated RF voltages for the fine and decade attenuators are given in Table 118 (taking the instrumental setting of  $1 \times 10^3$  as  $1.00 \times 10^3 \text{ mV}$ ).

The RF level was also monitored over a period of two months, using a Phillips GM 6060 voltmeter with RF probe, plugged into the RF source (SK 3). This showed the level to



Table 118. Calibrated RF voltages (mV) for the R10 instrument.

	Fine control							Decade control					
Instrumental	1	1.25	1.6	2	2.5	3.2	4	5	6.3	8.3	$10^2$	$10^3$	$10^4$
Calibrated	1.00	1.28	1.61	2.03	2.57	3.24	4.12	5.26	6.73	8.61	$1 \times 10^2$	$1 \times 10^3$	$0.888 \times 10^4$



be constant to within 99%.

(iii) Reproducibility of peak heights

It was found that peak heights changed randomly from day to day by as much as 18%, possibly because of variations in the sensitivity of the detector system, but variation within a day was at most 3% and probably much less. It was therefore essential that all saturation series were completed without a break.

Changing the N.M.R. tube appeared to affect the peak heights insignificantly.

(iv) Sweep rate and time constant

The choice of time constant is very largely determined by the sensitivity being used, in order to achieve tolerable signal to noise levels. With this provision, the shorter the time constant the better for achieving accurate peak heights. In fact, it was possible to use time constants which introduced negligible error.

The choice of sweep rate depends on whether negligible saturation is required (calibration of RF) or stationary conditions are required (saturation work). For the former, the best sweep rate was found by decreasing it until constant peak heights were obtained, this being achieved before saturation became appreciable.

For the saturation work, it would be ideal to stop the pen on the peak maximum and so measure the peak height. This, however, was not possible for two reasons; firstly the signal drifted very slightly and secondly, during saturation, the signal noise was such that the pen dug holes in the chart



paper if the sweep was stopped. Thus peak heights were measured by scanning the peak maximum at the slowest sweep rate available.

(v) Bridge control

Offsetting the bridge seemed to increase the peak heights. The bridge was always kept as near balanced as possible and the  $50\Omega$  resistor (see section (ii)) kept inserted.

(vi) High-sensitivity probe

During the course of this work, a new high-sensitivity probe was put into the instrument. This increased the peak heights, improving the signal to noise ratio, but otherwise made no difference. The RF level remained the same (shown by the unchanged value for the constant "a"), and the attenuators calibrated identically. Reproducibility was not improved.

(b) Instrumental calibration to evaluate absolute values of  $T_1T_2$ .

The saturation equation,  $h_s = \frac{h_u}{1 + \gamma^2 a^2 V^2 T_1 T_2}$ , gives rise to plots which yield values of  $\gamma^2 a^2 T_1 T_2$ . To evaluate  $T_1 T_2$ ,  $\gamma^2 a^2$  must be determined, which is possible using a standard solution whose relaxation times are known. For this, a paramagnetic solution where  $T_1 = T_2$  and  $T_2$  can be measured from the linewidth, would be ideal. A cobalt(II)-water solution was chosen since the short electronic relaxation time for cobalt(II) should ensure  $T_1 = T_2$ , and water gives a suitable singlet for linewidth measurement.



Two such solutions were investigated, the first approximately 0.05M in Co(II) with 5  $\mu$ l distilled water and 1  $\mu$ l dilute sulphuric acid (conc.  $H_2SO_4$  in distilled  $H_2O$ ) and the second approximately 0.04M in Co(II) with 1  $\mu$ l dilute sulphuric acid, both made up to 0.5 ml with  $D_2O$ . The acid was to ensure fast exchange. Peak heights were measured over a range of RF powers from  $2.5 \times 10^3$  to  $4.0 \times 10^4$  mV.

In both cases, the plots of  $h_s$  against  $h_s V^2$  (method 1) gave fairly good straight lines at low RF voltages but curved away at higher values (Figure 16). The plots of  $h_s^{-1}$  against  $V^2$  (method 2) were not very good straight lines (Figure 17).

The values of  $\gamma^2 a^2 T_1 T_2$ , and  $\gamma^2 a^2$  calculated from  $T_1 = T_2 = 1/\pi \Delta \nu_{1/2}$ , are given for each case in Table 119.

Table 119.  $\gamma^2 a^2 T_1 T_2$  and  $\gamma^2 a^2$  values calculated graphically from saturation studies on cobalt(II)-water solutions.

Molarity Co(II), $\underline{M}$	$\Delta \nu_{1/2}, \underline{Hz}$	$\gamma^2 a^2 T_1 T_2$		$\gamma^2 a^2$	
		Graphical method			
		1	2	1	2
0.05	9.1	$5.87 \times 10^{-9}$	$5.06 \times 10^{-9}$	$4.8 \times 10^{-6}$	$4.1 \times 10^{-6}$
0.04	6.7	$11.4 \times 10^{-9}$	$11.4 \times 10^{-9}$	$5.0 \times 10^{-6}$	$5.0 \times 10^{-6}$

The rather poor linearity of the graphs gives rise to a sizeable error. Taking the average value,  $\gamma^2 a^2 = 4.7 \times 10^{-6}$ . The rather large uncertainty in this figure suggested that it would be inadvisable to use this method to determine absolute  $T_1 T_2$  values. Further, the poor linearity had to be explained.



Figure 16. Plot of  $h_s$  against  $h_s V^2$  for a 0.05M Co(II) solution in  $D_2O$ , using the  $^{81}R10$  instrument.

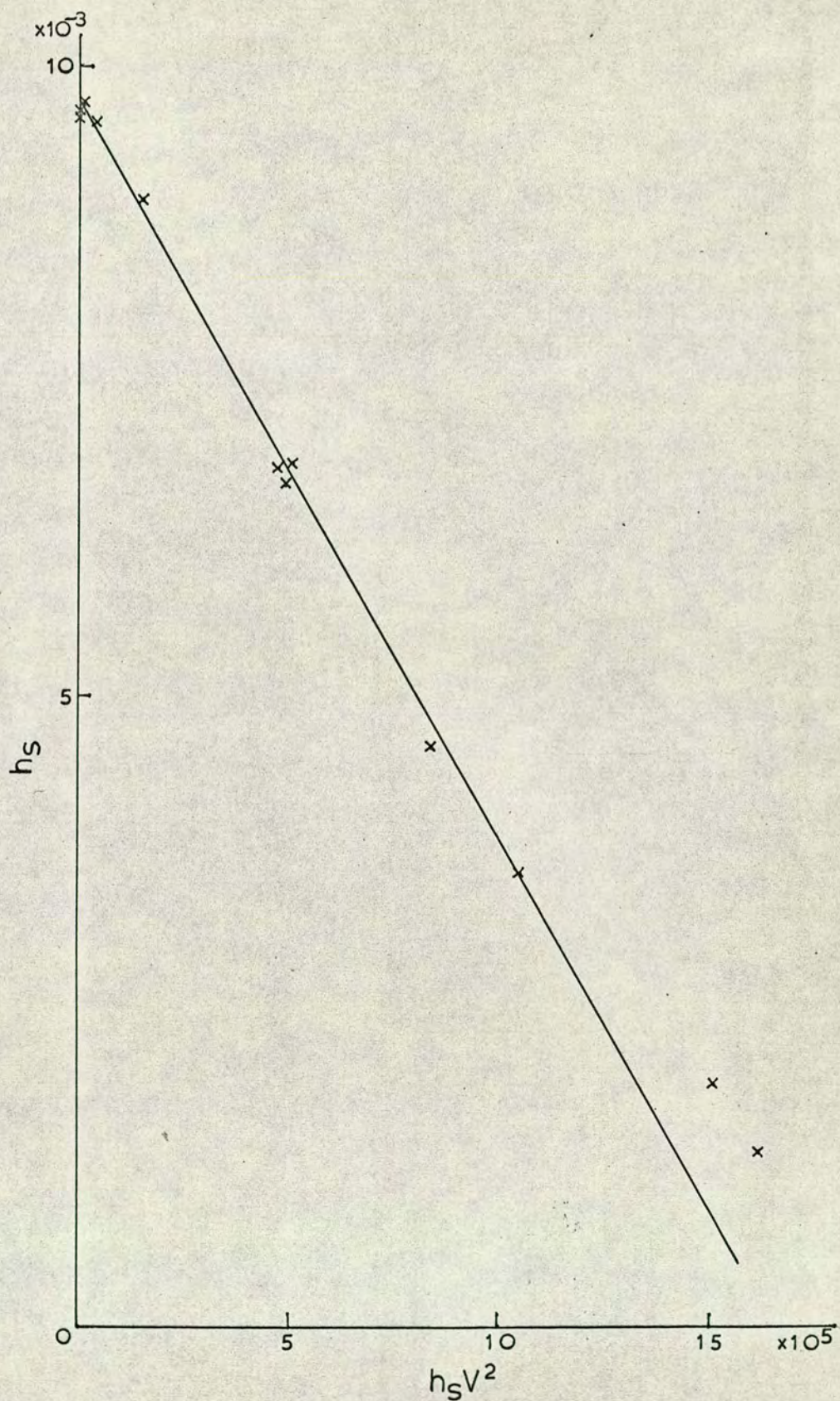
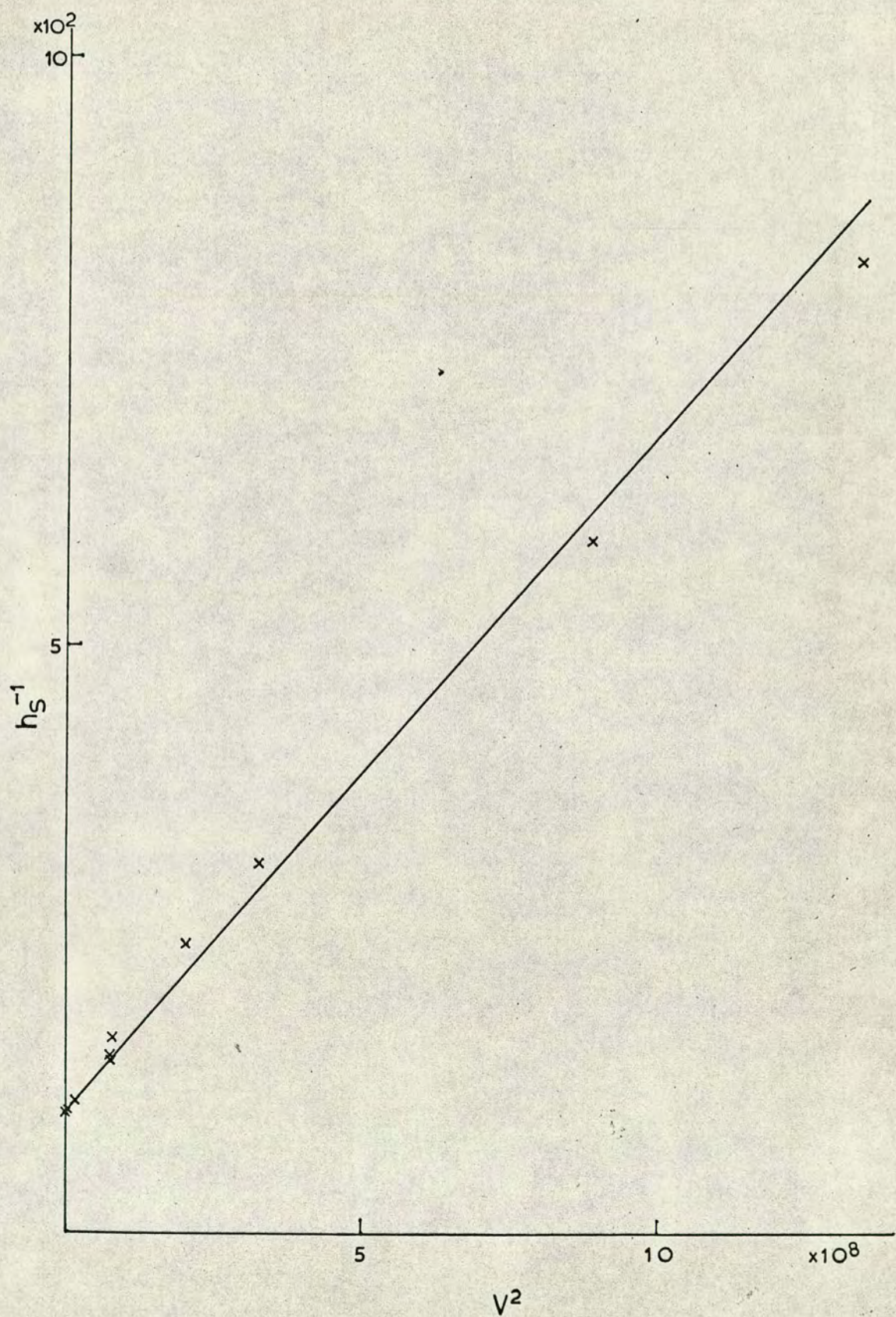




Figure 17. Plot of  $h_s^{-1}$  against  $V^2$  for a 0.05M Co(II) solution in  $D_2O$ , using the R10 instrument.





### Inhomogeneity of the RF field

The non-linearity of the saturation plots could be accounted for by inhomogeneity of the RF field. Such inhomogeneity would not be unexpected for the RLO instrument since the single short coil which is used both as transmitter and receiver is only slightly larger in diameter than the sample tube. In this case, the saturation equation becomes<sup>271</sup>

$$h_s = k \Sigma \frac{f(x,y)h(x,y)}{1 + c^2 V^2 h^2(x,y)} \quad \text{integrated over the whole volume of the sample.}$$

$h(x,y)$  is the shape function of the RF field and varies from 1 at the centre of the coil to near zero at the top and bottom of the sample;  $f(x,y)$  represents the detection efficiency relative to the centre of the coil, where  $f(x,y) = 1$ ;

$c^2 = \gamma^2 a^2 T_1 T_2$ . As there was no simple way of presenting this equation graphically to give meaningful results, alternative methods of evaluating  $T_1 T_2$  were sought.

#### (1) Curve-fitting

Since  $h_s = h/V = f(V,T)$ , if a plot of  $h_s$  against  $V$  is made for one value of  $T$ , then again for a second value of  $T$ , the second curve should be the same shape as the first and, by multiplying  $h_s$  and  $V$  by suitable constants, it should be possible to fit one curve over the other. The constant required for multiplying  $V$  is the ratio of the  $T$  values, since effectively it is correcting only for the change in  $T$  from one case to the other.

This curve-fitting can be conveniently done using plots of  $\log h_s$  against  $\log V$  since the ratio of the  $T$  values is



then given simply by the distance between the two curves in the V direction.

The two cobalt/water solutions studied above gave curves which overlapped very well (Figure 18), giving the ratio of T values as 1.41. This compared quite favourably with the ratio of 1.36 for the  $T_2$  values obtained from the linewidths. This method would thus appear to be satisfactory, giving relative T values, which, by comparison with a standard curve, can be given absolute values.

(2) Value of the RF field which gives maximum peak height

Each of the graphs

(a) h against V

(b) log h against V

(c) log h against log V,

where  $h = h_s V$ , gives a turning-point when  $V = 1/\gamma a T$ .

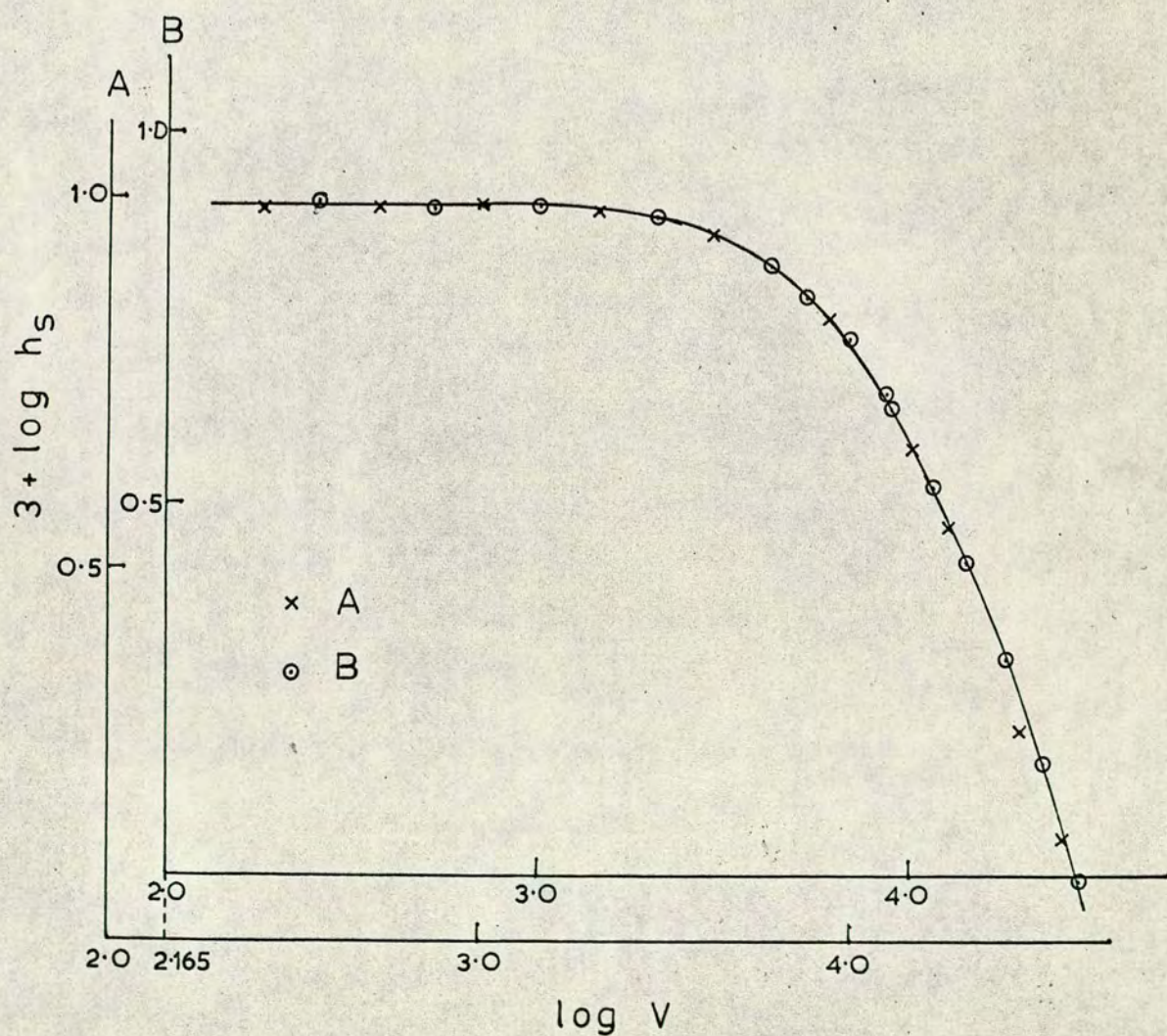
This could give a very convenient method of evaluating relative values of  $T_1 T_2$ , but it was found that in each case the turning point was rather broad and so there was considerable error in evaluating T.

Instrumental calibration using copper solutions

The two cobalt/water solutions gave similar although not identical values for  $\gamma^2 a^2$ , and gave log curves (plots of log  $h_s$  against log V) which overlapped very well allowing relative relaxation times to be evaluated. It seemed advisable to check the value for  $\gamma^2 a^2$  and also to ascertain whether the same log curve shape is applicable to other systems. For this, three copper solutions were investigated. They were



Figure 18. Log curves for 0.05M (A) and 0.04M (B) Co(II) solutions in  $D_2O$ , showing overlap of the curves. (R10 instrument)





12mM, 16mM and 34mM in copper(II) ( $\text{CuSO}_4 \cdot 3\text{H}_2\text{O}$ ), each solution containing 25  $\mu\text{l}$  dilute sulphuric acid and made up to 0.5 ml with  $\text{D}_2\text{O}$ .

The plot of  $h_s$  against  $h_s V^2$  was linear for the 12mM solution but curved at high RF powers for the more concentrated solutions, which were run at higher RF levels.

The values of  $\gamma^2 a^2 T_1 T_2$  and  $\gamma^2 a^2$  calculated assuming  $T_1 = T_2 = 1/\pi \Delta \nu_{1/2}$  are given in Table 120.

Table 120.  $\gamma^2 a^2 T_1 T_2$  and  $\gamma^2 a^2$  values calculated graphically from saturation studies on copper(II)-water solutions.

Molarity Cu(II), mM	$\Delta \nu_{1/2}$ , Hz	$\gamma^2 a^2 T_1 T_2$	$\gamma^2 a^2$
12	4.65	$12.4 \times 10^{-9}$	$2.6 \times 10^{-6}$
16	5.2	$10.2 \times 10^{-9}$	$2.7 \times 10^{-6}$
34	11.0	$1.7 \times 10^{-9}$	$2.0 \times 10^{-6}$

These figures for  $\gamma^2 a^2$ , which are not very concordant, are distinctly different from the values obtained with the cobalt solutions, (ca.  $4.7 \times 10^{-6}$ ).

This would therefore not seem to be a satisfactory method of calibrating the instrument to obtain absolute values for the relaxation times. The poor results may well be due to the non-linear plots arising from inhomogeneity of the RF field. In this case, the log curve method should give more satisfactory results.

The three log curves overlapped well with each other and with the curves from the cobalt solutions. The  $T_2$  ratios



(from linewidths) and the T ratios (from log curves) for the 16mM and 34mM copper solutions relative to the 12mM copper solution are given in Table 121, as are also the ratios for the 12mM copper solution relative to the 0.05M cobalt solution.

Table 121. Ratios of relaxation times for copper solutions with respect to each other and to a cobalt solution.

Solution	Solution for comparison	$T_2$ ratio	T ratio
16mM Cu(II)	12mM Cu(II)	0.90	0.91
34mM Cu(II)	12mM Cu(II)	0.42	0.39
12mM Cu(II)	0.05M Co(II)	1.96	1.55

Although the ratios for the copper solutions relative to each other are in fairly good agreement, the copper solutions do not agree with the cobalt solutions.

A possible reason for the inequality of the ratios is that  $T_1 \neq T_2$  for either Co(II) or Cu(II) or both. Bernheim and coworkers<sup>34</sup> have found that  $T_1 \approx T_2$  for both Cu(II) and Co(II) in aqueous solution. For the former,  $T_1 = T_2$  over a wide temperature range, whereas for Co(II),  $1.0 \leq T_1/T_2 \leq 1.17$ , and at 33°,  $T_1/T_2 = 1.1$ . Cox and Morgan<sup>274</sup> also found  $T_1 \approx T_2$  for temperatures under 300°K for 0.05M copper(II) nitrate solutions, and Nolle and Morgan<sup>35</sup> found that  $T_1 \approx T_2$  for Co(II), independent of frequency. They also found  $T_1 \approx T_2$  for Cu(II) at all frequencies. It would thus appear that for Cu(II),  $T_1 = T_2$  whereas for Co(II) it may vary



slightly, but such that  $1.0 \leq T_1/T_2 \leq 1.17$ .

It seems unlikely therefore that the discrepancy between the copper and cobalt solutions can be ascribed to inequality of  $T_1$  and  $T_2$ . It could be that  $T_2$  has been shortened, for example, by slow exchange. However, all these solutions contained acid which should ensure fast exchange of  $H^+$  or  $D^+$ .

It would be interesting to test the method with another system to see if more satisfactory results can be achieved.

#### Investigation of cobalt-ethanol solutions

Three solutions were investigated, 1%, 5% and 10% in ethanol and 0.1M, 0.1M and 0.2M in cobalt(II)  $[Co(ClO_4)_2 \cdot 6H_2O]$ , respectively, each in  $D_2O$  solvent. The second and third solutions contained a trace of acid.

With these solutions, two of the three signals in each spectrum are multiplets and so the height of any individual peak is augmented by contributions due to overlap. Rather than correct each peak height individually according to the equation given above (Section A), an alternative approach, applicable only to the curve-fitting method, was used. This involved modifying the standard cobalt curve (0.05M Co(II) in  $D_2O$  solution) to give new standard curves which incorporated the additional contributions due to overlap. A separate curve is required for each value of  $J/\Delta\nu_{1/2}$ , where  $\Delta\nu_{1/2}$  is the linewidth in the absence of saturation. Two sets of curves were calculated by computer, one set for a 1:1 doublet or centre peak of a 1:2:1 triplet (identical) and one set for a centre peak of a 1:3:3:1 quartet. Each set covered the



range of ratios  $1.0 \leq J/\Delta\nu_{\frac{1}{2}} \leq 5.0$ . The experimental curves can then be overlapped directly with the appropriate standard curve.

The curve for each of the ethanol signals fitted its appropriate standard curve very well. The value of  $\log V$  which corresponded to  $\log V = 3.00$  in the appropriate standard was noted for each curve.

Since  $V \times T = K$ , where  $K$  is a constant,

$$\text{or } \log V + \log T = \log K$$

and

$$T^2 = T_1 T_2 \quad ; \quad T_2 = 1/\pi \Delta\nu_{\frac{1}{2}}$$

then, if  $T_1 = T_2$ ,

$$\log V = \log \Delta\nu_{\frac{1}{2}} + \log K\pi$$

or, if  $T_1 = cT_2$ , where  $c$  is a constant,  $c \geq 1$ ,

$$\log V = \log \Delta\nu_{\frac{1}{2}} + \log K\pi c^{-\frac{1}{2}}.$$

Thus a plot of  $\log V$  against  $\log \Delta\nu_{\frac{1}{2}}$  will give a straight line, gradient = 1, and intercept =  $\log K\pi c^{-\frac{1}{2}}$ , provided that the ratio of  $T_1:T_2$  remains constant. This method of presenting the results should therefore indicate quite clearly whether  $T_1 = cT_2$  without making any assumptions about the equality of  $T_1$  and  $T_2$  for any one solution.

The  $\log V$  values corresponding to  $\log V = 3.00$  in the standards, and the linewidths for each cobalt/ethanol solution, as well as those previously determined for the cobalt/water and copper/water solutions, are given in Table 122.

The points fall on to two quite distinct lines (Figure 19), both with gradient 1.1, one for all the cobalt values (with intercept 1.92) and the other for the three copper values (with intercept 2.06). This suggests that



Figure 19. Plot of  $\log V$  against  $\log \Delta v_{1/2}$  for copper(II) and cobalt (II) solutions, using the R10 instrument.

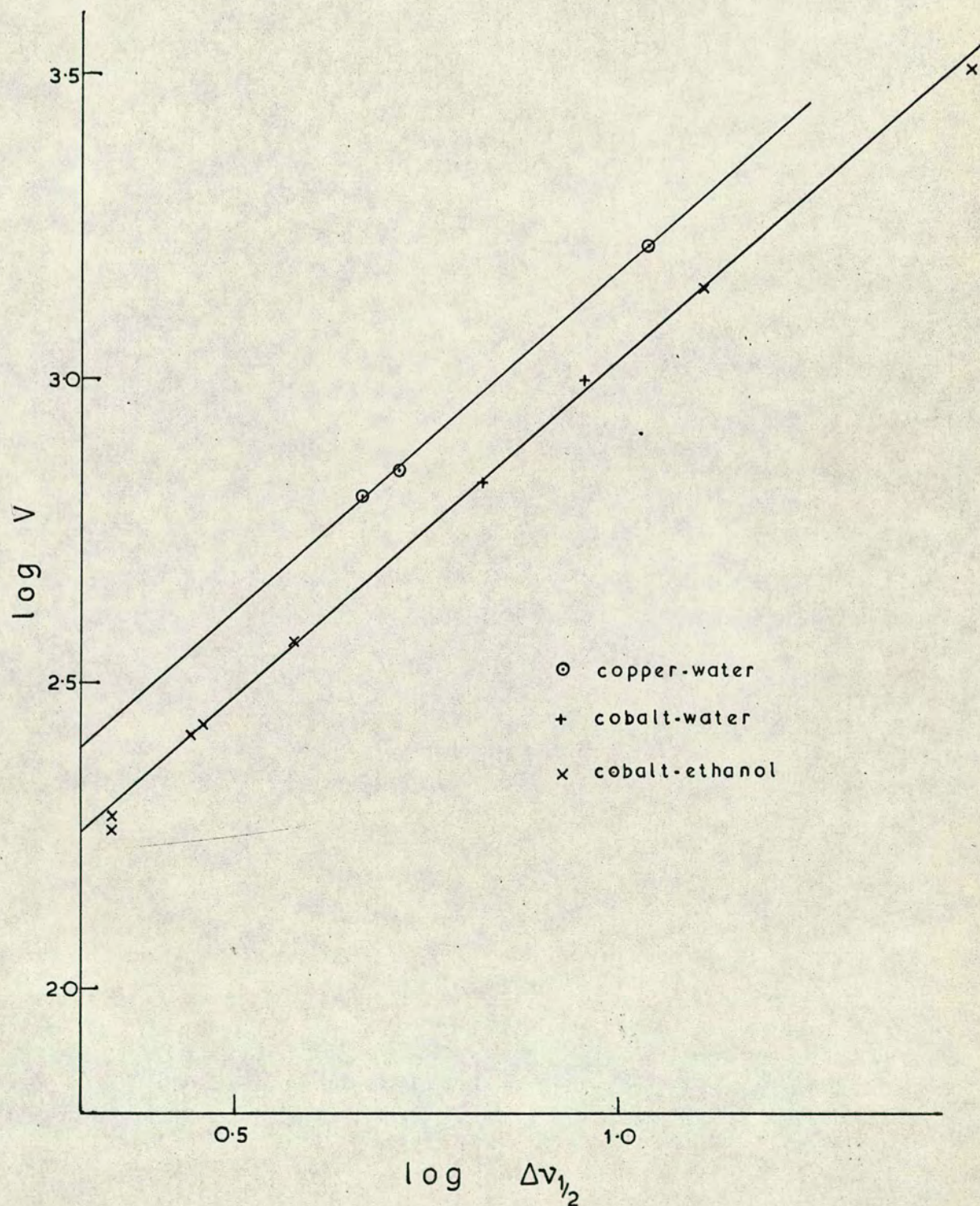




Table 122. Log V values (see text) and linewidths, in Hz, of signals in cobalt(II) and copper(II) solutions used for progressive saturation.

Conc. paramagnetic ion	Ligand	Signal	log V	$\Delta\nu_{\frac{1}{2}}$
0.1M Co(II)	1% EtOH	CH <sub>2</sub>	2.43	2.9
		CH <sub>3</sub>	2.26	2.3
0.1M Co(II)	5% EtOH	OH	3.15	13.0
		CH <sub>2</sub>	2.415	2.8
		CH <sub>3</sub>	2.28	2.2
0.2M Co(II)	10% EtOH	OH	3.51	29
		CH <sub>2</sub>	2.745	<u>ca.</u> 5
		CH <sub>3</sub>	2.57	3.8
0.05M Co(II)	H <sub>2</sub> O	H <sub>2</sub> O	3.00	9.1
0.04M Co(II)	H <sub>2</sub> O	H <sub>2</sub> O	2.86	6.7
12mM Cu(II)	H <sub>2</sub> O	H <sub>2</sub> O	2.81	4.65
16mM Cu(II)	H <sub>2</sub> O	H <sub>2</sub> O	2.85	5.2
34mM Cu(II)	H <sub>2</sub> O	H <sub>2</sub> O	3.22	11.0

for each ion the  $T_1/T_2$  ratio is constant. From the intercepts,

$$\log c_{\text{Co}}^{\frac{1}{2}} - \log c_{\text{Cu}}^{\frac{1}{2}} = 2.06 - 1.92 = 0.14,$$

$$\text{thus } c_{\text{Co}} = 1.9 c_{\text{Cu}}.$$

If  $T_1 = T_2$  for copper, then  $T_1 = 1.9 T_2$  for cobalt which, according to the literature (see above), is unacceptably large. The high ratio is almost certainly not due to slow exchange of  $\text{H}^+$  or  $\text{D}^+$ , as the one solution which contained no acid (0.1M Co(II) with 1% EtOH) gave values lying on the cobalt line.



Slow ligand exchange also seems unlikely since both ethanol and water solutions with cobalt gave values lying on one line whereas identical exchange rates would be improbable. The fact that the gradient was 1.1 rather than 1.0 in both cases should also be noted.

### (c) Conclusion

This progressive saturation method allows comparison of T values to be made for both singlet and multiplet signals. However, absolute values of T could not be calculated due to the difficulties encountered in calibrating the instrument. Although the curve-fitting procedure was convenient and seemed to overcome the problem caused by inhomogeneity, it led to incompatible results with regard to the  $T_1/T_2$  ratios of the solutions examined.

It was therefore decided to investigate progressive saturation on the HA 100 instrument in the hope that it would have a homogeneous RF field and so eliminate that possible source of error from the calculations.

## (D) PROGRESSIVE SATURATION USING THE HA 100 INSTRUMENT

### (a) Instrumental conditions and accuracy checks

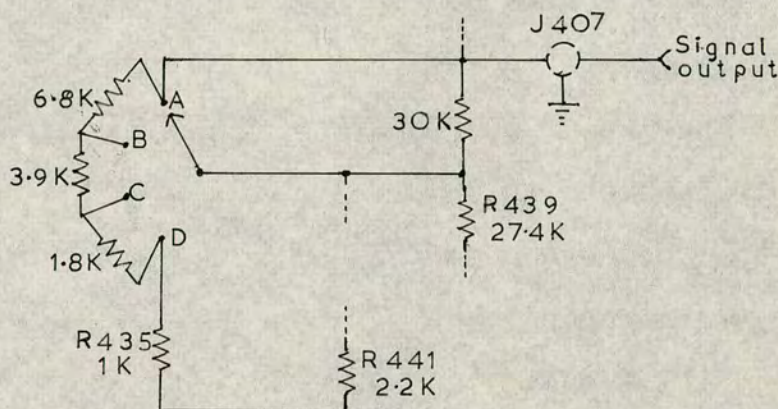
#### (i) Linearity of the recorder

This was checked in a similar way to that on the R10 instrument, the signal being generated this time by offsetting the amplifier balance with the Function switch at "Integral". The voltage, measured with a DVM plugged into the signal output (J407), proved proportion<sup>al</sup> to the signal height on the recorder to within 1%, which was considered quite satisfactory.



(ii) Output control

It was not possible to set the continuous fine output control with great accuracy and so work was initially carried out with the fine control at its maximum (1.0) and the coarse control at 0.1 (Tables 124-126). This proved very restricting. A new, step-wise fine control was then designed and fitted.



The controls were calibrated by generating and measuring a voltage as above. The calibrated values, which in some cases differed considerably from the nominal values, are given in Table 123.

(iii) Radiofrequency field

There are two ways of increasing the RF power:

- (1) by decreasing the RF attenuation
- (2) by increasing the modulation.

Although the former also increases the lock power, it was considered to be the preferable method as the RF attenuation buttons are easier to set reproducibly and to calibrate than the continuous modulation control.

As with the R10 instrument, a 0.3M copper sulphate



Table 123. Calibrated and nominal values for the fine and coarse output controls of the HA 100 instrument.

Nominal value		Calibrated value	
Coarse	Fine		
1.0	1.00 (A)	1.31	= 1.0 x 1.31
	0.498(B)	0.499	= 1.0 x 0.499
	0.245(C)	0.267	= 1.0 x 0.267
	0.0986 (D)	0.119	= 1.0 x 0.119
0.1	1.00	0.100	= 0.1 x 1.0*
	0.498	0.0499	= 0.1 x 0.499
	0.245	0.0247	= 0.1 x 0.247
	0.0986	0.00984	= 0.1 x 0.0984
0.01	1.00	0.01266	= 0.01266 x 1.0
	0.498	0.00630	= 0.01266 x 0.498
	0.245	0.00311	= 0.01266 x 0.246
	0.0986	0.00123	= 0.01266 x 0.0972

\* standard.

solution in water was used. However, a lock signal was required for this instrument, and, because the solution was fairly strongly paramagnetic, it was decided that an external lock, contained in a capillary tube (Wilmad precision co-axial capillary, outer diam.:0.08 ins, inner diam.: 0.05 ins.), would be desirable, giving a sharper signal. Acetone would appear to be suitable for a lock signal, but pure acetone was not usable as the difference in magnetic susceptibility between it and the paramagnetic solution gave rise to strong side-bands which gave the broad water peak the appearance of a broadened triplet. It has been shown that when spinning is stopped, the signal from a cylindrical annulus of liquid around a



central capillary consists of two absorption bands whose separation in Hz is given by <sup>275</sup>

$$n = 4\pi\nu_0 \left[ (\chi_1 - \chi_2) \left( \frac{a}{r} \right)^2 + (\chi_2 - \chi_3) \left( \frac{b}{r} \right)^2 \right]$$

where  $\nu_0$  is the fixed radiofrequency,  $a$  and  $b$  are the internal and external radii of the inner glass tube,  $r$  is the radius of the annulus and  $\chi_1$ ,  $\chi_2$  and  $\chi_3$  are the volume susceptibilities of the liquid in the inner tube, the glass, and the annular liquid respectively. Changing the susceptibility of the liquid in the inner tube will change the separation of the two signals.

In the present work, the two bands for the water signal from the outer annulus (spinning stopped) appeared as one very broad singlet. Addition of cobalt,  $\text{CoCl}_2 \cdot 6\text{H}_2\text{O}$ , to the acetone decreased the linewidth, the narrowest value being achieved with 21mg  $\text{CoCl}_2 \cdot 6\text{H}_2\text{O}$  per ml acetone. With the sample spinning, this change in susceptibility of the liquid in the inner tube also decreased the side-bands until a single peak of linewidth 80Hz was achieved with the above solution. An identical copper sulphate solution using an internal acetone lock in the normal way gave a water linewidth of 90 Hz.

The RF attenuator buttons were then calibrated in a similar manner to the calibration of the  $H_1$  control on the R10 instrument, and were found to be accurate to within 1.5%.

Although it seemed likely that most work would be carried out with the RF modulation at a maximum (i.e. at 1.0 mG), it was thought advisable to know accurately the ratio 1.0:0.1 on the coarse modulation control. The ratio was found, by the same method, to be 1.0:0.097.



(iv) Peak height measurement

Since the HA 100 instrument uses a locking system, thus eliminating signal drift, it should be possible to "sit" on the top of a peak to measure the stationary peak height. While this has the advantage of being far less tedious and probably more accurate, there is the disadvantage that the signal shape and position are not seen throughout the measurements. Various possible sources of error had to be checked.

The peak could move during the measurements if its chemical shift with respect to the lock showed any alteration. This was found to be the case with the water peak, due to change in temperature of the solution. Care was thus taken that the sample was at thermal equilibrium before measurements were made.

The phase could be wrong, but accurate initial phasing at a fairly high RF power seemed to give good phasing at all powers except the very highest.

The base-line was found by switching the frequency offset from 1500 (position for peak observation) to 2500. (It was possible to do this as the work was being carried out on field sweep, as indeed was almost all the work on the instrument, frequency sweep only being used for spin-decoupling work and occasionally for shift measurements where it proved convenient). This "base-line" was found to be slightly lower than the normal base-line, but the latter gradually approached the "2500 base-line" on moving further from the peak and so the "2500 base-line" is probably the more accurate, provided there is not a peak at "2500".



That equilibrium is attained very quickly was checked by measuring the peak height very quickly on switching the frequency offset from 2500 to 1500, then after about 30 seconds measuring it again. It was identical on every occasion.

In every saturation series, the entire signal was drawn out both at fairly low RF levels (for linewidth measurement) and at fairly high RF levels (for accurate phasing), thus providing a check that nothing unexpected (e.g. peak overlap) was occurring.

The method of "spotting" peak maxima and base-line thus appeared quite satisfactory, and the average of two values was taken each time.

#### (v) Effect of leakage

The leakage was always set at a minimum using a high RF power. The peak heights were found to be considerably dependent on the leakage, and, since the leakage increased with increasing RF power, this may introduce a considerable source of error. Investigation of this by carrying out several saturation series using different leakage values gave inconclusive results, suggesting that perhaps other factors, such as movement of the probe which is not fully supported or varying resolution, may also contribute comparable errors. It was hoped that, by careful minimisation of the leakage before starting a series, the error would be kept as small as possible.



(vi) Resolution

The resolution of the instrument was always optimised before starting a saturation series. Shimming was carried out manually and, provided a series was executed reasonably rapidly, it was found to maintain quite adequately.

After a considerable amount of this saturation work had been done, it was found that the magnet homogeneity was very poor, the sharp signals overlying broad humps. This was found to be due to the pole caps of the magnet being the wrong distance apart and was corrected by altering the shim plates behind the pole pieces. The resolution was dramatically improved. However, this caused very little change in the results obtained.

(b) Instrumental calibration to evaluate absolute values of  $T_1 T_2$ 

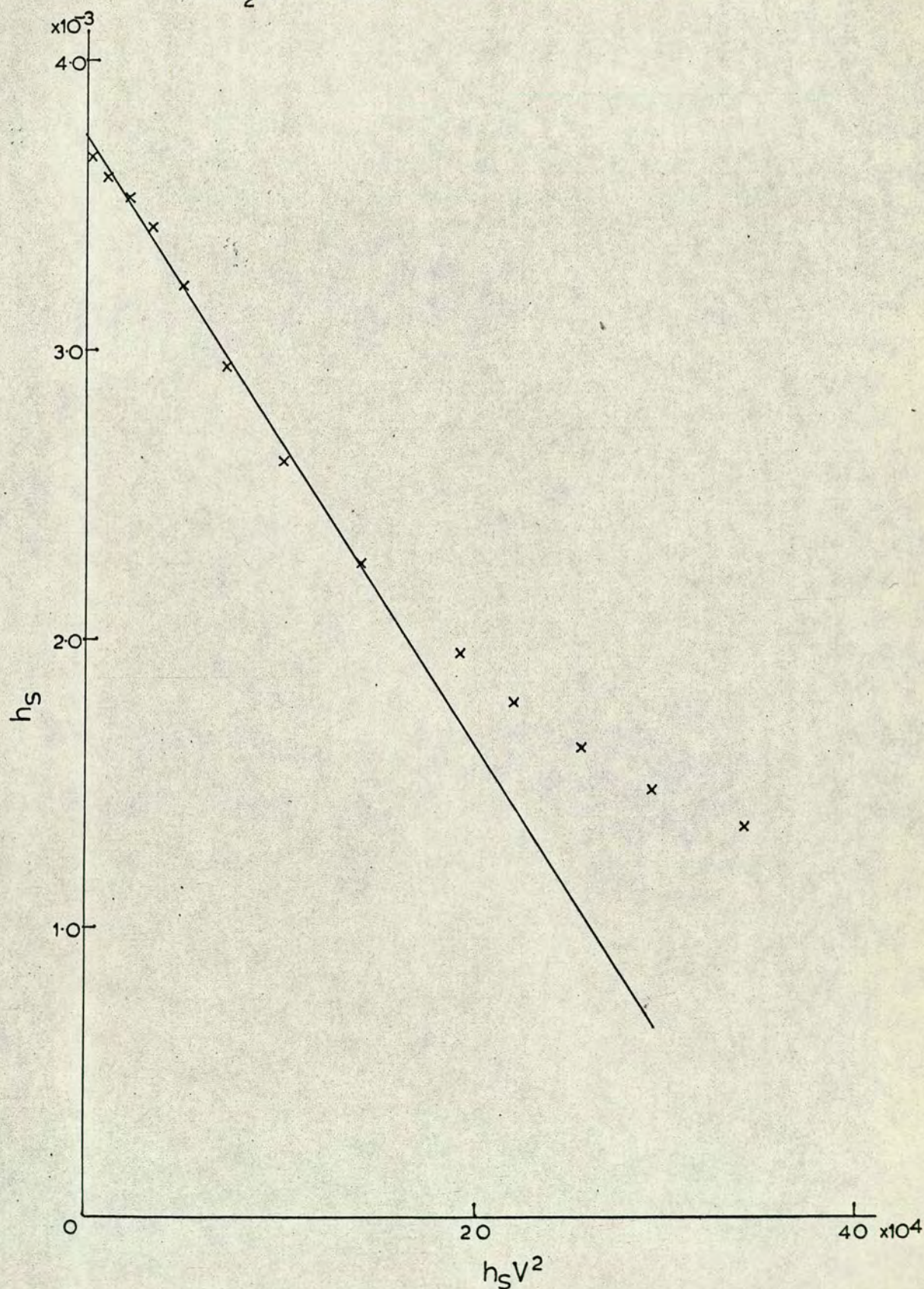
Since it would appear that the equality of  $T_1$  and  $T_2$  is more certain for copper than for cobalt, copper solutions were investigated with a view to calibration of the instrument. Two solutions, 16mM and 32mM in copper(II)  $[\text{CuSO}_4 \cdot 5\text{H}_2\text{O}]$ , with 25  $\mu\text{l}$  dilute sulphuric acid and 25  $\mu\text{l}$  acetone (for lock), each made up to 0.5 ml with  $\text{D}_2\text{O}$ , were used, RF powers from 40dB to 14dB (modulation 1.0 mG) being used.

The plots of  $h_s$  against  $h_s V^2$  (Figure 20) were reasonably linear except for RF powers greater than 20dB (16 mM solution) or 16dB (32mM solution). Values of  $\gamma^2 a^2 T_1 T_2$  were taken from the linear portion of the plots.

The values for  $\gamma^2 a^2 T_1 T_2$  and  $\gamma^2 a^2$ , assuming  $T_1 = T_2 = 1/\pi \Delta \nu_{\frac{1}{2}}$  are given in Table 124.



Figure 20. Plot of  $h_s$  against  $h_s V^2$  for a 16mM Cu(II) solution in  $D_2O$ , using the HA 100 instrument.





N.B. "a" would be expected to have a different value here from that on the R10 instrument.

Table 124.  $\gamma^2 a^2 T_1 T_2$  and  $\gamma^2 a^2$  values calculated graphically from saturation studies on copper(II)-water solutions.

Molarity Cu(II), mM	$\Delta v_{\frac{1}{2}}, \text{Hz}$	$\gamma^2 a^2 T_1 T_2$	$\gamma^2 a^2$
16	5.4	$1.05 \times 10^{-8}$	$3.03 \times 10^{-6}$
32	9.7	$0.32 \times 10^{-8}$	$2.98 \times 10^{-6}$

Although the values for  $\gamma^2 a^2$  are remarkably concordant, it would be advisable to substantiate them using a second system, for example a cobalt-water system.

#### Instrumental calibration using cobalt-water solutions

Two solutions, prepared identically to the copper solutions above, except containing 16mM and 30mM cobalt(II)  $[\text{Co}(\text{ClO}_4)_2 \cdot 6\text{H}_2\text{O}]$  instead of copper(II), were investigated.

The plots of  $h_s$  against  $h_s V^2$  again were linear except for the highest RF powers, and the gradient of the linear portion gave the  $\gamma^2 a^2 T_1 T_2$  values shown in Table 125.

Table 125.  $\gamma^2 a^2 T_1 T_2$  and  $\gamma^2 a^2$  values calculated graphically from saturation studies on cobalt(II)-water solutions.

Molarity Co(II), mM	$\Delta v_{\frac{1}{2}}, \text{Hz}$	$\gamma^2 a^2 T_1 T_2$	$\gamma^2 a^2$
16	3.9	$2.25 \times 10^{-8}$	$3.38 \times 10^{-6}$
30	6.35	$1.01 \times 10^{-8}$	$4.02 \times 10^{-6}$



The values for  $\gamma^2 a^2$  are not very concordant and, as was found for the R10 instrument, are greater than those for the copper solutions.

### Curve-fitting

Rather than form a standard curve from an arbitrarily chosen solution, it was decided to compare the log-curves for these four solutions with a theoretical standard curve, that is a log-curve given by

$$h_s = \frac{1}{a(1 + bV^2)} .$$

The log-curve given by  $h_s = \frac{1}{100(1 + 10^{-6}V^2)}$  was found to be suitable. As this theoretical curve assumes a homogeneous RF field, the experimental curves will not fit it if there is significant inhomogeneity.

All four curves did fit the theoretical plot very well for lower RF powers, but the points which deviated from linearity in the plots of  $h_s$  against  $h_s V^2$  also deviated from the curve (see Figure 21).

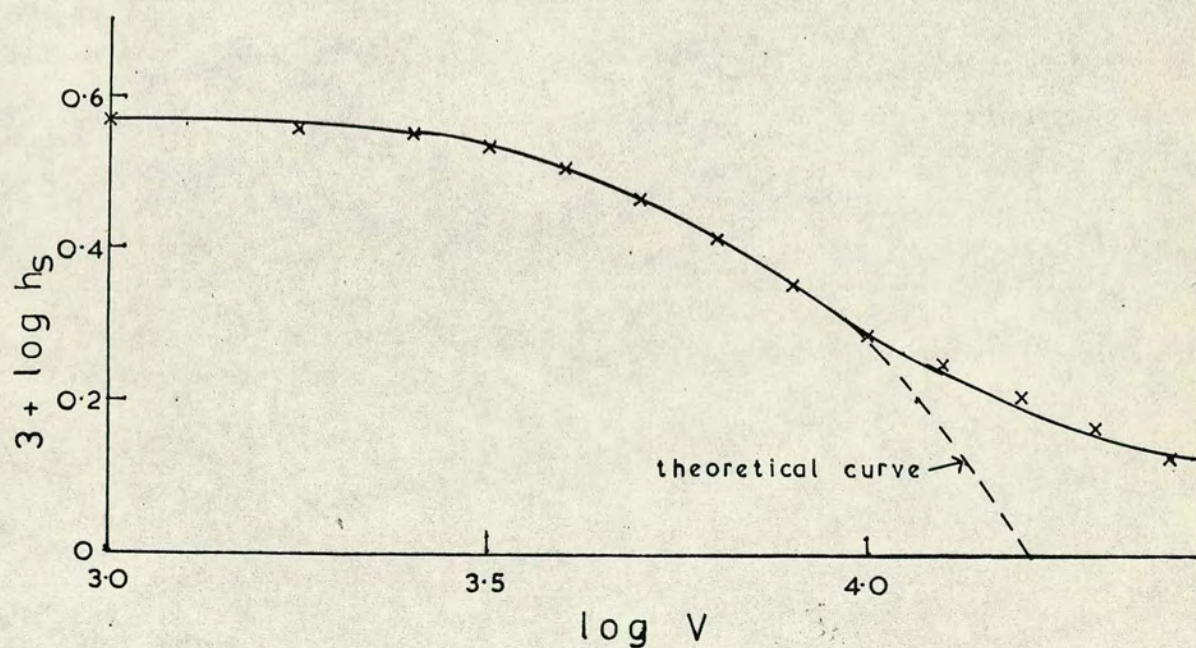
The log V values for these experimental curves corresponding to  $\log V = 3.00$  of the theoretical curve are given in Table 126.

Table 126. Log V values (see text) and linewidths, in Hz, of signals in copper(II) and cobalt(II) water solutions used for progressive saturation.

Paramagnetic ion	Molarity, mM	log V	$\Delta\nu_{1/2}$
Cu(II)	16	4.01	5.4
Cu(II)	32	4.26	9.7
Co(II)	16	3.82	3.9
Co(II)	30	4.01	6.35



Figure 21. Log curve for a 16mM Cu(II) solution in D<sub>2</sub>O,  
showing deviation from the theoretical curve.  
(HA 100 instrument)





The plot of  $\log V$  against  $\log \Delta\nu_{\frac{1}{2}}$  showed that the copper and cobalt points did not fit on one straight line. As there were only two points for each ion, best straight lines were drawn through each pair of points assuming a gradient of unity. The intercept,  $\log K\pi c^{-\frac{1}{2}}$ , for the copper line was 3.28 and for the cobalt line 3.22, from which, assuming  $T_1 = T_2$  for copper,  $T_1 = 1.15 T_2$  for cobalt which is theoretically possible.

However, these results were far from satisfactory. The anticipated improvement on changing to the HA 100 instrument has not been realised. The graphs still deviate substantially from theoretical, and other problems, such as irreproducible peak heights and errors due to the effect of the leakage, have been introduced. The only real advantage appeared to be the less tedious procedure involved in "sitting" on peak maxima rather than slow scanning.

It was at this inconclusive stage that the magnetic homogeneity was improved. It also appeared<sup>276</sup> that radiation damping<sup>277</sup> might be playing a considerable part in these results. Radiation damping arises from coupling between the spin system and its own radiated field and causes a reduction in the effective quality factor for the receiver coil. Since the effect is negligible away from the signal resonance and strongest at the signal maximum, it broadens and lowers the observed signal. It depends on the concentration of nuclei in the sample and so can be reduced by diluting the sample or using a smaller sample volume.



To test the contribution made by these two factors, four further copper solutions were investigated, two with comparable peak heights to those in the solutions previously investigated and two with smaller peak heights. The solutions were 8mM, 4mM, 4mM and 10mM in copper(II) and contained 9  $\mu$ l, 10  $\mu$ l, 5  $\mu$ l and 8.6  $\mu$ l dilute sulphuric acid (conc.  $\text{H}_2\text{SO}_4$  in distilled  $\text{H}_2\text{O}$ ), respectively, each solution having 25  $\mu$ l acetone and made up to 0.5 ml with  $\text{D}_2\text{O}$ .

The plot of  $h_s$  against  $h_s V^2$  for the first solution was again only linear for the lower RF powers, showing that the non-linearity was not due to poor magnetic field homogeneity. The second solution also gave a poor plot. The third and fourth solutions (with smaller peak heights though not necessarily smaller peak areas) both gave good plots (see Figure 22). It would thus appear that radiation damping may well be the cause of the non-linearity.

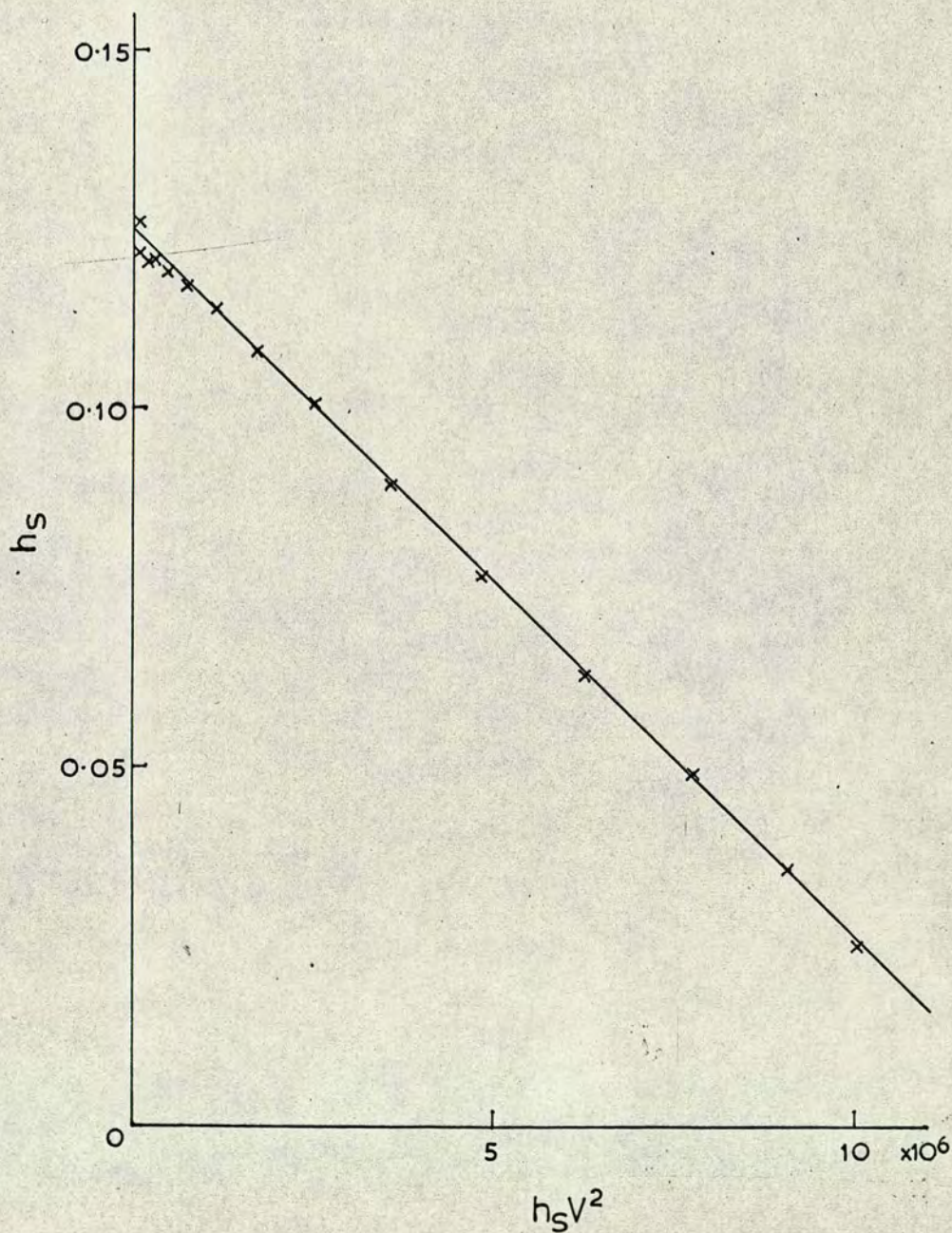
The  $\gamma^2 a^2 T_1 T_2$  values, calculated from the gradients of the plots of  $h_s$  against  $h_s V^2$ , and  $\gamma^2 a^2$  values, assuming  $T_1 = T_2$ , are given in Table 127.

Table 127.  $\gamma^2 a^2 T_1 T_2$  and  $\gamma^2 a^2$  values calculated graphically from saturation studies on copper(II)-water solutions.

Molarity Cu(II), <u>mM</u>	$\mu$ l $\text{H}_2\text{O}$	$\Delta\nu_{\frac{1}{2}}$ , <u>Hz</u>	$\gamma^2 a^2 T_1 T_2$	$\gamma^2 a^2$
8	9	3.0	$0.7 \times 10^{-8}$	$0.62 \times 10^{-6}$
4	10	1.95	$2.4 \times 10^{-8}$	$0.90 \times 10^{-6}$
4	5	2.10	$1.0 \times 10^{-8}$	$0.44 \times 10^{-6}$
10	8.6	3.8	$0.40 \times 10^{-8}$	$0.57 \times 10^{-6}$



Figure 22. Plot of  $h_s$  against  $h_s V^2$  for a 4mM Cu(II) solution in  $D_2O$ , using the HA 100 instrument. Lower intensity peak.





The value of "a" has again changed. The reason for this is not known. It was assumed that during the changes to the magnet and the major servicing which followed the RF level from the RF unit or the modulation level had in some way been altered.

The  $\gamma^2 a^2$  values show poor concordancy, even within those which gave good linear plots, and calibration is certainly not possible from these figures.

It seemed of interest to see how well the log-curves now fitted the theoretical curve, and whether they indicated a constant  $T_1/T_2$  ratio.

The first solution gave a log-curve which fitted the theoretical curve better than the previous solutions had done, but still deviated significantly. The curve for the second solution was a poor fit, but the other two gave very good fits, as would be expected from the linearity of the above plots.

The log V values corresponding to  $\log V = 3.00$  in the theoretical curve are given in Table 128.

Table 128. log V values and linewidths, in Hz, of signals in copper(II)-water solutions used for progressive saturation.

Molarity Cu(II), mM	$\mu\text{l H}_2\text{O}$	log V	$\Delta v_{1/2}$ , Hz
8	9	4.09	3.0
4	10	3.80	1.95
4	5	4.00	2.10
10	8.6	4.19	3.8



The plot of  $\log V$  against  $\log \Delta v_{\frac{1}{2}}$  was not linear, nor did a line with gradient unity pass through the two points for the curves which gave good overlap with the theoretical curve.

Thus, although reduction of the signal intensity has produced linear plots of  $h_s$  against  $h_s V^2$  and theoretical-shaped log-curves, it has not made calibration of the instrument with any accuracy any more possible, nor allowed confirmation of the equality of  $T_1$  and  $T_2$ .

(c) Measurement of the radiofrequency field by Torrey oscillations

Since it was not possible to calibrate the instrument using a standard solution, an alternative method was sought, the Torrey oscillation method of Leigh<sup>278</sup>. A sample of 10  $\mu$ l AnalaR chloroform in 0.5 ml deuteriochloroform with 3% TMS was used, providing a sharp chloroform signal. With the pen "sitting" on top of this peak, the modulation was rapidly switched from 0 mG to 1.0 mG, causing the pen to oscillate. The speed of oscillation depended on the RF power (attenuation) and was measured using a fast writing ultra-violet recorder (Honeywell 2106) plugged into the signal output. The chart speed of the recorder was determined simultaneously using a known frequency generated by a Muirhead oscillator and applied to the second channel of the recorder. The oscillations were measured for various RF powers.

The oscillation frequency,  $\Omega$  ( $\text{rad s}^{-1}$ ), is given by  $\Omega = \gamma H_1 c$  which, if  $\gamma H_1 > 10 \text{ rad s}^{-1}$  and  $T_2 > 1 \text{ s}$ , becomes  $\Omega = \gamma H_1$  with an error of less than  $\frac{1}{2}\%$ .  $\gamma = 26.75 \text{ rad s}^{-1} \text{ mG}^{-1}$ .



In this work,  $H_1 = aV$ , where  $V$  is the RF reading on the instrument (arbitrarily taken as  $1.0 \times 10^3$  units at 40dB attenuation and 1.0 mG modulation). Thus  $\Omega = \gamma a V$ . A plot of  $\Omega$  against  $V$  will therefore have a gradient  $\gamma a$ .

The plot was fairly linear (Figure 23) and gave  $\gamma a = 3.63 \times 10^{-4}$ .

The oscillations were also measured with two further solutions, one  $D_2O$  and the other  $D_2O$  with trace acid, both using acetone for lock signal and making measurements on the HOD signal. The plot of  $\Omega$  against  $V$  for the former was not very linear, the average gradient giving  $\gamma a = 4.3 \times 10^{-4}$ . The latter solution gave a good straight line yielding  $\gamma a = 3.77 \times 10^{-4}$ . These values suggest that the solvent has a small effect on the value of the RF field.

Changing the sweep offset was also investigated but this did not change the field significantly.

The absolute value of the RF field,  $H_1$ , can be calculated from

$$H_1 = aV = \frac{\gamma a \cdot V}{\gamma}$$

For the chloroform solution, at 0dB attenuation and 1.0 mG modulation ( $V = 1.0 \times 10^5$  units),

$$H_1 = \frac{3.6 \times 10^{-4} \times 1.0 \times 10^5}{26.75} \text{ mG}$$

$$= 1.35 \text{ mG} \quad (\text{nominal value } 1.0 \text{ mG})$$

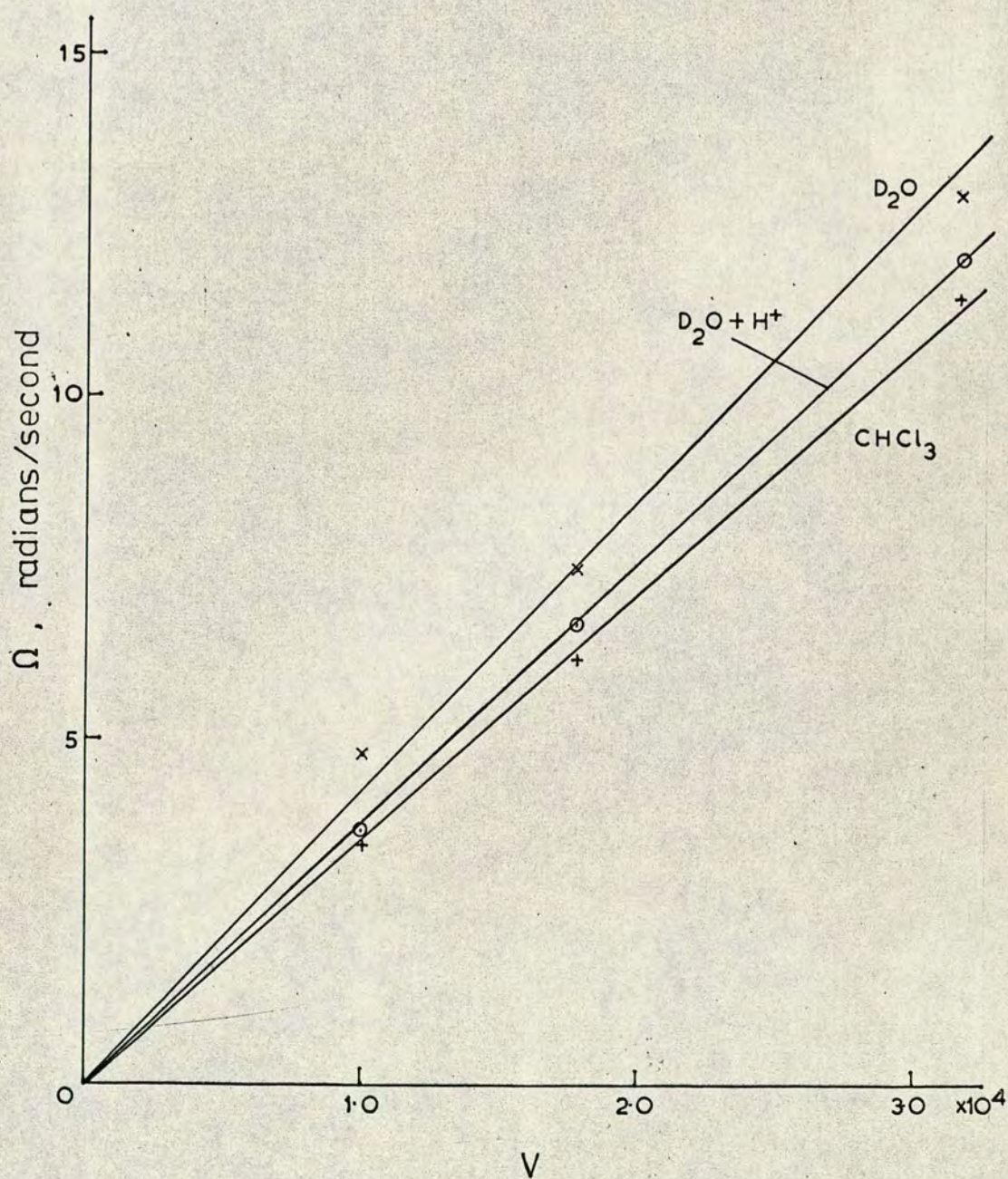
For the  $D_2O$  solution with trace acid,

$$H_1 = 1.42 \text{ mG} \quad (\text{nominal value } 1.0 \text{ mG}).$$

The absolute value of the RF field determined in this way was then used to calculate the magnitude of  $T_1 T_2$  as given by progressive saturation and this value was then compared



Figure 23. Plot of oscillation frequency against nominal RF field for evaluation of  $H_1$  by the method of Torrey oscillations.





with the value of  $T_2$  from the linewidth.

A solution 12mM in copper(II) with 10  $\mu$ l water (dilute sulphuric acid) and 25  $\mu$ l acetone made up to 0.5 ml with  $D_2O$  was progressively saturated. The plot of  $h_s$  against  $h_s v^2$  was linear giving  $\gamma^2 a^2 T_1 T_2 = 0.59 \times 10^{-8}$ . The appropriate value of  $\gamma a$  obtained by Torrey oscillations is  $\gamma a = 3.77 \times 10^{-4}$ , which gives  $T_1 T_2 = 0.041 \text{ s}^2$ .  $T_2$  measured from the linewidth is 0.084s, giving  $T_1/T_2 = 5.8$  which is unacceptably large.

Thus, although this method of measurement of  $H_1$  is fairly simple to execute, the results do not clarify the situation.

(d) Progressive saturation of the integral

Although Geet and Hume<sup>271</sup> found that saturation of the integral was a less satisfactory method of determining relaxation times, it may be that for multiplet signals it is more satisfactory than the peak height method as error due to overlap is avoided, the whole signal being accumulated by the integral.

The integral is proportional to  $Z^{\frac{1}{2}}$ <sup>271</sup> where  $Z$  is the saturation factor,

$$\text{i.e. } I = kZ^{\frac{1}{2}}H_1$$

$$\text{or } I_s = \frac{I}{V} = k' \frac{1}{(1 + \gamma^2 a^2 v^2 T_1 T_2)^{\frac{1}{2}}}$$

Thus a plot of  $I_s^2$  against  $I_s^2 v^2$  will have gradient  $-\gamma^2 a^2 T_1 T_2$ .

It is not possible to achieve stationary conditions while collecting an integral. Geet and Hume found that



accumulating the integral at a rate of 0.1 c.p.s. per second was sufficiently slow for relaxation times less than 1.3 second. Thus, at sweep width 100Hz, a sweep speed of 1000 seconds should be sufficiently slow for all paramagnetically broadened signals, but slower speeds may be required in diamagnetic solutions. In fact a speed of 1000 sec was found to be too fast for a diamagnetic solution of acetyl ferrocene, a slower speed (2500 s) causing a noticeable decrease in the measured integrals, particularly in the sharp singlet peak of the unsubstituted ring protons.

At these very slow sweep speeds, considerable errors may be introduced if the amplitude balance is not very carefully "zeroed" to eliminate base-line drift. Also accurate phasing of the signals is critical. The very slow sweep speeds also resulted in integral magnitudes too great for the instrument, even with very low intensity signals. A capacitor was inserted parallel to the integrator capacitor, which allowed about twenty times the integral to be gathered.

A solution of 0.2M acetyl ferrocene in deuteroacetone was progressively saturated, peak height and integral measurements being made for the two triplets of substituted ring protons.

The plots of  $h_s$  against  $h_s V^2$  were curved for both triplets, even when corrected for peak overlap.

The  $I_s^2$  v.  $I_s^2 V^2$  plots (Figure 24) were fairly linear for lower RF powers but curved downwards at higher values.

The  $\gamma^2 a^2 T_1 T_2$  values calculated from the "gradients" are given in Table 129.



Figure 24. Saturation of the integral. Plot of  $I_s^2$  against  $I_s^2 V^2$  for the 2,5- and 3,4-ring proton triplets of acetyl ferrocene, using the HA 100 instrument.

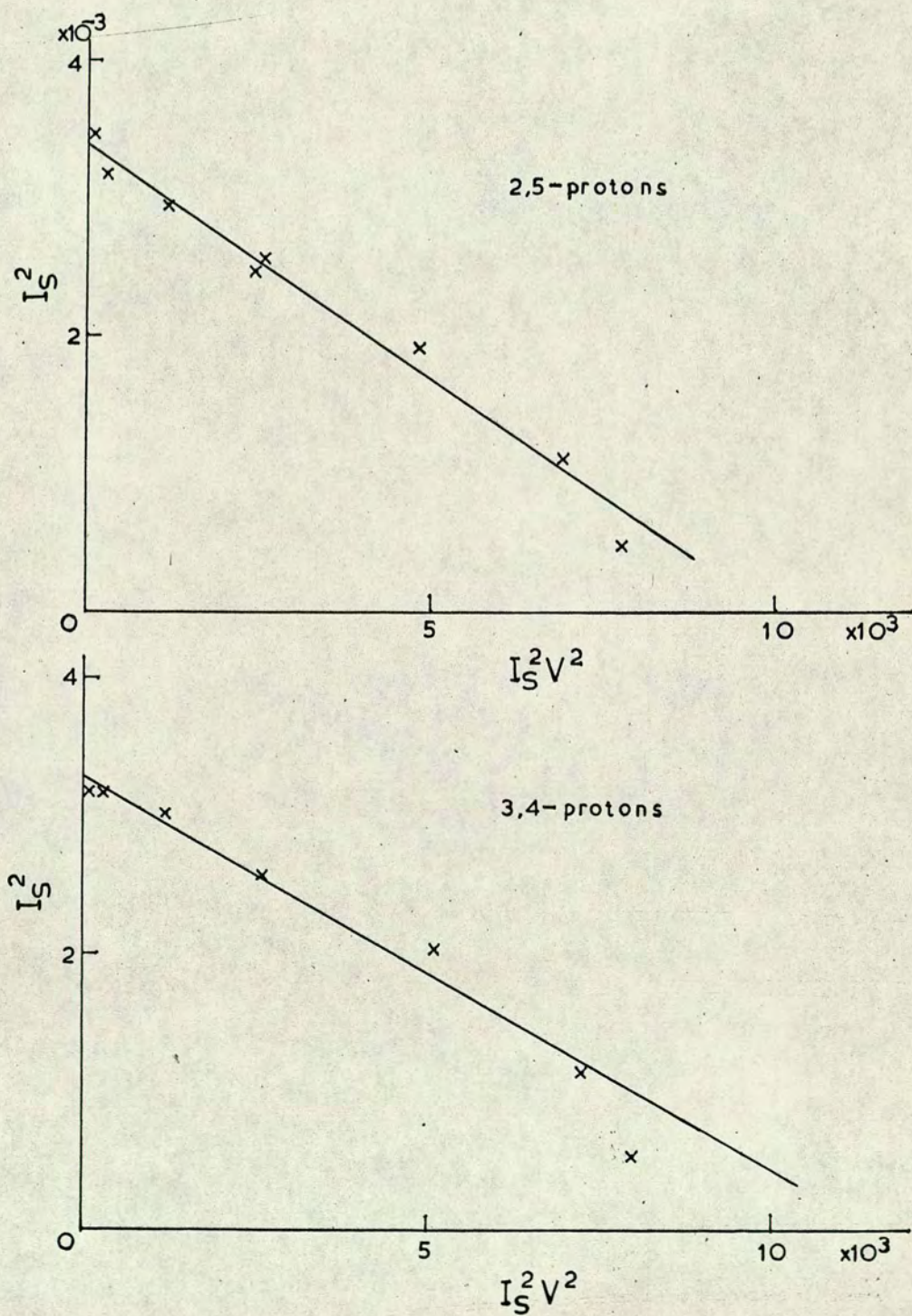




Table 129.  $\gamma^2 a^2 T_1 T_2$  values calculated graphically from saturation studies on acetyl ferrocene. Comparison of peak height and integral methods.

Method	$\gamma^2 a^2 T_1 T_2$ value	
	Triplet (1)	Triplet (2)
Peak height	$0.53 \times 10^{-6}$	$0.39 \times 10^{-6}$
Integral	$0.32 \times 10^{-6}$	$0.27 \times 10^{-6}$

The values in the two cases show very poor concordance, almost certainly due to the large error involved in measuring the "gradient" of non-linear plots.

Although it would obviously be of interest to investigate the integral method further using paramagnetic solutions, it is clear that the method provides no great advantage. It is very tedious, on account of the slow sweep speeds involved, a factor which also prevents its use with paramagnetic solutions which are not very stable, such as solutions of many ferricenium derivatives.

#### (e) Conclusion

The progressive saturation method on the HA 100 instrument has in some respects proved better than on the R10 instrument. The main advantage lies in the fact that stationary conditions may be achieved, giving greater accuracy and a much less time-consuming procedure. The problem of non-linear plots seems to have been solved by reducing signal intensity which reduces the radiation damping effect. However, irreproducible peak heights, perhaps due to slight changes in the probe position, or perhaps due to



leakage, are still a considerable problem.

In theory, calibration of the instrument should have allowed absolute values for relaxation times to be calculated, but this did not prove possible. Using standard paramagnetic solutions for which the equality of  $T_1$  and  $T_2$  would be expected, the relaxation times were not found to be equal, casting some doubt on the method. The alternative method of instrumental calibration using Torrey oscillations was also unsuccessful, again because the equality of  $T_1$  and  $T_2$  could not be confirmed.

We thus have a method by which qualitative comparisons of relaxation times can be made, but which, in its present form, does not allow absolute values to be calculated with any certainty.

The integral method appeared on preliminary investigation to be less satisfactory than the peak height method.

#### (E) APPLICATIONS OF PROGRESSIVE SATURATION

Progressive saturation was used in two areas of the above work:

- (a) with ferrocene derivatives
- (b) with amide complexes of cobalt perchlorate.

##### (a) Ferrocene derivatives

Investigation of progressive saturation in the present work arose from the work on ferrocene derivatives. It was suspected that the ring proton signals in some ferricenium derivatives were being selectively broadened, but linewidth measurements proved unsatisfactory due to extensive overlap of



peaks. It was hoped that progressive saturation would distinguish any differences in the relaxation times of these protons.

Work on the R10 instrument with oxidised ethyl ferrocenoate and on the HA 100 instrument with oxidised methyl ferrocenoate showed quite clearly that the substituted ferrocene ring protons in both these derivatives have shorter relaxation times than the unsubstituted ring protons (see Part III, Section C). The method however was not accurate enough to show up any difference that there might have been between the two pairs of substituted ring protons.

(b) Amide studies

During the work on cobalt complexes, the selective shifts produced by cobalt(II) perchlorate in sugar amide signals (see Part V, Section C(c)) gave inconclusive results for the acetyl signals. These signals showed widely differing shift to linewidth ratios. It was hoped that progressive saturation, by evaluating the relative relaxation times for these acetyl signals, would indicate whether the broadening was due to slow exchange.

The saturation studies did show up differences between the signals. Interpretation of the results, however, could only be tentative, partly because the results were not very precise, and partly because the system was so complicated that the various factors involved could not be separated.



BIBLIOGRAPHY

1. P.F. Swinton, Ph.D. thesis, Edinburgh, 1967.
2. B.R. Donaldson, Ph.D. thesis, Edinburgh, 1970.
3. H.M. McConnell and D.B. Chestnut, J. Chem. Phys., 1958, 28, 107.
4. E. Fermi, Z. Physik, 1930, 60, 320.
5. H.M. McConnell and C.H. Holm, J. Chem. Phys., 1957, 27, 314.
6. J.A. Happe and R.L. Ward, J. Chem. Phys., 1963, 39, 1211.
7. W.D. Horrocks and G.N. LaMar, J. Amer. Chem. Soc., 1963, 85, 3512.
8. E.A. LaLancette and D.R. Eaton, J. Amer. Chem. Soc., 1964, 86, 5145.
9. D.R. Eaton, J. Amer. Chem. Soc., 1965, 87, 3097.
10. R.E. Cramer and R.S. Drago, J. Amer. Chem. Soc., 1970, 92, 66.
11. R.J. Kurland and B.R. McGarvey, J. Magn. Resonance, 1970, 2, 286.
12. D.R. Eaton, A.D. Josey, W.D. Phillips and R.E. Benson, J. Chem. Phys., 1962, 37, 347.
13. W.D. Horrocks, J. Amer. Chem. Soc., 1965, 87, 3779.
14. R.J. Fitzgerald and R.S. Drago, J. Amer. Chem. Soc., 1967, 89, 2879.
15. D.R. Eaton, A.D. Josey and R.E. Benson, J. Amer. Chem. Soc., 1967, 89, 4040.
16. W.D. Horrocks and D.L. Johnston, Inorg. Chem., 1971, 10, 1835.
17. N. Bloembergen and W.C. Dickinson, Phys. Rev., 1950, 79, 179.
18. W.C. Dickinson, Phys. Rev., 1951, 81, 717.
19. H.M. McConnell and R.E. Robertson, J. Chem. Phys., 1958, 29, 1361.
20. G.N. LaMar, J. Chem. Phys., 1965, 43, 1085.
21. G.N. LaMar, W.D. Horrocks and L.C. Allen, J. Chem. Phys., 1964, 41, 2126.



22. examples are a) G.N. LaMar, J. Chem. Phys., 1964, 41, 2992.  
                   b) R.W. Kluiber and W.D. Horrocks, J. Amer. Chem. Soc., 1965, 87, 5350.  
                   c) R.W. Kluiber and W.D. Horrocks, Inorg. Chem., 1967, 6, 166.
23. M.L. Wicholas and R.S. Drago, J. Amer. Chem. Soc., 1968, 90, 2196.
24. W.D. Horrocks, Inorg. Chem., 1970, 9, 690.
25. W.D. Perry, R.S. Drago, D.W. Herlocker, G.K. Pagenkopf and K. Czworniak, Inorg. Chem., 1971, 10, 1087.
26. F. Bloch, Phys. Rev., 1946, 70, 460.
27. N. Bloembergen, E.M. Purcell and R.V. Pound, Phys. Rev., 1948, 73, 679.
28. I. Solomon, Phys. Rev., 1955, 99, 559.
29. N. Bloembergen, J. Chem. Phys., 1957, 27, 572.
30. N. Bloembergen and L.O. Morgan, J. Chem. Phys., 1961, 34 842.
31. R.G. Shulman, H. Sternlicht and B.J. Wyluda, J. Chem. Phys., 1965, 43, 3116.
32. H. Sternlicht, J. Chem. Phys., 1965, 42, 2250.
33. Z. Luz and S. Meiboom, J. Chem. Phys., 1964, 40, 2686.
34. R.A. Bernheim, T.H. Brown, H.S. Gutowsky and D.E. Woessner, J. Chem. Phys., 1959, 30, 950.
35. A.W. Nolle and L.O. Morgan, J. Chem. Phys., 1957, 26, 642; 1959, 31, 365.
36. T.J. Swift and R.E. Connick, J. Chem. Phys., 1962, 37, 307.
37. R.W. Kluiber and W.D. Horrocks, J. Amer. Chem. Soc., 1966, 88, 1399.
38. E. Gillies and M.C. Baird, Chem. Phys. Letters, 1970, 7, 451.
39. R. Engel, J. Chem. Soc. (C), 1971, 3554.
40. R. Engel and G. Nathan, J. Chem. Soc. (C), 1971, 3844.
41. L.S. Frankel, J. Chem. Phys., 1969, 50, 943.
42. R. Engel and A. Jung, J. Chem. Soc. (C), 1971, 1761.
43. S.S. Zumdahl and R.S. Drago, Inorg. Chem., 1968, 7, 2162.



44. L.S. Frankel, Inorg. Chem., 1969, 8, 1784.
45. R. Engel, Chem. Comm., 1970, 133.
46. J. Eisinger, R.G. Shulman and B.M. Szymanski, J. Chem. Phys., 1962, 36, 1721.
47. J. Eisinger, F. Fawaz-Estrup and R.G. Shulman, J. Chem. Phys., 1965, 42, 43.
48. H.M. McConnell and C.H. Holm, J. Chem. Phys., 1958, 28, 749.
49. D.A. Levy and L.E. Orgel, Mol. Phys., 1960, 3, 583.
50. H.P. Fritz, H.J. Keller and K.E. Schwarzhans, Z. Naturforsch. B, 1968, 23, 298.
51. M.F. Rettig and R.S. Drago, J. Amer. Chem. Soc., 1969, 91, 1361, 3432.
52. M.W. Dietrich and A.C. Wahl, J. Chem. Phys., 1963, 38, 1591.
53. H.P. Fritz, H.J. Keller and K.E. Schwarzhans, (a) Z. Naturforsch. B, 1966, 21, 809; (b) J. Organometallic Chem., 1966, 6, 652; 1967, 7, 105.
54. (a) R. Prins and F.J. Reinders, J. Amer. Chem. Soc., 1969, 91, 4929.  
(b) R. Prins, Mol. Phys., 1970, 19, 603.  
(c) R. Prins and A.R. Korswagen, J. Organometallic Chem., 1970, 25, C74.
55. D.R. Eaton, A.D. Josey, W.D. Phillips and R.E. Benson, Discuss. Faraday Soc., 1962, 34, 77.
56. D.R. Eaton, A.D. Josey, R.E. Benson, W.D. Phillips and T.L. Cairns, J. Amer. Chem. Soc., 1962, 84, 4100.
57. D.R. Eaton, A.D. Josey, W.D. Phillips and R.E. Benson, J. Chem. Phys., 1963, 39, 3513.
58. D.R. Eaton, W.D. Phillips and D.J. Caldwell, J. Amer. Chem. Soc., 1963, 85, 397.
59. D.R. Eaton and W.D. Phillips, J. Chem. Phys., 1965, 43, 392.
60. D.R. Eaton, W.R. McClellan and J.F. Weiher, Inorg. Chem., 1968, 7, 2040.
61. D. Doddrell and J.D. Roberts, J. Amer. Chem. Soc., 1970, 92, 5255.
62. R.H. Holm, A. Chakravorty and G.O. Dudek, J. Amer. Chem. Soc., 1964, 86, 379.
63. L. Sacconi, P. Paoletti and M. Ciampolini, J. Amer. Chem. Soc., 1963, 85, 411.



64. R.H. Holm and K. Swaminathan, Inorg. Chem., 1962, 1, 599.
65. L. Sacconi, M. Ciampolini and N. Nardi, J. Amer. Chem. Soc., 1964, 86, 819.
66. E.A. LaLancette, D.R. Eaton, R.E. Benson and W.D. Phillips, J. Amer. Chem. Soc., 1962, 84, 3968.
67. A. Chakravorty and R.H. Holm, Inorg. Chem., 1964, 3, 1010.
68. G.W. Everett and R.H. Holm, J. Amer. Chem. Soc., 1965, 87, 2117.
69. G.W. Everett and R.H. Holm, J. Amer. Chem. Soc., 1966, 88, 2442.
70. L.H. Pignolet, W.D. Horrocks and R.H. Holm, J. Amer. Chem. Soc., 1970, 92, 1855.
71. G.N. LaMar and E.O. Sherman, J. Amer. Chem. Soc., 1970, 92, 2691.
72. M.R. Rosenthal and R.S. Drago, Inorg. Chem., 1965, 4, 840.
73. R.H. Holm, G.W. Everett and W.D. Horrocks, J. Amer. Chem. Soc., 1966, 88, 1071.
74. B.B. Wayland and R.S. Drago, J. Amer. Chem. Soc., 1966, 88, 4597.
75. M. Wicholas and R.S. Drago, J. Amer. Chem. Soc., 1968, 90, 6946.
76. I. Bertini and L.J. Wilson, J. Chem. Soc. (A), 1971, 489.
77. D.W. Herlocker, R.S. Drago and V.I. Meek, Inorg. Chem., 1966, 5, 2009.
78. I. Bertini, D. Gatteschi and L.J. Wilson, Inorg. Chim. Acta, 1970, 4, 629.
79. R.J. Fitzgerald and R.S. Drago, J. Amer. Chem. Soc., 1968, 90, 2523.
80. G.N. LaMar, J. Phys. Chem., 1965, 69, 3212.
81. W.D. Horrocks and L.H. Pignolet, J. Amer. Chem. Soc., 1966, 88, 5929; 1968, 90, 922.
82. Z. Luz and R.G. Shulman, J. Chem. Phys., 1965, 43, 3750.
83. B.B. Wayland and W.L. Rice, Inorg. Chem., 1966, 5, 54.
84. F.A. Cotton and R.H. Soderberg, Inorg. Chem., 1964, 3, 1.
85. J.P. Fackler, J. Amer. Chem. Soc., 1962, 84, 24.



86. J.P. Fackler, Inorg. Chem., 1963, 2, 266.
87. R.W. Kluiber, R. Kukla and W.D. Horrocks, Inorg. Chem., 1970, 9, 1319.
88. I. Morishima, T. Yonezawa and K. Goto, J. Amer. Chem. Soc., 1970, 92, 6651.
89. D. Doddrell and J.D. Roberts, J. Amer. Chem. Soc., 1970, 92, 6839.
90. G.N. LaMar, Inorg. Chem., 1969, 8, 581.
91. G.N. LaMar, J. Amer. Chem. Soc., 1970, 92, 1806.
92. V.K. Fricke and H. Suhr, Ber. Bunsengesellschaft Phys. Chem., 1968, 72, 434.
93. R.W. Kluiber and W.D. Horrocks, Inorg. Chem., 1967, 6, 430.
94. J.W. Rakshys, Inorg. Chem., 1970, 9, 1521.
95. T. Yonezawa, I. Morishima, Y. Akana and K. Fukuta, Bull. Chem. Soc. Japan, 1970, 43, 379.
96. T. Yonezawa, I. Morishima and Y. Ohmori, J. Amer. Chem. Soc., 1970, 92, 1267.
97. W.A. Szarek, E. Dent, T.B. Grindley and M.C. Baird, Chem. Comm., 1969, 953.
98. E. Gillies, W.A. Szarek and M.C. Baird, Canad. J. Chem., 1971, 49, 211.
99. R.W. Kluiber and W.D. Horrocks, J. Amer. Chem. Soc., 1965, 87, 5350.
100. R.W. Kluiber, F. Thaller, R.A. Low and W.D. Horrocks, Inorg. Chem., 1970, 9, 2592.
101. R.W. Kluiber, and W.D. Horrocks, Inorg. Chem., 1966, 5, 152.
102. R.W. Kluiber and W.D. Horrocks, J. Amer. Chem. Soc., 1966, 88, 1399.
103. W.D. Horrocks, R.C. Taylor and G.N. LaMar, J. Amer. Chem. Soc., 1964, 86, 3031.
104. W.A. Szarek and M.C. Baird, Tetrahedron Letters, 1970, 2097.
105. E.B. Whipple and G.R. Evanega, Tetrahedron, 1968, 24, 1299.
106. G.N. LaMar, J. Magn. Resonance, 1969, 1, 185.



107. A. Forman, J.N. Murrell and L.E. Orgel, J. Chem. Phys., 1959, 31, 1129.
108. F. Röhrscheid, R.E. Ernst and R.H. Holm, Inorg. Chem., 1967, 6, 1315.
109. D.W. Larsen and A.C. Wahl, Inorg. Chem., 1965, 4, 1281.
110. G.N. LaMar, J. Chem. Phys., 1965, 43, 235.
111. W.D. Horrocks, R.H. Fischer, J.R. Hutchison and G.N. LaMar, J. Amer. Chem. Soc., 1966, 88, 2436.
112. G.N. LaMar, R.H. Fischer and W.D. Horrocks, Inorg. Chem., 1967, 6, 1798.
113. R.S. Milner and L. Pratt, Discuss. Faraday Soc., 1962, 34, 88.
114. C.C. Hinckley, J. Amer. Chem. Soc., 1969, 91, 5160.
115. C.C. Hinckley, J. Org. Chem., 1970, 35, 2834.
116. C.C. Hinckley, M.R. Klotz and F. Patil, J. Amer. Chem. Soc., 1971, 93, 2417.
117. J.K.M. Sanders and D.H. Williams, Chem. Comm., 1970, 422.
118. P.V. Demarco, T.K. Elzey, R.B. Lewis and E. Wenkert, J. Amer. Chem. Soc., 1970, 92, 5734, 5737.
119. N.S. Bhacca and J.D. Wander, Chem. Comm., 1971, 1505.
120. M.R. Vegar and R.J. Wells, Tetrahedron Letters, 1971, 2847.
121. J.K.M. Sanders and D.H. Williams, J. Amer. Chem. Soc., 1971, 93, 641.
122. B.L. Shapiro, J.R. Hlubucek, G.R. Sullivan and L.F. Johnson, J. Amer. Chem. Soc., 1971, 93, 3281.
123. F.A. Carey, J. Org. Chem., 1971, 36, 2199.
124. T. Okutani, A. Morimoto, T. Kaneko and K. Masuda, Tetrahedron Letters, 1971, 1115.
125. G.H. Wahl and M.R. Peterson, Chem. Comm., 1970, 1167.
126. I. Armitage, G. Dunsmore, L.D. Hall and A.G. Marshall, Chem. Comm., 1971, 1281.
127. L. Ernst, Chem.-Ztg., 1971, 95, 325.
128. H.V. Brederode and W.G.B. Huysmans, Tetrahedron Letters, 1971, 1695.



129. D.C. Remy and W.A.V. Saun, Tetrahedron Letters, 1971, 2463.
130. L. Ernst and A. Mannschreck, Tetrahedron Letters, 1971, 3023.
131. W.L.F. Armarego, T.J. Batterham and J.R. Kershaw, Org. Magn. Resonance, 1971, 3, 575.
132. H. Huber and C. Pascual, Helv. Chim. Acta, 1971, 54, 913.
133. K.J. Liska, A.F. Fentiman and R.L. Foltz, Tetrahedron Letters, 1970, 4657.
134. C.P. Casey and R.A. Boggs, Tetrahedron Letters, 1971, 2455.
135. P. Kristiansen and T. Ledaal, Tetrahedron Letters, 1971, 2817.
136. F.I. Carroll and J.T. Blackwell, Tetrahedron Letters, 1970, 4173.
137. M. Yoshimoto, T. Hiraoka, H. Kuwano and Y. Kishida, Chem. and Pharm. Bull. (Japan), 1971, 19, 849.
138. L.F. Johnson, J. Chakravarty, R. Dasgupta and U.R. Ghatak, Tetrahedron Letters, 1971, 1703.
139. L.H. Keith, Tetrahedron Letters, 1971, 3.
140. M.R. Willcott, J.F.M. Oth, J. Thio, G. Plinke and G. Shröder, Tetrahedron Letters, 1971, 1579.
141. Z.W. Wolkowski, Tetrahedron Letters, 1971, 825.
142. K.D. Berlin and S. Rengaraju, J. Org. Chem., 1971, 36, 2912.
143. A.H. Lewin, Tetrahedron Letters, 1971, 3583.
144. T.M. Ward, I.L. Allcox and G.H. Wahl, Tetrahedron Letters, 1971, 4421.
145. T.H. Siddall, Chem. Comm., 1971, 452.
146. R.F. Butterworth, A.G. Pernet and S. Hanessian, Canad. J. Chem., 1971, 49, 981.
147. R.R. Fraser and Y.Y. Wigfield, Chem. Comm., 1970, 1471.
148. K.K. Andersen and J.J. Uebel, Tetrahedron Letters, 1970, 5253.
149. P. Girard, H. Kagan and S. David, Bull. Soc. chim. France, 1970, 4515.



150. I. Armitage and L.D. Hall, Chem. and Ind., 1970, 1537.
151. I. Armitage and L.D. Hall, Canad. J. Chem., 1971, 49, 2770.
152. J.E. Herz, V.M. Rodriguez and P. Joseph-Nathan, Tetrahedron Letters, 1971, 2949.
153. M. Kishi, K. Tori and T. Komeno, Tetrahedron Letters, 1971, 3525.
154. L. Lacombe, F. Khuong-Huu-Laine, A. Pancrazi, Khuong-Huu-Quy and G. Lukacs, C.R. Acad. Sci. Ser. C. 1971, 272, 668.
155. O. Achmatowicz, A. Ejchart, J. Jurczak, L. Kozerski and J. St. Pyrek, Chem. Comm., 1971, 98.
156. D.G. Buckley, G.H. Green, E. Ritchie and W.C. Taylor, Chem. and Ind., 1971, 298.
157. F.F.L. Ho, J. Polymer. Sci., Part B, Polymer Letters, 1971, 9, 491.
158. A.R. Katritzky and A. Smith, Tetrahedron Letters, 1971, 1765.
159. M.I. Foreman and D.G. Leppard, J. Organometallic Chem., 1971, 31, C31.
160. M. Gielen, N. Goffin and J. Topart, J. Organometallic Chem., 1971, 32, C38.
161. J. Briggs, G.H. Frost, F.A. Hart, G.P. Moss, and M.L. Staniforth, Chem. Comm., 1970, 749.
162. J. Briggs, F.A. Hart and G.P. Moss, Chem. Comm., 1970, 1506.
163. L. Tomic, Z. Majerski, M. Tomic and D.E. Sunko, Chem. Comm., 1971, 719.
164. P. Bélanger, C. Freppel, D. Tizané and J.-C. Richer, Canad. J. Chem., 1971, 49, 1985.
165. G.V. Smith, W.A. Boyd and C.C. Hinckley, J. Amer. Chem. Soc., 1971, 93, 6319.
166. P. Kristiansen and T. Ledaal, Tetrahedron Letters, 1971, 4457.
167. P. Bélanger, C. Freppel, D. Tizané and J.C. Richer, Chem. Comm., 1971, 266.
168. P.H. Mazzocchi, H.J. Tamburin and G.R. Miller, Tetrahedron Letters, 1971, 1819.
169. B.D. Cuddy, K. Treon and B.J. Walker, Tetrahedron Letters, 1971, 4433.



170. D.R. Crump, J.K.M. Sanders and D.H. Williams, Tetrahedron Letters, 1970, 4419.
171. N. Ahmad, N.S. Bhacca, J. Selbin and J.D. Wander, J. Amer. Chem. Soc., 1971, 93, 2564.
172. W.D. Horrocks and J.P. Sipe, J. Amer. Chem. Soc., 1971, 93, 6800.
173. C. Beauté, Z.W. Wolkowski and N. Thoai, Tetrahedron Letters, 1971, 817.  
 Z.W. Wolkowski, Tetrahedron Letters, 1971, 821.  
 M. Witanowski, L. Stefaniak, H. Januszewski and Z.W. Wolkowski, Tetrahedron Letters, 1971, 1653.  
 C. Beauté, Z.W. Wolkowski, J.P. Merda and D. Lelandais, Tetrahedron Letters, 1971, 2473.  
 C. Beauté, Z.W. Wolkowski and N. Thoai, Chem. Comm., 1971, 700.
174. J. Briggs, F.A. Hart, G.P. Moss and E.W. Randall, Chem. Comm., 1971, 364.
175. G.M. Whitesides and D.W. Lewis, J. Amer. Chem. Soc., 1970, 92, 6979; 1971, 93, 5914.
176. H.L. Goering, J.N. Eikenberry and G.S. Koerner, J. Amer. Chem. Soc., 1971, 93, 5913.
177. R.R. Fraser, M.A. Petit and J.K. Saunders, Chem. Comm., 1971, 1450.
178. R.E. Rondeau and R.E. Sievers, J. Amer. Chem. Soc., 1971, 93, 1522.
179. L.R. Isbrandt and M.T. Rogers, Chem. Comm., 1971, 1378.
180. J.F. Caputo and A.R. Martin, Tetrahedron Letters, 1971, 4547.
181. J.E. Guillet, I.R. Peat and W.F. Reynolds, Tetrahedron Letters, 1971, 3493.
182. J.K.M. Sanders and D.H. Williams, Tetrahedron Letters, 1971, 2813.
183. D.G. Karraker, J. Chem. Educ., 1970, 47, 424.
184. A.F. Cockerill and D.M. Rackham, Tetrahedron Letters, 1970, 5149.
185. J. Goodisman and R.S. Matthews, Chem. Comm., 1972, 127.
186. W.D. Horrocks, J.S. Sipe and J.R. Lubner, J. Amer. Chem. Soc., 1971, 93, 5258.
187. I. Armitage, G. Dunsmore, L.D. Hall and A.G. Marshall, Chem. and Ind., 1972, 79.



188. H. Huber and J. Seelig, Helv. Chim. Acta, 1972, 55, 135.
189. K. Roth, M. Grosse and D. Rewicki, Tetrahedron Letters, 1972, 435.
190. J. Bouquant and J. Chuche, Tetrahedron Letters, 1972, 2337.
191. I.M. Armitage, V. Gibb, L.D. Hall and A.G. Marshall, 2nd International Conference on N.M.R. Spectroscopy, Surrey, 1972.
192. B. Bleaney, C.M. Dobson, B.A. Levine, R.B. Martin, R.J.P. Williams and A.V. Xavier, Chem. Comm., 1972, 791.
193. K.H. Hausser, H. Brunner and J.C. Jochims, Mol. Phys., 1966, 10, 253.
194. R.W. Kreilick, J. Chem. Phys., 1966, 45, 1922.
195. R.W. Kreilick, J. Chem. Phys., 1967, 46, 4260.
196. R.W. Kreilick, J. Amer. Chem. Soc., 1968, 90, 2711.
197. R.W. Kreilick, J. Amer. Chem. Soc., 1968, 90, 5991.
198. F. Yamauchi and R.W. Kreilick, J. Amer. Chem. Soc., 1969, 91, 3429.
199. R.W. Kreilick, Mol. Phys., 1968, 14, 495.
200. I. Morishima, K. Endo and T. Yonezawa, Chem. Phys. Letters, 1971, 9, 143, 203.
201. I. Morishima, K. Endo and T. Yonezawa, J. Amer. Chem. Soc., 1971, 93, 2048.
202. R.E. Connick and E.D. Stover, J. Phys. Chem., 1961, 65, 2075.
203. J.C. Sheppard and J.L. Burdett, Inorg. Chem., 1966, 5, 921.
204. Z. Luz and S. Meiboom, J. Chem. Phys., 1964, 40, 1058, 1066.
205. P.A. Zagorets, V.I. Ermakov and A.P. Grunau, Russ. J. Phys. Chem., 1965, 39, 826.
206. N.A. Matwiyoff and P.E. Darley, J. Phys. Chem., 1968, 72, 2659.
207. I.D. Campbell, P.E. Nixon and R.E. Richards, Mol. Phys., 1971, 20, 923.
208. L.S. Frankel, I.R. Stengle and C.H. Langford, Canad. J. Chem., 1968, 46, 3183.



209. R.E. Connick and R.E. Poulson, J. Chem. Phys., 1959, 30, 759.
210. R.L. Conger and P.W. Selwood, J. Chem. Phys., 1952, 20, 383.
211. R.W. Kreilick and S.I. Weissman, J. Amer. Chem. Soc., 1966, 88, 2645.
212. H. Sternlicht, R.G. Shulman and E.W. Anderson, J. Chem. Phys., 1965, 43, 3123.
213. J.E. Herz, J. Chem. Educ., 1966, 43, 599.
214. C.R. Hauser and J.K. Lindsay, J. Org. Chem., 1957, 22, 482.
215. V. Weinmayr, Chem. Abs., 1955, 49, 10364a.
216. K.L. Rinehart, K.L. Motz and S. Moon, J. Amer. Chem. Soc., 1957, 79, 2749.
217. R.A. Benkesser, D. Goggin and G. Schroll, J. Amer. Chem. Soc., 1954, 76, 4025.
218. V. Weinmayr, J. Amer. Chem. Soc., 1955, 77, 3009.
219. R.L. Schaaf, J. Org. Chem., 1962, 27, 107.
220. E.J. Kupchik and R.J. Kiesel, J. Org. Chem., 1966, 31, 456.
221. J.B. Lee, J. Amer. Chem. Soc., 1966, 88, 3440.
222. J.B. Lee and I.M. Downie, Tetrahedron, 1967, 23, 359.
223. R.C. Parish and L.M. Stock, J. Org. Chem., 1965, 30, 927.
224. M. Rosenblum, A.K. Banerjee, N. Danieli, R.W. Fish and V. Schlatter, J. Amer. Chem. Soc., 1963, 85, 316.
225. P.L. Pauson and W.E. Watts, J. Chem. Soc., 1962, 3880.
226. P.J. Graham, R.V. Lindsey, G.W. Parshall, M.L. Peterson and G.M. Whitman, J. Amer. Chem. Soc., 1957, 79, 3416.
227. Private communication from P.L. Pauson.
228. M. Rosenblum, J. Amer. Chem. Soc., 1959, 81, 4530.
229. E.G. Perevalova, N.A. Simukova, T.V. Nikitina, P.D. Reshetov and A.N. Nesmeyanov, Chem. Abs., 1961, 55, 17645e.
230. M.D. Rausch and A. Siegel, J. Organometallic Chem., 1969, 17, 117.



231. J. Tirouflet and G. Tainturier, Bull. Soc. chim. France, 1966, 2565.
232. M.D. Rausch and V. Mark, J. Org. Chem., 1963, 28, 3225.
233. A.S. Waggoner, A.D. Keith and O.H. Griffith, J. Phys. Chem., 1968, 72, 4129.
234. O.H. Griffith and A.S. Waggoner, Accounts Chem. Res., 1969, 2, 17.
235. A.R. Forrester, J.M. Hay and R.H. Thomson, "Organic Chemistry of Stable Free Radicals", Academic Press, 1968, ch. 5.
236. R. Brière, H. Lemaire and A. Rassat, Bull. Soc. chim. France, 1965, 3273.
237. E.G. Rozantsev, Chem. Abs., 1963, 59, 15252h.
238. D.R. Eaton and W.D. Phillips, Adv. Magn. Resonance, 1965, 1, 103.
239. E.B. Whipple and G.R. Evanega, Tetrahedron, 1968, 24, 1299.
240. M. Kerr, unpublished work.
241. T. Moroe, G. Indo, A. Komatsu and T. Yoshida, Chem. Abs., 1965, 62, 14736b.
242. R. Adams and L.M. Werbel, J. Amer. Chem. Soc., 1958, 80, 5799.
243. W.D. Johnson and N.V. Riggs, Austral. J. Chem., 1964, 17, 787.
244. W.H. Mills and R.M. Kelham, J. Chem. Soc., 1937, 274.
245. L.F. Fieser, Org. Synth., 1955, 35, 43.
246. N.K. Richtmyer, "Methods in Carbohydrate Chemistry", Vol. I, Whistler and Wolfrom, Academic Press, 1962, p. 108.
247. M.L. Wolfrom and A. Thompson, "Methods in Carbohydrate Chemistry", Vol. II, Whistler and Wolfrom, Academic Press, 1963, p. 212.
248. F. Micheel and O. Littmann, Annalen, 1928, 466, 115.
249. L.F. Fieser and M. Fieser, "Steroids", Chapman and Hall, 1959, p. 519.
250. L.F. Fieser and M. Fieser, "Steroids", Chapman and Hall, 1959, p. 287.



251. A.A. Zinov'ev and V.I. Naumova, Chem. Abs., 1960, 54, 11786h.
252. B.J. Hathaway, D.G. Holah and M. Hudson, J. Chem. Soc., 1963, 4586.
253. V. Gold and C. Tomlinson, Chem. Comm., 1970, 472.
254. B.J. Hathaway and A.E. Underhill, J. Chem. Soc., 1961, 3091.
255. W.D. Horrocks and J.R. Hutchison, J. Chem. Phys., 1967, 46, 1703.
256. N.S. Bhacca and D.H. Williams, "Applications of NMR Spectroscopy in Organic Chemistry", Holden-Day, 1964.
257. B. Coxon, Tetrahedron, 1965, 21, 3481.
258. N.A. Matwiyoff, Inorg. Chem., 1966, 5, 788.
259. B.B. Wayland, R.J. Fitzgerald and R.S. Drago, J. Amer. Chem. Soc., 1966, 88, 4600.
260. M. Wicholas and R.S. Drago, J. Amer. Chem. Soc., 1969, 91, 5963.
261. R.F.C. Brown, L. Radom, S. Sternhell and I.D. Rae, Can. J. Chem., 1968, 46, 2577.
262. B.F. Pedersen and B. Pedersen, Tetrahedron Letters, 1965, 34, 2995.
263. B.B. Wayland, R.S. Drago and H.F. Henneike, J. Amer. Chem. Soc., 1966, 88, 2455.
264. L.D. Hall, Adv. Carbohydrate Chem., 1964, 19, 51.
265. D. Horton, W.E. Mast and K.D. Philips, J. Org. Chem., 1967, 32, 1471.
266. R.U. Lemieux and J.D. Stevens, Can. J. Chem., 1965, 43, 2059.
267. T.D. Inch, J.R. Plimmer and H.G. Fletcher, J. Org. Chem., 1966, 31, 1825.
268. C.R. Narayanan and B.M. Sawant, Tetrahedron Letters, 1971, 1321.
269. K.J. Eisentraut and R.E. Sievers, J. Amer. Chem. Soc., 1965, 87, 5254.
270. R.I. Slavkina, D. Usubaliev and V.V. Serebrennikov, Chem. Abs., 1964, 61, 7918e.



271. A.L. Van Geet and D.N. Hume, Analyt. Chem., 1965, 37, 979.
272. E.G. Finer and R.K. Harris, Chem. Comm., 1969, 42.
273. Private communication from J. Tournier, Perkin-Elmer.
274. P.F. Cox and L.O. Morgan, J. Amer. Chem. Soc., 1959, 81, 6409.
275. D.C. Douglass and A. Fratiello, J. Chem. Phys., 1963, 39, 3161, and references there cited.
276. Private communication from R.K. Harris.
277. N. Bloembergen and R.V. Pound, Phys. Rev., 1954, 95, 8.  
C.R. Bruce, R.E. Norberg and G.E. Pake, Phys. Rev., 1956, 104, 419.  
S. Bloom, J. Appl. Phys., 1957, 28, 800.  
A. Szöke and S. Meiboom, Phys. Rev., 1959, 113, 585.  
R.B. Williams, Ann. N.Y. Acad. Sci., 1958, 70, 890.
278. J.S. Leigh, Rev. Sci. Instr., 1968, 39, 1594.